Atmospheric nitrate deposition on subalpine meadows of the Lautaret pass

Ilann Bourgeois

Communauté
UNIVERSITÉ Grenoble Alpes

THÈSE

Pour obtenir le grade de

DOCTEUR DE LA COMMUNAUTE UNIVERSITE GRENOBLE ALPES

Spécialité : **Biodiversité, Ecologie, Environnement**

Arrêté ministériel : 25 mai 2016

Présentée par

Ilann BOURGEOIS

Thèse dirigée par **Jean-Christophe CLEMENT** et **Joël SAVARINO**

préparée au sein du **Laboratoire d'Ecologie Alpine** et de **l'Institut des Géosciences de l'Environnement**
dans **l'École Doctorale Chimie et Sciences du Vivant**

Dépôt des nitrates atmosphériques sur les prairies subalpines du Lautaret

Thèse soutenue publiquement le **8 Décembre 2017**,
devant le jury composé de :

M. Didier VOISIN
Professeur à l'Université Grenoble Alpes, Président
M. André PORNON
Maitre de conférence à l'Université Toulouse III, Rapporteur
M. Jan KAISER
Professor, University of East Anglia, Rapporteur
M. Gordon HOLTGRIEVE
Assistant Professor, University of Washington, Examinateur
M. Jean-Christophe CLEMENT
Professeur à l'Université Savoie Mont Blanc, Directeur de thèse
M. Joël SAVARINO
Directeur de recherche au CNRS, co-Directeur de thèse

Remerciements

Quand vient le temps des remerciements, ça sent bon le dernier paragraphe, la page qui se tourne, le point « final » en somme. L'occasion de dire « Merci » à toutes les personnes qui, de près ou de loin, ont contribué à ce travail, scientifiquement d'abord, humainement surtout. Merci, donc…

Le triptyque directionnel : Joël, pour m'avoir suivi, fait confiance, et poussé de l'avant depuis bientôt 7 ans que nos chemins se sont croisés à Dôme C. J'espère avoir redressé la barre depuis les résines de Concordia… Merci pour le reste aussi: je n'oublie pas que San Diego, la thèse et le Stromboli, c'est grâce à toi ! JC, pour ta confiance inébranlable au cours de ces trois dernières années. Alors même que l'on ne se connaissait pas, tu as accepté de me laisser les rênes de ce sujet de thèse au Lautaret, et tu as su me laisser maître de mes choix au quotidien. Cette thèse n'est sans doute pas celle que tu avais imaginé initialement, mais j'espère qu'elle ne t'en satisfera pas moins. Didier, enfin. Si ta codirection de cette thèse n'a jamais été officialisée, elle n'en a pas été moindre à mes yeux pour autant. Ta curiosité inextinguible et les discussions fréquentes que nous avons eues ont toujours été matière à réflexion pour moi. Merci aussi pour les mots de soutien, distillés avec parcimonie mais toujours aux moments opportuns.

Le jury : André P. et Jan K., pour avoir accepté d'évaluer ce manuscrit et d'en avoir livrer une critique constructive qui saura profiter à mes futurs papiers. Gordon H., pour ta présence à ce jury et tes questions d'une pertinence rare.

Le groupe isotope pour avoir pagayé avec moi dans les méandres de l'isotopie. Mention spéciale à Nico pour ta bonne humeur et ta pédagogie infaillible, Albane pour le serrage de coude les longues soirées de labo, Elsa pour le soutien moral (et gastronomique !) et Joseph pour ta disponibilité et ton aide alors même que tu avais mis un terme à ta carrière scientifique.

L'équipe SAJF (Franck, Pascal, Camille, Rolland, Max, Christophe) pour les coups de main sur le terrain et pour tous les bons moments passés au col. Un remerciement tout particulier à Franck : si ton imagination débridée et ta disponibilité ont été un atout majeur pour cette thèse, ta compagnie a elle été un immense plaisir pour moi.

Un mot particulier pour les stagiaires de tout horizon (Sarah (x2), Cristiano, Nicolas et Solange) que j'ai eu le plaisir et la chance d'encadrer : cette thèse c'est aussi la vôtre. Merci pour votre implication et pour ne jamais avoir baissé les bras quand moi-même semblais couler sous la charge de travail.

Ce travail a été le fruit d'un travail de terrain et de laboratoire acharné, qui n'aurait pu avoir lieu sans l'aide précieuse de nombreux doctorants, permanents, stagiaires et amis que je citerai ici dans le désordre : Alban, Alexis, Olivier, Hélène, Julien, Fanny, Vincent, Erwann, Baptiste, Cindy, Lionel, Gabin, Bruno, Didier, Arthur, Shohei, Sakiko, Albane, Nico, Joseph, Benjamin et François.

C'est au travers de nombreuses discussions avec des scientifiques de tout bord que j'ai pu élargir les horizons de ce travail. Pour le temps qu'ils ont su m'accorder, un énorme merci à Julien R., Arnaud F., Bello M. et Rolland D. du LECA, Aurélie C., Julien N., Guillaume N., et Cédric L. de l'IGE, Mathieu S. de l'UPMC et Nicolas L. à l'INSA Val de Loire. Je voudrais aussi souligner ici l'accueil exceptionnel de l'équipe Microbiologie de l'Ecole Centrale de Lyon. Partager ces quelques jours avec vous a été un plaisir, merci donc à Tim V., Catherine L., Cécile T. et Romie T.

Laboratoire d'un jour, laboratoire toujours : au LGGE et ses membres, merci pour l'hospitalité au cours de ces trois années. Carole, merci d'avoir rendu cet accueil administrativement si facile. Pour le plaisir que j'ai toujours eu à échanger avec vous, merci Bruno J., Olivier A., Aurélien D., Olivier M., Eric L., Delphine S. et Hans-Werner J. Un mot tout particulier à Suzi et surtout Bruno, sans qui je n'aurais jamais mis les pieds au labo s'ils ne m'avaient fait confiance, il y a 8 ans de cela, pour hiverner à Dôme C.

Les amis, en vrac : Laure, mon pilier landais, des muxu et merci pour tout. Alban, le petit biscuit grenoblois, à bientôt quelque part, et merci pour tous les bons moments. Etienne et Olivier, mes co-bureaux Deluxe, ça a été un b(h)onneur pour moi de partager cette fin d'aventure avec vous. Merci ! Aux compagnons de galère, anciens et nouveaux thésards, bon vent : Julien de Combloux, Gaby, Marina, Cyrille, Thomas, Marion et Lucas, Joseph, Jean, Alexis, Jay, Maria, Camille. Merci à ma seconde famille, les coloc' : Aurèl' et Victor, les grands fous de l'ile verte, Tif et Marioune, les princesses de St Martin d'Hères, Kévin et Julien mini-Belge, les barbus de St Martin d'Hères. Que de souvenirs… Je ne vous remercierai jamais assez pour tous ces moments. Audrey, merci d'avoir toujours cru en moi. La réussite de cette thèse, c'est aussi un peu la tienne.

Papa, Maman, Hugo, Yaël, Néo et toute la famille, merci, évidemment… Une pensée pour toi, mon Pépé, je sais que tu aurais été fier de cet accomplissement. J'espère perpétuer dignement ton souvenir.

Hélène, je ne te remercierai jamais assez pour tout ce que je te dois… Tu étais apparue comme une évidence, tu es maintenant une certitude.

Résumé

L'accroissement des dépôts de nitrate atmosphérique ($NO_3^-{}_{atm}$) sur les bassins versants d'altitude, limités en ressources, entraîne des changements nets de disponibilité d'azote. Ces apports modifient la diversité biologique (végétation, microorganismes), les processus des sols liés à l'azote et conduisent à l'eutrophisation des cours d'eau. A terme, l'impact sur les populations humaines se traduira par la perte d'importants services fournis par ces écosystèmes (alimentation en eau, qualité du fourrage, contrôle de l'érosion, biodiversité). Si les effets des dépôts de $NO_3^-{}_{atm}$ sur les bassins versants pauvres en azote sont maintenant bien documentés, il n'en reste pas moins à comprendre les processus régissant la rétention de $NO_3^-{}_{atm}$ dans les écosystèmes de montagne. Pour ce faire, la variabilité spatio-temporelle de la répartition du $NO_3^-{}_{atm}$ dans tous les compartiments subalpins est ici étudiée en utilisant un traceur multi-isotopique (^{17}O, ^{18}O, ^{15}N) du NO_3^-. L'importante proportion de $NO_3^-{}_{atm}$ dans les cours d'eau de montagne, tout au long de l'année et plus particulièrement à la fonte des neiges, laisse à penser que les bassins versants sont cinétiquement saturés en azote. La composition isotopique du NO_3^- dans les eaux de surface illustre la transformation rapide de l'ammonium de la neige et confirme que la fonte des neiges est une période cruciale du cycle de l'azote dans les montagnes enneigées. La proportion de $NO_3^-{}_{atm}$ dans les sols varie, quant à elle, en fonction du type d'occupation des sols et des propriétés biotiques et abiotiques afférentes. Le suivi de la végétation a montré une forte teneur en $NO_3^-{}_{atm}$ dans les tissus, par assimilation racinaire et foliaire. Ces avancées scientifiques permettront, à terme, de mieux comprendre comment les dépôts de $NO_3^-{}_{atm}$ affectent l'environnement.

Mots-clés : Nitrate, dépôts atmosphériques, isotopes, subalpin, prairies

Abstract

Increasing rates of atmospheric nitrate ($NO_3^-{}_{atm}$) deposition in nutrients-poor mountainous regions have led to critical changes in nitrogen (N) availability, with consequences on biodiversity (plants, microbes), soil N turnover, and water nutrients status. This will ultimately affect human populations through the loss of critical ecosystem services (e.g., provision of clean freshwater, erosion control, biodiversity). If the impacts of $NO_3^-{}_{atm}$ deposition to N-limited basins are now well documented, little is known about the processes driving $NO_3^-{}_{atm}$ retention in subalpine ecosystems. In this context, new tools are necessary to better understand the fate of $NO_3^-{}_{atm}$ in mountains and to predict the mid and long-term ecological consequences of increasing $NO_3^-{}_{atm}$ deposition. This work uses a high-resolution multi-isotopic technique combining ^{17}O, ^{18}O and ^{15}N signatures of NO_3^- in the different subalpine compartments to understand the temporal and spatial evolution of $NO_3^-{}_{atm}$ partitioning in a subalpine watershed of the French Alps. Year-round elevated exports of $NO_3^-{}_{atm}$ in subalpine streams suggest that the watershed is kinetically N saturated, especially after snowmelt. The isotopic composition of NO_3^- in freshwaters also points at the rapid processing of snow ammonium, confirming that snowmelt is a “hot moment” for N cycling in seasonally snow-covered catchments. The monitoring of soils reveals varying $NO_3^-{}_{atm}$ proportions depending on the land management regimes and implied biotic and abiotic characteristics. Two dominant subalpine plants showed high proportions of $NO_3^-{}_{atm}$ in organs acquired by both root and foliar uptake. These scientific breakthroughs will ultimately lead to a better understanding of how $NO_3^-{}_{atm}$ deposition affects the environment.

Keywords: Nitrate, atmospheric deposition, isotopes, subalpine, grasslands

Table of contents

1 Introduction

1.1 Nitrate positioning in the Nitrogen biogeochemical cycle: an isotopic perspective

How best to start this manuscript than by paraphrasing J.N. Galloway and colleagues introduction to their authoritative article of 2004 about Nitrogen (N) cycle (Galloway et al., 2004). There, the authors cited a couplet from the *Rime of the Ancient Mariner* (by Samuel Taylor Coleridge, 1772-1834): "Water, water everywhere and all the boards did shrink; water, water everywhere nor any drop to drink". Beyond its pure poetical beauty, this couplet was a statement that although sailors were surrounded by abundant seawater, they couldn't drink it because of its form. The analogy with nitrogen is explicit for enlightened minds, and here is why.

1.1.1 About nitrogen and nitrate

Nitrogen (N) is an essential nutrient for life on Earth. It is present at every stages of the biosphere – from being associated with other major elements (carbon (C), oxygen (O), sulfur (S), etc.) in deoxyribonucleic acid (DNA) nucleotides to representing the main constituent (78 %) of the atmosphere as N_2 – and necessary to sustain life forms, from microorganisms to vertebrates (Galloway et al., 2008). Paradoxically, despite its prominent abundance N is often a limiting nutrient of net primary productivity in unperturbed systems (Vitousek and Howarth, 1991) due its unavailability to most living organisms (99 % of N is unavailable to 99 % of life on Earth, Galloway et al., 2008). The reason is that N is almost exclusively under the form of molecular nitrogen (N_2), which is not usable as such by most organisms because of the strength of the triple bond linking the two N atoms. To become available, N needs to be "fixed", that is, removed from the atmosphere to be associated with other atoms such as O and hydrogen (H) to form reactive N species (Nr). Here, Nr designates all chemically, biologically and radiatively (re)active N molecules that can be found in Earth's envelopes (Galloway et al., 2004). Natural processes susceptible to provide enough energy to achieve the transformation of N_2

to Nr are Biological Nitrogen Fixation (BNF) and lightning. BNF occurs via N fixing organisms which include a surprisingly small number of algae and bacteria, many of them forming symbiotic relationships with higher plants to convert gaseous N into plant-usable Nr (Hipkin et al., 2004).

Human activities, and more specifically N fixing food-production and energy-making processes have doubled the flux of Nr delivered to the environment (Vitousek et al., 1997), a number projected to increase in the future (Figure 1-1). Detrimental effects of too much Nr in the environment have now been widely monitored, and are well documented (Fowler et al., 2013; Galloway et al., 2008; Vitousek et al., 1997), a perfect illustration of Rosalind famous saying "Too much of a good thing" (*As you like* it, William Shakespeare, 1564-1616). More details about the ecological consequences of enhanced Nr inputs to ecosystems are given in section 1.2, but among the most noticeable is biodiversity loss (Clark et al., 2013).

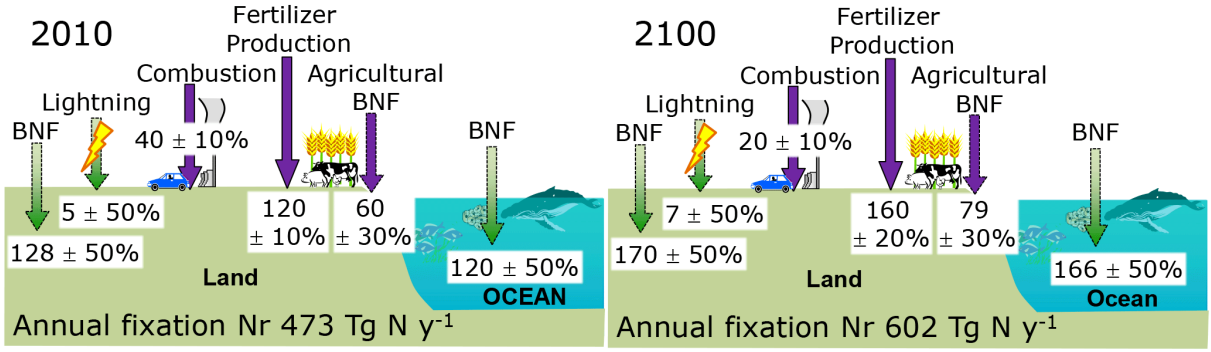

Figure 1-1: Current (left) and future (right) estimates of global Nr fixation with in green the natural processes (Biological Nitrogen Fixation (BNF) and lightning) and in purple human driven processes (agriculture, combustion, industrial activities). After Fowler et al., 2015.

Among Nr species, nitrate (NO_3^-) is of particular importance both to the environment and to humans. With ammonium (NH_4^+), they constitute the quasi totality of N inorganic forms. Plants acquire N mainly under the form of inorganic N at temperate latitudes (Epstein and Bloom, 2016; Miller and Cramer, 2005), even if organic N (N_{org}) such as urea or amino acids can also be absorbed (Hachiya and Sakakibara, 2016). As such, changes in the available amounts and imbalance in the supply of dissolved inorganic nitrogen (DIN) forms can alter vegetation diversity and even cause significant toxicity to plants (Britto and Kronzucker, 2013; Hachiya and

Sakakibara, 2016). NO_3^- is also characterized by a high solubility in water, and can be transported far from the original source to the river lower reaches, or accumulate in groundwater (Spalding and Exner, 1993). It is the most ubiquitous chemical contaminant in the world's aquifers, a situation leading to adverse effects both on humans and the environment. The World Health Organization (WHO) has adopted a 10 mg L^{-1} $N\text{-}NO_3^-$ limit as a maximum standard for safe drinking water. Exceedance of NO_3^- concentrations above this limit is thought to increase risks of reproductive problems, methemoglobinemia and cancer, although it is still subject to scientific controversy (Fewtrell, 2004; Mensinga et al., 2003; Powlson et al., 2008; Van Grinsven et al., 2006). NO_3^- can also impact human health *via* indirect ecological feedbacks, especially when anthropogenic NO_3^- inputs drive significant changes in the environment (Townsend et al., 2003). For all these reasons, NO_3^- dynamics and fate in the environment have been the scope of hundreds of studies over the past several decades, and still is at the center of important scientific questions in the 21st century.

1.1.2 Nitrate isotopologues

Nitrate is constituted of one N atom and three O atoms. These elements have two (^{14}N, ^{15}N) and three (^{16}O, ^{17}O, ^{18}O) stable isotopes, respectively, with m the number of nucleons of ^{m}X isotope (X being any element of the Mendeleev table). The relative proportion of heavy *vs* light isotopes of a given element is expressed as a ratio (e.g., $R^{15} = n(^{15}N) / n(^{14}N)$, $R^{17} = n(^{17}O) / n(^{16}O)$ and $R^{18} = n(^{18}O) / n(^{16}N)$).
The isotopic enrichment (or depletion) of a sample, relative to a standard reference, is expressed in ‰ and calculated using the δ notation as follows:

$$\delta_{sample} = (R_{sample} / R_{standard}) - 1 \qquad \text{(Eq. 1.1)}$$

Reference standards (*i.e.*, stable compounds, abundant, non-toxic, easy to handle and store) are specific to each element. Atmospheric N_2 is the reference standard for N (Mariotti, 1984), and the Vienna Standard Mean Ocean Water (VSMOW) the reference standard for oxygen (International Atomic Energy Agency). By definition,

standards have a δ value of 0 ‰. Here, most of the discussion will turn around the variations of $\delta^{15}N$ and $\delta^{18}O$ of nitrate.

Stable isotopes biogeochemistry focuses on the evolution of isotopic ratios in samples when submitted to physical, chemical or biological processes in the environment. Three mechanisms can lead to fractionation: equilibrium (or thermodynamic), kinetic and nuclear spin. For the purpose of this manuscript, no distinction between these processes will be made and "fractionation" will refer to any of these mechanisms from now onwards, unless specified otherwise. Interested readers can refer to Michener and Lajtha (2007) or Hayes (2004) for a very nice introduction to the fundamentals of stable isotopes in the environment. Isotopic fractionation can be quantified using a fractionation factor (α), which can be defined as the ratio of two isotopic ratios:

$$\alpha = R_{product} / R_{substrate} \qquad \text{(Eq. 1.2)}$$

Where R is the isotopic ratio of the instantaneous product ($R_{product}$) and substrate ($R_{substrate}$). Isotope effects are generally small (*i.e.*, $\alpha \approx 1$); therefore it is common practice to report the deviation of fractionation factors from unity as follows:

$$\varepsilon = \alpha - 1 \qquad \text{(Eq. 1.3)}$$

Where ε is the result of the isotopic fractionation process, which either enrich ($\varepsilon > 0$) or deplete ($\varepsilon < 0$) the substrate with heavy isotopes relative to the product. Other formulations for fractionation factors are also sometimes used, with different mathematical solutions, and are thoroughly reviewed elsewhere (Bao et al., 2016; Faure, 1998; Hayes, 2004). The application of stable isotopes biogeochemistry to nitrate has enabled sizable scientific breakthroughs in the understanding of nitrogen cycling in ecosystems, of which an overview is given in the following section.

1.1.3 Sources and sinks of nitrate in terrestrial ecosystems

As stated above, NO_3^- is an important link of N cycling in terrestrial ecosystems, at the crossroads of a variety of N sources, transformations and sinks (Figure 1-2). The $\delta^{15}N$ and $\delta^{18}O$ of NO_3^- reflect the original sources (or mixing of sources) of N and O from which it is derived and the subsequent processes that potentially caused fractionation effects. Most existing N sources have now been documented for their $\delta^{15}N$ ranges, but isotopic fractionation effects of terrestrial processes are still to be further constrained. An overview of the current state of knowledge on N fractionations in the N cycle have recently been published, with emphasize on the discrepancies between experimentally and theoretically calculated fractionation factors (Denk et al., 2017). Still, a number of studies have laid the ground for isotopic characterization of the main biological processes affecting NO_3^-, as described below.

Among the sources of NO_3^-, ***nitrification*** is a two-step process of NH_4^+ oxidation to NO_3^-, and the only natural terrestrial production pathway of NO_3^-. Nitrification is in majority mediated by several different autotrophic bacteria and archaea for the purpose of deriving metabolic energy. Although it exists other nitrifiers capable of oxidizing N forms to nitrate (e.g., heterotrophic nitrification), for the purpose of this work they will all be grouped together and referred to as “nitrifiers” from now onwards, unless specifies otherwise. The production of intermediary nitrite (NO_2^-) is usually the limiting step of this process, yielding ^{15}N-depleted NO_3^- in the end. Note that depending on the initial ammonium source, the resulting NO_3^- will have different (or overlapping) $\delta^{15}N$ values. A summary of $\delta^{15}N$-NO_3^- ranges, depending on the NH_4^+ substrate used in the nitrification process, is given in Figure 1-3. Note that whereas nitrification is a naturally occurring NO_3^- production process, the NH_4^+ substrate can originate from either natural or anthropogenic sources.

During the nitrification process, three oxygen isotopes are associated to the N-NH_4^+ atom, two of which are supposed to come from soil-water and one from atmospheric O_2 ($\delta^{18}O$ = 23.88 ‰, Barkan and Luz, 2005). Therefore, theoretical $\delta^{18}O$ values of nitrate produced by nitrification can be calculated as:

$\delta^{18}O\text{-}NO_3^- = 1/3\ (\delta^{18}O\text{-}O_2) + 2/3\ (\delta^{18}O\text{-}H_2O)$ (Eq. 1.4)

This calculation assumes a number of hypotheses (e.g., no fractionation resulting from the incorporation of these O atoms) that are extensively discussed elsewhere (Kendall et al., 2007; Rose et al., 2015b; Snider et al., 2010). $\delta^{18}O\text{-}NO_3^-$ from nitrification are generally in the range of -15 to 15 ‰, with most studies reporting positive values (Kendall et al., 2007; Snider et al., 2010).

The other "natural" source of nitrate, ***atmospheric deposition***, will be further discussed in section 1.1.4. Range for $\delta^{15}N$ of atmospheric nitrate is -15 to 15 ‰, and 60 to 90 ‰ for $\delta^{18}O$ (Durka et al., 1994; Kendall et al., 2007). Seasonal variations in $\delta^{15}N$ and $\delta^{18}O$ of NO_3^- have been measured, reflecting the contribution of several sources ($\delta^{15}N$) and production pathways in the atmosphere ($\delta^{18}O$) at different periods of the year (Elliott et al., 2007; Freyer, 1991; Savarino et al., 2007, 2013).

Nitrate can also be produced artificially for ***fertilization*** purpose by the Haber-Bosch process, which consists in fixing atmospheric N_2 into ammonia (NH_3), followed by its oxidation to NO_3^- using atmospheric O_2. Consequently, the isotopic composition of thus produced NO_3^- is similar to air (*i.e.*, $\delta^{15}N = 0 \pm 5$ ‰ (Mariotti, 1984) and $\delta^{18}O = 23.88$ ‰ (Barkan and Luz, 2005).

There are three main removal pathways, or sinks, of NO_3^- in terrestrial systems. NO_3^- ***uptake*** and ***assimilation*** by plants and microbes refer to the transport of external NO_3^- into organism cells and subsequent transformation to organic forms during biosynthesis, respectively. While different fractionation factors for $N\text{-}NO_3^-$ isotopes have been reported during uptake (Denk et al., 2017), there are generally considered negligible (Karsh et al., 2014; André Mariotti et al., 1982). A large range of N fractionations (-30 to 0 ‰) has also been measured for NO_3^- assimilation in field and laboratory experiments (Denk et al., 2017; Kendall et al., 2007). Interestingly, assimilation was shown to cause coupled $\delta^{15}N$ and $\delta^{18}O$ changes along a 1:1 line in residual NO_3^-, highlighting the utility of a dual isotope approach to decipher biological processes in the environment (Granger et al., 2004, 2010a; Karsh et al., 2012; Treibergs and Granger, 2017).

Denitrification refers to the dissimilatory reduction of NO_3^- into gaseous compounds, (nitric oxide (NO), nitrous oxide (N_2O) and eventually N_2) and occurs only in anaerobic conditions, which are predominant in saturated soils and riparian sediments usually found in wetlands (Clément et al., 2002; Sebilo et al., 2003, 2006). The first steps of this reducing process are often limiting, yielding strong N and O fractionations (-40 to -5 ‰). Similarly to assimilation, $\delta^{15}N$ and $\delta^{18}O$ of residual nitrate covariate along lines with slopes ranging from 0.4 to 1.0 during denitrification (Clément et al., 2003b; Granger et al., 2008; Kendall et al., 2007; Wexler et al., 2014).

NO_3^- can also be removed by ***leaching*** from soils through hydrological flow paths, a processed not yielding any isotopic fractionation (Semaoune et al., 2012).

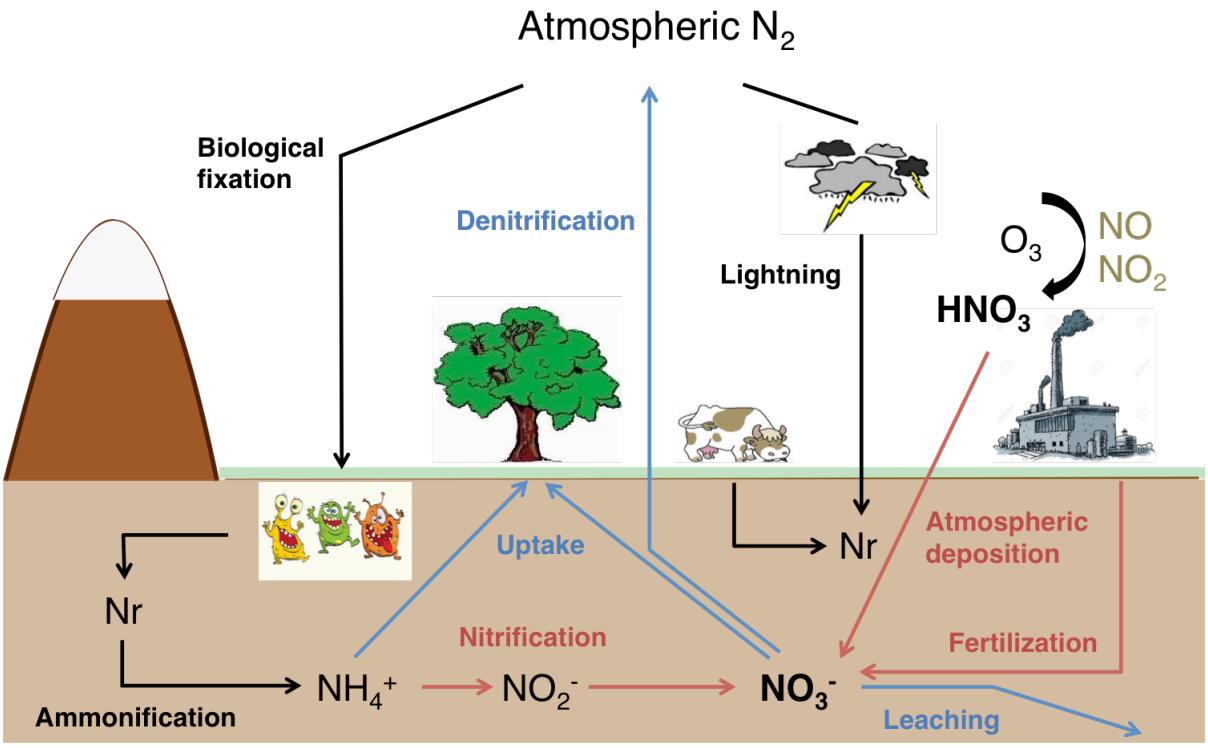

Figure 1-2: A very simplified representation of the processes, sources (in red) and sinks (in blue) involved in the terrestrial N cycle, featuring NO_3^- as the nerve center.

Sources and processes affecting NO_3^- in terrestrial ecosystems can be plotted in a dual isotope plot featuring $\delta^{15}N$ and $\delta^{18}O$ on the x and y-axes, respectively (Figure 1-3). It is customary to report measured $\delta^{15}N$ and $\delta^{18}O$ values on such plot to determine *where NO_3^- comes from*, and *which processes it undergoes* in a studied system.

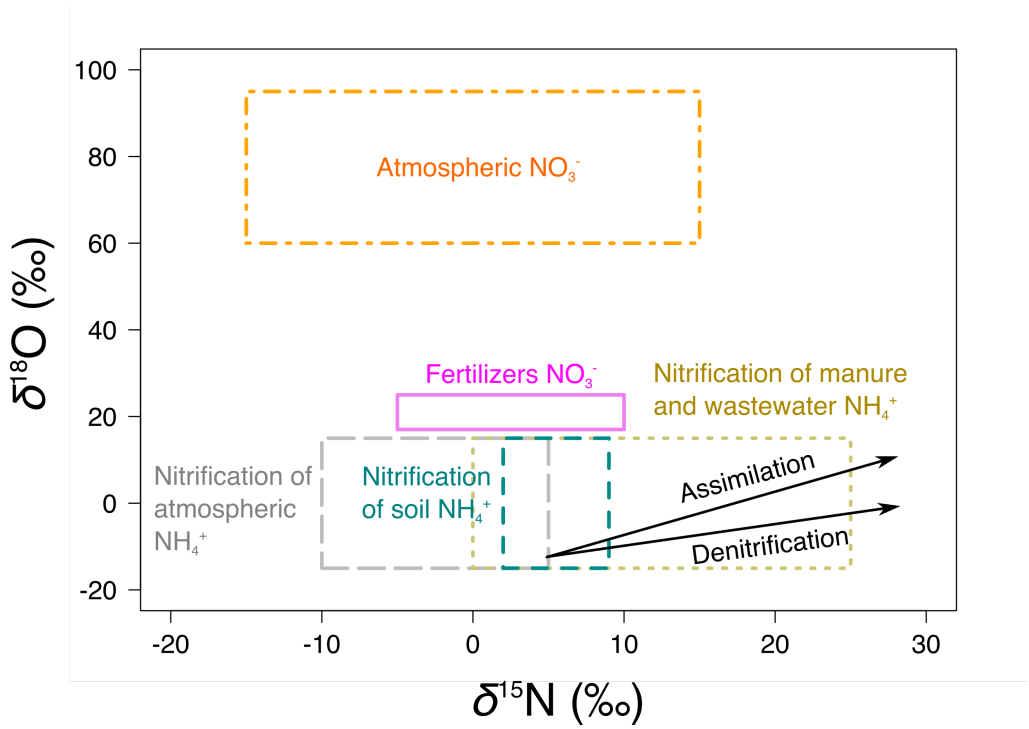

Figure 1-3: A dual isotope plot showing the typical range of $\delta^{18}O$ and $\delta^{15}N$ of NO_3^- derived or nitrified from various sources. Colored boxes denote potential sources of NO_3^-. The black lines indicate the expected slope for data resulting from denitrification (slope = 0.5) and assimilation (slope = 1). After Kendall et al. (2007).

Other dissimilatory reduction processes, such as the dissimilatory reduction of NO_3^- to ammonium (DNRA), have been scarcely investigated for their fractionation factors. However, necessary environmental conditions for these processes to occur (*i.e.*, strong reducing conditions with high sulfide concentrations) are seldom met, and therefore they will not be further discussed here (Thamdrup and Dalsgaard, 2002; Trimmer and Nicholls, 2009). Biological N fixation, mineralization and volatilization isotopic effects are not discussed here as well because these processes only affect soil N_{org} and NH_4^+ pools, with no direct impact on the isotopic composition of nitrate. Note that anammox and commamox processes, which can potentially impact nitrate pool evolution over time, will not discussed here as they are assumed not to be predominant. More details on N terrestrial cycling can be found in the Chapter 6 of Sutton (2011).

1.1.4 Focus on atmospheric deposition of NO_3^-

NO_3^- is produced in the atmosphere by several mechanisms, all implying the oxidation of nitrogen dioxide (NO_2) by reactive atmospheric species (e.g., O_3, OH, NO_3, halogens) to varying extents. NO_2, along with NO, play a major role in atmospheric chemistry, especially because of their intertwined relationship with O_3 (and peroxyl radicals) in a diurnal cycle (Crutzen, 1970; Leighton, 1961). In an attempt of clarity, all forms of NO_3^- in the atmosphere (*i.e.*, gaseous nitric acid (HNO_3) and particulate nitrate (p-NO_3) in the dry fraction, dissolved NO_3^- in precipitation) will be referred to under the shared denomination of "atmospheric nitrate" or "$NO_3^-{}_{atm}$" in this manuscript. The constant interaction between NO_x species (NO_2 and NO) and O_3 is of particular relevance regarding the isotopic composition of $NO_3^-{}_{atm}$. Indeed, measurements of O isotopic enrichment in the main terrestrial reservoirs of O-bearing species showed the following first order relationship:

$$\delta^{17}O \approx 0.52 * \delta^{18}O \qquad \text{(Eq. 1.5)}$$

This relationship translates the doubled fractionation effects on $\delta^{18}O$ relative to $\delta^{17}O$ during the production and transformation of these species, due to a mass difference between ^{18}O and ^{16}O twice superior to the mass difference between ^{17}O and ^{16}O. Such isotopic fractionations are called "mass-dependent".

The laboratory discovery of a significant deviation of ozone isotopes from this mass-dependent terrestrial fractionation line (TFL) has opened the gate to a whole new world of isotopic investigation (Thiemens and Heidenreich, 1983). ^{17}O and ^{18}O enrichment during O_3 production in the atmosphere leads to a deviation from the proportionality law described in (Eq. 1.5Eq. 1.5), and is called "mass-independent" fractionation (MIF). This deviation from the TFL, illustrated in Figure 1-4, is called "^{17}O excess" and noted as $\Delta^{17}O$, of which its linear expression is written as:

$$\Delta^{17}O = \delta^{17}O - 0.52 * \delta^{18}O \qquad \text{(Eq. 1.6)}$$

Note that this formulation of $\Delta^{17}O$ is the one that will be used in the remainder of this manuscript, and that an extensive review of all mathematical expressions of the ^{17}O excess and their significance can be found elsewhere (Bao et al., 2016; Coplen, 2011). Additionally, an IUPAC project led by Jan Kaiser will soon provide an update in terminology and suitable definitions to use in multiple stable isotope systems. Also, an explanation on the cause of this mass-independent fractionation of oxygen isotopes in O_3 in the first place can be found in Gao and Marcus (2001); Hathorn and Marcus (2000) and Janssen and Marcus (2001).

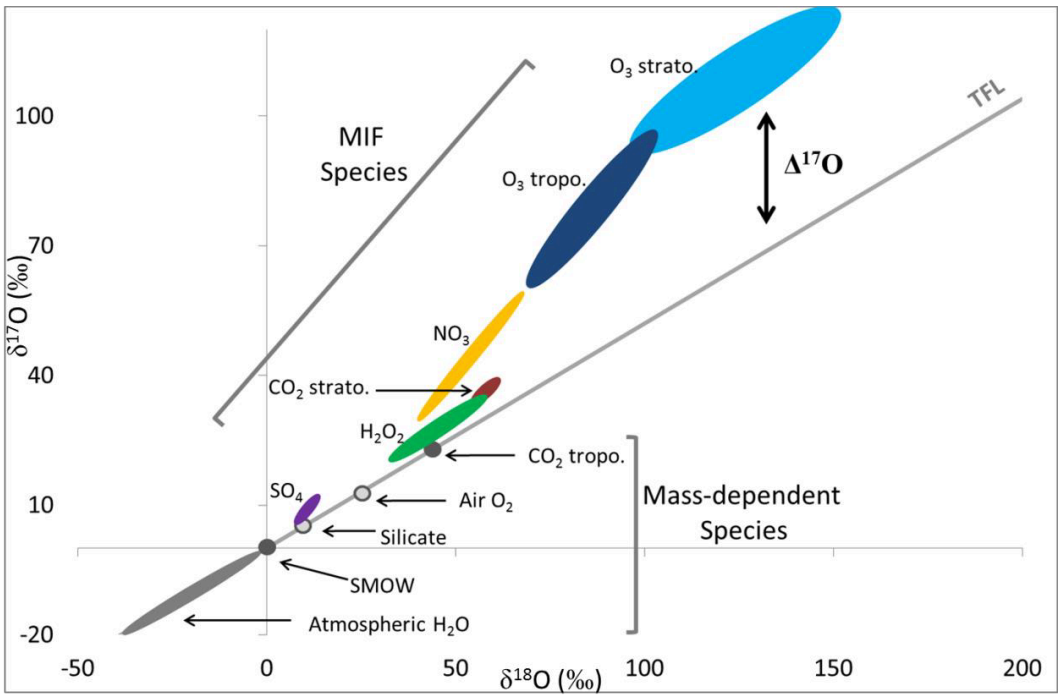

Figure 1-4: Oxygen isotopic compositions of atmospheric species as measured to date of publication (Thiemens, 2006). TFL represents the oxygen terrestrial fractionation line based on mass dependent fractionation ($\delta^{17}O = 0.52 * \delta^{18}O$). MIF (mass independent fractionation) species are atmospheric derived compounds that are equally enriched in ^{17}O and ^{18}O. The deviation of MIF species from the TLF is denoted $\Delta^{17}O$ ($\Delta^{17}O \approx \delta^{17}O - 0.52 * \delta^{18}O$). After Riha, (2014). SMOW stands for Standard Mean Ocean Water.

As ozone interacts with NO_x at almost every step of the nitrate making process (Figure 1-5), this ^{17}O excess is transferred to the final product of the Leighton cycle (*i.e.*, NO_3^-). Briefly, the high reactivity of NO_2 and NO in the troposphere drives a fast succession of photo-dissociation reactions of NO_2 to NO and oxidation of NO to NO_2 by O_3 (Savarino et al., 2008). Therefore, NO_2 oxygen composition results principally

from O_3, and the ^{17}O excess in transferred accordingly (Morin et al., 2007). In reality, other oxidants (e.g., peroxyl radicals) dilute this transfer of mass-independent fractionation signature by contributing O atoms with $\Delta^{17}O$ values of 0 into the Leighton cycle. Depending on the oxidation pathway of the terminal step of the Leighton cycle (*i.e.*, NO_2 ➔ HNO_3), the produced NO_3^- is either further enriched in ^{17}O excess (nighttime oxidation by O_3) or diluted (e.g., during daytime oxidation by OH radical) (Morin et al., 2011). $\Delta^{17}O$ of $NO_3^-{}_{atm}$ is, like for most atmospheric reservoirs that involve O_3 in their production mechanisms (e.g., SO_4^{2-}, ClO_4^-), representative of the oxidation pathways leading to its formation (Alexander et al., 2009), and has enabled major breakthrough in understanding the oxidative capacity of Earth atmosphere (Morin et al., 2008; Savarino et al., 2013; Thiemens, 2006).

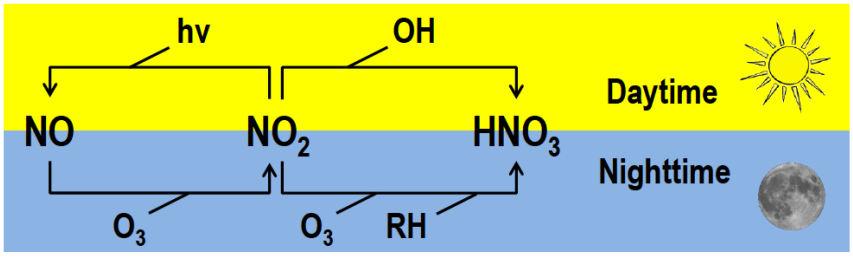

Figure 1-5: Simplified representation of the Leighton cycle leading to the production of $NO_3^-{}_{atm}$. After Erbland (2011).

In biogeochemical studies, $\Delta^{17}O$ is usually not used as a proxy of the oxidative pathways leading to $NO_3^-{}_{atm}$ formation, but rather as a tracer of atmospheric inputs of NO_3^- in a given system. Because of its mathematical expression (Eq. 1.6), $\Delta^{17}O$ is not affected by mass-dependent fractionation processes and is conserved in terrestrial reservoirs upon deposition, until $NO_3^-{}_{atm}$ is completely biologically recycled (*i.e.*, until the original O mass-independent isotopic signature is lost). Indeed, when $NO_3^-{}_{atm}$ undergoes a full assimilation - mineralization - nitrification cycle, the oxygen atoms forming the new NO_3^- will derive from air O_2 and soil H_2O as described in (Eq. 1.4), losing its initial ^{17}O-excess. Biologically produced NO_3^- and anthropogenic fertilizers have $\Delta^{17}O$ values of 0 (with the notable exception of the atmospheric originated Chilean saltpeter (Michalski et al., 2004a)), **making $\Delta^{17}O$ a unique tool to quantify the direct contribution of unprocessed $NO_3^-{}_{atm}$ to an ecosystem** (Michalski et al., 2004b, 2015) (Figure 1-6). $\Delta^{17}O$ is a conservative tracer of $NO_3^-{}_{atm}$

inputs, and **enables the study of N deposition in ecosystems without perturbing them** (e.g., unlike ^{15}N pool dilution experiments, which often involve unrealistic doses of N in a very short timeframe that potentially bias the results). However, $\Delta^{17}O$ is not panacea by itself and its utilization yields powerful insights on N cycling sources and processes especially when coupled to the classical dual isotope approach (*i.e.*, $\delta^{15}N$ and $\delta^{18}O$) presented in section 1.1.3. This **multi-isotopic method** will be at the heart of the scientific interests tackled in this thesis manuscript.

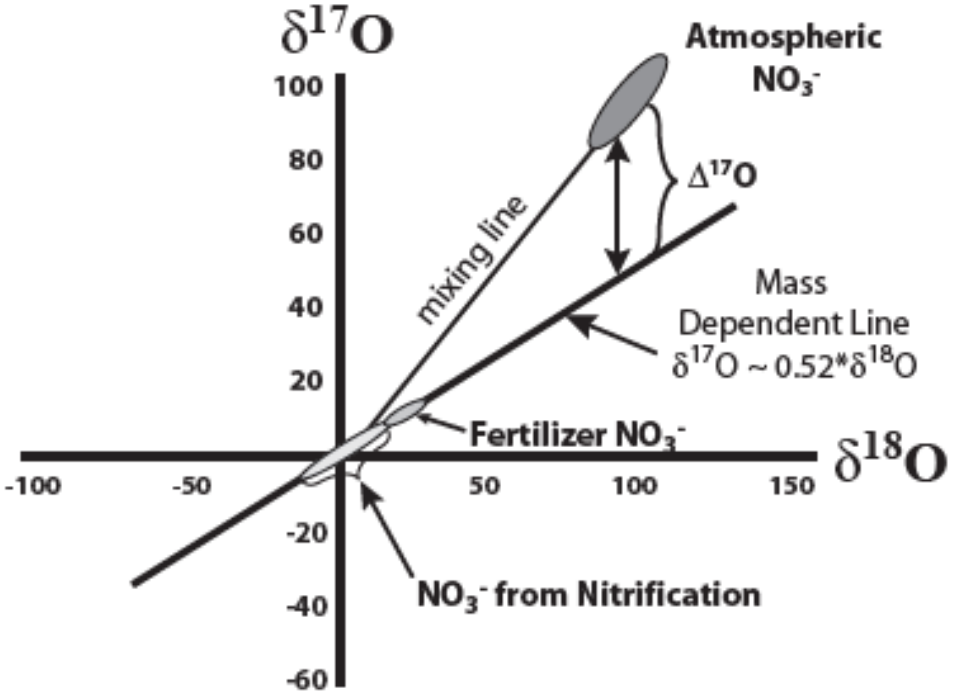

Figure 1-6: Oxygen isotopic compositions of NO_3^- species as measured to date of publication. The mass dependent line represents the oxygen terrestrial fractionation line ($\delta^{17}O = 0.52 * \delta^{18}O$). $NO_{3\ atm}^-$ deviates from the TFL because of equal enrichment in ^{17}O and ^{18}O. The deviation from the TFL is denoted $\Delta^{17}O$ ($\Delta^{17}O \approx \delta^{17}O - 0.52 * \delta^{18}O$). Biologically produced NO_3^- and anthropogenic NO_3^- fertilizers have $\Delta^{17}O$ values of 0 (*i.e.*, no deviation from the TFL). After Michalski et al. (2002).

Three main processes produce the quasi-totality of NO_x of which $NO_{3\ atm}^-$ is derived from in the troposphere: **fixation** of N_2, **oxidation** of N_{org} during combustion and **emission** during the various processes of the N cycling. **Fixation of N_2** encompasses the natural (lightning) and anthropogenic (e.g., fossil fuel combustion in vehicle engines, industrial energy production) processes occurring at temperature > 1500 °C, leading to the production of "thermal" NO_x (Young, 2002). **Oxidation of N_{org} during combustion** refers to the oxidation of N contained in any fuel during

combustion at lower temperatures than the formation threshold for "thermal" NO_x. Coal burning and biomass fires are principally responsible for the making of these "fuel" NO_x. Finally, **N cycling in soils** leads to emissions of NO as a byproduct of processes conducted by microorganisms on Earth surface (e.g., nitrification, denitrification, etc.).

According to United States (US) emissions inventories surveying the past few years, *ca* 90 % of NO_x emitted in the country are due to anthropogenic activities (https://www.epa.gov/air-emissions-inventories/air-pollutant-emissions-trends-data). Globally, fossil-fuel combustion is the main contributor to NO_x emissions (58 %), followed by soils (22 %), and biomass burning (14 %), the rest being mostly produced by lightning (Fowler et al., 2015). Even more preoccupying, NO_x (and NH_x, *i.e.* NH_3 and NH_4^+) emissions are projected to be 17 times higher in 2050 compared to the pre-industrial era (Galloway et al., 2008). Because of the long-range transport of $NO_3^-{}_{atm}$ on continents and oceans (Galloway et al., 2003), atmospheric deposition is a major source of nutrients to remote ecosystems in pristine environments (Holtgrieve et al., 2011). High altitude watersheds in the mountains are iconic of remote ecosystems being increasingly affected by atmospheric deposition of N, as discussed in section 1.2.

1.2 Mountains, sentinels of change

This title was chosen in reference to the Belmont Forum call for proposal, as it perfectly illustrates how sensitive a mountain ecosystem can be to global change. There is a lot of information to be inferred from the changes observed in altitude (> 1500 m a.s.l.) catchments, a forewarning message of the transformations to be expected in the future in more resilient systems.

1.2.1 Alpine and subalpine environments are sensitive to N deposition

Alpine and subalpine environments are especially vulnerable to increasing inputs of Nr *via* atmospheric deposition. In the European Alps, an ice-core record showed 5-folds higher Nr deposition nowadays compared to estimated pre-industrial levels (Preunkert, 2003), although N deposition rates are on the decline in the Alps (Rogora et al., 2006). The N sensitivity of terrestrial ecosystems is logically a function of atmospheric deposition rates of Nr and the strength of Nr sinks (*i.e.*, plants, soils and microorganisms). Harsh bioclimatic conditions have led mountainous soils to be nutrients poor, and N is often the primary limiting factor of plants before phosphorus (P) (Körner, 2003). Nitrogen cycling in alpine and subalpine systems is slow (Robson et al., 2007, 2010), because of temperature limited mineralization rates (Miller et al., 2007), high retention of inorganic N in soils organic matter and substantial competition between plants and microbes for N resource during the growing season (Legay et al., 2013; Robson et al., 2010). These criteria make herbaceous-dominated grasslands, typical of these systems, very likely candidates to ecological changes under increasing Nr deposition rates (Bowman et al., 2006).

The notion of "**critical load**" have been introduced by scientists and policy makers in an attempt to determine the minimum input of a pollutant leading to a significant change of an ecological indicator (e.g., nitrogen saturation status), and is increasingly used to set pollution standards worldwide (Bobbink et al., 2011). Among grasslands and tall forbs habitats, alpine and subalpine grasslands are the most sensitive to N deposition, with a critical load for these ecosystems estimated to 1 - 4 kg-N ha^{-1} yr^{-1} (Baron et al., 2011; Bobbink et al., 2011; Bowman et al., 2006; Nanus

et al., 2017). Changes in species composition, or acidification of surface freshwaters are early ecological indicators of N deposition detrimental effects, and often used as metrics to measure and evaluate ecosystems response to increased Nr supply and the saturation stage (Baron et al., 2011; Bowman et al., 2006; Chapin et al., 1997). The **nitrogen saturation** concept has first been introduced to qualify an ecosystem where Nr inputs (e.g., atmospheric deposition) outbalance the biological demand, leading to losses of unused N generally through leaching (Aber et al., 1989). This approach has been revisited in a conceptual model where the rate of Nr inputs exceeds the rate of Nr assimilation in an ecosystem and its remediation capacity (Lovett and Goodale, 2011), certainly more adequate to describe N status in alpine and subalpine watersheds where multiple drivers control the N budget (Barnes and Raymond, 2010; Burns, 2003; Rose et al., 2015b).

It would not be possible to discuss Nr deposition in mountains without mentioning the considerable amount of research that has been conducted in the Rocky Mountains in the US. There, probably the most comprehensive study of atmospheric N inputs ecological consequences in alpine ecosystems has been conducted over the last two decades, and is still on-going, providing an unique insight on both short-term and long-term changes in all compartments of mountains (Figure 1-7). Over the past twenty years, patterns in atmospheric N deposition were evaluated, showing that dry deposition can contribute up to 10-30% of the total N inputs in alpine catchments (Burns, 2003; Mladenov et al., 2012) and that deposited Nr often originates from distant sources after long-range transport (Wasiuta et al., 2015a, 2015b). Stream chemistry was shown to respond to variations in N deposition rates (Mast et al., 2014), to the point of episodic acidification and NO_3^- leakage in the Green Lakes Valley of the Colorado Front Range (Williams and Tonnessen, 2000). Changes in plants functional traits, soil mineralization rates and soil microbial communities were also documented (Baron et al., 2005; Nemergut et al., 2008), and increased uptake of Nr by vegetation had locally led to a 10 % turnover of its biodiversity at the species level (McDonnell et al., 2014). Most noticeable impacts were observed in lakes where acidification and eutrophication driven by N atmospheric deposition induced significant changes in phytoplankton nutrient

limitation, diatoms species composition and amphibians populations (Baron et al., 2011; Burns, 2004; Elser et al., 2009; Wolfe et al., 2003). Evidently, ecological changes cited above are not specific to the Rocky Mountains, and similar impacts have been widely monitored elsewhere (Bassin et al., 2013, 2015; Boutin et al., 2017; Clément et al., 2012; Gill, 2014; Hobbs et al., 2016; Nanus et al., 2017). Nitrogen deposition is considered as the second main driver of alpine ecosystem changes behind climate change (Sala et al., 2000).

Another particular feature of alpine and subalpine catchment relative to N deposition resides in the seasonal snow-cover, which aggregates a fraction of winter atmospheric N deposits (Campbell et al., 2007; Williams et al., 2009). In high altitude catchments, about half of the year's N deposits are estimated to be retained in the snowpack (Hiltbrunner et al., 2005) and released at spring during **snowmelt**, when plant demands is high (Bilbrough et al., 2000). Release of snowpack nitrate as an ionic pulse, which magnifies its concentration, is considered as a "hot moment" in these ecosystems, and deemed responsible for episodic acidification of alpine and subalpine streams (Lepori et al., 2003; Williams et al., 2009; Williams and Tonnessen, 2000). Other studies also demonstrated that part of this ionic pulse at snowmelt could results from the flushing of soil inorganic N reservoirs by melt water (Campbell et al., 2002; Kendall et al., 1995). The importance of hydrology in linking atmospheric N deposition with terrestrial reservoirs has clearly been delineated in these ecosystems (Balestrini et al., 2013; Rose et al., 2015b).

Seasonal snow-cover is also an important control of N availability in alpine and subalpine soils. Thinner snowpack was shown to promote higher N-related microbial activity in subalpine meadows (Jusselme et al., 2016), consistent with previous findings showing that snow depth and timing controlled soil heterotrophic activity during winter (Brooks et al., 1999; Brooks and Williams, 1999). A shift of microbial communities at snowmelt (Lipson et al., 2002) was deemed responsible for the release of immobilized inorganic N in soils at the beginning of the growing season (Schmidt and Lipson, 2004).

Finally, N-related changes in altitude catchments are likely to have social and economic impacts because of indirect ecological feedbacks on human population, by analogy with coastal and estuarine environments (Dodds et al., 2009), and low altitude terrestrial systems (Clark et al., 2017). Therefore, preservation of high-altitude habitats is a growing necessity in terms of biodiversity conservation, erosion control and water quality insurance, and will be a major challenge to address in the upcoming years.

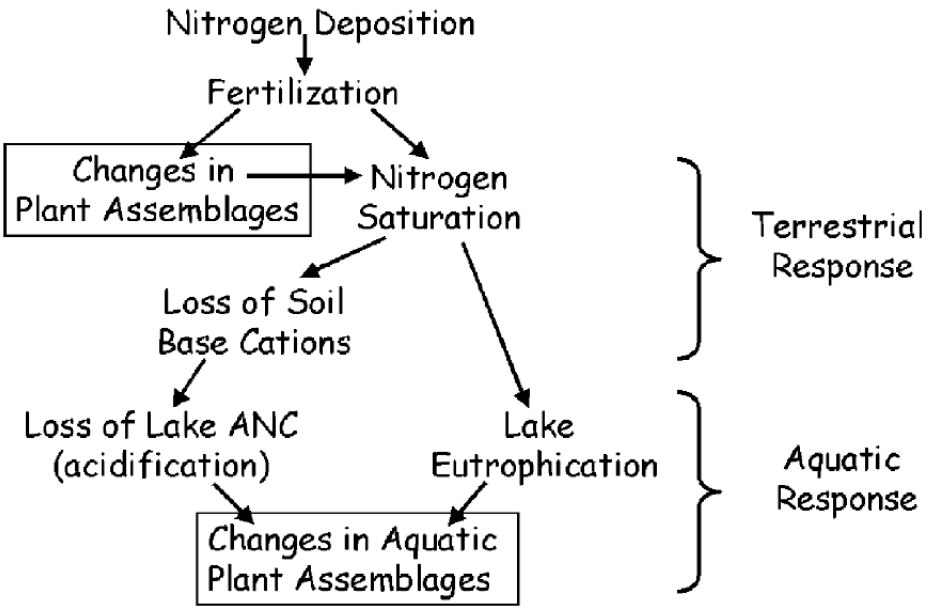

Figure 1-7: A simplified version of the nitrogen cascade, illustrating the effects of nitrogen deposition on terrestrial and aquatic ecosystems. ANC stands for Acid Neutralization Capacity. After Baron et al. (2005).

1.2.2 Subalpine meadows at the Lautaret pass

Most of the work presented in this manuscript was undertaken in the Romanche Valley, between the village of Villar d'Arènes (1650-m a.s.l.) and the Lautaret pass (2058-m a.s.l.), in the French Alps (45°02'N, 6°20'E). This experimental site will be cited as the "Lautaret pass" in the rest of this manuscript.

The Lautaret pass stands about one hour and a half drive away from Grenoble (205-m a.s.l.) and has been the University of Grenoble-Alpes (UGA) outpost for ecological research in mountains for more than 30 years (Figure 1-8). The site is equipped with scientific infrastructure (e.g., laboratories, experimental platforms) and sleeping

facilities, favoring the good achievement of on-site research projects. As part of the Long Term Ecological Research (LTER) network, this site is managed by the Station Alpine Joseph Fourier (SAJF). The SAJF is a logistical unit from UGA and CNRS dedicated, among other tasks, to support science at the Lautaret pass (Figure 1-9).

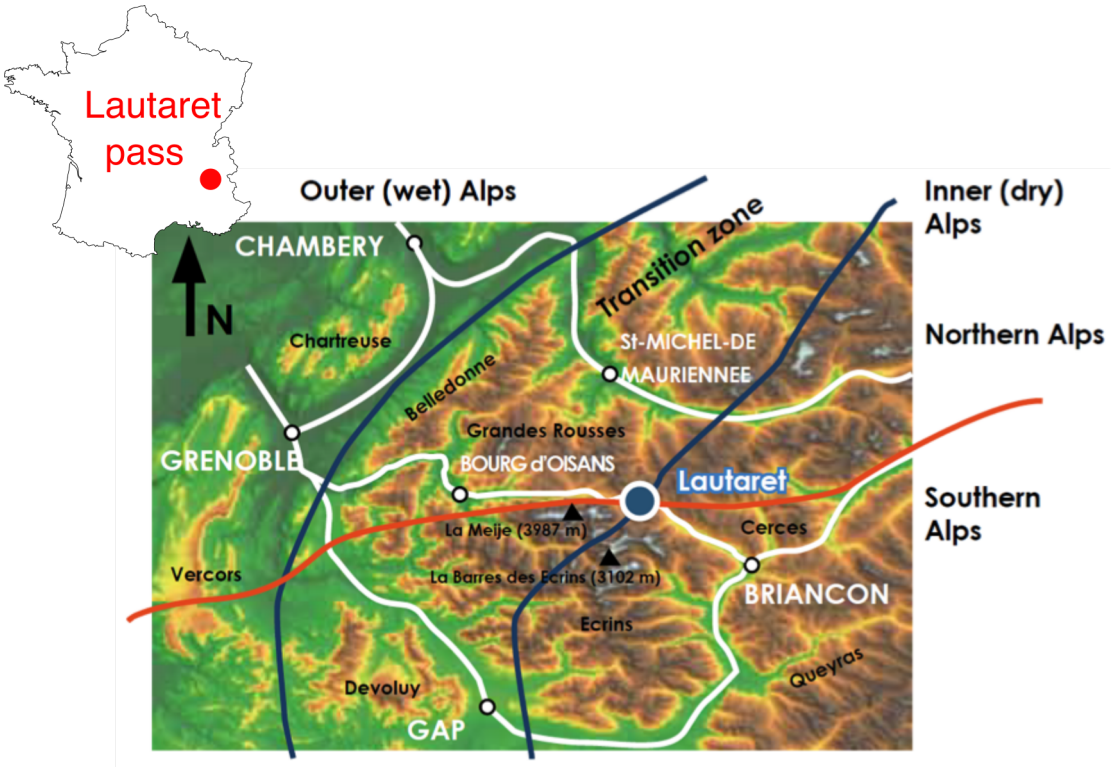

Figure 1-8: Geographical location of the Lautaret pass. The black lines delineate a shift in climatic characteristics, and the red line the boundary between Southern and Northern Alps. Modified from Baptist (2007).

As explained above, the Lautaret pass has been the siege of a large number of studies, in which the meteorological, hydrotopographic and biogeomorphic properties of the site have been extensively described (Baptist, 2007; Grassein, 2009; Legay et al., 2013; Quétier, 2006). In an effort of brevity and clarity, only relevant information to the comprehension of the rest of the manuscript will be presented here.

The meteorological conditions at the Lautaret pass are typical of the subalpine zone and dominated by a strong continental influence. Mean monthly temperatures range from -7°C in February to +16°C in July (Legay, 2013; Quétier, 2006). Marked temperature differences between winter and summer generally come with an uneven

temporal distribution of precipitation, featuring a mostly arid period in summer and wet conditions in winter, with an annual mean of 960 mm (Quétier, 2006). The snow-cover in winter can be as high as 3-m in accumulation zones, and is permanent from November to April (south-facing slope) or May (north-facing slope), considerably limiting the vegetation growth period from May (or June) to September (Robson et al., 2010). **The Lautaret Pass received an estimated 6-8 kg-N ha^{-1} yr^{-1} in 2015, of which *ca* 4 kg-N as HNO_3** (GEOS-Chem v11-01, GEOS-FP, resolution: 2x2.5; Angot, *personal communication*).

Figure 1-9: Panoramic view on the Lautaret pass, taken from the road to the Galibier pass.

The subalpine meadows found at the Lautaret pass are not representative of the climactic cover by *Pinus cembra* that should be prevalent at this altitude (Ozenda, 1985). Subalpine regions are an ecotone between the lower dense coniferous forests and the higher permanent alpine grasslands (Körner, 2003). Therefore, it should not be surprising to find scattered tree groves in these regions. The absence of forests at the Lautaret pass illustrates human influence, and more specifically the **past agro-pastoral practices** which roots spread back to the Middle-Age, that have modified both the topography and the vegetation cover of this valley. The soils have been intensively managed to produce the necessary fodder to sustain cattle during the long winter months, but the intensification of agriculture in plains has progressively led to the decline of mountainous agricultural practices over the past 50 years (Girel et al., 2010). **Current land-management** varies from plot to plot, where the most extensive practice consists in mowing and manuring activities in spring and summer and the less extensive practice is the simple cessation of activity except for occasional grazing (Quétier et al., 2007). As a consequence, subalpine meadows at

the Lautaret pass show a vegetal functional diversity that differs depending on their past land-use – which shaped the actual topography of these meadows (*i.e.*, terraced or unterraced, Figure 1-10) – and their actual agricultural trajectory – the past and current practices (e.g., mowing, manuring, grazing) – (Quétier et al., 2007).

The conjunction of climatic and anthropic factors has thus favored the setting of specific vegetal communities, making these subalpine meadows among the most diversified ecosystems, in terms of plant species, in Europe (Quétier, 2006). Herbaceous species are dominated by graminoïds, among which *Poaceae* is the most abundant family (Figure 1-10). Mown and fertilized terraces are mostly covered by fast maturing species showing exploitative traits associated to high resource uptake strategies (*i.e.*, ***Dactylis glomerata***). When not fertilized, mown terraced meadows vegetation shifts to an increased presence of intermediary (in terms of speed) growing species such as *Bromus erectus*, but *Dactylis glomerata* remains a co-dominating species. Finally, abandoned grasslands are highly dominated by ***Festuca paniculata*** (> 70 % of communities biomass), mainly because of no interest to cattle and because it releases allelopathic compounds in soils that chemically inhibit the development of other species (Binet et al., 2013; Quétier et al., 2007; Viard-Crétat et al., 2012), thus slowing N cycling rates and decreasing specific diversity.

Figure 1-10: The left panel shows typical terraced meadows, an inherited topography from past agricultural practices. The right panel illustrates the rich biodiversity of high patrimonial value subalpine grasslands. © S. Aubert.

It has been shown that changes in agricultural practices, and cessation of ancestral activities such as mowing induce important changes in plants and microorganisms' communities and in the ecosystem services they provide. Impairment of ecosystem services such as the loss of patrimonial species, decrease of water and fodder quality and N retention capacity in soils have thus been described at the Lautaret pass (Lavorel et al., 2011) (Figure 1-11). **However, how these changing land-uses relate to increasing N deposition has only scarcely been studied, and the potential synergetic effect on soils N cycling is still to be assessed.**

Figure 1-11: Illustration of ecosystem services loss caused by N deposition. The left panel shows signs of advanced eutrophication – evidenced by algal bloom – in a subalpine stream of the Lautaret pass in July 2016. Shift of biodiversity can also lead to erosion control issues, occasioning landslides as it happened close to the Chambon lake (right panel, © www.lemedia05.com).

1.2.3 Positioning of this study in the current state ok knowledge

Subalpine meadows are vulnerable to N deposition because of their oligotrophic and acidic properties, and susceptible to ecological changes. Compared to higher alpine regions where human presence is rare, and to lower forested or agricultural catchments, they have received little scientific attention regarding the ecological effects of atmospheric nitrogen inputs despite being a critical zone in terms of ecosystem services. Even more, subalpine meadows illustrate the transition between mostly human-influenced (lowlands) and almost totally natural systems (uplands), which make them a unique territory to understand how biota meets N deposition in semi-natural conditions. Whereas the understanding of the ecological **impacts** of enhanced atmospheric N deposition in subalpine meadows have been

the object of extensive studies in the French Pyrenees (Boutin, 2015), this work aims at providing insights on the **dynamics** and **processes** leading to such monitored impacts. With focus on NO_3^-, which harmfulness potential is widely recognized (see section 1.1), we intended to investigate the **fate** and the partitioning of atmospheric deposits in and between the different compartments that constitute the subalpine ecosystem.

The utilization of $\Delta^{17}O\text{-}NO_3^-$, initially an atmospheric chemistry tracer of oxidative pathways in the troposphere (see section 1.1), in terrestrial environment studies is scarce (less than 15 published scientific papers), mainly because of the difficulties to measure $\delta^{17}O$ with high accuracy and because of the relative novelty of its discovery. Among the few studies that have used the NO_3^- triple isotope tracer ($\Delta^{17}O$, $\delta^{18}O$ and $\delta^{15}N$), most focused on forested catchments (Costa et al., 2011; Rose et al., 2015a; Sabo et al., 2016; Tsunogai et al., 2014), groundwater or surface water reservoirs (Dietzel et al., 2014; T. Liu et al., 2013; Saccon et al., 2013; Tsunogai et al., 2011, 2016) or semi-arid natural or urban systems (Dejwakh et al., 2012; Michalski et al., 2004b; Riha et al., 2014; Wang et al., 2016), and only two on alpine surface waters (Darrouzet-Nardi et al., 2012; Hundey et al., 2016). This work aims at increasing this growing body of literature, and at further pushing the limits of $\Delta^{17}O$ utilization by applying it to a new ecosystem, and to new environmental matrices.

1.3 Objectives, structure and overview

To avoid – as much as possible – redundancy with the *Methods* sections of the four scientific papers that consist the core of this manuscript, an overview of the field and analytical techniques used during the 3 years of this Ph.D. thesis will be given in Appendix A – Methods. Readers are invited to peruse this section as considerable amount of time was spent collecting and analyzing samples during this doctoral work.

1.3.1 Scientific questions and manuscript structure

The importance of studying nitrate deposition in subalpine systems has been extensively discussed in section 1.2, and the ecological vulnerability of these systems highly motivated this project. Another title to this manuscript could have been "***What becomes of atmospheric nitrate in a subalpine watershed after being deposited?***" which sums up pretty well what this doctoral work has been about these past three years. In a nutshell, this works aims at **tracing** and **quantifying** $NO_3^-_{atm}$ in the various compartments that constitute the subalpine ecosystem, and will try to specifically answer the following questions:

Chapter 2 What is the isotopic composition of $NO_3^-_{atm}$ deposited at the Lautaret pass? Is it exported in streams, and what are the drivers controlling the seasonal variations of these exports? Does snowmelt release $NO_3^-_{atm}$ as an ionic pulse? What are the other sources of NO_3^- in streams, and how does it translate in terms of saturation? Are the controls of $NO_3^-_{atm}$ exports the same along a montane to urban gradient?

These questions will be addressed through two scientific articles. The first article, in review for *Environmental Science & Technology*, treats the deposition and the seasonal dynamics of $NO_3^-_{atm}$ exports at the subalpine stage only. It focuses on the biological and hydrological drivers of seasonal variability in $NO_3^-_{atm}$ exports. The second article tackles the dynamics of $NO_3^-_{atm}$ in streams along a montane to urban

gradient and the ecological implication for both subalpine and urban environments. This article is in review for *Science of the Total Environment*.

Chapter 3 How much $NO_3^-_{atm}$ is retained in soils? How does $NO_3^-_{atm}$ / $NO_3^-_{ter}$ ratio vary in time, and what does it mean in terms of N cycling rates and processes? Are these variations the same in meadows that differ by their past and current land uses? What does it mean in a context of changing agro-pastoral practices at the Lautaret pass?

This is still on-going work, and results obtained so far are presented under the form of a scientific article to comply with the general format of this Ph.D. manuscript. Here, I focus on three subalpine meadows with different management treatments, and I evaluate the ecological ramification of the variability in NO_3^- isotopic composition ($\Delta^{17}O$, $\delta^{18}O$ and $\delta^{15}N$) in soil extracts and leachates. I also aim at constraining what are the dominant biological processes at play in soils.

Chapter 4 How much $NO_3^-_{atm}$ is absorbed by subalpine plant species? Is there enough NO_3^- in plant tissues to perform isotopic analyses? How can we adapt existing extraction protocols to perform $\Delta^{17}O$-NO_3^- analysis in plants? What do we learn from such measurements in terms of plant metabolism rates? What are the ecological ramifications of the measured levels of $NO_3^-_{atm}$ in plants?

These questions will be addressed under the form a scientific article that is in review for the *Proceedings of the National Academy of Sciences*. I present the isotopic composition of NO_3^- ($\Delta^{17}O$, $\delta^{18}O$ and $\delta^{15}N$) in the organs of two dominant subalpine plant species, and segregate the respective contribution of root and foliar uptake to plant NO_3^- contents. A conceptual framework provided in Figure 1-12 sums up all scientific interests that will be addressed in this Ph.D. manuscript.

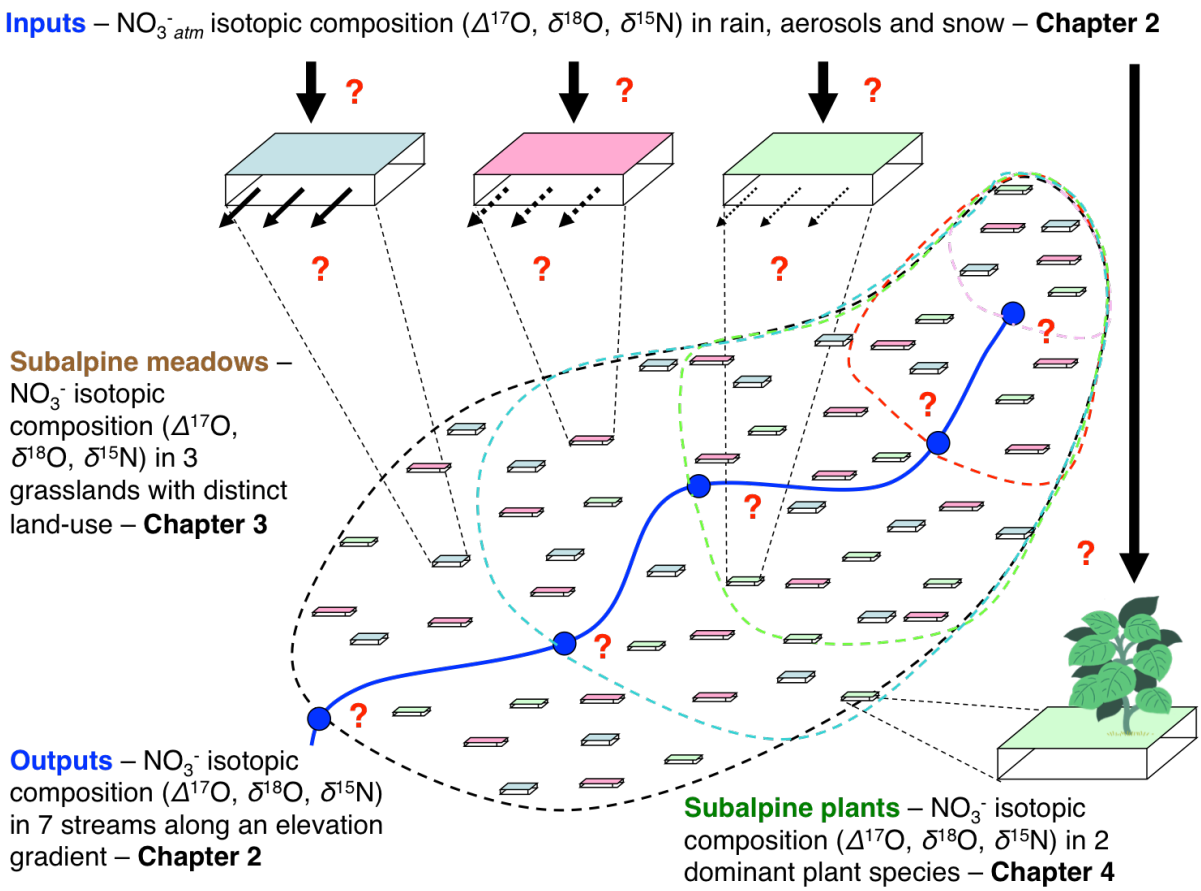

Figure 1-12: Conceptual framework and general structure of this study. The dotted lines delineate watersheds with increasing size (and altitude range). Blue points and line are for streams. Colored boxes illustrate the variety of subalpine meadows management regimes at the Lautaret pass. The red question marks translate the scientific questions addressed in this study.

1.3.2 Main scientific achievements

The main scientific findings that will be presented in this doctoral work can be summarized in five highlights as follows:

- Deposited atmospheric nitrate and ammonium both contribute to the N balance of a subalpine watershed, especially at snowmelt.
- Year-round presence of atmospheric nitrate in streams suggests that atmospheric inputs exceed the remediation capacity of subalpine freshwaters.
- Biotic and abiotic processes that depend on the land-management regimes and the basins characteristics drive atmospheric nitrate turnover in subalpine soils.
- The $\Delta^{17}O$ tracer can be used to monitor vegetation assimilation pathways and to infer plants uptake strategies.

- The $\Delta^{17}O$ tracer, when coupled to $\delta^{18}O$ and $\delta^{15}N$ of nitrate, helps not only to trace $NO_3^-_{atm}$ fate, but also to better understand N cycling processes in all spheres of the environment.

1.3.3 An overview of this doctoral work in two figures

The sampling strategy during this Ph.D. consisted in spending one day per week at the Lautaret pass, and this for more than two years. In Figure 1-13, the readers are provided with an overview of the study site and its geographical range, as well as the sampling locations. This monitoring led to a total of **1377 samples analyzed** for NO_3^- isotopes ($\Delta^{17}O$, $\delta^{18}O$ and $\delta^{15}N$), major ions (NH_4^+, SO_4^{2-}, Cl^-, Ca^{2+}) and other parameters, and a few dozen still waiting in the cold room at the Institute of Geosciences for Environment (IGE). Table 1-1 sums up the main field experiments and laboratory analyzes conducted to achieve the scientific objectives of this study.

Figure 1-13: Representation of the study area. The upper map represents the Romanche Valley in the central French Alps, situated 90 km away from the city of Grenoble. The boundaries of the different studied watersheds are delimited in yellow. In orange is the position of the SAJF research facilities and location for snow, aerosols and rain sampling. The lower map illustrate Grenoble conurbation. Streams are shown in blue, and in red are the sampling locations. The green / brown dots indicate the meadows where soils and plants were collected. Maps were extracted from www.geoportail.fr.

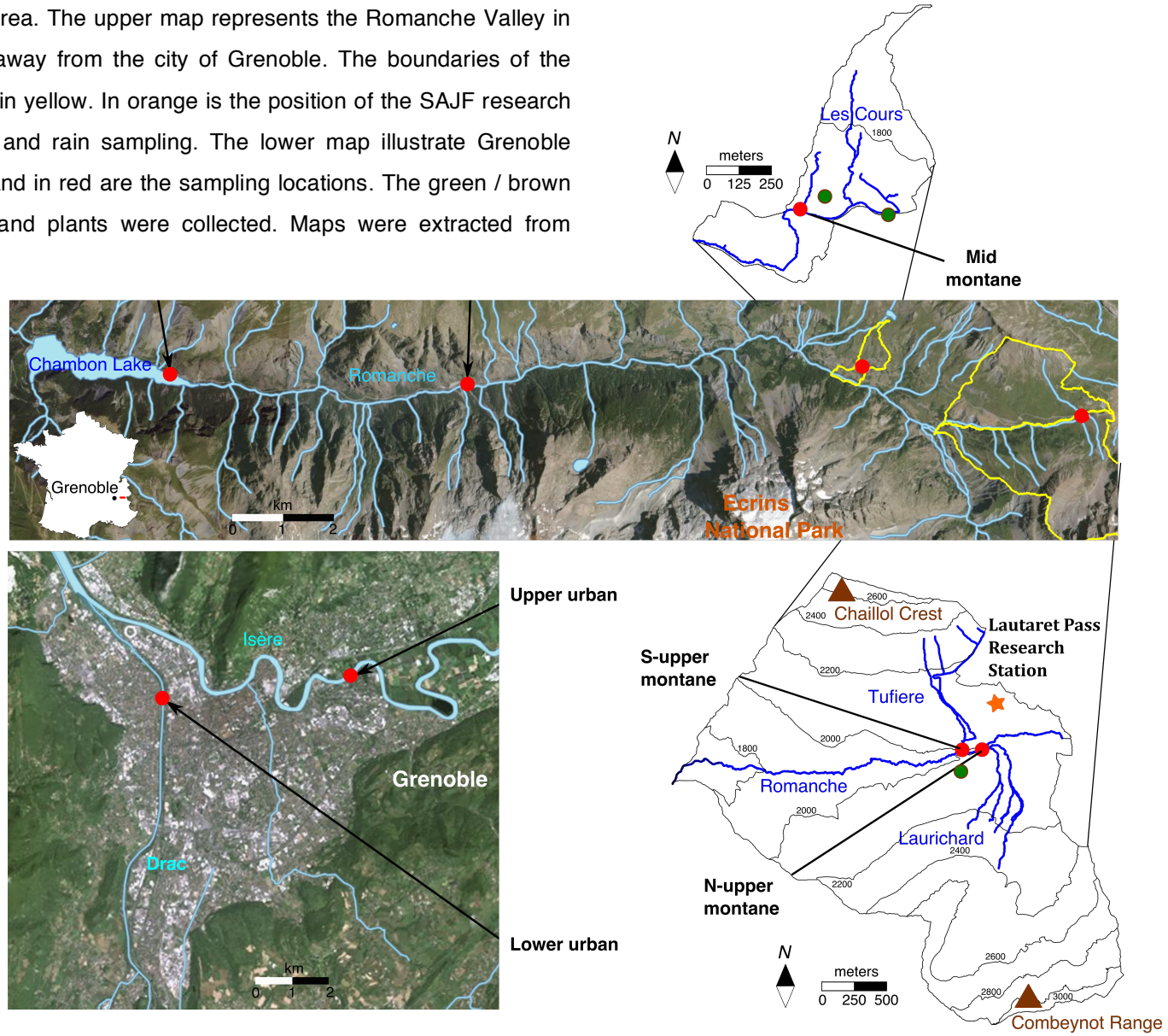

Table 1-1: Summary of the main field experiments, laboratory analyses and where to find the data.

	Aerosols	**Wet & Dry deposition**	**Snow**	**Streams**	**Soils**	**Plants**
Aspect	Filters	Rain Rinsed dust in MQ water	Snow Pits (2015) Bulk snow (2016)	River water	Leachates Extracts	Roots Leaves + stems
Year collected	2015 ($PM_{2.5}$) 2016 (PM_{10})	2016	2015 2016	2015 2016	2015 (experimental) 2016 (growing season only)	2016 (growing season only)
Sampling frequency	1 / week	1/ 2 weeks	1 / month (pit) 1 / week (bulk snow)	1 / week (per stream)	3 / month (per meadow)	3 / month (per meadow)
Type of analysis	$\Delta^{17}O$, $\delta^{18}O$, $\delta^{15}N$, $[NO_3^-]$, $[NH_4^+]$, $[SO_4^{2-}]$, $[Ca^{2+}]$, $[Cl^-]$	$\Delta^{17}O$, $\delta^{18}O$, $\delta^{15}N$, $[NO_3^-]$, $[NH_4^+]$, $[SO_4^{2-}]$, $[Ca^{2+}]$, $[Cl^-]$	$\Delta^{17}O$, $\delta^{18}O$, $\delta^{15}N$, $[NO_3^-]$, $[NH_4^+]$, $[SO_4^{2-}]$, $[Ca^{2+}]$, $[Cl^-]$	$\Delta^{17}O$, $\delta^{18}O$, $\delta^{15}N$, $[NO_3^-]$, $[NH_4^+]$, $[SO_4^{2-}]$, $[Ca^{2+}]$, $[Cl^-]$, H_2O isotopes	$\Delta^{17}O$, $\delta^{18}O$, $\delta^{15}N$, $[NO_3^-]$, $[NH_4^+]$, TDN, TON, OM, bulk density, microbial N	$\Delta^{17}O$, $\delta^{18}O$, $\delta^{15}N$, $[NO_3^-]$, $[NH_4^+]$
Number of samples	65	31	164	566	231	320
Corresponding chapter	Chapter 2, Appendix 3	Chapters 2, 3 and 4	Chapter 2	Chapter 2	Chapter 3	Chapter 4

2 Atmospheric nitrate in streams: seasonal dynamics, spatial variations and controlling factors

This chapter describes the breakthroughs in our understanding of what drives $NO_3^-_{atm}$ exports in subalpine streams, and if these exports are varying before reaching downstream populated areas. A particular focus is given on the snowmelt period to evaluate its role in transferring accumulated $NO_3^-_{atm}$ in the snowpack to the surrounding environment. The section 2.1 describes the seasonal variations of $NO_3^-_{atm}$ exports in three subalpine streams over one year and offers an explanation to these variations based on hydrological and topographical considerations. The section 2.2 depicts the spatial heterogeneity of $NO_3^-_{atm}$ exports in seven freshwater reservoirs along an altitude gradient, and gives insights on the different drivers that explain such pattern. A summary of the scientific conclusions is provided in section 2.3, and the main findings will be put in perspective with the terrestrial N cycle in subalpine meadows.

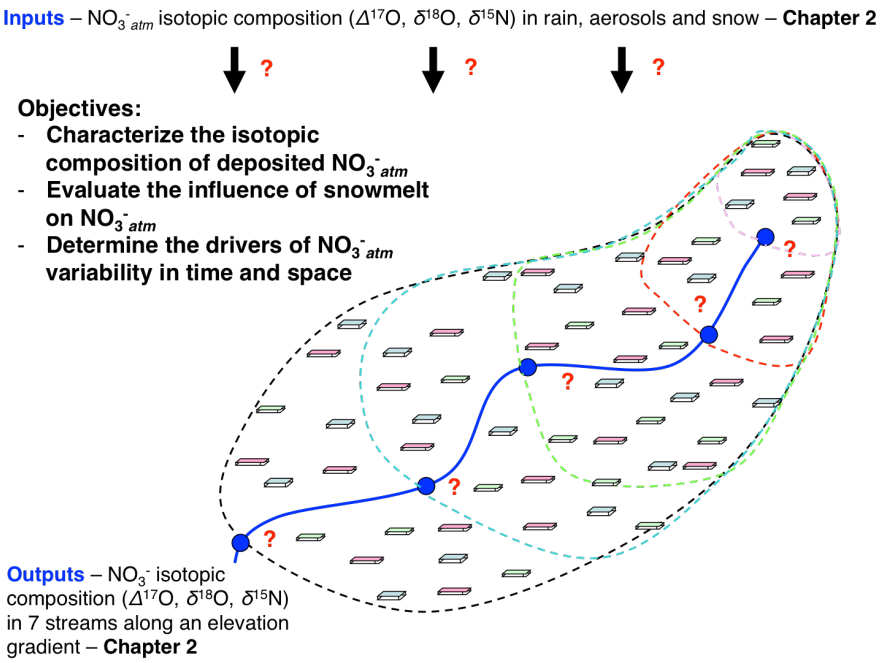

Figure 2-1: Positioning of this chapter in the conceptual framework of this study, and related objectives it will answer to.

2.1 Ins and outs of atmospheric nitrate at the Lautaret pass

After:

Bourgeois, I. ; Savarino, J. ; Caillon, N. ; Angot, H. ; Barbero, A. ; Delbart, F. ; Voisin, D. and Clément, J.-C.: Tracing the fate of atmospheric nitrate in a subalpine watershed using $\Delta^{17}O$, in review for *Environmental Science & Technology*.

Abstract

Nitrogen is an essential nutrient for life on Earth, but in excess, it can lead to environmental issues. Understanding the nitrogen budget (*i.e.*, inputs and outputs) is essential to evaluate the prospective decay of the ecosystem services that subalpine headwater catchments provide, especially as these ecosystems experience increased anthropogenic nitrogen deposition. Here, we use a multi-isotopic tracer ($\Delta^{17}O$, $\delta^{15}N$ and $\delta^{18}O$) of nitrate in aerosols, snow and streams to assess the fate of atmospherically deposited nitrate in the subalpine watershed of the Lautaret pass (French Alps). We show that atmospheric deposition contributes significantly to stream nitrate pool year-round, either by direct inputs (up to 35 %) or by *in situ* nitrification of atmospheric ammonium (up to 35 %). Snowmelt in particular leads to high exports of anthropogenic nitrate, most likely fast enough to impede assimilation by surrounding ecosystems. Yet, in a context of climate change, with shorter snow seasons, and increasing nitrogen emissions, our results hint at possibly stronger ecological consequences of nitrogen atmospheric deposition in the close future.

2.1.1 Introduction

Reactive Nitrogen (Nr) has long been known for its duality. At low to moderate concentrations, it is an essential nutrient for natural ecosystems in general, and plant nutrition in particular (Epstein and Bloom, 2016). In excess, Nr becomes an environmental issue for endemic terrestrial plant species and aquatic ecosystems (Aber et al., 1989; Galloway et al., 2003; Vitousek et al., 1997), and may pose threats to human health (Ward et al., 2005). Human activities have increased N inputs to the environment by 150% over the last century (Galloway et al., 2004), with a rising contribution – among other distribution processes – of atmospheric deposition

(Galloway et al., 2008; Matson et al., 2002). Fossil-fuel combustion, agriculture and food production are responsible for direct or indirect emissions of atmospheric N-species with the capacity to reach remote ecosystems such as mountainous regions (Baron et al., 2005; Preunkert, 2003) where Nr equilibrium is very sensitive to small perturbations (Baron et al., 2000; Kirchner et al., 2014). Alpine and subalpine watersheds are particularly vulnerable to this increasing Nr-supply (Burns, 2004; Clark et al., 2013), as they are usually N-limited ecosystems (Kaye and Hart, 1997). The critical load for these ecosystems has been estimated to 1-4 kg-N ha^{-1} yr^{-1}, making alpine and subalpine grasslands the most sensitive to N deposition among grasslands and tall forb habitats (Baron et al., 2011; Bobbink et al., 2011; Nanus et al., 2017). In some regions of the globe, such as in the Colorado Front Range, USA, shifts from N-limitation to N-saturation state have been observed leading to regional and national policies to regulate this phenomenon (Baron, 2006; Williams and Tonnessen, 2000; Wolfe et al., 2003). As a consequence of increasing N deposition, a slow but persistent change of alpine and subalpine landscape has been noticed in several regions (Bassin et al., 2013; McDonnell et al., 2014). Species more competitive for nitrogen uptake tend to develop in abundance at the expense of usually oligotrophic native plants, leading to plant diversity loss and changes in ecosystem functioning and services. Freshwater quality and erosion control are, per instance, threatened by this cascade of changes (Bowman et al., 2006; Chapin et al., 1997). Yet, and mainly because of the paucity of monitoring facilities in isolated areas and of the logistical difficulties in accessing these regions, key biogeochemical processes regulating N cycling in mountains are still not well understood (Mast et al., 2014).

More specifically, atmospheric nitrate (NO_3^-) and ammonium (NH_4^+), deriving principally from anthropogenic NO_x (NO and NO_2) and agricultural NH_3 emissions, are transferred to the land surface through wet and dry deposition. Dissolved inorganic nitrogen (DIN) species (*i.e.*, NO_3^- and NH_4^+) are of capital importance in ecological studies given their high solubility in water; the strong hydrological connectivity and typical topography of alpine and subalpine watersheds can lead to a fast transport and a potentially long reach of the above-mentioned nutrients in

surrounding ecosystems (Campbell et al., 1995; Clow and Sueker, 2000). Traditionally, environmental studies on NO_3^- sources partitioning are essentially based on $\delta^{15}N$ and $\delta^{18}O\text{-}NO_3^-$ values (Kendall et al., 1995; Mayer et al., 2002; Ohte et al., 2008), to constrain the biogeochemical processes affecting the various N forms in mountains. Yet, the wide range of observed values for $\delta^{15}N$ and $\delta^{18}O\text{-}NO_3^-$ from atmospheric and other sources limits accurate quantification of contributing sources (T. Liu et al., 2013; Michalski et al., 2004b).

In this study we focus – for the first time (to the best of our knowledge) – on year-round NO_3^- dynamics in a mountainous watershed in the French Alps, using a multi-isotopic ($\Delta^{17}O$, $\delta^{18}O$, $\delta^{15}N$) tracer of NO_3^- in subalpine surface waters. This relatively new method has been increasingly used, as it enables a more refined understanding of atmospheric NO_3^- ($NO_3^-_{atm}$) contribution to ecosystems N pool (Michalski et al., 2004b; Rose et al., 2015a; Tsunogai et al., 2016). With the aim to clearly delineate the fate of atmospheric Nr in a subalpine watershed, we first characterized the triple isotopic composition of NO_3^- in aerosols and snow deposited in high altitude catchments (> 1500m a.s.l.) of the central French Alps (*i.e.*, the input flux). Second, we evaluated the fate of the deposited $NO_3^-_{atm}$ by monitoring NO_3^- riverine exports from the watersheds (*i.e.*, the output flux).

We hypothesized that (i) the triple isotopes approach will enable a clear delineation of NO_3^- sources and the quantification of their respective contribution to small and medium-scale watersheds N budget and (ii) seasonal dynamics of $NO_3^-_{atm}$ exports in stream will provide additional insights on N cycling controls in high altitude catchments.

2.1.2 Material and methods

2.1.2.1 Study site

The studied catchments are located in the upper Romanche valley, near the Lautaret pass (central French Alps, Figure 2-2). The experimental site is part of the national research infrastructure for the study of continental ecosystems and their biodiversity (AnaEE – France, https://www.anaee-france.fr), and of the Long Term Ecological Research network (LTER, https://lternet.edu). The streams monitored

throughout 2015 are located close to the research facilities of the Alpine Research Station (Station Alpine Joseph Fourier (SAJF), CNRS-UGA, UMS 3370, https://www.jardinalpindulautaret.fr), where atmospheric and climatic parameters were monitored (Figure 2-3).

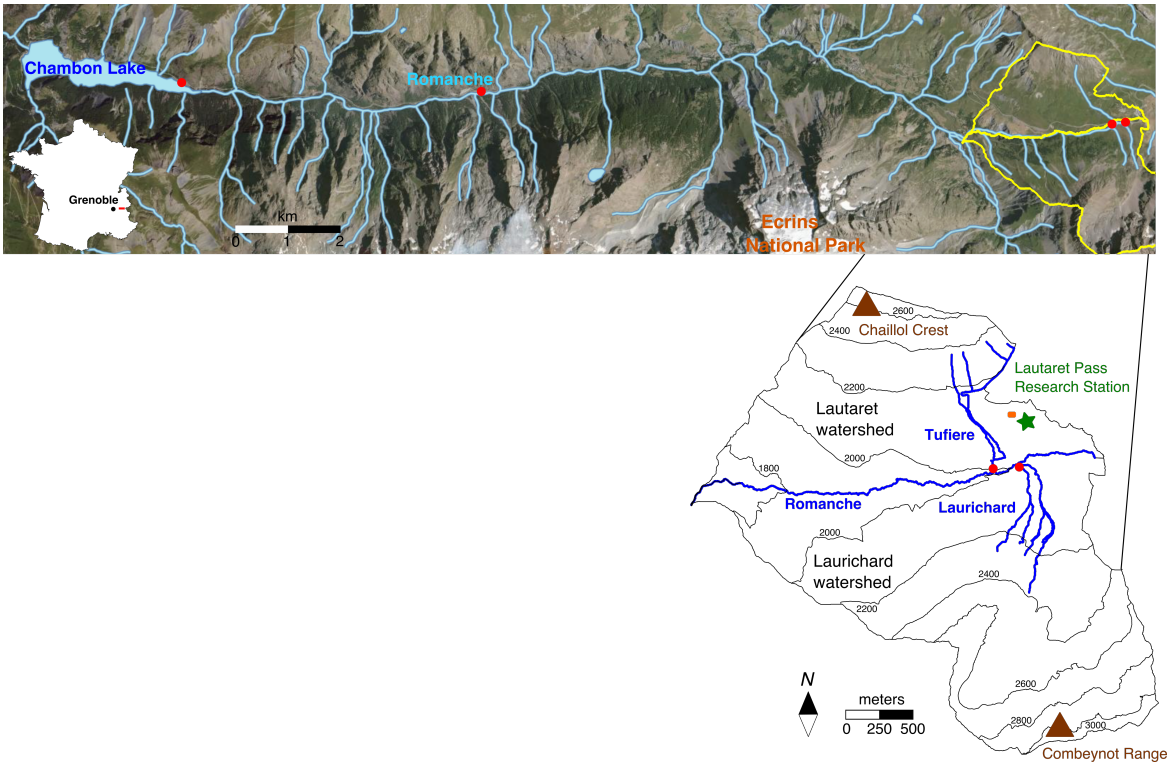

Figure 2-2: Map of the Lautaret pass study area. The upper map represents the Romanche Valley in the central French Alps, situated 90 km away from the city of Grenoble (~ 163 000 inhabitants). The boundaries of Lautaret and Laurichard watersheds are delimited in yellow. Streams are shown in blue. Streams and snow sampling localizations are indicated in red and orange, respectively.

The climate is subalpine with a strong continental influence. The annual precipitation in 2015 (year of study) was 537 mm, significantly drier than the mean annual precipitation of 956 mm observed between 2004 and 2013 (Legay et al., 2013). In 2015, *ca* 45 % of the precipitation occurred during the growing season from snowmelt (in April) to late September. Winters are cold and snowy. The mean temperature was -7.5 °C in February 2015 and 13.9 °C in July 2015. More detailed information about the sampling site can be found elsewhere (Clément et al., 2012; Legay et al., 2013).

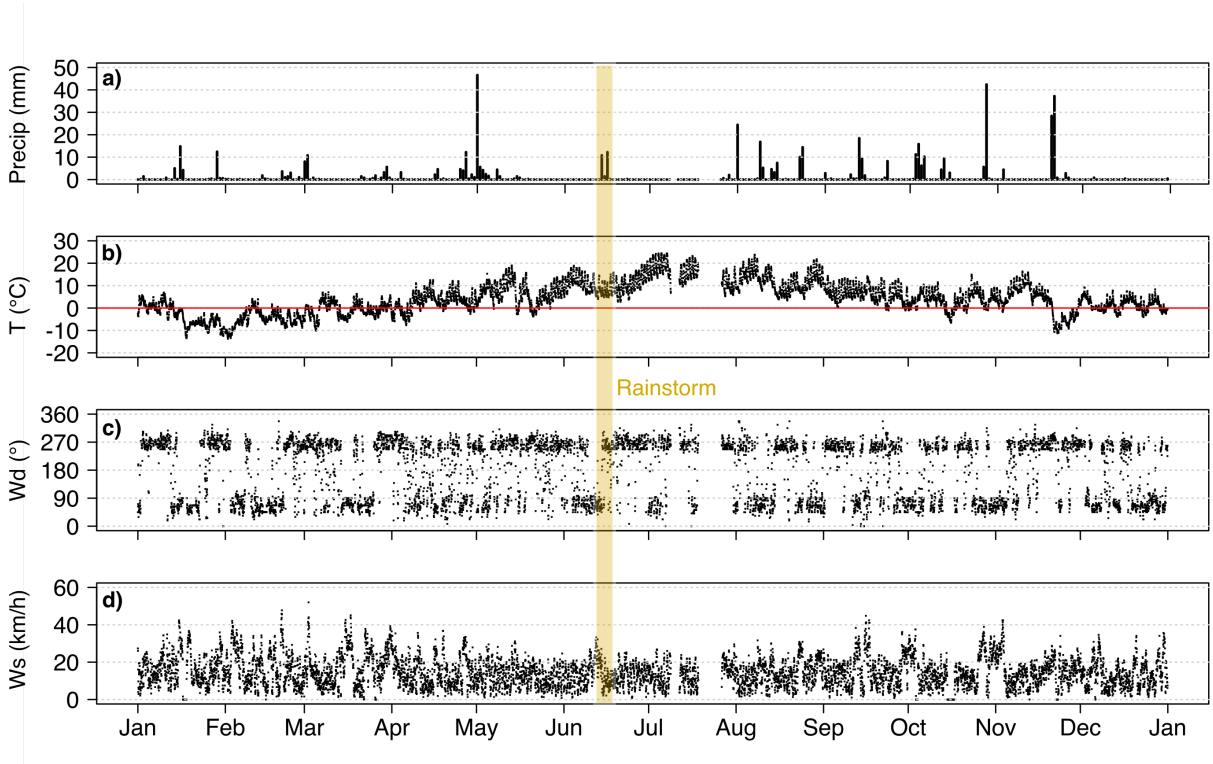

Figure 2-3: Meteorological conditions at the Lautaret pass in 2015 with a) precipitation amount (mm) summed daily; b) temperature (*T* in °C); c) wind direction (Wd in °, 0° being North) and d) wind speed (Ws in $km.h^{-1}$). The annual precipitation amount was 560 mm and the mean annual temperature was 3.8°C.Highlighted in yellow is a two-days rainstorm that occurred mid-June.

The first studied sub-watershed (hereafter called Lautaret) is mainly constituted of calcareous substrate and extends over 3.4 km². At the outlet of this sub-watershed runs a stream called Tufiere. Samples were collected at an altitude of *c.* 2015 m a.s.l, just before the stream merges with the outlet of the second sampled watershed (Figure 2-2). Altitude on this watershed spans from 1665 to 2725 m a.s.l. Mean slope is 25%, and the vegetation cover Normalized Difference Vegetation Index (NDVI) is 0.38.

The second sub-watershed (hereafter called Laurichard) is constituted of granitic rocks on an ancient volcanic layer and extends over 5.3 km². It is part of the North exposed side of the Combeynot mountain range, which highest peak culminates at 3155 m. The Laurichard stream, fed in part by glacier melt, runs down this mountainous area and is sampled downhill, just before it joins the Tufiere stream. Altitude on this watershed ranges from 1665 to 3155 m a.s.l. Mean slope is 30%, and the vegetation cover NDVI is 0.33.

The last river is Romanche, which integrates the response of the whole Romanche Valley, and is fueled by smaller tributaries such as Tufiere and Laurichard from the Lautaret pass and the Ecrins National Park down to the artificial Chambon Lake. Our sampling point for this river is about 1000 m lower in altitude and approximately 12 km away from the first two tributaries (contributing area ≈ 220-km²).

2.1.2.2 Field sampling

Aerosols were collected on the Lautaret watershed from November 2014 to September 2015 using a homemade apparatus (similar to a Digitel® DA77) equipped with a Digitel® $PM_{2.5}$ cutting head. We used QMA Whatman quartz filters for aerosols collect, burnt at 800 °C for 1 h to lower the blank signal (Jaffrezo et al., 2005). Filters were changed on a weekly basis, thus accumulating enough material for isotopic analysis. Airflow was fixed at 0.5 m^3 per minute.

From December 2014 to April 2015 a snow pit (SP) was dug every month on the Lautaret watershed to provide profiles of $NO_3^-{}_{atm}$ concentration and isotopic values in the snowpack. For each pit, snow was dug until the soil was reached, then after cleaning the vertical profile, samples were collected every 3 cm starting from surface snow.

Water samples were collected in the three streams (Figure 2-2, in red) from November 2014 to December 2015 to obtain a full one-year hydrological cycle and stream N chemistry. The samples were taken according to the Niwot Ridge LTER protocol (Williams and Melack, 1991). Samples were taken on a weekly basis when possible, and at most 2 weeks separated two consecutive samples.

More details regarding aerosols, snow and water sampling can be found in the section 2.1.5. Unfortunately, neither rivers discharge measurements nor wet deposition collect could be done at the time of the study because of lacking equipment. Appreciation of snowmelt timeframe, peak and length was based on visual observation of snow cover and rivers flow. The Laurichard stream could not be sampled from mid-January to mid-April as the riverbed was completely covered by the snowpack.

2.1.2.3 Samples pre-treatment and NO_3^- concentration analysis

Aerosols samples were analyzed by extracting NO_3^- from filters, immersed in 40-mL of ultrapure water in a centrifugal ultrafiltration unit (Milipore Centricon plus-70, 100 000 Daltons), shaken a few times, and then centrifuged at 4500-RPM for 20 minutes. The extract was then collected in a 50-mL Corning® centrifuge tube and kept frozen until further analysis.

Water and snow samples underwent the same pre-treatment for isotopic analysis. Frozen samples were melted at room temperature overnight before being filtered using 0.45-µm Whatman GD/X syringe filters linked to a peristaltic pump. Ultimately, aerosols, snow and stream samples were concentrated using an anionic resin (0.6-mL AG 1-X8 resin, Cl^--form, Bio-Rad) with recovery efficiency over 98.5% and eluted with 10 mL of a 1-M NaCl solution for isotopic analysis (Templer and Weathers, 2011). Sample aliquots were taken before the resin concentration step for $[NO_3^-]$ determination using a Continuous Flow Analysis spectrophotometer (SEAL Analyzer QuAAtro) based on cadmium-reduction of NO_3^- to nitrite (Wood et al., 1967). $[NO_3^-]$ values are given with an uncertainty of 0.02 mg L^{-1}, calculated as the mean standard deviation of ten successive measurements of the calibrating standards.

2.1.2.4 Isotopic analysis

Aerosols, snow and river samples were analyzed for $\Delta^{17}O$, $\delta^{18}O$ and $\delta^{15}N$ of NO_3^- using the bacterial denitrifier technique in combination with the N_2O gold decomposition method (Casciotti et al., 2002; Kaiser et al., 2007; Morin et al., 2008). More details about the analytical procedure can be found elsewhere (Morin et al., 2009) and in the section 2.1.5.

All samples isotopic values were corrected for any isotopic effect possibly occurring during the procedure by processing simultaneously international reference materials (International Atomic Energy Agency USGS 32, USGS 34 and USGS 35) through the same analytical batch. The isotopic standards were prepared in the same background matrix as samples (*i.e.*, 1-M NaCl). Standard deviation of the residuals from the linear regression between the measured reference standards (n=20) and their expected values served as indicator of the accuracy of the method. In our study,

the $\Delta^{17}O$, $\delta^{18}O$ and $\delta^{15}N$ values of aerosols, snow and streams NO_3^- are given, with respect to atmospheric N_2 (AIR) and Vienna Standard Mean Ocean Water (VSMOW) standards, with a mean uncertainty of 0.2, 1.4 and 0.4 ‰ respectively.

2.1.2.5 End-member mixing analysis

The triple stable isotope approach using $^{18}O/^{16}O$ and $^{17}O/^{16}O$ enables exclusive quantification of unprocessed $NO_3^-_{atm}$. Because chemical pathways leading to the production of atmospheric NO_3^- involve NO_x oxidation by ozone, which is the bearer of ^{17}O-excess in the first place, it shows a significant positive deviation from the terrestrial fractionation line (TFL: $\delta^{17}O \approx 0.52 * \delta^{18}O$) (Kaiser, 2011; Thiemens, 2006). $\Delta^{17}O$ is a quantification of this deviation from the TFL, calculated as $\Delta^{17}O = \delta^{17}O - 0.52 * \delta^{18}O$ in the present work. $\Delta^{17}O$ value of atmospheric NO_3^- generally ranges between 20 and 35 ‰ in temperate latitudes (Morin et al., 2009; Savarino et al., 2007) whereas $\Delta^{17}O$ value of NO_3^- from all other sources (industrial fertilizers, nitrification) or biologically processed $NO_3^-_{atm}$, is 0 (Michalski et al., 2004b, 2015). In this study, we used these two distinct $\Delta^{17}O$ values as end-members in a simple mixing model to quantify unprocessed $NO_3^-_{atm}$ proportion in streams. Calculation of atmospheric contribution, noted f_{atm}, was derived from the following equation:

$$\Delta^{17}O\text{-}NO_3^-_{sample} = f_{atm} * \Delta^{17}O\text{-}NO_3^-_{atm} + (1- f_{atm}) * \Delta^{17}O\text{-}NO_3^-_{ter} \quad \text{(Eq. 2.1)}$$

With f_{atm} (= $\%NO_3^-_{atm}$), the mole fraction of the atmospheric contribution (Michalski et al., 2004b), $\Delta^{17}O\text{-}NO_3^-_{sample}$ the measured value of $\Delta^{17}O\text{-}NO_3^-$ in a sample and $\Delta^{17}O\text{-}NO_3^-_{ter}$ the value of ^{17}O-excess of terrestrial NO_3^- ($NO_3^-_{ter}$). As $\Delta^{17}O\text{-}NO_3^-_{ter}$ = 0 ‰ (Michalski et al., 2004b), Eq. 2.1 simplifies to

$$f_{atm} = \Delta^{17}O\text{-}NO_3^-_{sample} / \Delta^{17}O\text{-}NO_3^-_{atm} \quad \text{(Eq. 2.2)}$$

Choice for the atmospheric end-member values of $\Delta^{17}O\text{-}NO_3^-_{atm}$ is further discussed in section 2.1.4.1. Post-deposition processes such as denitrification or assimilation should enrich $\delta^{18}O$ and $\delta^{15}N$ along a 2:1 to 1:1 line (Granger et al., 2010b; Kendall et al., 2007), but co-occurring soil production of NO_3^- by nitrification

can lead to lower enrichment proportions (Granger and Wankel, 2016). However, $\Delta^{17}O$ values are unaffected because they are independent of the absolute $\delta^{18}O$ values (Michalski et al., 2004b), and therefore provide a robust quantification of unprocessed $NO_3^-{}_{atm}$., and subsequently, of $NO_3^-{}_{ter}$.

2.1.2.6 Statistical analysis

We used two non-parametric statistical tests in our study. The choice for non-parametric tests lies in the small population size of the aerosols (n=26), snow (n=30, 22, 29, 36 and 26 for December, January, February, March and April SP, respectively), and stream water samples (n=42, 29 and 28 for Tufiere, Laurichard and Romanche, respectively). A Mann-Whitney test was applied on river samples to determine whether mean concentrations and isotopic values were significantly different between streams. A Spearman test was applied to evaluate the correlation between stream water parameters (typically $\Delta^{17}O$, $\delta^{18}O$, $\delta^{15}N$ and $[NO_3^-]$). Differences and correlations were held significant when the *p* value reached a 0.01 credible interval. All statistical analyses were conducted using R software (v3.2.3).

2.1.3 Results

2.1.3.1 Nitrate input to ecosystems: $NO_3^-{}_{atm}$

Evolution of mean concentration, $\Delta^{17}O$, $\delta^{18}O$ and $\delta^{15}N$ of NO_3^- in snow pits throughout the winter, and in aerosols throughout year 2015 can be found in Figure 2-4 and in Table 2-1. First snow falls occurred mid-November 2014 with several freeze-thaw events before it started to accumulate. On days of snow pits sample collect, snowpack depths were 66, 64, 139, 142 and 101 cm in December 2014, January, February, March and April 2015, respectively. Maximum snow accumulation (*ca* 1.6-m) occurred early March 2015 (see section 2.1.5). By the end of April 2015, the snowpack had completely melted. In December and January, low $[NO_3^-]$ were measured in all snow pits layers (Figure 2-4). In February and March, a peak of $[NO_3^-]$ up to 5-mg L^{-1} between 70 and 90-cm of snow accumulation was recorded. This peak was also measured in April (orange line in Figure 2-4a), but at a lower depth (40 to 60-cm) and to a lesser extent (2.7-mg L^{-1}), due to elution of the snowpack NO_3^- by snowmelt water. $\Delta^{17}O$-NO_3^- in snow varied between 20 and 35 ‰ (Figure 2-4b),

well within the atmospheric range of NO_3^- isotopic values reported in the literature (Morin et al., 2009; Savarino et al., 2013). $\delta^{18}O$ and $\delta^{15}N$ values were between 60 and 90 ‰ and -10 and 0 ‰, respectively (Figure 2-4c and d), consistent with a reservoir exclusively made of $NO_3^-_{atm}$ (Kendall et al., 2007). Mean (± standard deviation) isotopic values of snow NO_3^- were 29.3 ± 1.6, 77.0 ± 5.6 and -3.6 ± 1.6 ‰ for $\Delta^{17}O$, $\delta^{18}O$ and $\delta^{15}N$, respectively.

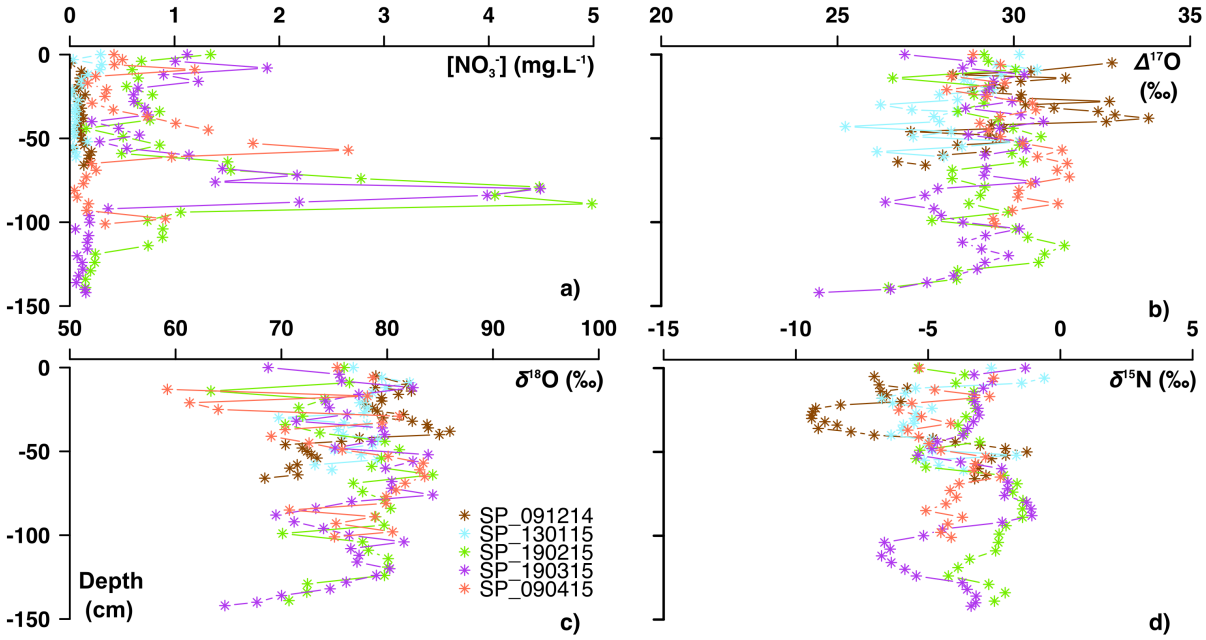

Figure 2-4: NO_3^- concentration and isotopic profiles of 5 snow pits (SP_ddmmyy) dug in winter 2014-2015, on a monthly basis. On X-axis is a) $[NO_3^-]$ (mg L^{-1}); b) $\Delta^{17}O$ (‰); c) $\delta^{18}O$ (‰) and d) $\delta^{15}N$ (‰). On Y-axis is snow depth as measured on day of collect. Brown, blue, green, purple and orange colors stand for December, January, February, March and April snow pit, respectively. The layer at 150 cm depth corresponds to the first non-melted snow of the winter. The deepest collected layer for each pit was about 2 cm above the soil, to avoid any NO_3^- exchange at the soil-snow interface.

Mean isotopic values of NO_3^- in aerosols were also consistent with other measurements of particulate NO_3^- (Elliott et al., 2009), featuring significantly lower mean $\Delta^{17}O$-NO_3^- and $\delta^{15}N$-NO_3^- in summer (23.1 ± 2.4 and -6.5 ± 3.4 ‰, respectively) than in winter (28.9 ± 1.7 and -1.0 ± 1.7 ‰, respectively), a temporal pattern discussed in the section 2.1.7. Winter aerosols NO_3^- isotopic values were in the range of the snowpack NO_3^- values.

Table 2-1: Mean volume-weighted concentration and concentration-weighted isotopic values for NO_3^- in snow pits (SP) and aerosols at the Lautaret pass. SP mean values are always calculated over the entire depth of the snow pack. Dates for SP are given in a dd/mm/yy format. SD is the standard deviation.

	Snow depth (cm)	$\delta^{15}N$ (‰)	$\delta^{18}O$ (‰)	$\Delta^{17}O$ (‰)	$[NO_3^-]$ ($mg.L^{-1}$)
		Mean (SD)	Mean (SD)	Mean (SD)	Mean (SD)
SP 09/12/14	66	-5.5 (2.7)	77.0 (5.0)	29.8 (1.9)	0.1 (0.4)
SP 13/01/15	64	-3.6 (1.7)	76.6 (7.2)	28.6 (2.5)	0.1 (0.9)
SP 19/02/15	139	-2.4 (1.2)	77.7 (4.5)	29.3 (1.2)	1.2 (1.3)
SP 19/03/15	142	-2.3 (1.6)	76.3 (4.6)	28.5 (1.3)	0.9 (1.0)
SP 09/04/15	104	-4.1 (1.1)	77.2 (6.8)	30.1 (1.0)	0.6 (0.6)
Aerosols (summer)	-	-6.5 (3.6)	62.9 (6.5)	23.1 (2.4)	0.1 (0.1) mg m^{-3}
Aerosols (winter)	-	-1.0 (1.7)	74.7 (4.4)	28.9 (1.0)	0.1 (0.2) mg m^{-3}

2.1.3.2 Nitrate output in rivers

All streams $[NO_3^-]$ data can be found in the Table 2-2. Laurichard showed significantly higher year-round $[NO_3^-]$ compared to the other streams, with a mean value of 2.6 ± 1.3-mg L^{-1}. Mean annual $[NO_3^-]$ was 0.09 ± 0.06-mg L^{-1} and 1.02 ± 0.48-mg L^{-1} in Tufiere and Romanche, respectively. Seasonal variations were similar in all streams, featuring higher $[NO_3^-]$ in late spring and lower $[NO_3^-]$ in summer (Figure 2-5a).

Tufiere had the widest range in $\Delta^{17}O\text{-}NO_3^-$ values, varying from 0.5 to 10.3 ‰, with a mean value of 3.2 ± 2.4 ‰. $\Delta^{17}O\text{-}NO_3^-$ values in Laurichard ranged from 0.8 to 8.2 ‰, with a mean value of 2.8 ± 1.7 ‰. In Romanche, $\Delta^{17}O\text{-}NO_3^-$ values remained above 3 ‰ for a period spanning several months, with a mean value of 4.3 ± 2.3 ‰ (Figure 2-5b). Mean $\Delta^{17}O\text{-}NO_3^-$ was significantly higher in Romanche than in Tufiere and Laurichard, whereas there was no significant difference between Tufiere and Laurichard mean $\Delta^{17}O\text{-}NO_3^-$ (p-value = 0.5). All streams showed similar range for $\delta^{18}O\text{-}NO_3^-$ and $\delta^{15}N\text{-}NO_3^-$, between -5 and 25 ‰ for $\delta^{18}O\text{-}NO_3^-$ and between -6 and

13 ‰ for δ^{15}N-NO_3^-. Our findings were somewhat in the same range of previously measured NO_3^- isotopic values in alpine streams (Burns and Kendall, 2002; Campbell et al., 2002; Mayer et al., 2002), although higher spanning δ^{18}O-NO_3^- values found elsewhere might be due to analytical bias (Rose et al., 2015b).

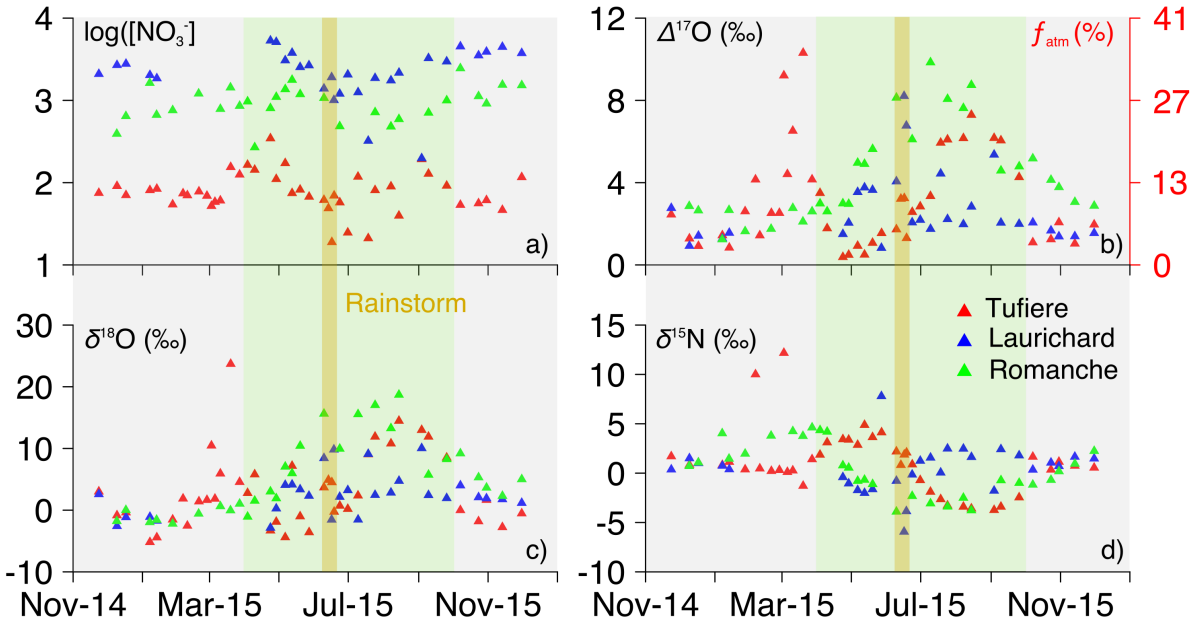

Figure 2-5: Seasonal variations of a) log([NO_3^-] in µg L^{-1}) (for an easier comparison of streams [NO_3^-]); b) Δ^{17}O (‰) and corresponding f_{atm} (%, the relative amount of atmospheric nitrate in streams); c) δ^{18}O (‰) and d) δ^{15}N (‰) of NO_3^- in streams. Red, blue and green colors stand for Tufiere, Laurichard and Romanche, respectively. Highlighted in yellow is a two-days rainstorm that occurred mid-June. The grey frames highlight the dormant season while the green one highlights the growing season. Transitions between both seasons are snowmelt period in spring, and plant senescence in autumn.

Table 2-2: Volume-weighted [NO_3^-] in streams at the Lautaret pass. Nitrate concentrations are given with an uncertainty of 0.02 mg L^{-1}.

Date (dd/mm/yy)	Tufiere	Laurichard	Romanche
23/11/14	0.07	2.09	
09/12/14	0.09	2.69	0.39
17/12/14	0.07	2.78	0.64
07/01/15	0.08	2.03	1.63
13/01/15	0.08	1.85	0.67
27/01/15	0.05		0.76
05/02/15	0.07		
09/02/15	0.07		
19/02/15	0.08		1.21
26/02/15	0.07		
02/03/15	0.05		
05/03/15	0.06		
10/03/15	0.06		0.79
19/03/15	0.15		1.43
27/03/15	0.13		0.86
03/04/15	0.16		0.97
09/04/15	0.14		0.27
23/04/15	0.35	5.33	0.80
28/04/15	0.11	5.12	1.10
06/05/15	0.17	3.06	1.37
12/05/15	0.07	3.78	1.77
19/05/15	0.08	2.54	1.19
27/05/15	0.07	2.66	1.07
09/06/15	0.06	1.39	0.79
13/06/15	0.05	1.91	
16/06/15	0.02	1.01	
18/06/15	0.07	1.20	
23/06/15	0.06	2.06	0.48
30/06/15	0.02	1.25	
09/07/15	0.12	0.32	
18/07/15	0.02	1.87	
24/07/15	0.08	1.75	0.72
07/08/15	0.09	2.17	0.48
14/08/15	0.04	0.20	0.59
03/09/15	0.19	3.26	
09/09/15	0.13	2.97	0.71
25/09/15	0.09	4.53	1.00
07/10/15	0.05	3.52	2.45
23/10/15	0.06	3.90	1.12
30/10/15	0.06	4.47	0.91
13/11/15	0.05	3.75	1.55
30/11/15	0.12	1.91	1.53

2.1.4 Discussion

2.1.4.1 Atmospheric nitrate end-member

Our choice to use snow-NO_3^- as the atmospheric end-member laid on simple but robust assumptions. First, snow is a good conservator of atmospheric nitrate in high accumulation sites (> 30 cm of snow accumulation) and preserves its isotopic composition (Hastings, 2004; Savarino et al., 2007). Second, the snowpack is representative of winter bulk deposition, as it aggregates both wet and dry deposition (Campbell et al., 2007; Williams et al., 2009). Third, most of $NO_3^-_{atm}$ measured in streams was assumed to come from snowmelt, as previously observed in other seasonally snow-covered catchments (Brooks and Williams, 1999; Williams et al., 2009). Little temporal variation of NO_3^- concentration and isotopic values in snow pits profiles, along with no isotopic evidence of post-deposition processes further supported this assumption (section 2.1.6, Figure 2-4 and Figure 2-9). By inputting mean snow $\Delta^{17}O\text{-}NO_3^-$ in Eq. 2.2, we obtained:

$$f_{atm} = \Delta^{17}O\text{-}NO_3^-_{sample} / 29.3 \qquad \text{(Eq. 2.3)}$$

The error range on f_{atm} was inferred from snow $\Delta^{17}O\text{-}NO_3^-$ standard deviation, and calculated as 2 %.

It must be underlined that snow as atmospheric end-member might not account correctly for wet or dry deposition in summer. Wet deposition has *de facto* been shown to contribute significantly to freshwaters systems, either through direct inputs due to flashy hydrology (Campbell et al., 2002; Rose et al., 2015a) or through indirect contribution *via* enhanced nitrification (Nanus et al., 2008). We show that summer deposition (wet or dry) as atmospheric end-member results in higher calculated $NO_3^-_{atm}$ fraction in streams, up to 6% in this study (see section 2.1.7). For that reason, all calculated f_{atm} values in the following sections must be considered as a lower estimate of $NO_3^-_{atm}$ inputs in this system.

2.1.4.2 Identification of terrestrial nitrate sources

No correlation was found between $\Delta^{17}O\text{-}NO_3^-$ and $[NO_3^-]$ in Tufiere, Laurichard and Romanche (Figure 2-6a, b and c), indicating that $NO_3^-_{atm}$ is not the main contributor to streams nitrogen load on a yearly basis. For all streams, $\Delta^{17}O\text{-}NO_3^-$ was significantly correlated to $\delta^{18}O\text{-}NO_3^-$ (Figure 2-6d, e and f) with the best correlation found in Romanche. Deviations from linear regressions are attributed to occasionally intense biological processes affecting $\delta^{18}O$ signal but leaving $\Delta^{17}O$ intact. Otherwise, the strong linear correlations observed here suggest that mixing of sources more than biological processes could explain the observed seasonal variations of NO_3^- isotopic values. As a consequence, by extrapolating this linear relationship to $\Delta^{17}O\text{-}NO_3^- = 0$ (*i.e.*, 100 % terrestrial NO_3^-), we can determine the mean $\delta^{18}O$ value of $NO_3^-_{ter}$ produced in the three watersheds: -6.0, -4.6 and -6.6 ‰ in Tufiere, Laurichard and Romanche, respectively. These results for $NO_3^-_{ter}$ were consistent with other studies estimation of $\delta^{18}O\text{-}NO_3^-_{ter}$ in streams, either calculated *via* the same method (Darrouzet-Nardi et al., 2012; Michalski et al., 2004b) or deduced from measured $\delta^{18}O$ values of soil-water and O_2, assuming they respectively contributed to NO_3^--O accordingly to $\delta^{18}O\text{-}NO_3^- = 1/3\ (\delta^{18}O\text{-}O_2) + 2/3\ (\delta^{18}O\text{-}H_2O)$ (Kendall et al., 2007; Rose et al., 2015b). Note that our approach (*i.e.*, $\Delta^{17}O$ *vs* $\delta^{18}O$) might yield lower uncertainty compared to the traditional one (*i.e.*, $\delta^{18}O$ calculation) which comes with a number of assumptions and caveats that are thoroughly dissected elsewhere (Rose et al., 2015b; Snider et al., 2010). Conversely, we found a significant negative correlation between $\Delta^{17}O\text{-}NO_3^-$ and $\delta^{15}N\text{-}NO_3^-$ (Figure 2-6g, h and i) in the three streams, with once again the best fit for Romanche. With the same method as cited above, we can infer the mean $\delta^{15}N\text{-}NO_3^-_{ter}$: 4.4, 5.0 and 6.1 ‰ in Tufiere, Laurichard and Romanche, respectively. These values characterizing the $NO_3^-_{ter}$ end-member are typical of NO_3^- produced from soil NH_4^+ nitrification (Kendall et al., 2007). On the other hand, extrapolating this correlation to $\Delta^{17}O\text{-}NO_3^- = 29.3$ ‰ (*i.e.*, 100% $NO_3^-_{atm}$) should give $\delta^{15}N\text{-}NO_3^-_{atm}$ and $\delta^{18}O\text{-}NO_3^-_{atm}$ consistent with otherwise measured snow NO_3^- isotopic values. We found values of 77.7, 79.0 and 74.7 ‰ for $\delta^{18}O\text{-}NO_3^-_{atm}$ in Tufiere, Laurichard and Romanche, respectively, consistent with the mean $\delta^{18}O$ value of 77.0 ‰ measured for snow NO_3^- (Table 2-1). Surprisingly, $\delta^{15}N\text{-}NO_3^-_{atm}$ values of *ca* -30 ‰ were inferred in all

streams, far from measured δ^{15}N-NO_3^- in snow and aerosols (Table 2-1) and from existing literature data showing a range of δ^{15}N values for NO_3^- between -15 and 15 ‰ (Guha et al., 2017; Kendall et al., 2007; Mara et al., 2009; Xue et al., 2009). This suggested that a two end-members mixing model cannot account for the different sources of N that might have served as substrate for nitrification in subalpine meadows, and the subsequent large distribution of δ^{15}N-$NO_3^-_{ter}$.

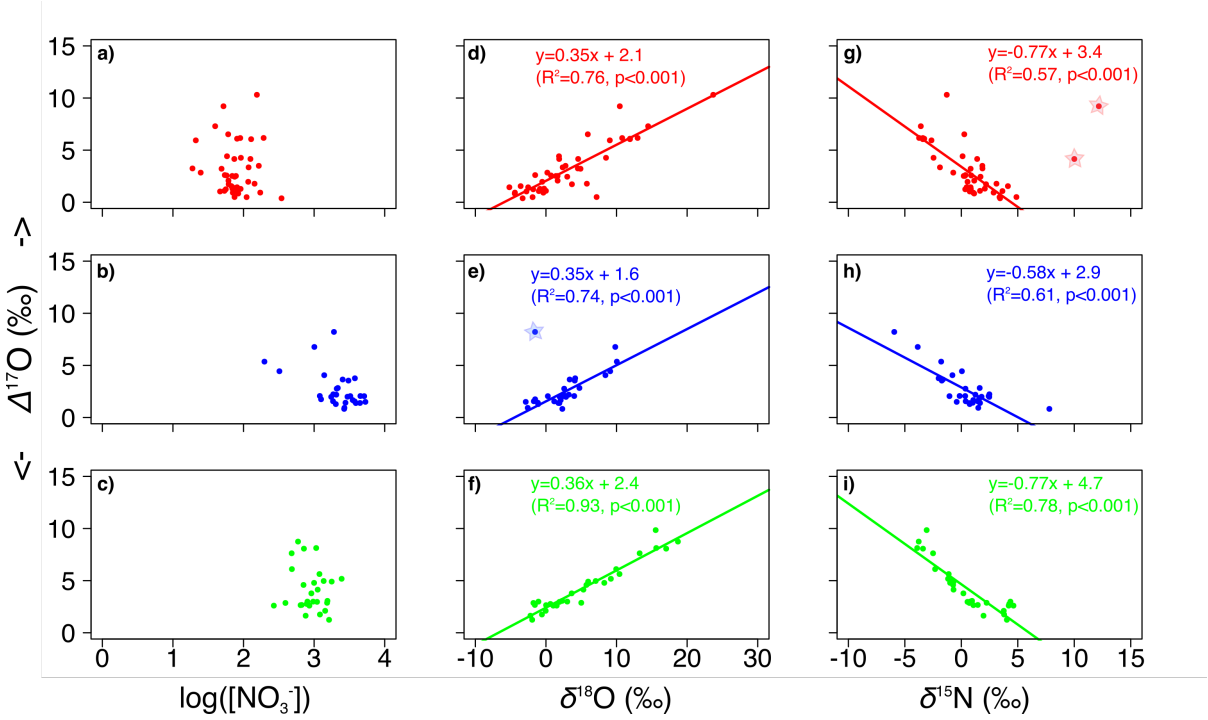

Figure 2-6: Correlation between nitrate Δ^{17}O (‰) and a), b), c) log([NO_3^-]); d), e), f) δ^{18}O (‰); g), h), i) δ^{15}N (‰). Red, blue and green colors stand for Tufiere, Laurichard and Romanche, respectively. Outliers (surrounded by stars) were not considered in the linear regression model, as we assume they result from biological processes (e.g., denitrification) and would blur determination of NO_3^- sources.

Similar work in alpine watersheds in the Colorado Front Range suggested that possible sources of NO_3^- in streams, apart from snow $NO_3^-_{atm}$, could be nitrification of snow NH_4^+ in the snowpack and in soils during snowmelt, or flushing of soil NO_3^- produced under the snowpack during winter (Kendall et al., 1995). Nitrification in the snowpack is highly unlikely; indeed, such a process would have overprinted snow Δ^{17}O-NO_3^- values, which is not the case here (see section 2.1.6 and Figure 2-4). However, the dual isotopes plot presented in Figure 2-7 hints at a stronger contribution of atmospheric N deposition – either as snow or rain – than previously assessed in subalpine watersheds. Deposition of $NH_4^+_{atm}$ in particular was likely to

enrich soils N pool, and could account for part of $NO_3^-{}_{ter}$ exported in streams. Snow at the Lautaret pass has been shown to hold a non-negligible pool of NH_4^+ – equivalent to NO_3^- pool (Clément et al., 2012) – whereas undetectable [NH_4^+] was monitored in all streams (data not shown) suggesting that NH_4^+ released from snow is either adsorbed on clay minerals or biologically processed. If the entire snow-NH_4^+ pool (if considered about roughly the same size as snow-NO_3^- pool) was nitrified in soils and exported as NO_3^- into streams during snowmelt, it would account for as much as 54 and 18 % of $NO_3^-{}_{ter}$ production in Tufiere and Laurichard, respectively (Figure 2-5b). The additional $NO_3^-{}_{ter}$ exported in streams can only be explained by soil leaching at snowmelt. Strong microbial activity under the snowpack is not uncommon in cold mountainous regions (Brooks and Williams, 1999; Hiltbrunner et al., 2005; Jusselme et al., 2016; Legay et al., 2013) and could justify the observed pattern. At snowmelt, cold adapted microbial communities massively turn over when confronted to warmer air temperatures (Schmidt and Lipson, 2004), releasing nitrified N from lysed cells into the soils where it leaches towards groundwater and streams (Williams et al., 1996). Sources of nitrified N under the snowpack may be related to soil organic matter and litter decomposition (Saccone et al., 2013) or soil NH_4^+ pool resulting from previous year's N deposits (Kendall et al., 1995; Williams et al., 1996). At this point we cannot conclude which source contributed the most to $NO_3^-{}_{ter}$ yield, but overwinter isotopic monitoring of N pools under the snowpack might bring clarification.

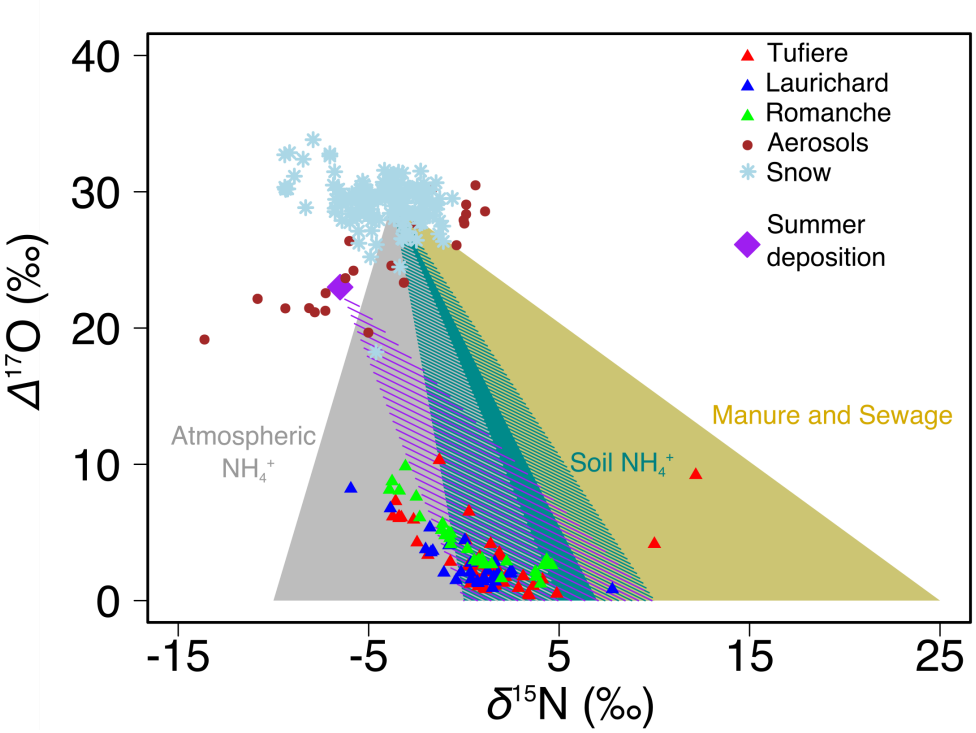

Figure 2-7: Dual isotopes plot ($\Delta^{17}O$ *vs.* $\delta^{15}N$) illustrating the mixing between three sources of NO_3^- in our study sites. The plain triangles feature the mixing range between snow $NO_3^-_{atm}$ and NO_3^- from nitrified $NH_4^+_{atm}$ in grey, NO_3^- from nitrified soil NH_4^+ in turquoise and NO_3^- from manure or sewage in beige. Dashed triangles of similar colors illustrate the overlapping of sources $\delta^{15}N\text{-}NO_3^-$ values. The dashed purple triangle illustrates the mixing range between $NO_3^-_{atm}$ and NO_3^- from nitrified soil NH_4^+ if summer deposition was the atmospheric end-member. When $\Delta^{17}O\text{-}NO_3^-$ values are high, $\delta^{15}N\text{-}NO_3^-$ is characteristic of nitrified $NH_4^+_{atm}$, delineating the coupled contribution of anthropogenic N deposition *via* direct inputs ($NO_3^-_{atm}$) and indirect inputs (nitrified $NH_4^+_{atm}$). Decreased contribution of atmospheric N sources (low $\Delta^{17}O\text{-}NO_3^-$ values) results in a higher proportion of $NO_3^-_{ter}$.

2.1.4.3 Seasonal variations of atmospheric nitrate exports

All stream water samples in this study had positive $\Delta^{17}O\text{-}NO_3^-$ values, showing unquestionable inputs of $NO_3^-_{atm}$ in all streams year-round (Figure 2-5b). However, Tufiere and Laurichard, although sampled at the same altitude, showed different NO_3^- export patterns, certainly due to different hydrological behaviors and respective basins characteristics (Rose et al., 2015b).

NO_3^- dynamic in Tufiere were most likely governed by snowmelt. Brief but high peaks of ^{17}O-excess of NO_3^- in March 2015, coincident with higher [NO_3^-], were attributed to direct runoff of snowmelt water to the stream (Campbell et al., 2002; Darrouzet-Nardi et al., 2012). Rapid melting of the lower watershed snowpack

washed away labile $NO_3^-{}_{atm}$ deposits and contributed up to 35 % of the total stream NO_3^- pool. Leached $NO_3^-{}_{ter}$ from snow-free soils by subsurface melt or rain water accounted for both higher [NO_3^-] and lower $\Delta^{17}O\text{-}NO_3^-$ in the stream later in spring (Liu et al., 2004). Gentle hillslopes and the calcareous substrate of the Lautaret sub-watershed were also likely to facilitate snowmelt water infiltration and mixing with groundwater, a common feature in subalpine catchments (Cowie et al., 2017). Starting early May, a slow but persistent increase in $\Delta^{17}O\text{-}NO_3^-$ suggested a resurgence of $NO_3^-{}_{atm}$ loaded water entering the stream, increasing $NO_3^-{}_{atm}$ proportion up to 25 % again at the end of August. Significantly higher precipitation in May and in August, compared to the previous months (Figure 2-3) could have triggered this resurgence by filling the aquifer with rain water, thus flushing stored water. The wide temporal range of this $\Delta^{17}O$ increase, encompassing six months from May to October, is in line with a temporally spread transit time of infiltrated melt water along an altitude gradient. Direct contribution of rain $NO_3^-{}_{atm}$ was unlikely to explain such pattern, given the low response of Tufiere [NO_3^-] and $\Delta^{17}O\text{-}NO_3^-$ to the storm in June (Figure 2-3). Considering the basin topography and geology (*i.e.*, gentler slopes and higher vegetation cover), most rain N inputs were certainly retained in soils or assimilated before either infiltration or direct runoff of rainwater in Tufiere (Nanus et al., 2008).

In contrast, $NO_3^-{}_{atm}$ contributed only between 4 and 15 % of total NO_3^- in Laurichard stream from April to May (Figure 2-5b), coincident with the snowmelt period for this northern exposed watershed. Laurichard rock glacier is an actively monitored permafrost-related landform, which increased surface velocities over the past twenty years hint at increased permafrost temperatures, possibly to the point of thawing (Bodin et al., 2009). Considerably higher year-round [NO_3^-] in Laurichard compared to snow-fed Tufiere – by 1-2 orders of magnitude – suggested that Laurichard NO_3^- exports were mainly driven by increasing soil exposure (Williams et al., 2007) more than any other geomorphic or biogeographic feature (Saros et al., 2010). Sources of such elevated levels of NO_3^-, while still debated (Slemmons et al., 2013; Williams et al., 2016), were likely linked to glaciers retreat and permafrost thawing leading to enhanced stream solutes fluxes (Barnes et al., 2014; Hood and

Scott, 2008), increased nitrification and/or mobilization of stored N from disturbed soils (Louiseize et al., 2014). Steeper slopes (Figure 2-2), and potentially increased deposition loading because of increased orographic precipitations (Williams and Tonnessen, 2000) – relative to the Lautaret watershed – were certainly responsible for the occasional higher $\Delta^{17}O\text{-}NO_3^-$ peaks, concomitant with rain events (Figure 2-3). Lower vegetation cover – and therefore reduced plant $NO_3^-{}_{atm}$ uptake– and the poor buffering capacity of Laurichard watershed granitic bedrock are additional factors that could have fostered punctually enhanced exports of $NO_3^-{}_{atm}$ from wet deposition (Balestrini et al., 2013; Rose et al., 2015b). The storm in June 2015 (Figure 2-3) led to the strongest input of $NO_3^-{}_{atm}$ in this stream, accounting for 29 % of Laurichard NO_3^- pool (Figure 2-5b). Simultaneous $\Delta^{17}O\text{-}NO_3^-$ peaks and $[NO_3^-]$ minima in July and September were further evidence of this flashy hydrology and illustrated stream glacial melt water dilution by rain.

Conversely, we did not observe an early snowmelt runoff-linked peak in Romanche stream water $\Delta^{17}O\text{-}NO_3^-$ in spring. Instead, $NO_3^-{}_{atm}$ contribution increased steadily from April to July (34 % of $NO_3^-{}_{atm}$ on July 9th) then declined until reaching a baseflow value of about 5 % of $NO_3^-{}_{atm}$ during the dormant season. Romanche is the main stream of the valley, fueled by myriad smaller tributaries like Tufiere and Laurichard. Lower altitude catchments contributed most in spring, but as air temperature and solar radiation increased in summer, melting snowpack from higher watersheds of the Ecrins National Park may have led to enhanced $NO_3^-{}_{atm}$ export in Romanche stream.

Why $[NO_3^-]$ decreased from Laurichard to Romanche is uncertain, but dilution by snow-fed streams like Tufiere between sampling locations is a possibility. Other possible sinks include denitrification, in-stream algal and phytoplankton assimilation or uptake by the riparian vegetation (Hall Jr et al., 2009). Denitrification and assimilation should discriminate $\delta^{18}O$ against $\delta^{15}N$ of residual NO_3^- following a line with a positive slope (*i.e.*, enrich the residual nitrate with heavier isotopes), which was not observed in our study (Figure 2-8). However, frequent recharge of NO_3^- by

smaller tributaries such as Laurichard may have overprinted any biological isotopic signature (Granger and Wankel, 2016).

On all basins, the strong controls seemingly exerted either by snowmelt (Tufiere and Romanche) or by glacier melt water (Laurichard) on stream $NO_3^-{}_{atm}$ exports precluded a higher contribution from direct summer deposition of $NO_3^-{}_{atm}$. Wet deposition loads of $NO_3^-{}_{atm}$ to streams were either buffered by vegetation uptake and/or soil immobilization on Lautaret watershed, subdued by high $NO_3^-{}_{ter}$ except on intense rain events on Laurichard watershed, or combined with the wide temporal response of the Romanche to snowmelt from uplands. Nevertheless, summer deposition of $NH_4^+{}_{atm}$ contributed significantly to subalpine N pool and was partly responsible for the $NO_3^-{}_{ter}$ exports in streams.

Simultaneous monitoring of $\Delta^{17}O\text{-}NO_3^-$, streams discharge, water isotopes and chemical tracers of hydrological paths remain needed to further constrain water sources and their respective contribution to NO_3^- exports in subalpine streams. Longer monitoring of streams exports is also warranted to better evaluate annual variability in this subalpine watershed, as year 2015 was significantly drier than previous years at the Lautaret pass. Hydrological responses to rain events, and resulting NO_3^- export dynamics under different precipitation conditions, need to be assessed.

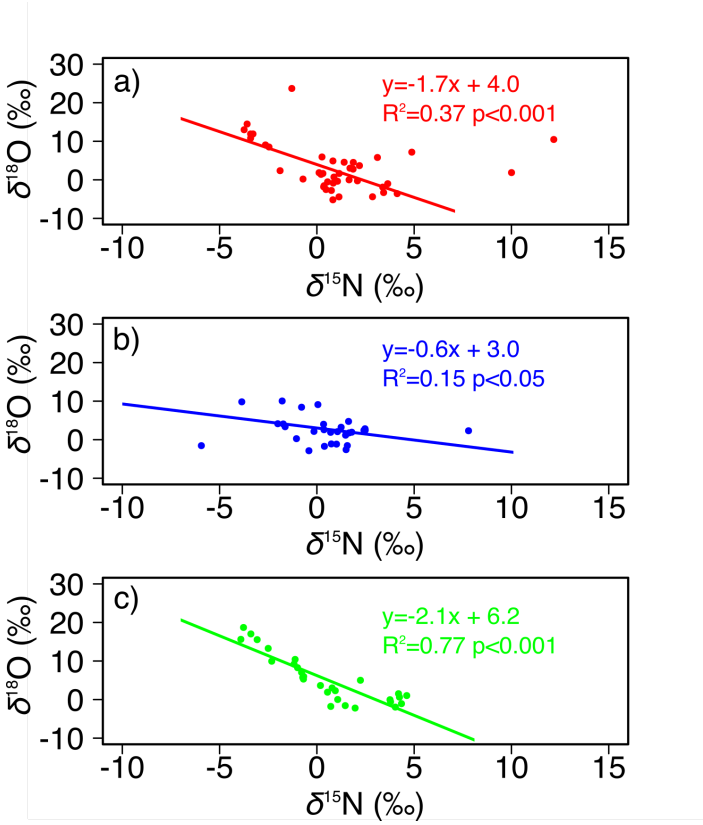

Figure 2-8: Correlation between stream water nitrate $\delta^{18}O$ (‰) and $\delta^{15}N$ (‰) in a) Tufiere (red), b) Laurichard (blue) and c) Romanche (green). Outliers were not considered in the linear regression model, for easier comparison with Figure 2-6. Negative slopes indicate that mixing, more than biological processes, governs NO_3^- budget in streams.

2.1.4.4 Nitrogen saturation and ecological implication

Despite presenting different N export dynamics, all streams shared uninterrupted presence of NO_3^- year-round, with a significant contribution from atmospheric deposition. In a supposedly N-limited ecosystem, such a pattern was unexpected as demand for dissolved inorganic nitrogen (DIN) from plants and microbial communities in spring and summer should have exceeded mobile NO_3^- reservoir in soils, precluding leaching to the streams.

Nitrogen saturation has first been evaluated in an ecosystem subjected to increasing N deposition (Aber et al., 1989). Several stages of saturation have been distinguished, ranging from 0 (N-limited ecosystem) to 3 (fully saturated ecosystem characterized by N-leaching and higher streams [NO_3^-]). [NO_3^-] in Tufiere and Romanche was within the range of reported alpine and mountain stream [NO_3^-]

(Balestrini et al., 2013), but [NO_3^-] in Laurichard was higher than in streams pinned as indicators of stage 2 or 3 (Rose et al., 2015a). However, similar seasonal variations of [NO_3^-] in Tufiere, Laurichard and Romanche – high in spring after snowmelt, decreasing in summer, then increasing again as air temperature starts falling down (Figure 2-5a) – were symptomatic of plants and microbial biomasses working as N sinks during the growing season. Evaluation of N saturation according to the conceptual model of biological demand exceeded by N supply does not take into account other drivers of N exports (Rose et al., 2015b), and may not be adapted to describe the N saturation state of subalpine watersheds. Another approach to N saturation has been described as kinetic N saturation, where the rate of N inputs exceeds the rate of N assimilation in an ecosystem and its remediation capacity, and can lead to intensive exports of N in streams (Lovett and Goodale, 2011). Given the highest percentage of unprocessed $NO_3^-{}_{atm}$ during hydrological events, our results provided additional evidence that catchment hydrology is certainly responsible for the kinetic N saturation in subalpine watersheds. Anyhow, assessment of N deposition load could help us estimate whether the critical threshold has been crossed, as evidenced in other alpine environments (Baron et al., 2011; Boutin et al., 2015; Nanus et al., 2017), and will be the object of future studies.

N inputs at the watershed scale, through $NO_3^-{}_{atm}$ direct contribution or $NH_4^+{}_{atm}$ nitrification, are likely to substantially impact surrounding ecosystems, especially during the growing season following snowmelt. For instance, the lake Chambon, a freshwater reservoir fueled by the Romanche stream, which supplies downhill villages and cities – including Grenoble (163 000 inhabitants) – with drinking water, showed high $NO_3^-{}_{atm}$ contribution from May to November (up to 25 %, Table 2-3). While [NO_3^-] in the lake averaged 2.0 ± 0.8-mg L^{-1} during the growing season, far below the limit of 50-mg L^{-1} (guideline value from The World Health Organization translated in the EU Water Framework Directive 2000/60/EC), the presence of $NO_3^-{}_{atm}$ in this elevated freshwater reservoir is yet another warning signal of potential threats due to atmospherically deposited pollutants. Evidence of lakes fertilization by atmospheric deposition in high altitude watersheds has been demonstrated before (Hundey et al., 2016). Fast cycling dynamics of high atmospheric Nr in lakes

(Tsunogai et al., 2011) can lead to well-documented ecological consequences such as acidification (Baron et al., 2011), shift of algal and phytoplankton communities (Hobbs et al., 2016; Spaulding et al., 2015) and disturbance of lakes food web (Elser et al., 2009), and highlight the necessity to protect critical water resources. In winter, limited hydrological connectivity between soils and streams cannot explain the year-round export presence of unprocessed $NO_3^-{}_{atm}$ in subalpine streams, highlighting the potential contribution of groundwater contamination to streams exports. Previous studies also showed that most alpine and subalpine plants acquire N during snowmelt (Bilbrough et al., 2000). In traditionally N-poor subalpine ecosystems, increasing inputs of $NO_3^-{}_{atm}$ together with climate change could accelerate diversity and composition losses of plant communities. In a 21st century with a shorter snow season, a higher fraction of the yearly deposited NO_3^- will be brought to subalpine ecosystems at a slower rate, during the growth season, instead of abruptly at snowmelt. If NO_3^- saturation is indeed kinetic – as our study suggested – then this climate driven change in NO_3^- influx timing could result in higher NO_3^- absorption in the environment, and lead to capacity saturation. This would come with a wide number of changes in the ecosystem, which have been extensively detailed elsewhere at a global scale (Aber et al., 1989; Galloway et al., 2008; Vitousek et al., 1997), and more specifically in high altitude catchments (Baron et al., 2000; Elser et al., 2009; Nanus et al., 2017).

These findings emphasize the need for more joint monitoring of subalpine soils and plant communities, with the objective a better understanding of atmospheric N deposition consequences on biogeochemical cycling in these semi-isolated ecosystems. In particular, prospective studies should continue focusing on potential synergetic effects of land use management coupled with atmospheric deposition on ecosystems alteration, to better orient policy makers in N emissions mitigation and adaptation efforts.

Table 2-3: Volume-weighted concentrations and concentration-weighted isotopic values of NO_3^- in the lake Chambon.

Date (dd/mm/yy)	$[NO_3^-]$ (mg.L^{-1})	$\delta^{18}O$ (‰)	$\Delta^{17}O$ (‰)	$\delta^{15}N$ (‰)	f_{atm} (%)
06/05/15		4.0	3.2	0.8	11
12/05/15	1.8	3.0	3.7	0.4	13
19/05/15	3.0	5.1	4.2	1.1	14
23/06/15	1.2	12.5	6.2	-1.5	21
30/06/15		1.2	7.4	-2.9	25
25/09/15	2.8	11.2	5.4	-1.9	18
07/10/15	2.9	10.1	5.0	-0.6	17
23/10/15	1.3	6.6	4.3	-1.5	14
30/10/15	1.6	6.7	4.3	-1.4	14

2.1.5 Appendix 1

The aerosol collector was installed about 200-m uphill from the SAJF research station with no traffic in direct vicinity except for occasional hikers. A 1-min sampling blank was performed every month to track possible contaminations associated with the analytical procedure. Blanks were always negligible (*i.e.*, three orders of magnitude lower than the lowest $[NO_{3\,atm}^-]$ in samples) and thus no blank correction was applied to any isotope measurement. After sampling, filters were folded to avoid any loss, immediately wrapped in aluminum foil, and conserved on site in clean sealed plastic bags at -20°C until further chemical analysis. All handling operations were designed to reduce potential contaminations as much as possible (gloves, clean surface, fast transport, *etc.*). The sampling area for snow pits was chosen close – within 50-m – to the aerosols collector on the Lautaret sub-watershed (Figure 2-2, in orange) and was delimited by poles and rope to avoid trespassing by hikers and cross-country skiers. Snowpack depth spatial variability was not evaluated. However, the snow sampling location was carefully chosen on a rather flat area, to avoid as much as possible blowing or accumulation effects of wind. Our accumulation

measurements were consistent with other measurements on the site at the same period and with regional models predictions (Charrois, 2017). Each snow sample was stored in a 2-L Whirl-Pack® bag, placed in a cooler with ice and brought back to the lab to be stored at -20°C. Visual check indicated that snow did not melt upon arrival to the laboratory except for April 2015 where a small amount of snowmelt water (about 5-mL) was observed in the bags. The maximum accumulation of snow (early March) was determined by continuous measurement of snow height with an acoustic sensor (Campbell SR50A-L) (Charrois, 2017). Stream samples were collected in 1-L Nalgene bottles, previously washed 3 times in laboratory with ultrapure water (18.2 MΩ.cm at 25 °C) and rinsed three more times with stream water before collection. All samples were then kept at -20°C on site until further treatment.

Isotopic analyses were performed using the bacterial denitrifier technique in combination with the N_2O gold decomposition method (Casciotti et al., 2002; Kaiser et al., 2007; Morin et al., 2008). Briefly, the denitrifying *Pseudomonas aureofaciens* bacteria convert NO_3^- to N_2O under anaerobic conditions. N_2O is then flushed into an in-house built processing line, where it is thermally decomposed in a gold furnace heated to 880 °C into a N_2/O_2 mixture. These are subsequently separated by gas chromatography (GasBench II with a 10 m Agilent J&W CP-Molsieve 5Å GC Column CP7535I5) then injected into a mass spectrometer (Thermo Finnigan MAT 253) for O and N isotopic analysis.

2.1.6 Appendix 2

Based on the vertical profiles of snowpack NO_3^- isotopic values (Figure 2-4), we provide evidence that post-deposition processes such as nitrification, denitrification, photolysis or uptake did not affect $NO_3^-{}_{atm}$ concentrations and isotopes. First of all, emphasis should be put on the very good agreement of the measured NO_3^- isotopic values in the snowpack and the literature about $NO_3^-{}_{atm}$ isotopic values (Guha et al., 2017; Kendall et al., 2007). However, and because of the large range for $NO_3^-{}_{atm}$ isotopic values in the literature, post-deposition processes could affect $NO_3^-{}_{atm}$ isotopes and still be in line with expected values for an atmospheric reservoir. The comparison of winter particulate NO_3^- (p-NO_3^-) isotopic

values with snow NO_3^- isotopic values did not support that hypothesis. In case of processes leading to NO_3^- supply (nitrification) or loss (denitrification, photolysis, uptake), snow residual NO_3^- should have been respectively depleted or enriched in ^{15}N and ^{18}O compared to p-NO_3^-. However, winter p-NO_3^- isotopic values were concordant with snow NO_3^- (Table 2-1), with differences lower than the calculated standard deviation (SD) for the mean values. Additionally, we did not observe temporal loss of NO_3^- between two consecutive pits, with the exception of April pit when lower [NO_3^-] is likely due to snowpack elution by melted snow (Figure 2-4). Little to no correlation between $\delta^{18}O$ and $\delta^{15}N$ is further evidence that $NO_3^-{}_{atm}$ and its isotopic signature were rather well conserved in the snowpack (Figure 2-9a). The only enrichment line in the April pit can be explained by lower isotopic values of snow surface NO_3^- (Figure 2-9a), illustrating the seasonal shift in $NO_3^-{}_{atm}$ sources or oxidation pathways, as explained in section 2.1.7. The $\Delta^{17}O$ / $\delta^{18}O$ plot of snowpack NO_3^- also shows little deviation from linear correlation that would indicate mass-dependent fractionating processes such as volatilization, biological uptake or denitrification (Figure 2-9).

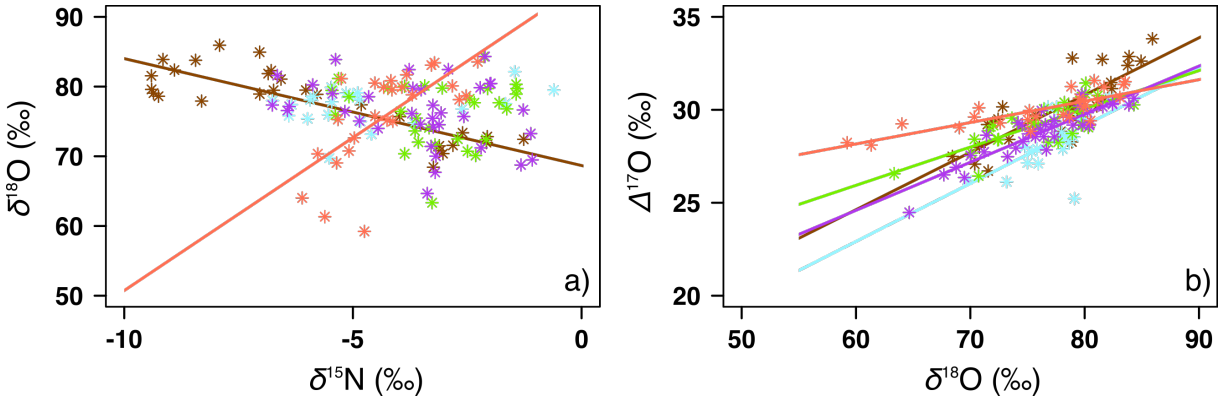

Figure 2-9: Correlation between snow nitrate a) $\delta^{18}O$ (‰) and $\delta^{15}N$ (‰); b) $\Delta^{17}O$ (‰) and $\delta^{18}O$. Brown, blue, green, purple and orange colors stand for December 2014, January 2015, February 2015, March 2015 and April 2015 snow pit, respectively. In the left panel, correlations were significant only for December and April ($p<0.05$). In the right panel, all correlations were significant ($p<0.001$).

2.1.7 Appendix 3

Snow NO_3^- as atmospheric end-member for the two end-members mixing model presented in section 2.1.2.5 is likely to not account well for wet deposition inputs in summer. Indeed, it has been demonstrated in several studies that, because

of either different sources or different oxidation pathways, seasonal variations often lead to lower isotopic values of NO_3^- – including $\Delta^{17}O$ (Savarino et al., 2013) – in summer compared to winter (Beyn et al., 2014; Elliott et al., 2009). This was also illustrated at the Lautaret pass by lower p-NO_3^- isotopic values in summer compared to winter (Table 2-1). Therefore, to choose a winter over a summer atmospheric end-member is likely to impact subsequent quantification of $NO_3^-_{atm}$ proportion in a given ecosystem. However, we show here that lower $\Delta^{17}O$ of wet deposition NO_3^- during the growing season only strengthens our conclusions since a previously used $\Delta^{17}O$-NO_3^- value of 25 ‰ (Costa et al., 2011; Michalski et al., 2004b) for summer wet deposition end-member would lead to:

$$f_{atm} = \Delta^{17}O\text{-}NO_3^-_{sample} / 25 \qquad \text{(Eq. 2.3bis)}$$

Instead of, for snow as atmospheric end-member:

$$f_{atm} = \Delta^{17}O\text{-}NO_3^-_{sample} / 29.3 \qquad \text{(Eq. 2.3)}$$

For a river sample with a $\Delta^{17}O$ = 10.3 ‰ (highest value measured in streams in 2015, Figure 2-5b), Eq. 2.3 gives *ca* 35 % of atmospheric NO_3^- whereas Eq. 2.3bis gives *ca.* 41 % of atmospheric NO_3^- in the stream. To use snow NO_3^- as atmospheric end-member enables the quantification of the minimum contribution of atmospheric NO_3^- in streams N pool. Rain NO_3^-, with lower isotopic values, results in a higher calculated contribution of $NO_3^-_{atm}$, and only tunes up with the conclusions of the manuscript (high contribution of $NO_3^-_{atm}$ and potential ecological consequences).

Acknowledgments

This study was supported by grants from the Labex OSUG@2020 (“Investissements d’avenir” - ANR10 LABX56), the ARC - Environnement Région Rhone-Alpes and the Grenoble-Chambéry DIPEE CNRS. This work also benefited from the National Research Agency support (“Investissements d’avenir” - ANR11 INBS-0001AnaEE-Services) and from the SAJF research station (UMR 3370, UGA/CNRS) infrastructures and competences. The study took place on the long-term

ecological research site Zone Atelier Alpes, a member of the ILTER-Europe. We would like to thank J.-L. Jaffrezo, F. Masson, V. Lucaire, E. Vince, C. Arnoldi and S. Albertin for help with either laboratory or field work. We acknowledge J. Renaud for help with SIG.

2.2 Atmospheric nitrate exports in streams from the Lautaret pass to Grenoble

After:

Bourgeois, I. ; Savarino, J. ; Némery, J., Caillon, N. ; Albertin, S. ; Delbart, F. ; Voisin, D. and Clément, J.-C.: Atmospheric nitrate export in streams along a montane to urban gradient, in review for *Science of the Total Environment*.

Abstract

As an increasing fraction of human population lives in cities, there is a growing need to understand how human activities couple and decouple with natural biogeochemical cycles. Excessive urbanization exacerbates the nitrogen (N) pollution of freshwaters. The study of the N cycle is thus of major interest to promote adapted remediation policies. Here, we focus on atmospheric nitrate exports in streams along a montane to urban gradient, using a multi-isotopic tracers approach ($\Delta^{17}O$, $\delta^{15}N$, $\delta^{18}O$ of nitrate and $\delta^{2}H$ of water). We show that montane streams have higher proportions of atmospheric nitrate compared to urban streams, and export more atmospheric nitrate on a yearly basis (0.35 *vs* 0.10-kg N ha^{-1} yr^{-1}). In urban areas, downstream nitrate flux is totally explained by groundwater, whereas in the catchment head export flows are dominated by key events such as snowmelt. Based on the measurements of $\delta^{15}N$ and $\delta^{18}O$-NO_3^- we conclude that the biological processes of denitrification or assimilation do not dominate in any streams in our study. On the other hand, the observed low $\delta^{15}N$ and $\delta^{18}O$ range of stream terrestrial nitrate compared to literature suggests that atmospheric deposition may have been a widely underestimated direct source of N pollution to the environment.

2.2.1 Introduction

Atmospheric nitrogen (N) deposition has increased 10-fold over the past century, increasingly contributing to the global N resource (Galloway et al., 2004). Anthropogenic activities such as fossil-fuel combustion, agriculture and fertilizers use are responsible for this increase (Fowler et al., 2015; Galloway et al., 2008; Vitousek

et al., 1997), with impacts even in remote ecosystems (Hastings et al., 2009; Holtgrieve et al., 2011; Preunkert, 2003). The consequences of high N loading on the environment have now been well documented and are evidenced in every sphere of the total environment (Aber et al., 1989; Clark et al., 2017; Elser et al., 2009; Matson et al., 2002). To address this issue, global efforts are underway to alleviate N inputs into ecosystems, aiming at "minimizing the consequent harm to humans and the environment" (International Nitrogen Initiative).

Nitrate concentrations and fluxes in soils and streams have often been used to assess the N saturation status in watersheds (Aber et al., 1989; Baron and Campbell, 1997; Lovett and Goodale, 2011). However, N exports in stream depend on multiple parameters such as basin topography (Balestrini et al., 2013; Clow and Sueker, 2000), land-cover (Barnes et al., 2014; Williams et al., 2016) and land-management (Barnes and Raymond, 2010; Burns et al., 2009; Lefebvre et al., 2007). As streams integrate many processes at the watershed scale, it is important to evaluate the respective contribution of biological and anthropogenic sources to downstream N exports, and to clarify the fate of deposited N in the environment, in order to understand the origin and the development of N saturation.

Montane ecosystems are particularly sensitive to increased N inputs by atmospheric deposition (Baron et al., 2000, 2005, 2011), as they are traditionally N-limited (Kaye and Hart, 1997). Critical loads for these ecosystems are among the lowest for pristine environments (Baron et al., 2011; Bowman et al., 2006; Nanus et al., 2017), making them vulnerable to long-range transport of atmospheric N emitted from distant sources (Mast et al., 2014; Wasiuta et al., 2015b). Nitrogen is mostly exported as nitrate (NO_3^-) from alpine and subalpine watersheds, typically showing a pulse at spring as soils subsurface NO_3^- reservoirs are flushed by snowmelt water (Kendall et al., 1995; Williams et al., 2009; Williams and Melack, 1991). Nevertheless, atmospheric deposition of N has also been shown to contribute significantly, either directly or indirectly, to year-round NO_3^- exports from montainous catchments (Bourgeois et al., in review; Hundey et al., 2016).

On the other hand, atmospheric deposition is a major source of N to urban areas, which receive much higher loads than adjacent environments (Bettez and Groffman, 2013; Fang et al., 2011; Hall et al., 2014; Rao et al., 2014; Templer et al., 2015). Local and regional emissions and subsequent deposition of fuel-combustion derived NO_x and ammoniac (NH_3) are responsible for such pattern (Galloway et al., 2004; Kean et al., 2000). NO_x are oxidized into NO_3^- within hours (Beirle et al., 2011), then scavenged from the atmosphere by wet and dry deposition (Hertel et al., 2012). In the atmosphere, NH_3 is in equilibrium with ammonium (NH_4^+), the other primary component of bulk N deposition. Because of the particular topography of urban basins (extended impervious surface, rapid precipitation runoff), urbanization can lead to high N exports to freshwater bodies (Groffman et al., 2004; Riha et al., 2014), with major ecological, economic and health consequences (Dodds et al., 2009).

So far, little attention has been paid to the control of atmospheric NO_3^- ($NO_3^-_{atm}$) exports from upland streams to urban reaches, down in the valley. Snowmelt derived groundwater, rather than surface water, was shown to drive NO_3^- exports across a montane to urban watershed in Salt Lake City, Utah, with little differences between snowmelt and baseflow hydrological regimes (Hall et al., 2016). Also, efficient soils subsurface N retention and denitrification were put forward to explain the low export of N from fertilizers or atmospheric deposition in streams. An increase in NO_3^- concentration was observed only when groundwater intercepted NO_3^- leaking from sewers. Other studies also hint at a high contribution of groundwater to baseflow in streams in various environments (Clément et al., 2003a; Ravazzani et al., 2016; Winter, 2007), with supposedly low exports of $NO_3^-_{atm}$. However, on occasional extreme hydrological events, enhanced exports of $NO_3^-_{atm}$ were generally measured in stormflow (Campbell et al., 2002; Pellerin et al., 2012; Rose et al., 2015b; Sebestyen et al., 2014).

Here, we combined isotopic and hydro-chemical techniques to evaluate the drivers of $NO_3^-_{atm}$ inputs and removal in streams along a montane to urban gradient. We hypothesized that, although the contribution from other sources (e.g., sewage, nitrification, fertilizers) is expected to increase in urban areas, higher atmospheric N

inputs should lead to increased $NO_3^-_{atm}$ exports along the gradient. We also hypothesized that urban stream $NO_3^-_{atm}$ exports should suffer less temporal variability than subalpine streams, if a well-equilibrated groundwater reservoir controls most of these streams discharge.

2.2.2 Material and methods

2.2.2.1 Study site and selected streams

The Lautaret pass is located in the central French Alps at 2058 m a.s.l., and dominates the Romanche Valley down to Grenoble (90 km away and 250 m a.s.l.). The Grenoble conurbation counts around 500 000 inhabitants, and is the biggest alpine metropolis in France (Figure 2-10).

We choose to sample 6 streams and one lake from the Lautaret pass to Grenoble, draining watersheds of increasing size and with distinct geomorphic and biogeographic characteristics (Table 2-4). Two alpine streams were sampled at *ca* 2000-m a.s.l., draining either the South exposed side of the Lautaret pass (S-upper montane, n=157) or its North exposed side (N-upper montane, n=93) where the stream is thought to be mainly fed by glacier melt. The mid montane stream (n=67) was sampled at *ca* 1600-m a.s.l., about 6-km away from the Lautaret pass. All three streams are tributaries of the Romanche (lower montane stream, n=127), which was sampled about 15-km away from the Lautaret pass at *ca* 1000-m a.s.l., before ending in the Chambon lake. The lake (*ca* 900-m a.s.l., n=29) is an artificial reservoir managed by the French national electricity company (EDF), about 21-km away from the Lautaret pass. The two urban sites were located around Grenoble (*ca* 210-m a.s.l.), either upstream from the main urbanized area (upper urban stream, n=48) or downstream from it (lower urban stream, n=45), and were separated by *ca* 8-km. Note that whereas the lower urban stream partly derives from the Romanche and the Chambon lake, the upper urban stream, called Isère, stems from a totally different alpine valley. The upper urban stream flows along residential areas, gardens and some arable fields prior to its sampling location whereas the lower urban site abuts industrial developments as well as residential neighborhoods (Dutordoir, 2014).

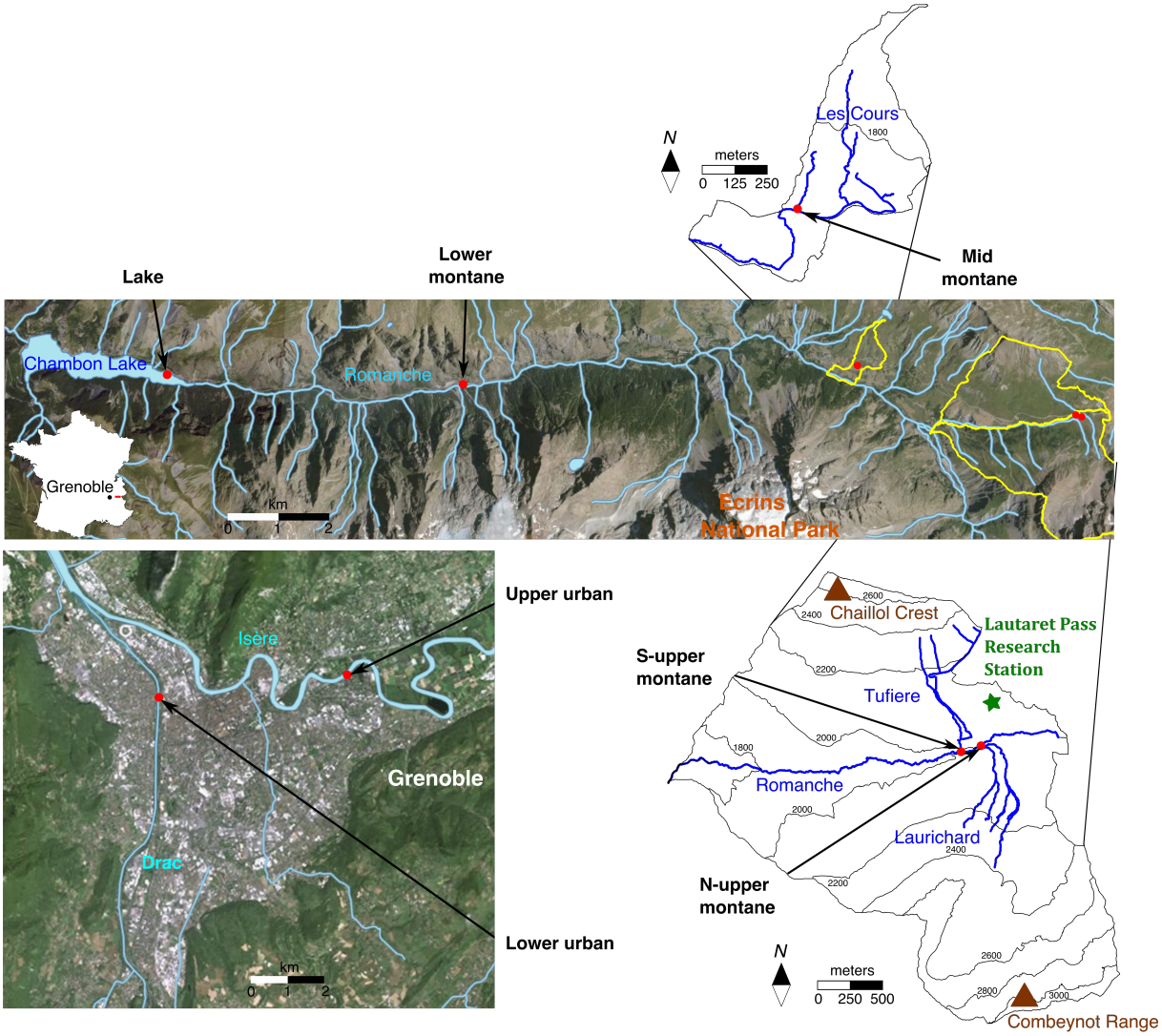

Figure 2-10 : Map of the Lautaret pass study area. The upper map represents the Romanche Valley in the central French Alps, situated 90 km away from the city of Grenoble. The boundaries of the S-upper, N-upper and mid montane watersheds are delimited in yellow. In green is the position of the Lautaret pass research station. The lower map illustrate Grenoble conurbation. Streams are shown in blue, and in red are the sampling locations. Maps were extracted from www.geoportail.fr.

Table 2-4: Characteristics of the Romanche Valley and Isere watersheds along the montane to urban gradient. Data were obtained using QGIS (Renaud, *personal communication*). The geology characteristics were inferred from Bodin (2007); Dutordoir (2014) and Mano et al. (2009).

Watershed	S-upper montane	N-upper montane	Mid montane	Lower montane	Upper urban	Lower Urban
Main regime	Snowmelt	Glacier melt	Snowmelt	Snowmelt	Snowmelt - Rainfall	Snowmelt - Rainfall
Altitude range (m a.s.l.)	1667-2725	1667-3155	1618-1980	1050-4088	210-2650	210-4088
Size (km^2)	3.4	5.3	0.5	220	5720	3600
Mean slope (%)	25	30	17	28	22	22
Geology	Calcareous	Granitic and ancient volcanic rocks	Calcareous	60% Marls and carbonates, 40% Metamorphic and crystalline rocks	77 % Marls and carbonates, 15 % Metamorphic and crystalline rocks, 8% glacial deposits	Crystalline rocks (granite, gneisses and amphibolites)
Land cover	30% alpine meadows (grazed), 27% uncovered, 26% abandoned grasslands, 13% terraced meadows, some habitations	Mostly uncovered and abandoned grasslands	80% terraced meadows (mown for hay), 13% alpine meadows, one village	60% Uncovered, 40% Forest or low vegetation, a few villages	74% Forest and semi-natural vegetation, 22% Agricultural fields, 4% Urbanized areas	81% Forest and semi-natural vegetation, 16% Agricultural fields, 3% Urbanized areas

2.2.2.2 Deposition and streams sampling, discharge and conductivity

Separated wet and dry deposition were collected using an atmospheric deposition collector (WADOS Kroneis GmbH Austria) at the S-upper montane site from April 2016 to April 2017. A heated moisture sensor connected to a moving lid above funnels ensured the separated collection. The deposition collector was

installed on the roof of the Lautaret pass alpine research station (SAJF, https://www.jardinalpindulautaret.fr) to reduce the impact of ground turbulences and input of soil particles. Samples were collected about every three weeks. Precipitation samples were kept at 4°C during the sampling period, then frozen until further analysis. After exposure to the atmosphere, the dry deposition funnel was rinsed with 500 mL of ultrapure water (18.2 MΩ.cm at 25°C), and the sample was stored at -20°C.

Stream and lake water was sampled at all sites according to the Niwot Ridge LTER protocol (Williams and Melack, 1991). In short, samples (total n=566) were collected manually in 1-L Nalgene bottles, previously washed 3 times in laboratory with MilliQ water and rinsed three times with stream water before collection. All samples were then kept at -20°C until further treatment. Water samples were collected on a weekly to monthly basis from January 2015 to December 2016, with increased sampling frequency in the upper tributaries from April to May 2016. During this intensive sampling period, water was collected using three automatic water samplers (Teledyne ISCO® 3700) every two or three hours at the S-upper and lower montane sites. Water conductivity, which was shown to be a good proxy of discharge (Weijs et al., 2013), and water temperature were also intensively monitored (2 minutes stepwise) over that period using CTD-Diver® sensors. Spring sampling was sporadic in the N-upper montane site because of persistent snow cover. Winter sampling was not possible at the lake site as it was frozen.

Discharge data was obtained from the national discharge-monitoring network (Banque Hydro) or measured every hour for both lower montane and urban site. Stream stage at the upper urban site was monitored every 30 minutes using water level gauge sensor (OTT®) at Grenoble Campus station (more details in Mano, 2008; Némery et al., 2013). Discharge was estimated from stage measurements by using rating curve (water level *vs* discharge) (Némery et al., 2013). Continuous discharge could not be measured at the upper and mid montane sites due to their torrential behavior. Precipitation data were obtained from the Alpine Mountain Meteorological Office Network (www.romma.fr) at the upper montane site and using a rain gauge

(Précis Mécaniques®) on a building roof of the Grenoble Campus, close to the upper urban site.

2.2.2.3 Chemical and isotopic analysis

All stream and deposition samples were left to unfreeze at ambient temperature prior to being filtered using 0.45-µm Whatman GD/X syringe filters linked to a peristaltic pump. They were subsequently analyzed for ion concentrations ($[NH_4^+]$, $[NO_3^-]$, $[SO_4^{2-}]$, $[Cl^-]$, $[Ca^{2+}]$) using a colorimetric technique (Gallery Plus, Thermo Fisher Scientific, Waltham, Massachusetts, USA) with an analytical error of ± 0.01 mg L^{-1}. Major ions such as sulfate and calcium and chloride are often used as hydro-chemical tracers of water flowpaths or water sources (Briand, 2014; Devito et al., 2000; Hall et al., 2016; Stoewer et al., 2015), and were measured to identify the dominating hydrological regimes in our studied sites.

All samples were concentrated on an anionic resin (0.6-mL AG 1-X8 resin, Cl^--form, Bio-Rad) with recovery efficiency over 98.5% (Erbland, 2011) and eluted with 10-mL of a 1-M NaCl solution for isotopic analysis (Templer and Weathers, 2011). Isotopic analyses of NO_3^- ($\Delta^{17}O$, $\delta^{18}O$ and $\delta^{15}N$) were conducted on an MAT 253 IRMS using an adapted version of the denitrifier method (Kaiser et al., 2007; Morin et al., 2008). More details about the experimental setup can be found elsewhere (Bourgeois et al., in review). The analytical errors were ± 0.4, 1.5 and 0.3 ‰ for $\Delta^{17}O$, $\delta^{18}O$ and $\delta^{15}N$ of NO_3^-, respectively.

A subset of stream, rain and snow samples (collected in winter 2015-2016 accordingly to Bourgeois et al., 2017 in review) were sent for δ^2H and $\delta^{18}O$ analyses on a Picarro L2130-i at the Laboratoire des Sciences et du Climat (LSCE) in Paris, France. The analytical error was ± 0.7 and 0.2 ‰ for δ^2H and $\delta^{18}O$ of H_2O, respectively.

2.2.2.4 NO_3^- sources appointment

A number of previous studies have used the dual isotopes approach ($\delta^{18}O$ and $\delta^{15}N$ of NO_3^-) to track the spatio-temporal variability of sources contribution to NO_3^- pools in a large variety of environmental matrixes (Campbell et al., 2002; Durka

et al., 1994; Elliott et al., 2009; Yang and Toor, 2016). Biochemical processes such as denitrification or assimilation have also been shown to enrich residual NO_3^- in heavier isotopes (here ^{15}N and ^{18}O) in distinguishable patterns (Granger et al., 2004, 2010a; Granger and Wankel, 2016; Treibergs and Granger, 2017). Pathways for NO_3^- removal in the environment have thus been thoroughly discussed (Clément et al., 2003b; Emmerton et al., 2001; Estrada et al., 2017; Fang et al., 2015; Lefebvre et al., 2007; Liu et al., 2013a; Wexler et al., 2014). However, the isotopic fingerprint of biological processes can lead to inaccurate NO_3^- source appointment in some cases, especially in delineating the respective contribution of the microbial and the atmospheric sources (Michalski et al., 2004b; Riha et al., 2014; Rose et al., 2015a).

In the past few years, a growing number of studies have used an isotopic particularity of $NO_3^-_{atm}$ to quantify the contribution of atmospheric deposition to terrestrial N pools (Bourgeois et al., in review; Costa et al., 2011; Hundey et al., 2016; Tsunogai et al., 2014). $NO_3^-_{atm}$ is enriched in ^{17}O due to its production pathways (i.e., oxidation of NO_x by O_3), showing a deviation from the Terrestrial Fractionation Line (Thiemens, 2006). $\Delta^{17}O$ is a quantification of this deviation, calculated as $\Delta^{17}O = \delta^{17}O - 0.52 * \delta^{18}O$ in the present work. $\Delta^{17}O$ value of $NO_3^-_{atm}$ generally ranges between 20 and 35 ‰ in temperate latitudes (Morin et al., 2009; Savarino et al., 2007), whereas $\Delta^{17}O$ value of NO_3^- from all other sources (industrial fertilizers, nitrification) or of biologically processed $NO_3^-_{atm}$, is 0 (Michalski et al., 2004b, 2015). In this study, we used these two distinct $\Delta^{17}O$ values as end-members in a simple mixing model to quantify unprocessed $NO_3^-_{atm}$ proportion (f_{atm}) in streams, according to Bourgeois et al., in review:

$$f_{atm} = \Delta^{17}O\text{-}NO_3^-_{sample} / \Delta^{17}O\text{-}NO_3^-_{atm} \qquad \text{(Eq. 2.2)}$$

The atmospheric fraction (f_{atm}) and the terrestrial fraction of NO_3^- ($f_{ter} = 1 - f_{atm}$) can be used to remove the isotopic influence of $NO_3^-_{atm}$ on samples, and allow for a better interpretation of biological processes that affect $\delta^{15}N$ and $\delta^{18}O$ (Dejwakh et al., 2012; Riha et al., 2014). $\delta^{18}O$ *vs* $\delta^{15}N$ plots have been intensively used to evaluate sources of N and potential processes (denitrification, assimilation) in the

environment (Burns et al., 2009; Durka et al., 1994; Griffiths et al., 2016; Kendall et al., 1995; Liu et al., 2013a). However, because of strongly distinct $\delta^{18}O\text{-}NO_3^-{}_{atm}$ values compared to $\delta^{18}O\text{-}NO_3^-{}_{ter}$, even a low f_{atm} can lead to scatter in a dual-isotope plot. Removing the atmospheric $\delta^{15}N$ and $\delta^{18}O$ components from environmental samples lead to an easier assessment of biological processes, such as assimilation in our case. This isotope correction was applied on our samples using the isotopic mass balances from Riha et al. Riha et al. (2014):

$$\delta^{18}O_{ter} = (\delta^{18}O_{sample} - \delta^{18}O_{atm} * f_{atm}) / f_{ter} \quad \text{(Eq. 2.4)}$$

$$\delta^{15}N_{ter} = (\delta^{15}N_{sample} - \delta^{15}N_{atm} * f_{atm}) / f_{ter} \quad \text{(Eq. 2.5)}$$

Where $\delta^{15}N_{atm}$ and $\delta^{18}O_{atm}$ were inferred from NO_3^- in wet and dry deposition (see section 2.2.3.2).

2.2.2.5 Fluxes of NO_3^- and $NO_3^-{}_{atm}$

N-NO_3^- fluxes were calculated at each site – when possible – on a weekly basis (F_m in kg-N w^{-1}) using the mean weekly discharge (Q_m in m^3 s^{-1}) and instantaneous concentrations ($[NO_3^-]_i$ in mg N-NO_3^- L^{-1}), as follows:

$$F_m = Q_m * [NO_3^-]_I \quad \text{(Eq. 2.6)}$$

Total specific annual stream fluxes of N-NO_3^- (F_{tot} in kg N ha^{-1} yr^{-1}) were calculated as the annual sum of weekly N-NO_3^- exports during the study period (2015 and 2016), as follows:

$$F_{tot} = (\sum_m Fm) / (\text{watershed area}) \quad \text{(Eq. 2.7)}$$

Finally, total annual N-$NO_3^-{}_{atm}$ fluxes (F_{atm}) were calculated for each year by multiplying the total annual stream flux of N-NO_3^- (F_{tot}) by the discharge-weighted annual mean f_{atm} (see Eq. 2.2) in the stream, according to Rose et al. (2015a):

$F_{atm} = F_{tot} * f_{atm}$ (Eq. 2.8)

When $[NO_3^-]$ or $\Delta^{17}O$ values were not available for a given date, they were replaced by the mean $[NO_3^-]$ or $\Delta^{17}O\text{-}NO_3^-$ values measured on the previous and the following dates. Note that the use of instantaneous $[NO_3^-]$ to calculate weekly streams $N\text{-}NO_3^-$ fluxes might over or under estimate the real $N\text{-}NO_3^-$ yield in streams.

2.2.2.6 Statistical analysis

A Mann-Whitney test was applied on river samples to determine whether mean concentrations and isotopic values were significantly different between streams. A Spearman test was applied to evaluate the correlation between stream water parameters (typically $\Delta^{17}O$, $\delta^{18}O$, $\delta^{15}N$ and ion concentrations). Differences and correlations were held significant when the *p* value reached a 0.05 credible interval. All statistical analyses were conducted using R software (v3.2.3).

2.2.3 Results

2.2.3.1 Precipitation and discharge

Cumulated precipitation was 537 and 609 mm in 2015 and 804 and 740 mm in 2016 at the upper montane and the urban sites, respectively. Discharge at the lower montane site reflects a snowmelt influenced hydrological regime. It peaked up to 30 $m^3\ s^{-1}$ in spring, and was significantly higher from April to October compared to the rest of the year. Discharge at both urban sites is consistent with a hydrological regime driven by snowmelt in spring-summer (main maximum), and rainfall in autumn (secondary maximum), a dual contribution similar to what was obtained in the Colorado Front Range (Cowie et al., 2017). At the upper urban site, discharge peaked up to 900 $m^3\ s^{-1}$ whereas maximum discharge was 300 $m^3\ s^{-1}$ at the lower urban site, a difference due to the streams draining two distinct watersheds (Figure 2-11).

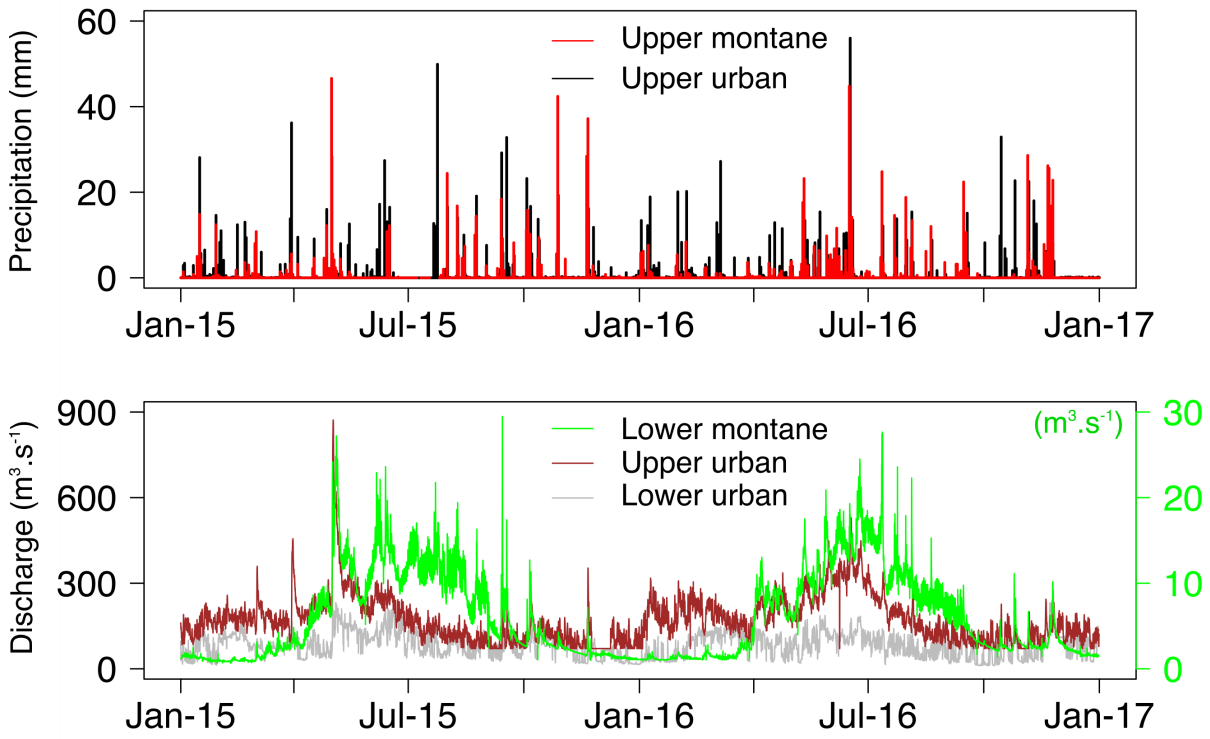

Figure 2-11: Hydrological conditions featuring a) daily precipitation (mm) and b) daily discharge (m^3 s^{-1}) at sites along the montane to urban gradient. Line colors denote sites as indicated in legend. Note the specific y-axis for discharge at the lower montane site.

2.2.3.2 Isotopic composition of NO_3^- in precipitation and streams

Mean annual $NO_3^-_{atm}$ isotopic values, reported in Table 2-5, were non-significantly higher in dry deposition than in wet deposition (significant only for δ^{15}N-NO_3^-), a pattern widely monitored at temperate latitudes (Beyn et al., 2014; Freyer, 1991; Mara et al., 2009). Mean Δ^{17}O-NO_3^- in precipitation and dry deposition were 26.4 ± 3.2 and 24.7 ± 3.5 ‰, respectively. These values are consistent with previously reported data for Δ^{17}O-$NO_3^-_{atm}$ (Costa et al., 2011; Hundey et al., 2016; Michalski et al., 2004b). The mass-weighted mean Δ^{17}O value for total deposition was 25.6 ± 3.3 ‰, and was used to quantify the atmospheric component of NO_3^- pools in streams (see section 2.2.2.4). Mean annual total δ^{18}O-$NO_3^-_{atm}$ (70.8 ± 7.2 ‰) and δ^{15}N-$NO_3^-_{atm}$ (-4.8 ± 5.9 ‰) are also consistent with a reservoir of exclusively $NO_3^-_{atm}$ (Kendall et al., 2007), and these values were used to correct samples from their atmospheric δ^{18}O and δ^{15}N components (see Eq. 2.4 and Eq. 2.5).

Table 2-5: Mean NO_3^- isotopic values in wet and dry deposition collected at the Lautaret pass from April 2016 to April 2017. The last row shows the inferred isotopic values of the atmospheric end-member used in this study.

	$\Delta^{17}O$ (‰)	$\delta^{18}O$ (‰)	$\delta^{15}N$ (‰)
Dry deposition (n=16)	26.4 ± 3.2	71.4 ± 6.3	-3.4 ± 5.6
Wet deposition (n=15)	24.7 ± 3.5	65.4 ± 8.1	-6.3 ± 1.7
Atmospheric end-member	**25.6 ± 3.3**	**70.8 ± 7.2**	**-4.8 ± 5.9**

Significantly higher annual mean $\Delta^{17}O\text{-}NO_3^-$ was measured in montane streams compared to urban streams, with the surprising exception of the mid montane site (1.0 ± 0.7 ‰), which exhibited the lowest values (Figure 2-12a). Both upper and lower urban, along with the mid montane streams were also characterized by the highest annual mean $\delta^{15}N\text{-}NO_3^-$ (3.7 ± 1.0 ‰, 4.9 ± 5.6 ‰ and 4.0 ± 2.0 ‰, respectively) (Figure 2-12c). The lake, fueled by the lower montane stream, presented the highest annual mean $\Delta^{17}O\text{-}NO_3^-$ (5.1 ± 1.8 ‰) and $\delta^{18}O\text{-}NO_3^-$ (8.6 ± 6.2 ‰), and the lowest $\delta^{15}N\text{-}NO_3^-$ (-0.2 ± 2.4 ‰) (Figure 2-12). It must be stressed out again that the lake was only sampled when unfrozen (i.e., late spring, summer and autumn), potentially biasing NO_3^- mean isotopic values at this site.

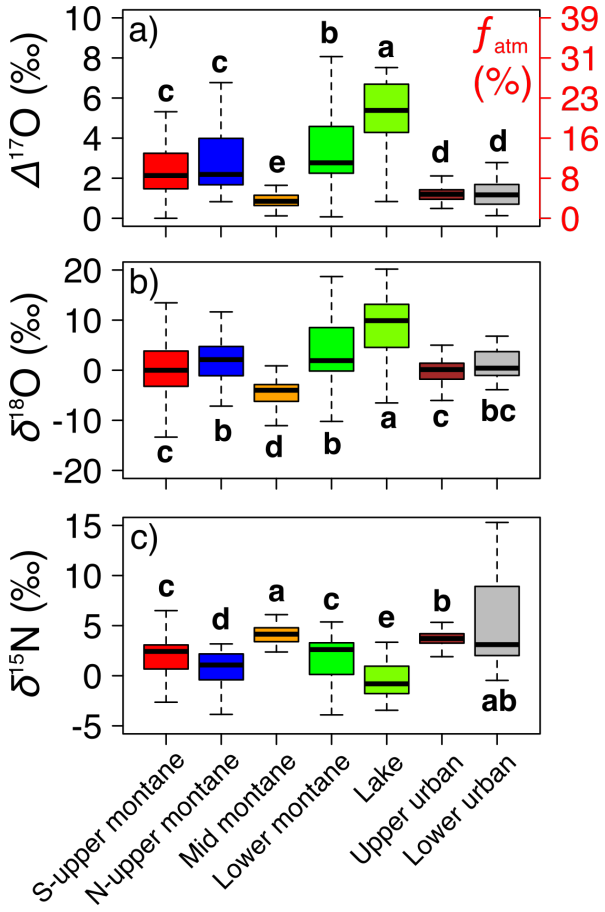

Figure 2-12: Two years isotopic composition of NO_3^- in streams, with a) $\Delta^{17}O$ (‰) (and corresponding f_{atm} (%) on the red y-axis), b) $\delta^{18}O$ (‰) and c) $\delta^{15}N$ (‰). Different letters denote significant differences in NO_3^- isotopic composition among sites (e.g., a site with *ab* letters is significantly different from sites with letters from *c* onwards. However, it means that it is not significantly different from sites with *a* or *b* letters).

2.2.3.3 Comparison of dissolved solutes across sites

Solutes concentration varied by up to 3 orders of magnitude among precipitation and streams samples (Table 2-5 and Figure 2-13). $[NH_4^+]$ was low in both dry and wet deposition at the S-upper montane site, and mostly (> 90 %) under the detection limit (< 0.01-mg L^{-1}) in all streams. $[NO_3^-]$ was significantly higher in rain samples compared to stream samples. The highest mean annual $[NO_3^-]$ was measured in the lower urban stream (1.4 ± 0.5-mg L^{-1}) and the lowest in the S-upper montane stream (0.2 ± 0.2-mg L^{-1}). $[NO_3^-]$ at the N-upper montane, mid montane, lower montane and upper urban sites were not statistically different (1.4 ± 1.3, 1.1 ± 0.6, 1.0 ± 0.6 and 1.1 ± 0.4-mg L^{-1}, respectively). $[SO_4^{2-}]$ and $[Ca^{2+}]$ were both very low in precipitation relative to streams. The S-upper montane stream exhibited the

highest annual mean [SO_4^{2-}] and [Ca^{2+}] (98.5 ± 39.5 and 44.5 ± 18.2-mg L^{-1}, respectively), followed by the upper urban stream (74.1 ± 26.9 and 35.2 ± 13.1-mg L^{-1}, respectively), and the lowest concentrations were measured at the N-upper montane site (22.1 ± 35.9 and 16.5 ± 16.0-mg L^{-1}, respectively). [Cl^-] was very low in precipitation samples and in most montane streams (mean values all < 3-mg L^{-1}), respectively. Higher annual mean [Cl^-] were measured in the urban streams (4.7 ± 1.8 and 16.6 ± 12.3-mg L^{-1} for the upper and lower urban stream, respectively).

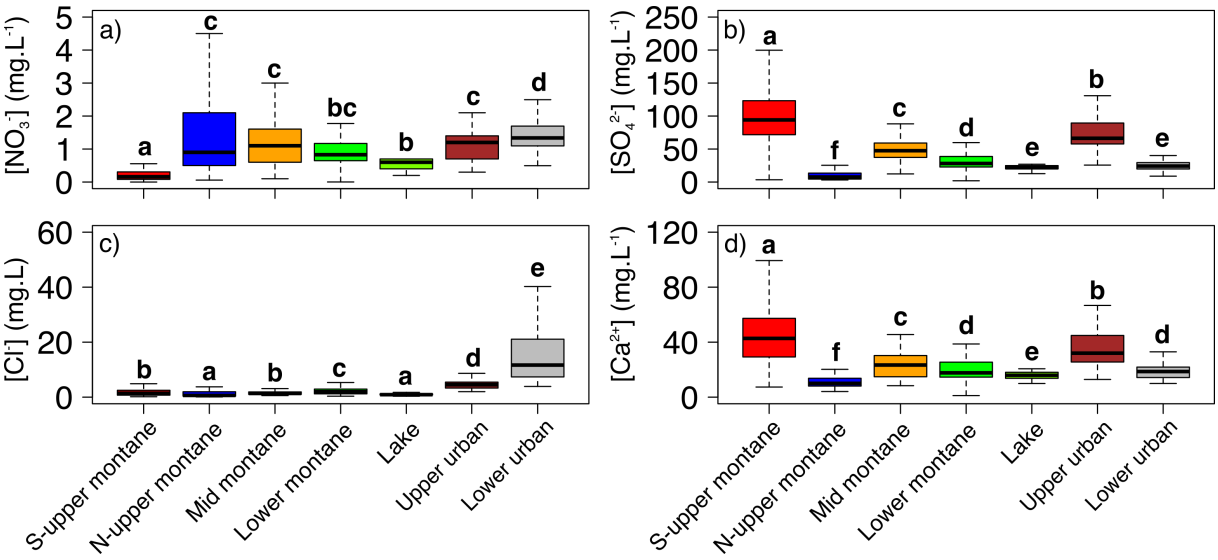

Figure 2-13: Two years solute concentrations in streams, with a) [NO_3^-] (mg L^{-1}), b) [SO_4^{2-}] (mg L^{-1}), c) [Cl^-] (mg L^{-1}) and d) [Ca^{2+}] (mg L^{-1}). Different letters denote significant differences in NO_3^- isotopic composition across sites. (e.g., a site with *ab* letters is significantly different from sites with letters from *c* onwards. However, it means that it is not significantly different from sites with *a* or *b* letters).

2.2.3.4 Trends in isotope composition of NO_3^- across sites

Seasonal variations of stream NO_3^- isotopes and corresponding f_{atm} are shown in Figure 2-14. The three montane streams followed a similar pattern of seasonal variations in 2015 and 2016. At the S-upper montane site, $\Delta^{17}O\text{-}NO_3^-$ and $\delta^{15}N\text{-}NO_3^-$ were significantly negatively correlated, with brief but high $\Delta^{17}O\text{-}NO_3^-$ peaks in spring, followed by a slow but continuous increase peaking late summer/beginning of autumn. At the N-upper site, a saw tooth pattern in summer and autumn occurred right after a small but temporally wider increase at snowmelt, in early summer. $\Delta^{17}O\text{-}NO_3^-$ and $\delta^{15}N\text{-}NO_3^-$ in the mid montane stream presented little variations throughout the seasons, apart from a raise in $\delta^{15}N\text{-}NO_3^-$ in spring / summer

2016. $\Delta^{17}O\text{-}NO_3^-$ and $\delta^{15}N\text{-}NO_3^-$ were significantly negatively correlated in the lower montane stream and in the lake, with significantly higher $\Delta^{17}O\text{-}NO_3^-$ from April to October – relative to the rest of the year – in a very similar way to discharge (Figure 2-11). Finally, $\Delta^{17}O\text{-}NO_3^-$ and $\delta^{15}N\text{-}NO_3^-$ were not correlated and did not vary much in urban streams, except for some occasional high $\delta^{15}N$ peaks in spring and winter 2015 at the lower urban site.

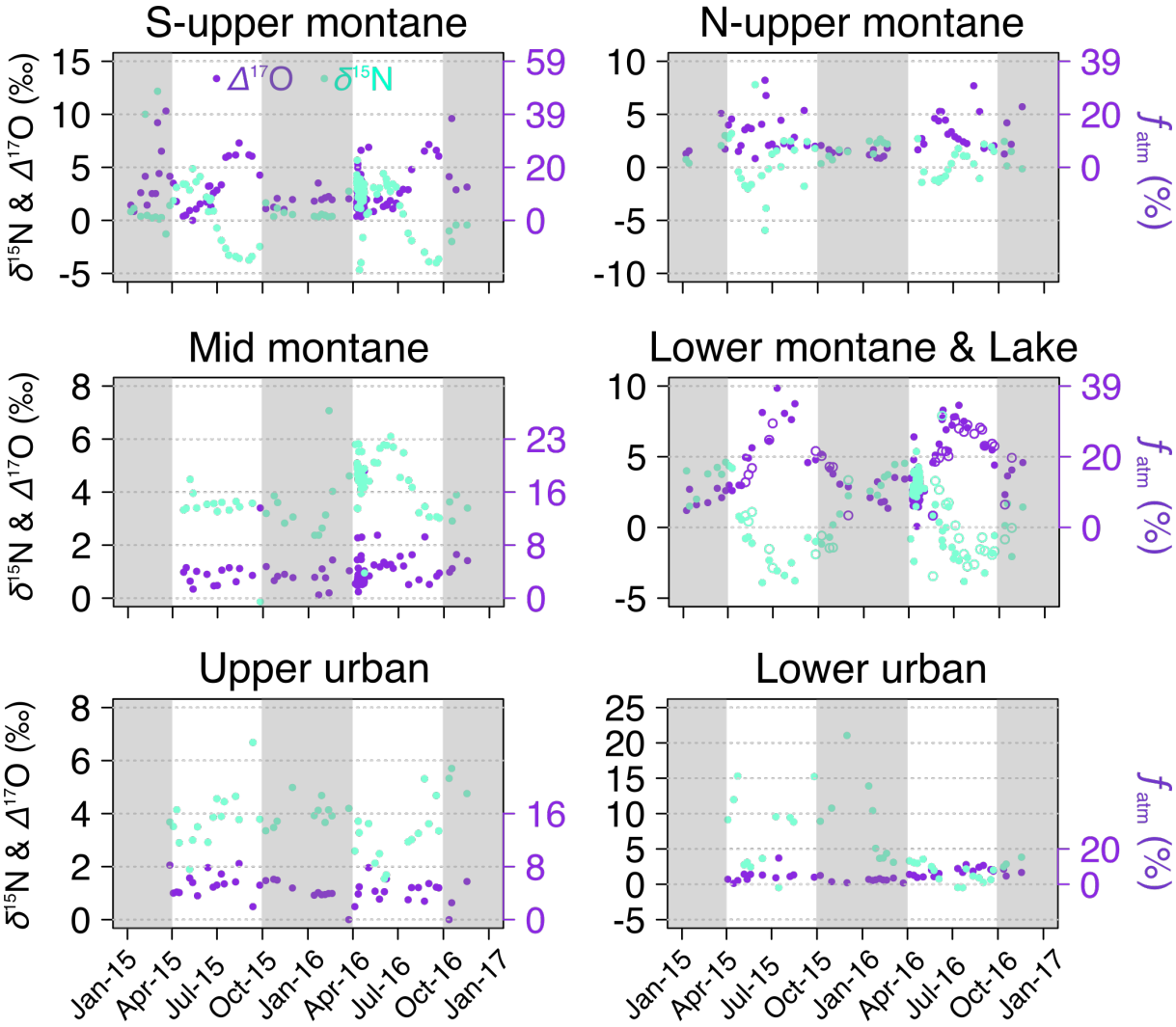

Figure 2-14: Seasonal variations of $\Delta^{17}O\text{-}NO_3^-$ and $\delta^{15}N\text{-}NO_3^-$ (‰) in streams. Point colors denote isotopes as indicated in legend. Range of corresponding f_{atm} (%) is indicated on the secondary y-axis. on the red y-axis). Highlighted in grey is the dormant season (October-April). Note the different y-axes scales across the different panels.

2.2.4 Discussion

2.2.4.1 NO_3^- exports in streams

Little differences in streams [NO_3^-] along the elevation gradient came as a surprise, as we expected the contribution from anthropogenic activities to streams N pool to increase when getting closer to urbanized areas (Groffman et al., 2004). The range of [NO_3^-] at the montane sites is consistent with measured concentrations in other Alpine valleys (Balestrini et al., 2013), and in elevated sites of the Colorado Front Range (Baron and Campbell, 1997; Campbell et al., 1995). The N-upper montane sites had a much wider range than the S-upper montane site, which is attributed to glacier melt influence (Barnes et al., 2014; Bourgeois et al., in review). [NO_3^-] in urban streams was low when compared to other concentrations measured in urban settings, such as the Tucson basin where values up to *ca* 62-mg L^{-1} were determined (Dejwakh et al., 2012) or up to *ca* 26-mg L^{-1} in the Gwynns Falls watershed (Groffman et al., 2004).

Even more surprising is the significantly higher contribution of atmospheric deposition as a NO_3^- source to streams at the montane sites relative to the urban sites – exception made of the mid montane site (Figure 2-12). The Chambon lake showed the highest f_{atm}, although it is possible that sampling of this reservoir exclusively in summer resulted in a biased estimate of mean annual $NO_3^-{}_{atm}$. High $NO_3^-{}_{atm}$ inputs in montane streams (up to 47%) clearly outline the influence of the melting snowpack releasing its load of atmospheric nitrate (Bourgeois et al., in review). Surprisingly, the mid montane stream exported the lowest proportion of $NO_3^-{}_{atm}$. Basins topography has been demonstrated to exert a strong control over NO_3^- dynamics in altitude catchments (Balestrini et al., 2013; Clow and Sueker, 2000), and much smoother slopes on this watershed (Table 2-4) are certainly responsible for this behavior by impeding direct runoff to stream during hydrological extremes (e.g., snowmelt). Low f_{atm} in urban streams is intriguing, as it poses a stark contrast with other findings, which showed an increasing f_{atm} in streams along an urbanization gradient (Riha et al., 2014), or high $NO_3^-{}_{atm}$ inputs in urban runoff (Yang and Toor, 2016). In urban areas, the combination of more impervious surface area coupled to

higher atmospheric deposition inputs is a strong driver that was expected to promote a higher proportion of $NO_3^-{}_{atm}$ to reach the urban streams, relative to montane sites.

We calculated the annual fluxes (kg-N ha^{-1} yr^{-1}) of total NO_3^- and total $NO_3^-{}_{atm}$ at the lower montane and both urban sites for 2015 and 2016 (Table 2-6). While urban streams generally produced higher total NO_3^- fluxes during the two years of the study, higher total $NO_3^-{}_{atm}$ fluxes are estimated at the lower montane site where $NO_3^-{}_{atm}$ represented *ca* 21% of the total annual NO_3^- flux. Elevated N deposition in the Alps – also illustrated by higher [NO_3^-] in wet and dry deposition compared to streams (Table 2-5) – is a well documented phenomenon (Kirchner et al., 2014; Rogora et al., 2006). Sustained nitrogen deposition in addition to the steep slopes of the lower montane watershed (Table 2-4) are likely to account for the higher total $NO_3^-{}_{atm}$ flux at the montane site. Grenoble conurbation is also remarkable in that its land cover is mainly constituted of forest and lower vegetation (64 %) followed by agricultural fields (24 %), and impervious surfaces (10 %) only a minor surface occupation (UE-SOeS, CORINE Land Cover, 2006). $NO_3^-{}_{atm}$ inputs are thus likely to move to multiple sinks, be biologically recycled or lost *via* different processes (e.g., denitrification, photolysis (Clément et al., 2003b; Ye et al., 2016)) before being collected by the urban streams (Rao et al., 2014). Furthermore, a strong decoupling between atmospheric N deposition and urban soils N cycling has also been evidenced recently, pointing at a distinct urban biogeochemical N cycle that would need further investigation (Decina et al., 2017). Finally, NH_3 – emitted by engine exhausts (Kean et al., 2000) and local fertilization (Decina et al., 2017) – can contribute significantly to urban atmospheric N together with NO_3^- (Decina et al., 2017; Rao et al., 2014) because of short atmospheric lifetime of ammonia (Hertel et al., 2012). In the montane sites, N deposition occurred mainly as NO_3^- (Table 2-5), further tipping the balance towards a higher proportion of $NO_3^-{}_{atm}$ exports in the lower montane stream.

Table 2-6: Mean discharge-weighted annual [NO_3^-] (mg L^{-1}) and f_{atm} (%), annual fluxes of total NO_3^- and total $NO_3^-{}_{atm}$ in streams and deduced annual contribution of $NO_3^-{}_{atm}$ yield to the total NO_3^- flux at three sites along the montane to urban gradient for years 2015 and 2016.

	Mean discharge-weighted annual [NO_3^-] (mg L^{-1})		Mean discharge weighted f_{atm} (%) based on $\Delta^{17}O$ (‰)		Total NO_3^- flux (kg N ha^{-1} yr^{-1})		Total $NO_3^-{}_{atm}$ flux (kg N ha^{-1} yr^{-1})		Contribution of $NO_3^-{}_{atm}$ yield to total NO_3^- flux (%)	
	2015	2016	2015	2016	2015	2016	2015	2016	2015	2016
Lower montane	1.0	0.9	22	19	1.9	1.4	0.4	0.3	21	21
Upper urban	1.0	1.2	5	4	2.0	2.6	0.1	0.1	5	4
Lower urban	1.7	1.3	4	5	4.8	2.1	0.2	0.1	4	5

2.2.4.2 Hydrology: a ubiquitous driver of $NO_3^-{}_{atm}$ exports?

Seasonal variations of $NO_3^-{}_{atm}$ are driven by hydrology

Seasonal variations of $NO_3^-{}_{atm}$ exports at the montane sites reflected the influence of hydrologic and topographic features of the basins, and are thoroughly discussed elsewhere (Bourgeois et al., in review). The S-upper montane site exports are likely governed by quick runoff to streams in the early stages of spring, followed by a diffuse resurgence of infiltrated snowmelt water in summer and autumn. Interestingly, the period between each event lasts about 5 months both in 2015 and in 2016, an indicator of either the water transit time in the calcareous substrate of the watershed or of the aquifer refill time before flushing to the stream. The N-upper montane stream is supposedly driven mostly by glacial melt, leading to higher [NO_3^-] than its southern counterpart by 1 order of magnitude (Figure 2-13). Occasional higher f_{atm} are linked with rainstorm events (Figure 2-3). The lower montane stream and the lake had very similar seasonal variations of $\Delta^{17}O$-NO_3^-, featuring the gradual melting of upstream snowpack throughout the growing season. The mid montane and the urban streams showed no marked seasonal variation, a behavior we attribute to the buffering effect of soils and the higher N cycling rates inherent to more

intensive land management treatments (Table 2-4), which probably dampened $NO_3^-{}_{atm}$ inputs to streams.

Groundwater dominates streams $NO_3^-{}_{atm}$ exports, to some extent

Year-round detectable $\Delta^{17}O\text{-}NO_3^-$ translates the continuous $NO_3^-{}_{atm}$ exports in all streams, even during baseflow (Figure 2-14). Most studies focusing on NO_3^- dynamics in runoff reported $NO_3^-{}_{atm}$ only during stormflow or snowmelt periods (Burns et al., 2009; Campbell et al., 2002; Pellerin et al., 2012). However, these studies used the dual isotope approach (*i.e.*, $\delta^{18}O$ and $\delta^{15}N$ of NO_3^-), which was demonstrated to not account so well for $NO_3^-{}_{atm}$ in streams compared to the $\Delta^{17}O$ tracer (Michalski et al., 2004b; Rose et al., 2015a). In a growing body of works using $\Delta^{17}O\text{-}NO_3^-$ in streams, $NO_3^-{}_{atm}$ presence during baseflow is a unifying feature (Rose et al., 2015a; Sabo et al., 2016; Tsunogai et al., 2016). In all these studies, f_{atm} ranged from 1-12 % in baseflow, except for a coniferous watershed in West Virginia, which led to f_{atm} of 54 % in stream, possibly due to low sampling resolution (n=4). Here, f_{atm} ranged from 1-20 % in all streams during the dormant season (in grey, Figure 2-14), except for high $\Delta^{17}O\text{-}NO_3^-$ peaks at the S-upper montane site in March 2015 due to a shorter winter this year (Bourgeois et al., in review).

Significant correlations between rock-derived solutes (SO_4^{2-} and Ca^{2+}) in all streams (Figure 2-15) points at groundwater contribution to streams as a unifying feature along the montane to urban gradient. Varying concentrations of rock-derived solutes are in good agreement with the geologic characteristics of each watershed (*i.e.*, highest concentrations in the S-upper montane and the upper urban streams draining calcareous basins, lowest concentrations in the N-upper montane stream draining a less erodible bedrock, see Figure 2-13 and Table 2-4). These findings are also consistent with $NO_3^-{}_{atm}$ exports being mainly driven by surface or subsurface runoff at the N-upper montane site, as opposite to underground flowpaths in the S-upper montane stream. However, even if groundwater contributes at all sites to streams water, its influence on streams ionic exports changes in the urban reaches.

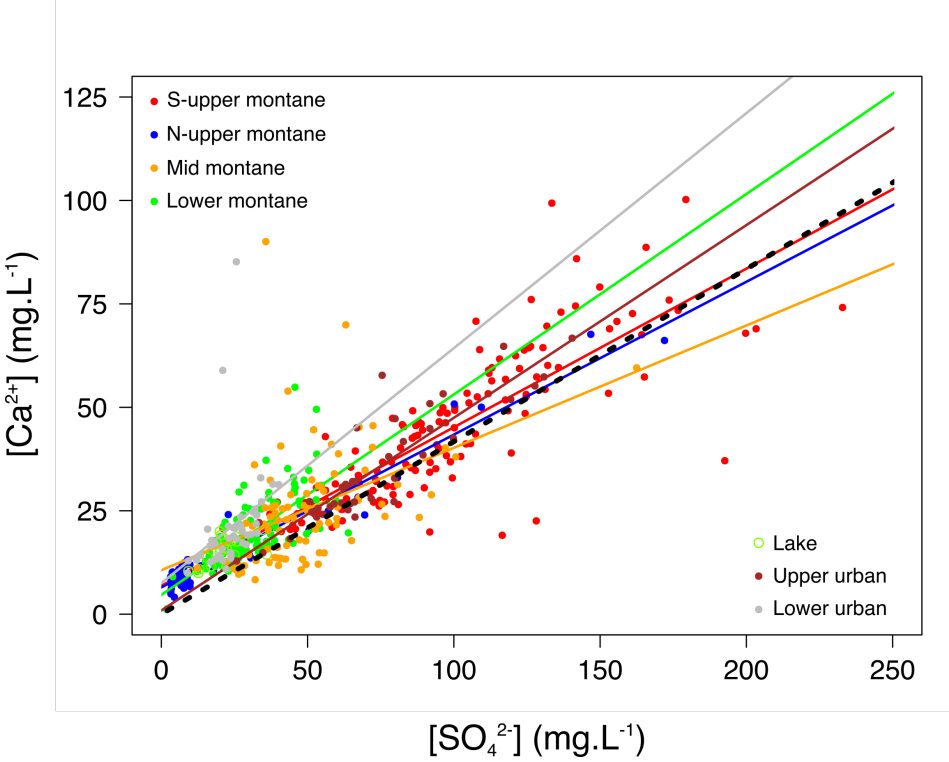

Figure 2-15: Relationships between $[SO_4^{2-}]$ and $[Ca^{2+}]$ at all sites. Linear regressions were plotted only when significant. Different colors denote different sites as shown by legend. The dashed black line shows the expected slope of 0.42 if both ionic species were in equimolar proportions.

No or near static correlations between either NO_3^- isotopes or conservative ions and discharge (Figure 2-16) imply that a geochemically equilibrated groundwater reservoir dominates stream exports at the urban sites, instead of surface runoff (Hall et al., 2016). In contrast, $\Delta^{17}O\text{-}NO_3^-$ increased significantly with discharge at the lower montane site, highlighting the influence of snowmelt on $NO_3^-{}_{atm}$ exports (Figure 2-16a). Decreasing weathering products concentrations with high flow also evidence the dilution of groundwater by surficial water at snowmelt (Figure 2-16d and f). No significant correlation of $[NO_3^-]$ with discharge in any stream implies a homogenized NO_3^- pool in groundwater reservoirs by infiltrated snowmelt inputs. In line with this hypothesis, a dual isotope plot of water suggested that snowmelt more than rain fueled the streams, even down to the outskirts of Grenoble (Figure 2-17). Other studies also reported similar findings of underground reservoirs fed by snowmelt in mountains vicinity (Brooks et al., 1999; Hall et al., 2016; Williams et al., 2009).

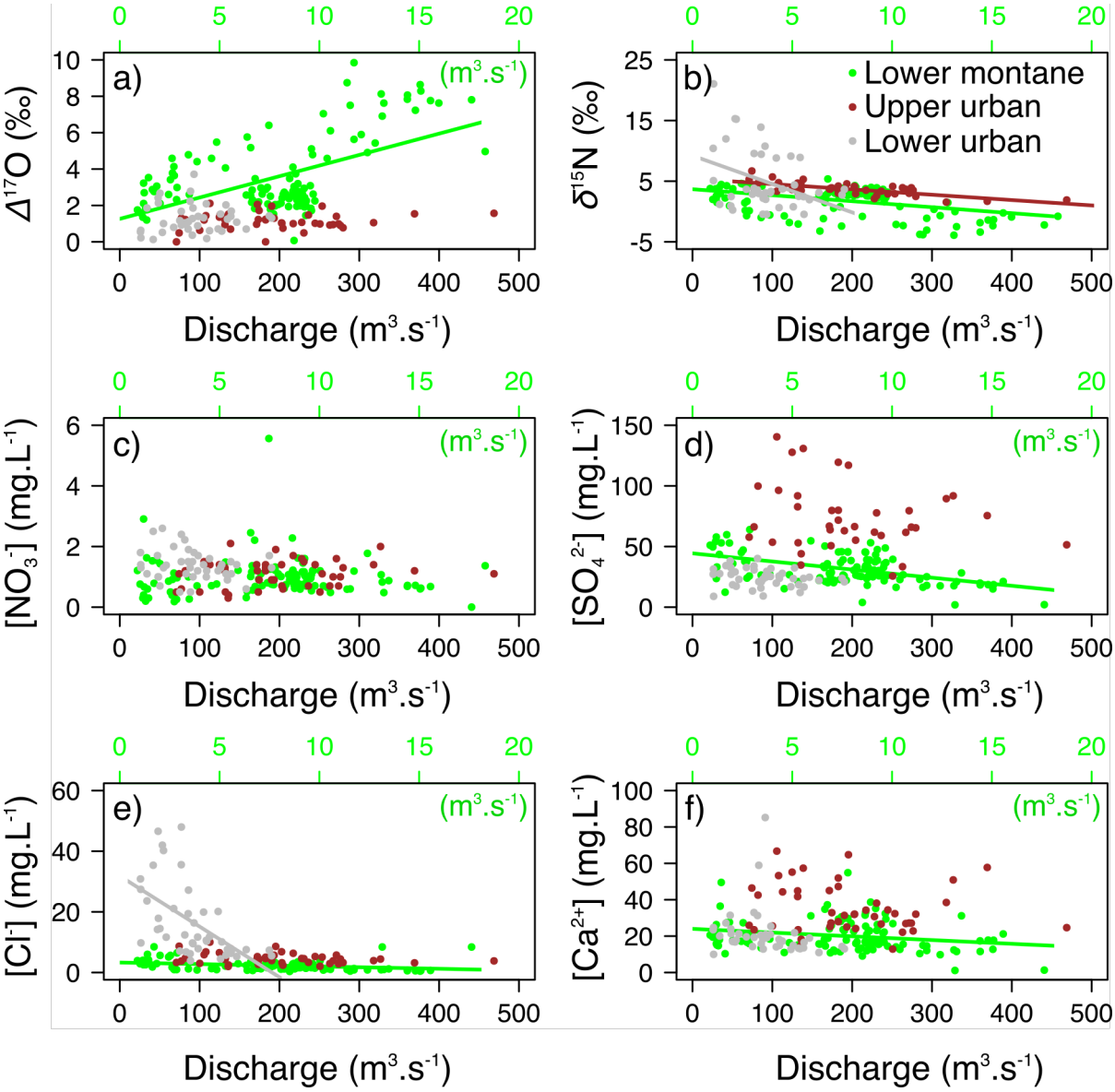

Figure 2-16: Relationships of nitrate isotopes and solutes concentration with discharge at three sites along the montane to urban gradient. Linear correlations were plotted only if significant. Note the differences in the y-axis scales among the panels, and the specific x-axis for discharge at the lower montane site (in green). Point colors denote sites as indicated in legend.

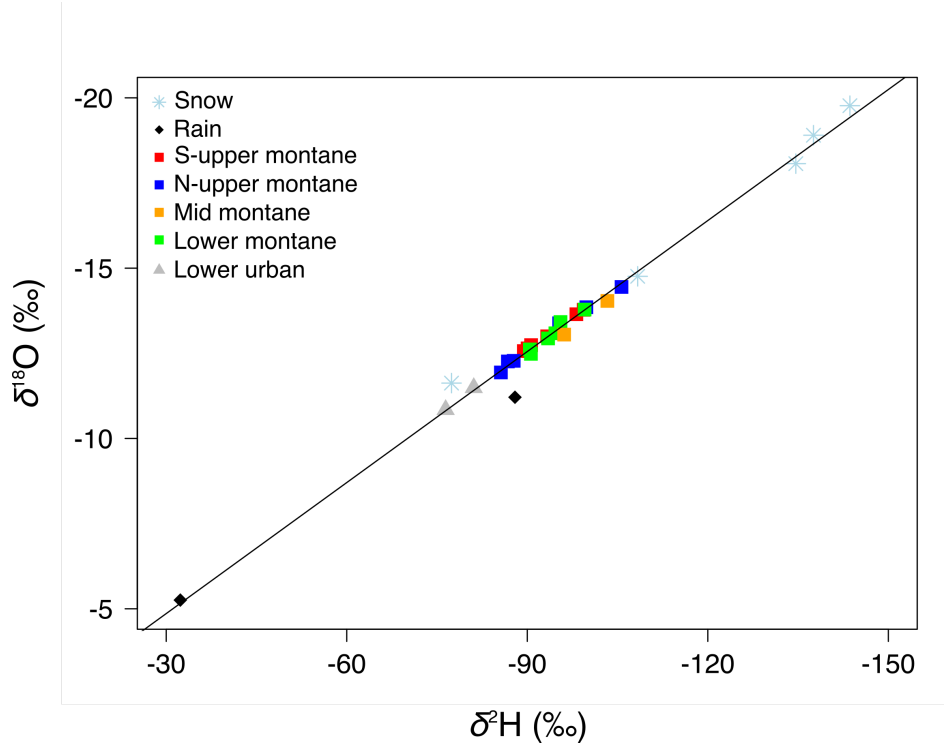

Figure 2-17: Dual isotope plot ($\delta^{18}O$ *vs* $\delta^{2}H$) of water in rain, snow and streams along the montane to urban watershed. The significant regression line (R^2 = 0.99) shows the dual contribution of snowmelt and rain to streams water. Different colors denote different sites as shown by legend.

Snowmelt period in montane streams

The intensive sampling campaign during spring 2016 at the S-upper montane and the lower montane sites, aiming at capturing the diurnal variability of NO_3^- concentration and isotopic composition, provided no evidence of specific temporal pattern for any solutes in the streams (data not shown). However, $\Delta^{17}O\text{-}NO_3^-$ at the S-upper montane site followed what looked like a diurnal pattern, even if difficult to significantly ascertain given the broad 95% confidence interval. Similar pattern is not seen in the lower montane stream (Figure 2-18). On the other hand, conductivity (at both sites) and discharge (lower montane site only) showed very pronounced diurnal variations, highlighting the hydrological influence of snowmelt during the day (Figure 2-18b and c), also consistent with previous studies in the same location (Mano et al., 2009).

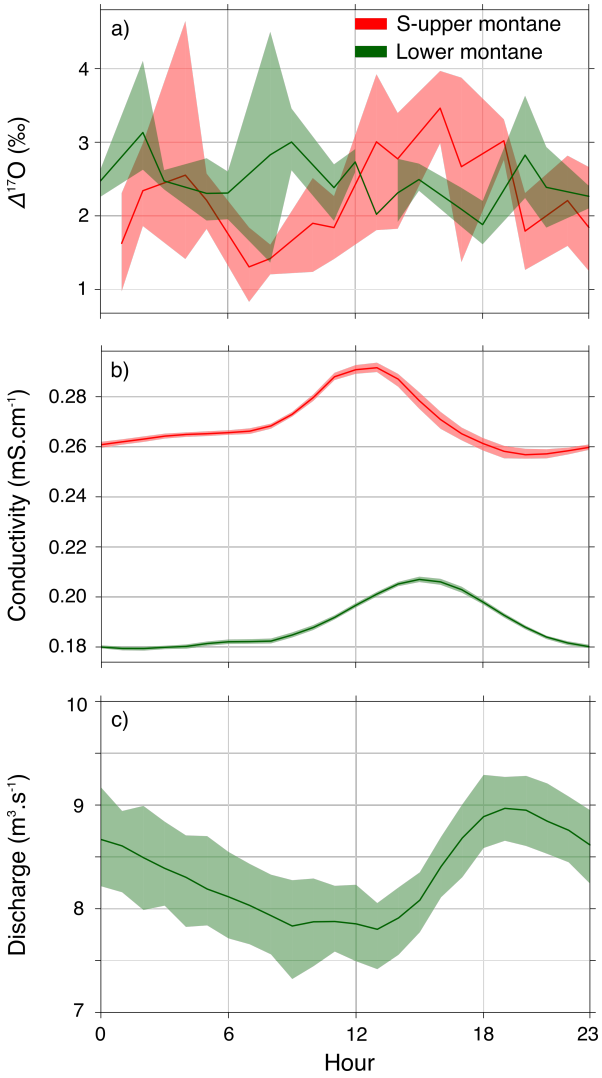

Figure 2-18: Diurnal variations of a) $\Delta^{17}O$ (‰), b) conductivity (mS.cm^{-1}) and c) discharge (m^3.s^{-1}). Variations were evaluated on period ranging from April 8 to April 24 in 2016, with a 3h-stepwise sampling frequency in streams. The envelope around the mean shows the 95% confidence interval.

At the lower montane site, discharge and conductivity were negatively correlated (Figure 2-19), certainly because their diurnal variations were driven by distinct hydrological regime (*i.e.*, baseflow for conductivity, snowmelt for discharge). That conductivity is controlled by baseflow is also supported by significant positive correlations between weathering solutes and conductivity at the S-upper montane site (Figure 2-19c). Therefore, assuming a similar relationship between conductivity and discharge would have existed in the S-upper montane stream, and considering that conductivity and $\Delta^{17}O\text{-}NO_3^-$ were also negatively correlated (Figure 2-19a), snowmelt-induced discharge certainly controlled the diurnal variations of $NO_3^-{}_{atm}$ exports. In contrast to another study showing in stream diurnal [NO_3^-] variations at

snowmelt in northern Vermont (Pellerin et al., 2012), we did not observe any significant temporal trend in any of the two streams here. However, given the shorter time period with specific focus on snowmelt and the much broader temporal resolution of sampling in our study, it is possible that we missed out some hot moments. It must also be emphasized that the lower montane stream was only on the rising limb of discharge when sampled, at the very beginning of snowmelt. Thus the absence of observed diurnal cycle at this site at this time may not be representative of day-night variations later in the season.

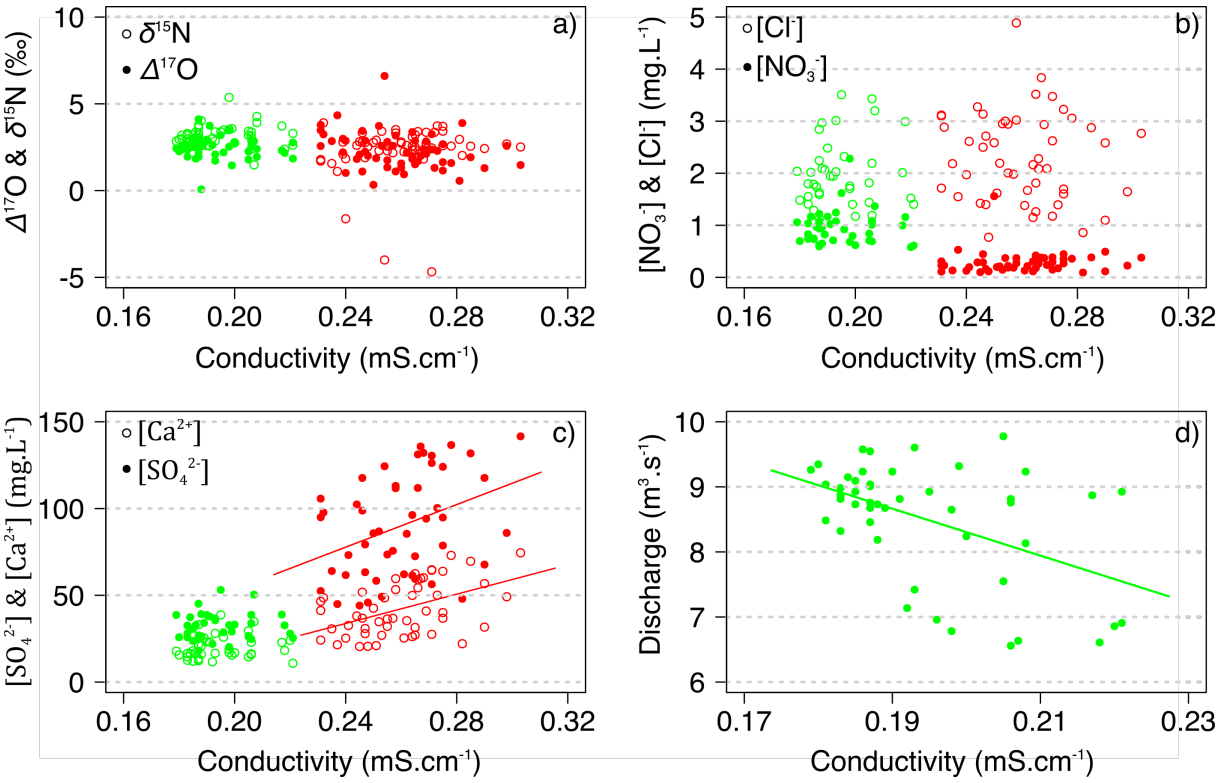

Figure 2-19: Relationships of NO_3^- isotopes, solute concentration and discharge with conductivity during snowmelt (April 8 to April 24 in 2016) at the S-upper montane (in red) and the lower montane (in green) sites. Linear regressions were plotted only if significant. Full or open circles feature either a) different NO_3^- isotopes or b) and c) different solute concentrations.

2.2.4.3 Sources of $NO_3^-{}_{ter}$

Isotopic values of $NO_3^-{}_{ter}$ (*i.e.*, NO_3^- corrected from the atmospheric component accordingly to Eq. 2.4 and Eq. 2.5) are reported in a dual isotope ($\delta^{18}O$ and $\delta^{15}N$) plot in Figure 2-20. This allows the evaluation of the respective contribution of terrestrial sources of $NO_3^-{}_{ter}$ to streams. Here, most $\delta^{15}N$-$NO_3^-{}_{ter}$ in streams span a 0

to 7 ‰ range, suggesting that nitrification of NH_4^+ is the main source of stream $NO_3^-_{ter}$ contents. This is in line with watersheds land cover consisting principally in natural or semi-natural vegetation (Table 2-4), where NO_3^- fertilizers use is unlikely. Only very few samples (n=4) had both $\delta^{15}N\text{-}NO_3^-_{ter}$ and $\delta^{18}O\text{-}NO_3^-_{ter}$ characteristic of NO_3^- fertilizers. It is complicated to segregate the substrate of nitrification (*i.e.*, deposited atmospheric NH_4^+ ($NH_4^+_{atm}$) or mineralized soil NH_4^+ ($NH_4^+_{org}$) that led to the production of $NO_3^-_{ter}$ in streams. Nitrification of $NH_4^+_{atm}$ and $NH_4^+_{org}$ produces NO_3^- with overlapping $\delta^{15}N$ ranges (Kendall et al., 2007). However, a fraction of samples, mostly from montane streams, had $\delta^{15}N\text{-}NO_3^-_{ter}$ lower than 0 ‰, consistent with nitrification of $NH_4^+_{atm}$ (Bourgeois et al., in review; T. Liu et al., 2013).

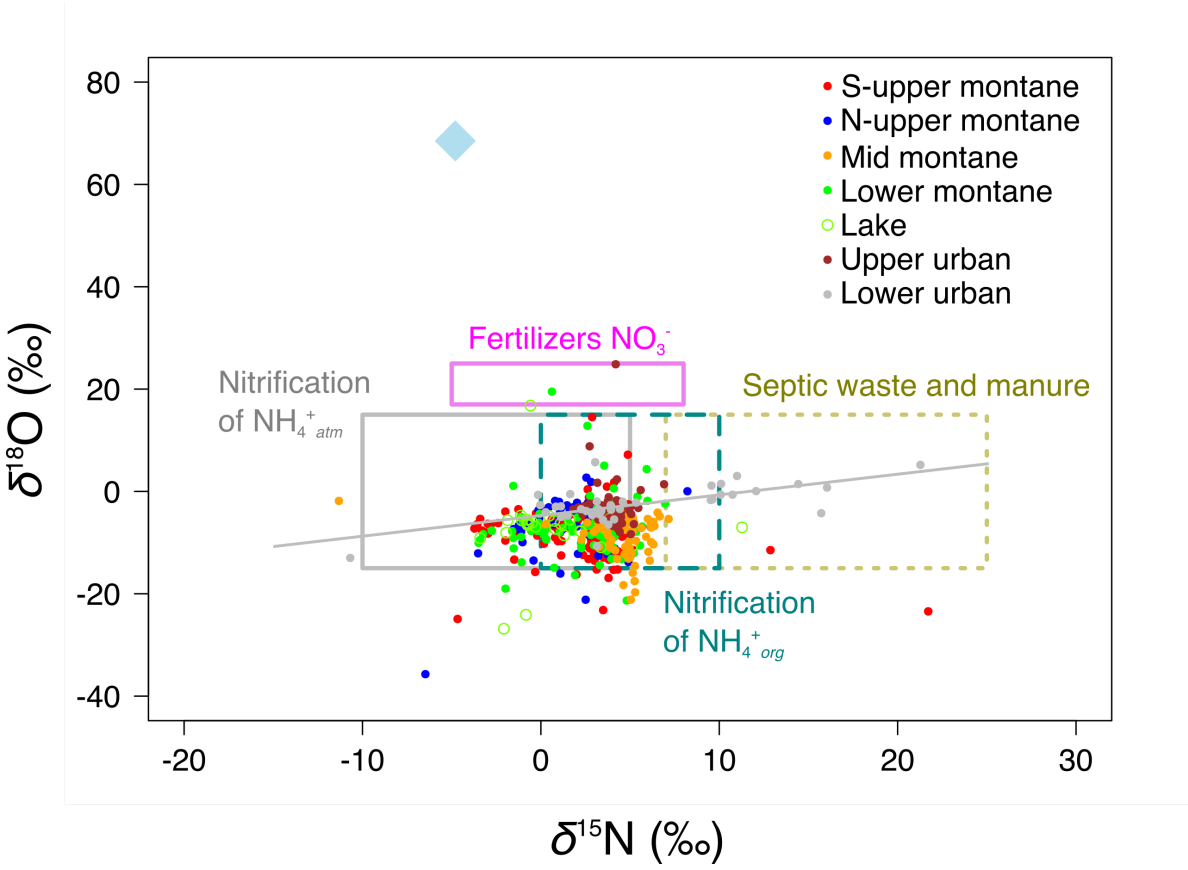

Figure 2-20: Dual isotopes plot ($\delta^{18}O$ *vs* $\delta^{15}N$) illustrating the mixing between distinct sources of $NO_3^-_{ter}$ (non-atmospheric) in streams. All isotopic values were obtained by the $\Delta^{17}O$ transform of NO_3^- collected at all sites (see section 2.2.2.4). The colored boxes represent the reported range for NO_3^- terrestrial sources, featuring atmospheric ammonium ($NH_4^+_{atm}$) in grey, mineralized ammonium ($NH_4^+_{org}$) in turquoise, manure or sewage derived NH_4^+ in beige and fertilizers NO_3^- in violet (Kendall et al., 2007). Linear regressions were plotted only when significant. The blue diamond reflects the isotopic composition of $NO_3^-_{atm}$ as measured in this study. Point colors denote sites as indicated in legend.

Weak negative correlations between $\delta^{18}O\text{-}NO_3^-$ and $\delta^{15}N\text{-}NO_3^-$ at all sites, exception made of the lower urban site, indicate that biological processes such as denitrification or assimilation do not control NO_3^- cycling in streams. Indeed, such processes should enrich residual $\delta^{18}O\text{-}NO_3^-$ and $\delta^{15}N\text{-}NO_3^-$ along a positively correlated line (Granger et al., 2008, 2010a; Kendall et al., 2007), in a similar fashion to what is observed at the lower urban site. Yet, that $\delta^{15}N\text{-}NO_3^-$ was significantly correlated to $[Cl^-]$ in this stream (data not shown) rather suggests that the high $\delta^{15}N\text{-}NO_3^-$ values are due to interception of sewage-originated wastewater (Hall et al., 2016). Decreasing $\delta^{15}N\text{-}NO_3^-$ and $[Cl^-]$ with discharge (Figure 2-16b and e) at this specific site also supports a groundwater origin of these nitrate pollution episodes.

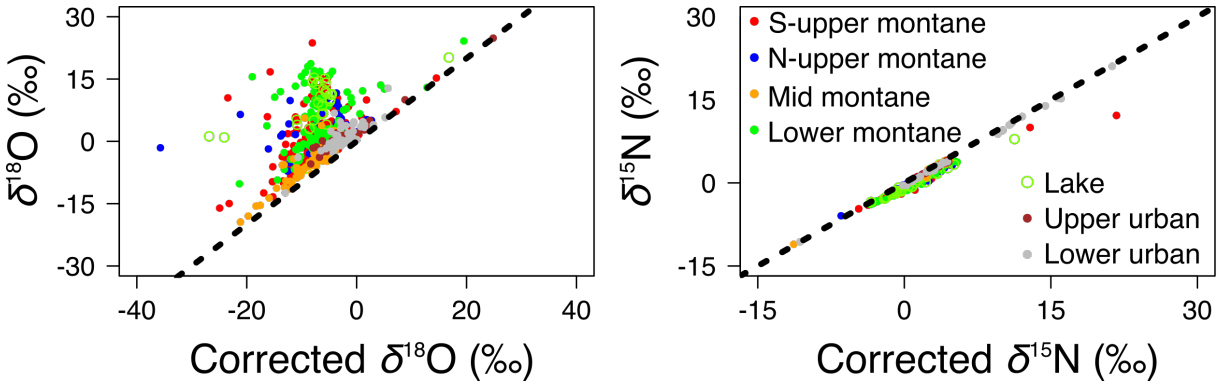

Figure 2-21: Dual isotope plots of $\delta^{18}O\text{-}NO_3^-$ (left) and $\delta^{15}N\text{-}NO_3^-$ (right). On the y-axes is the sample isotopic composition in streams as measured over the two years of this study, and on the x-axes is the corresponding isotopic composition after correction for the atmospheric component (see section 2.2.2.4). The dotted black lines feature the 1:1 slope expected if no $NO_{3\,atm}^-$ had contributed to streams N pool. Different colors denote different sites as shown by legend.

Very interestingly, $\delta^{18}O\text{-}NO_{3\,ter}^-$ values as low as -20 ‰ were obtained after removing the atmospheric imprint (Figure 2-20 and Figure 2-21). These results diverge considerably from widely reported high values of $\delta^{18}O\text{-}NO_3^-$ in freshwater systems (Burns and Kendall, 2002; Campbell et al., 2002; Griffiths et al., 2016; Jin et al., 2015; Riha et al., 2014; Tsunogai et al., 2016). The theoretical range for $\delta^{18}O\text{-}NO_{3\,nit}^-$ (*i.e.*, theoretical $\delta^{18}O\text{-}NO_3^-$ after nitrification) is -15 to 15 ‰, assuming soil-water and O_2 respectively contribute to NO_3^--O accordingly to $\delta^{18}O\text{-}NO_3^- = 1/3\ (\delta^{18}O\text{-}O_2) + 2/3\ (\delta^{18}O\text{-}H_2O)$ (Kendall et al., 2007). Here, a subset of 5 snow-water samples and 2 rain samples were analyzed for $\delta^{18}O$, with respective mean values of -16.6 ‰ and -8.2 ‰. Soil-water isotopes were not directly measured, but assimilated to

precipitation water isotopes. Assuming $\delta^{18}O$ values of air-O_2 around 23.88 ‰ (Barkan and Luz, 2005), we end up with $\delta^{18}O\text{-}NO_3^-$ = -3.3 (if the end-member is snow water) and +2.3 ‰ (if the end-member is rain water) for $NO_3^-{}_{nit}$. Even though this approach comes with a number of assumptions and caveats (Rose et al., 2015b; Snider et al., 2010), the calculated values are significantly higher – by *ca* 4 ‰ – than the mean annual $\delta^{18}O\text{-}NO_3^-{}_{ter}$ (Table 2-7). In a study focusing on an estuarine system in San Francisco Bay, it was postulated that rapid recycling of NO_3^- under low [NO_3^-] conditions (< 0.9-mg L^{-1}) could result in an increased incorporation of H_2O-O atoms into the NO_3^- molecule (Wankel et al., 2006). Another work focusing on nitrification in forests soils of central Japan attributed low $\delta^{18}O\text{-}NO_3^-$ to a combination of O atoms exchange between H_2O and NO_2^- and kinetic isotope fractionation associated with oxygen incorporation throughout the nitrification process in acidic soils (Fang et al., 2012). The latter hypothesis could possibly apply to our generally acidic subalpine soils characterized by slow N cycling (Robson et al., 2007), but further investigation is warranted to understand the cause of ^{18}O depleted NO_3^-. Anyhow, these findings suggest that atmospheric deposition of NO_3^- could have possibly been underestimated (e.g., up to 5 % in this study, see Table 2-7) in most studies focusing on NO_3^- dynamics and source partitioning in terrestrial and aquatic ecosystems.

Table 2-7: The second column gives the mean annual $\delta^{18}O\text{-}NO_3^-$ (‰) measured in streams. The third column shows the mean annual $\delta^{18}O\text{-}NO_{3\,ter}^-$ (‰) after sample isotopic compositions were corrected for the atmospheric imprint, and the proportion of $NO_{3\,atm}^-$ when using the corrected value as microbial end-member. Fourth column presents the calculated theoretical $\delta^{18}O\text{-}NO_{3\,nit}^-$ when using the approach detailed in section 2.2.4.3, and the proportion of $NO_{3\,atm}^-$ when using this theoretical value as microbial end-member.

	Mean annual $\delta^{18}O\text{-}NO_3^-$ (‰)	Mean annual $\delta^{18}O\text{-}NO_{3\,ter}^-$ (‰) and deduced % $NO_{3\,atm}^-$	Calculated $\delta^{18}O\text{-}NO_{3\,nit}^-$ (‰) and deduced % $NO_{3\,atm}^-$
S-upper montane	0.7	-7.7 (11%)	-3.3 (6%)
N-upper montane	2.8	-6.3 (12%)	-3.3 (9%)
Mid-montane	-4.9	-8.0 **(4%)**	-3.3 **(0%)**
Lower montane	4.1	-6.8 (15%)	-3.3 (11%)
Lake	8.6	-7.3 (22%)	-3.3 (17%)
Upper urban	1.1	-2.6 **(5%)**	2.3 **(0%)**
Lower urban	0.9	-2.8 **(5%)**	2.3 **(0%)**

2.2.5 Conclusions

Ours results showing higher $NO_{3\,atm}^-$ exports in a montane stream relative to urban streams have several key implications. First, we shed light on the contribution of snowmelt-derived groundwater to year-round $NO_{3\,atm}^-$ exports in all streams at baseflow. This suggests that contamination of groundwater by $NO_{3\,atm}^-$ may be a widespread phenomenon, regardless of emitting sources proximity (Dejwakh et al., 2012; Dietzel et al., 2014; Stoewer et al., 2015). Second, we provide evidence that hydrological events (e.g., snowmelt) are the main controls of upland $NO_{3\,atm}^-$ exports, whereas a chemically equilibrated groundwater reservoir dominates discharge in urban streams. In a context of climate change, with temporally shorter and shallower snow coverage of altitude catchments, decreasing exports of $NO_{3\,atm}^-$ by snowmelt water could result in proportional $NO_{3\,atm}^-$ enrichment of alpine soils. However, how this would correlate with otherwise reported snow cover removal effects on microbial communities, N retention, plants biomass and soil respiration is a complex question

yet to be addressed (Brooks et al., 2011; Gavazov et al., 2017; Sorensen et al., 2016; Vankoughnett and Henry, 2013). Third, we emphasize on the convenient association of $\Delta^{17}O$, $\delta^{15}N$ and $\delta^{18}O$ as a potent tool to unravel the respective atmospheric and terrestrial sources contribution to NO_3^- pools. The lower $\delta^{18}O\text{-}NO_3^-{}_{ter}$ than theoretically expected suggests that atmospheric deposition could have been underestimated in most pristine and urban environments. We recommend that more work be conducted using the triple isotope technique to revise our assessment of $NO_3^-{}_{atm}$ ubiquity in the environment.

Acknowledgments

This study was supported by grants from the Labex OSUG@2020 ("Investissements d'avenir" - ANR10 LABX56), the ARC - Environnement Région Rhone-Alpes, the Grenoble-Chambéry DIPEE CNRS. This work also benefited from the National Research Agency supports ("Investissements d'avenir" - ANR11 INBS-0001AnaEE-Services and "FloodScale project" - ANR 2011 BS56 027) and from the SAJF research station (UMR 3370, UGA-CNRS) infrastructures and competences. The study took place on a Long Term Ecological Research site of the ZAA (Zone Atelier Alpes) and the Isère Campus monitoring site is a CNRS-labeled site of the ZABR (Rhone Basin Long Term Ecological Research site). We would like to thank G. Nord, J.-L. Jaffrezo, F. Masson, V. Lucaire, E. Vince and C. Arnoldi for help with either laboratory or field work. We also want to acknowledge J. Renaud for help with SIG.

2.3 Synthesis

2.3.1 Summary of the main results

In the first part of this chapter (section 2.1), we specifically focus on the seasonal dynamics of $NO_3^-{}_{atm}$ proportion in three subalpine streams. Streams exhibit very different patterns, which are attributed to the different topographical and geomorphic characteristics of the watersheds. The nature of the watershed bedrock, the mean slope and the land cover are thought to be controls of particular relevance in this study. Interestingly, **snowmelt** leads to an increased $NO_3^-{}_{atm}$ proportion in all three streams, but $\Delta^{17}O\text{-}NO_3^-$ is decoupled from $[NO_3^-]$. This indicates that the ionic pulse observed in most alpine settings at snowmelt likely results from a flushing of subsurface soil N reservoirs. Using a combined $\Delta^{17}O\text{-}NO_3^-$ and $\delta^{15}N\text{-}NO_3^-$ plot, we also point at the possibly high contribution of **atmospheric ammonium** trapped in the snowpack to subalpine soils N pool. If this were more widely confirmed, these findings would shed light on an important, but overlooked, sensitivity of seasonally snow-covered catchments to ammonium deposition, rather than nitrate.

In the second part of the previous chapter (section 2.2), we show that the contribution of $NO_3^-{}_{atm}$ to the total NO_3^- fluxes in streams decreases when nearing urban settings. This suggests that atmospheric N deposition relative implication in **freshwaters eutrophication** is more important at the subalpine stage compared to the urban stage. However, year-round quantifiable $NO_3^-{}_{atm}$ in all streams point at **groundwater contamination** by atmospheric N deposition, echoing findings from other studies (section 2.2.4.1). The main other source of nitrate to streams is the nitrification of soil ammonium, with surprisingly low inputs from fertilizers and sewage wastewater in urban streams. Finally, the low $\delta^{18}O\text{-}NO_3^-{}_{ter}$ measured in all streams come as an intriguing feature, and differ from the values commonly reported in literature (section 2.2.4.3). If the reasons why are yet to be addressed, it raises a significant questioning on the conclusions drawn in other NO_3^- source partitioning studies that relied only on $\delta^{18}O$- and $\delta^{15}N\text{-}NO_3^-$. Even further, it indicates that **conjoint monitoring of $\Delta^{17}O$, $\delta^{18}O$ and $\delta^{15}N$ of nitrate should be more**

systematically performed when the aim is to assess how much atmospheric N deposition contributes to a system.

2.3.2 Results situated in the conceptual framework

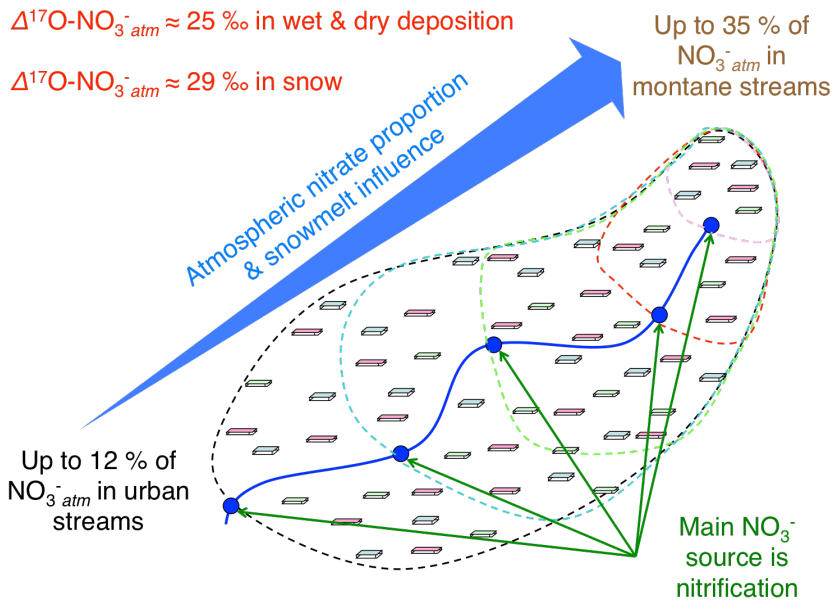

Figure 2-22: Main results from the chapter 2 placed in the study context.

2.3.3 Linkage with the other terrestrial compartments

Streams are often used to assess the stage of N saturation of a given ecosystem (see section 2.1.4.4). High NO_3^- leaching rates, and therefore high $[NO_3^-]$ in streams are usually associated with elevated N saturation status. Here, variable $[NO_3^-]$ from a subalpine stream to the other, and seasonal trends in $\Delta^{17}O\text{-}NO_3^-$ rather point at a kinetic saturation of the system. But do snowmelt and precipitation really impede atmospheric $NO_3^-{}_{atm}$ uptake or immobilization in soils, and therefore limit the ecological impact of atmospheric N deposition? Is $NO_3^-{}_{atm}$ retained in soils? If so, is it rapidly processed by microorganisms, indicating that N-limitation is still a controlling factor of net primary production? These are the questions that arise after this chapter, and they will be addressed in the following one.

3 Atmospheric nitrate in soils: seasonal dynamics, land use influence and implication for N turnover

This chapter describes the breakthroughs in our understanding of the N cycle in subalpine meadows. Three specific meadows, with land use spanning a management gradient, are more specifically the object of the study presented here. The section 3.1 describes the temporal variations of $NO_3^-{}_{atm}$ in three subalpine meadows, and the influence of the management treatments on $NO_3^-{}_{atm}$ retention in soils. Based on isotopic considerations, nitrification sources and pathways are also discussed and constrained. The section 3.2 provides complementary information relative to microbial genes abundance in soils, and presents future directions aiming at coupling isotopic and genomic data. A summary of the scientific conclusions is provided in section 3.3, and the main findings will be put in perspective with the terrestrial N cycle in subalpine meadows.

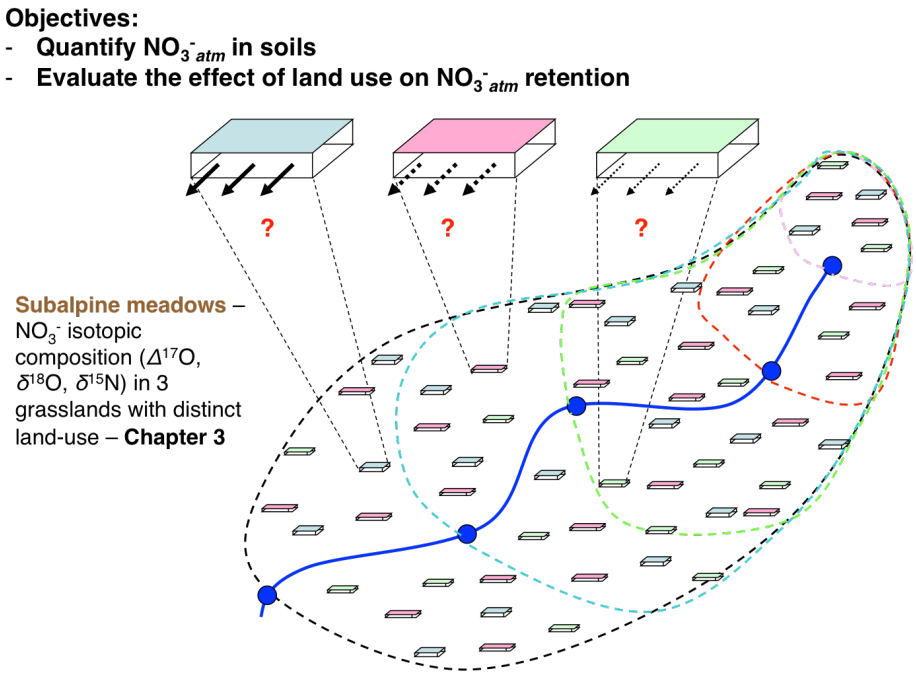

Figure 3-1: Positioning of this chapter in the conceptual framework of this study, and related objectives it will answer to.

3.1 Drivers of nitrate turnover in subalpine soils at the Lautaret pass

This chapter is still on-going work, and results obtained so far are presented under the form of a scientific article to comply with the general format of this Ph.D. manuscript.

Abstract

It is well established that increasing nitrogen (N) inputs in ecosystems generate a cascade of various ecological and environmental issues (e.g., eutrophication, water quality, biodiversity loss). However, the usual specific markers to trace the fate of N in ecosystems still strongly limits our capacity to reveal the mechanisms and processes at play, and thus our capacity to propose conservative actions. Here, we propose a completely new strategy to track atmospheric N inputs into a subalpine ecosystem. We coupled monthly $\delta^{18}O$, $\delta^{15}N$ and concentration measurements of nitrate (NO_3^-), common tools for probing N in ecosystems, with $\Delta^{17}O\text{-}NO_3^-$, a conservative tracer of atmospheric N deposition, in three subalpine grasslands soils with distinct management at the Lautaret pass, French Alps.

We provide isotopic evidence that on average 0-6 % of soil NO_3^- derives directly from atmospheric deposition, without undergoing any microbial reprocessing. This proportion was lower than expected, and point at several removal mechanisms that strongly depend on land management. Low and seasonally constant $\delta^{18}O\text{-}NO_3^-$ in all meadows are *in situ* evidence of kinetic isotopic effects during nitrification, and potentially equilibrium isotopic fractionation. Low but temporally variable $\delta^{15}N\text{-}NO_3^-$ in all fields imply a combination of multiple sources and non-conservative behavior. Kinetic fractionation during mineralization and nitrification, atmospherically deposited ammonium and denitrification are the most likely candidates to explain the observed variability. Altogether, these results suggest that subalpine meadows are still N limited. We also strongly recommend that future NO_3^- isotopic studies in environmental matrixes as complex as soils do not solely rely on isotopes to decipher the processes at play, but also draw on ancillary data.

3.1.1 Introduction

Understanding the fate of deposited atmospheric nitrogen (N) in pristine environment is essential to assessing and mitigating the ecological consequences of increasing atmospheric N deposition worldwide (Fowler et al., 2013; Galloway et al., 2004; Holtgrieve et al., 2011). Past studies have indicated that atmospheric N deposition has an important function in N cycling of alpine and subalpine ecosystems (Baron et al., 2000, 2005; Burns, 2004). N critical load – defined as the minimum input of a pollutant before an "harmful effect" to an ecological sensitive indicator (Bowman et al., 2006) – for these systems is estimated to be 1-4 kg-N ha^{-1} yr^{-1}, ranging among the lowest established for natural environments (Baron et al., 2011; Bobbink et al., 2011; Nanus et al., 2017). In the European Alps, atmospheric deposition has delivered N loads around 10-fold higher than this critical threshold (Kirchner et al., 2014; Rogora et al., 2006), a seemingly unifying feature across mountainous regions globally (Bai et al., 2010; Baron et al., 2011; Boutin et al., 2015; Phoenix et al., 2006; Zong et al., 2016).

Remote subalpine grasslands are generally characterized by nutrients-poor soils (Körner, 2004), and even low atmospheric N inputs can substantially increase bioavailable N contents, which was shown to particularly affect plant species composition and biodiversity in these systems (Bassin et al., 2013; Boutin et al., 2017; Stevens, 2004). However, there are contrasting reports in the literature on the effects of deposited atmospheric N on grassland soil N pools and turnover rates (Bassin et al., 2015; Clément et al., 2012; Phoenix et al., 2003). Bassin et al. (2015) conducted ^{15}N tracer studies and concluded that subalpine soils N pools remained unaffected by atmospheric N deposition. Similarly, Clément et al. (2012) documented undisturbed N cycling rates in subalpine meadows after snowmelt, considered as a « hot moment » for nutrients bio-availability because of the sudden transfer of stocked atmospheric N in snow to surrounding compartments (Bilbrough et al., 2000; Robson et al., 2007; Williams and Melack, 1991). On the other hand, Phoenix et al. (2003) reported that 38-89 % of deposited atmospheric N was retained in grassland soils. Resolving the fate and impact of atmospheric N in soils upon deposition is therefore crucial for understanding its impacts on subalpine ecosystems.

To further complicate the picture, other factors have been shown to play an important role in controlling subalpine soil N pools and turnover. Seasonal snow cover is a major driver of change in microbial communities (Jusselme et al., 2016; Lipson et al., 2002; Schmidt and Lipson, 2004), with in turn consequences on N cycling (Legay et al., 2013, 2016). Agricultural land-management is also deemed responsible for altering N processes in subalpine grasslands, either *via* past (Gill, 2014; McGovern et al., 2014) or current (Robson et al., 2007, 2010) practices. To decouple atmospheric N deposition effects on soils N cycling from other factors of change is challenging, and new techniques are needed to further comprehend what becomes of atmospheric N in soils.

Recently, a new isotopic approach has been shown to effectively discriminate atmospheric nitrate ($NO_3^-{}_{atm}$) from terrestrial nitrate in soils ($NO_3^-{}_{ter}$), and enable quantitative insights into atmospheric $NO_3^-{}_{atm}$ contribution to the environment (Michalski et al., 2004b). Most terrestrial reservoirs of NO_3^- show mass-dependent relationships between its oxygen (O) isotopes, accordingly to $\delta^{17}O \approx 0.52 * \delta^{18}O$ (Miller, 2002; Young et al., 2002). A noticeable exception to this rule is ozone (O_3), which exhibits equal ^{17}O and ^{18}O enrichment upon formation (Thiemens and Heidenreich, 1983). This deviation from the terrestrial fractionation line is most commonly defined as $\Delta^{17}O = \delta^{17}O - 0.52 * \delta^{18}O$. $NO_3^-{}_{atm}$ is characterized by high $\Delta^{17}O$ values (20 - 35 ‰ (Savarino et al., 2013)), which translate its photochemical formation pathway in the atmosphere when its precursors (NO_x) react with O_3 (Alexander et al., 2009). In contrast, terrestrial NO_3^- ($NO_3^-{}_{ter}$) and NO_3^- fertilizers have $\Delta^{17}O$ values close to 0 (Michalski et al., 2004b, 2015). This makes $\Delta^{17}O$ a unique tool to track and quantify the fraction of soil NO_3^- deriving directly from unprocessed atmospheric deposition relative to other terrestrial sources and turnover (Costa et al., 2011; Michalski et al., 2004b). NO_3^- dual isotopes ($\delta^{18}O$ and $\delta^{15}N$) co-variation has also been intensively used to infer the dominant biological processes in a given system such as vegetation and microbial N assimilation, and microbial nitrification and denitrification (Kendall et al., 2007). Nitrification, an aerobic microbial activity transforming ammonium (NH_4^+) into nitrite (NO_2^-) and NO_3^-, comes with a decoupling of $\delta^{18}O$-NO_3^- and $\delta^{15}N$-NO_3^- because whereas N isotopes of NO_3^- reflect the original

N source from which it is derived (Kendall et al., 2007), O isotopes of NO_3^- illustrate the nitrification pathway leading to its production (Buchwald and Casciotti, 2010; Casciotti et al., 2010). In case of heterotrophic microbial denitrification, or plant and microbial assimilation, $\delta^{18}O$ and $\delta^{15}N$ are expected to vary along a 1:2 to 1:1 line (Granger et al., 2004, 2008, 2010a; Karsh et al., 2012; Treibergs and Granger, 2017), enabling a clear appreciation of the processes at play in a system (Bourgeois et al., *in review*; Clément et al., 2003b; Fang et al., 2015; Swart et al., 2014; Wexler et al., 2014).

Here, we conduct and report isotopic measurements ($\Delta^{17}O$, $\delta^{18}O$, and $\delta^{15}N$) of extracted and leached NO_3^- in soils and in precipitation collected at the Lautaret pass, French Alps. We evaluate whether a significant fraction of soil NO_3^- stems from direct atmospheric deposition inputs, and what are the main biological processes at play driving N cycling in these soils. We hypothesize that (i) an increasing proportion of $NO_3^-{}_{atm}$ should be measured in less extensively managed grasslands as a result of low N turnover rates, and (ii) that more $NO_3^-{}_{atm}$ should be find in leachates, relative to extracts, if leaching is indeed an efficient $NO_3^-{}_{atm}$ removal process as suggested by stream exports (see Chapter 2).

3.1.2 Material and methods

3.1.2.1 Study site and sampling procedure

From April to October 2016, samples were collected on a monthly basis in three distinct meadows of the Lautaret pass (2058-m a.s.l.), located in the French Alps (Figure 3-1). The study sites are thoroughly described elsewhere (Bourgeois et al., *in review*; Clément et al., 2012; Robson et al., 2007). Briefly, the surrounding meadows of the Lautaret pass are under the combined influence of mountainous climatic conditions (a cold and wet winter with extensive snow cover from November to April followed by a short plant growing season from May to September), agricultural practices (organic fertilization, mowing, grazing) and modified topography (terraces) (Quétier et al., 2007). In light to this assemblage of climatic and human drivers, oligotrophic soils and rich plant biodiversity have been maintained over the past decades (Körner, 2003; Robson et al., 2007)

.

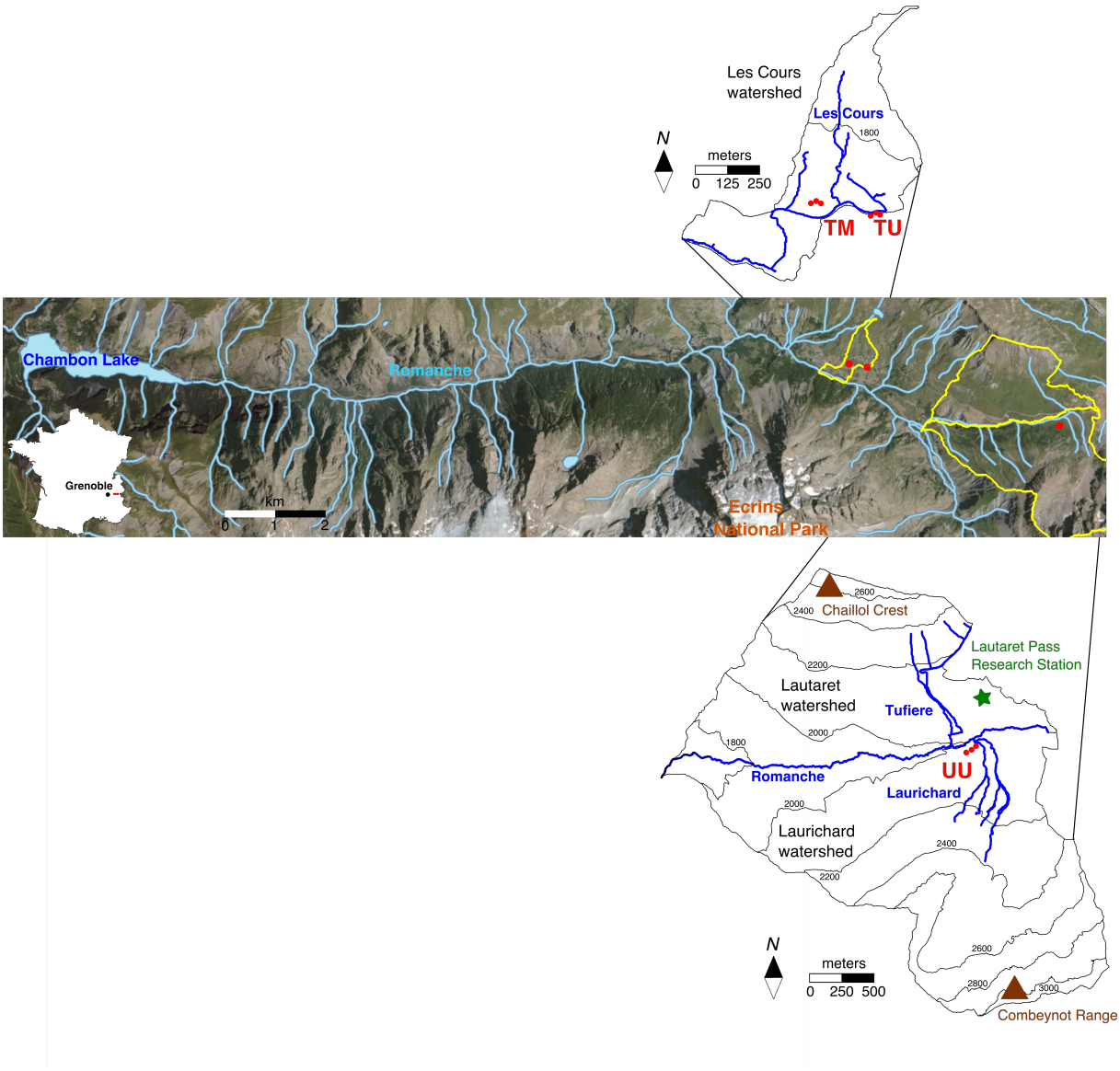

Figure 3-2: Map of the Lautaret pass study area. The central map represents the Romanche Valley in the central French Alps, situated 90 km away from the city of Grenoble (~ 163 000 inhabitants). The boundaries of Lautaret, Laurichard and Les Cours watersheds are delimited in yellow. Streams are shown in blue. The localization of soils sampling in three meadows with different land-management is indicated in red. The meadows are labeled as TM (terraced-mown), TU (terraced-unmown) and UU (unterraced-unmown.

Here, sampling was performed on 9 fields, *i.e.* 3 replicates for each of 3 distinct land management regimes, featuring:

(i) Terraced meadows, manured in May (*ca* 8-kg N ha^{-1} yr^{-1}) (Robson et al., 2007), mown for hay in August and grazed in autumn (TM hereafter).

(ii) Terraced meadows, unmown but grazed in summer (TU hereafter).

(iii) Unterraced and unmown grasslands where very light grazing occurs during livestock transhumance (UU hereafter).

The management practices in the area have been stable since at least 2003 (Legay et al., 2013). Soil characteristics are given in Table 3-1.

Table 3-1: Soil characteristics (0-8 cm depth) and ecosystem properties of the three management treatments. OM stands for Organic Matter. NMP stands for Net Mineralization Potential. pH_{H2O} values were reported from Robson et al. [2007].

	Terraced Mown meadows	Terraced Unmown meadows	Unterraced Unmown meadows
OM (%)	16.7 ± 4.0^{a}	18.4 ± 4.0^{ab}	20.3 ± 6.3^{b}
Bulk density ($g.cm^{-3}$)	0.72 ± 0.19^{a}	0.65 ± 0.17^{a}	0.44 ± 0.11^{b}
Porosity (%)	68 ± 5^{a}	70 ± 6^{a}	78 ± 2^{b}
pH_{H2O}	6 - 7^{a}	6 - 7^{a}	4 - 5^{b}
NMP (µg N-NH_4^+ g^{-1} d^{-1})	14.9 ± 4.7^{a}	18.9 ± 7.8^{b}	11.5 ± 6.1^{c}
Microbial biomass (µg g^{-1} dw)	51.0 ± 9.7^{a}	45.7 ± 19.1^{a}	37.2 ± 16.5^{b}

Prior to sampling, each of the 9 locations was divided in two subplots, separated by *ca* 10-cm, where a soil core was taken using a corer of 4.5-cm diameter and 8-cm length, bringing the total soil samples to n=18 (3 meadows * 3 replicates * 2 cores) per sampling date. All soil cores were immediately labeled, placed in a cool box, and frozen until further manipulation. Samples were removed at monthly intervals, from late April just after snowmelt to October. In parallel, wet and dry deposition samples were collected – every three weeks when possible – using an atmospheric deposition collector (WADOS Kroneis GmbH Austria) from April 2016 to October 2016, thus spanning the same timeframe as soil sampling. Precipitation

samples were stored frozen until further analysis. The dry deposition funnel was rinsed with 500-mL of ultrapure water (18.2-MΩ cm^{-1}), and the sample was stored frozen.

3.1.2.2 Sample extraction and analysis

Systematically, one soil core was homogenized by hand and sieved (5.6-mm). Visible roots and rocks were removed before the homogenized core was sub-sampled in 10-g aliquots. One aliquot served for N extraction by adding 50-mL ultrapure water before mechanical shaking for 1-h at 300-RPM (referred as "soil extracts" hereafter). All extracts were centrifuged (400-RPM for 10-min) and the supernatant was carefully recovered. Another filtration step (0.22-µm Whatman GD/X syringe filters linked to a peristaltic pump) followed before analysis. The second aliquot was used for chloroform fumigation (for 7 days) and subsequent ultrapure water extraction to quantify microbial N (Brookes et al., 1985). Nitrogen Mineralization Potential (NMP) was determined by incubating a third aliquot with 50-mL ultrapure water for 7 days at 40°C. During this process, organic N is mineralized and accumulates as NH_4^+, providing information on the potential mineralization rate in the meadows (Waring and Bremner, 1964). Finally, the last aliquot was oven-dried for 7 days at 70°C to determine soil moisture, before being burned at 550°C for 5 hours to determine % organic matter (OM).

The second soil cores were carefully wrapped in aluminum foil with holes and placed upon graduated cylinders. Then each soil core was leached with 100-mL of distilled water and potentially leached NH_4^+ and NO_3^- were measured from percolates (De Vries et al., 2011). Leached waters (*ca* 40-mL, referred as "soil leachates" hereafter) were recovered before being centrifuged and filtered similarly to soils extracts.

Precipitation samples were left to melt at ambient temperature prior to being filtered on 0.45-µm quartz filters (QMA Whatman).

All samples were subsequently analyzed for [NH_4^+] and [NO_3^-] using a colorimetric technique (Gallery Plus, Thermo Fisher Scientific, Waltham, Massachusetts, USA) with an analytical error of ± 0.01-mg L^{-1}. All soil extracts were also analyzed for total dissolved nitrogen (TDN) by mixing 2.5-mL of sample with 2.5-mL of an oxidative potassium persulfate solution (Williams et al., 2009). Dissolved organic nitrogen (DON) concentration was determined as the difference between TDN concentration and the sum of mineral N form concentrations. All concentrations are given in µg-N g^{-1} dry soil weight (dw). Isotopic analyses were conducted on an MAT 253 IRMS using an adapted version of the denitrifier method (Kaiser et al., 2007). The analytical error was ± 0.6, 1.6 and 0.2 ‰ for $\Delta^{17}O$, $\delta^{18}O$ and $\delta^{15}N$ of NO_3^-, respectively.

3.1.2.3 Calculation of the atmospheric contribution

The atmospheric contribution (f_{atm}) was calculated using a two-source mixing model as previously described (Bourgeois et al., *in review*). Briefly, $\Delta^{17}O\text{-}NO_3^-{}_{atm}$ end-member was chosen as the mean concentration-weighted value of $\Delta^{17}O\text{-}NO_3^-$ in wet and dry deposition collected at the Lautaret pass from April to October 2016 (Table 3-2), with a value of 24.4 ± 2.4 ‰ (-6.0 ± 4.1 and 66.6 ± 5.8 ‰ for $\delta^{15}N$ and $\delta^{18}O\text{-}NO_3^-{}_{atm}$, respectively). Respective contribution of atmospheric deposition in samples was thus inferred from the following equation:

$$f_{atm} = \Delta^{17}O\text{-}NO_3^-{}_{sample} / 24.4 \qquad \text{(Eq. 3.1)}$$

With f_{atm} (= $\%NO_3^-{}_{atm}$), the mole fraction of the atmospheric contribution and $\Delta^{17}O\text{-}NO_3^-{}_{sample}$ the measured value of $\Delta^{17}O\text{-}NO_3^-$ in a sample (Bourgeois et al., *in review*).

Mole fractions of NO_3^- (f_{atm} and $f_{ter} = 1 - f_{atm}$) can be used to remove the isotopic influence of $NO_3^-{}_{atm}$ on $NO_3^-{}_{sample}$ (Dejwakh et al., 2012; Riha et al., 2014), which allows for a better interpretation of biological processes that affect its $\delta^{15}N$ and $\delta^{18}O$ values, as stated in section 1. Because of significantly higher $\delta^{18}O\text{-}NO_3^-{}_{atm}$ values compared to $\delta^{18}O\text{-}NO_3^-{}_{ter}$, even a small f_{atm} can lead to scatter in a dual isotope plot. Removing the atmospheric $\delta^{15}N$ and $\delta^{18}O$ components from

environmental samples should allow an easier assessment of biological processes, such as nitrification and denitrification in our case. This isotope correction was applied on our samples using the isotopic mass balances from Riha et al. (2014):

$$\delta^{18}O_{ter} = (\delta^{18}O_{sample} - \delta^{18}O_{atm} * f_{atm}) / f_{ter} \quad \text{(Eq. 3.2)}$$

$$\delta^{15}N_{ter} = (\delta^{15}N_{sample} - \delta^{15}N_{atm} * f_{atm}) / f_{ter} \quad \text{(Eq. 3.3)}$$

$\delta^{15}N_{atm}$ and $\delta^{18}O_{atm}$ were inferred from NO_3^- in wet and dry deposition, and are given in Table 3-2.

Table 3-2: Mean NO_3^- and NH_4^+ concentrations and NO_3^- isotopic values in wet and dry deposition collected at the Lautaret pass from April to October 2016, and associated standard deviations. The last row gives the inferred isotopic values for this study atmospheric end-member.

Deposition	$[NH_4^+]$ (µg L^{-1})	$[NO_3^-]$ (µg L^{-1})	$\Delta^{17}O$ (‰)	$\delta^{18}O$ (‰)	$\delta^{15}N$ (‰)
Dry deposition (n=10)	-	-	25.1 ± 2.7	69.1 ± 5.7	-5.1 ± 6.2
Wet deposition (n=9)	0.5 ± 0.2	5.5 ± 3.2	23.6 ± 2.0	63.8 ± 6.0	-7.1 ± 1.7
Atmospheric end-member	-	-	24.4 ± 2.4	66.6 ± 5.8	-6.0 ± 4.1

3.1.2.4 Data analysis and statistics

Note that each data point in Figure 3-6 represents the mean value of three soil replicates per sampling date in order to account for spatial variability. All statistical analyses were conducted using R software (v3.2.3). A Mann-Whitney test was applied to determine significant differences of mean concentrations and isotopic values of NO_3^- and NH_4^+ between soil extracts and leachates, among or across land managements and on an annual (Table 3-3) or seasonal (Figure 3-4) basis. Differences and correlations were held significant when the *p* value reached a 0.05 credible interval.

3.1.3 Results

3.1.3.1 NO_3^- isotopes in wet and dry deposition

Mean $\Delta^{17}O\text{-}NO_3^-$ in wet and dry deposition over the study period is 25.1 ± 2.7 ‰ and 23.6 ± 2, respectively (Table 3-1). These values are consistent with previously reported data for $\Delta^{17}O\text{-}NO_3^-_{atm}$ (Costa et al., 2011; Hundey et al., 2016; Michalski et al., 2004b). The mass-weighted mean $\Delta^{17}O$ value for total deposition is 24.4 ± 2.4 ‰, and is used to quantify the atmospheric component of NO_3^- pools in streams (Eq. 3.1). Mean annual total $\delta^{18}O\text{-}NO_3^-_{atm}$ (66.6 ± 5.8 ‰) and $\delta^{15}N\text{-}NO_3^-_{atm}$ (-6.0 ± 4.1 ‰) are also consistent with a reservoir of exclusively $NO_3^-_{atm}$ (Kendall et al., 2007), and these values are used to correct samples from their atmospheric $\delta^{18}O$ and $\delta^{15}N$ components (Eq. 3.2 and Eq. 3.3).

3.1.3.2 Soil N pools and NO_3^- isotopes

As presented in Figure 3-3, DON is the most abundant form in all soils, and its proportion increases with decreasing land management intensity. Similarly, NH_4^+ proportion increases with decreasing land management intensity, at the expense of the NO_3^- pool, which represent only 11% of TDN in the UU meadow.

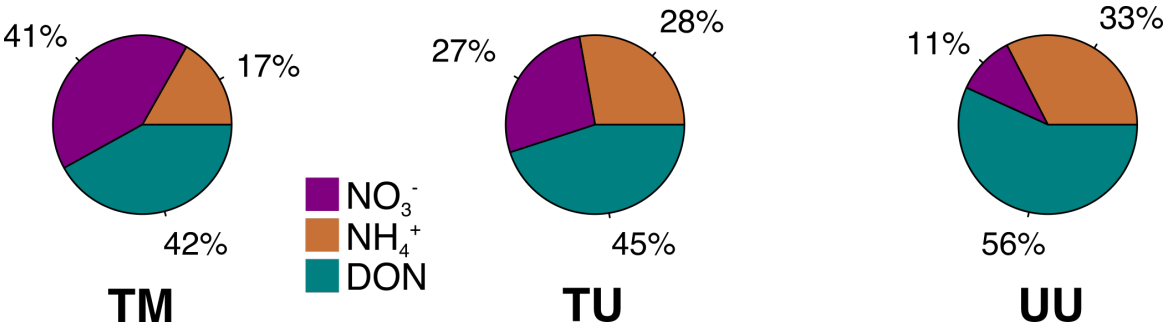

Figure 3-3: Soil N pools repartition across different land management at the Lautaret pass. Different colors delineate different N forms as indicated in the legend.

Table 3-3 gives the mean $[NH_4^+]$, $[NO_3^-]$ and NO_3^- isotopic values ($\Delta^{17}O$, $\delta^{18}O$ and $\delta^{15}N$) in soil extracts and soil leachates over the study period. Mean annual $[NH_4^+]$ in soil extracts were not significantly different across meadows, and ranged from 4.8 ± 3.1 µg-N g^{-1} dw in TM fields to 13.6 ± 23.2 µg-N g^{-1} dw in TU fields. Mean $[NO_3^-]$ in soil extracts were significantly higher in the terraced meadows (TM and TU)

compared to the UU grassland, but showed no difference between them. [NH_4^+] and [NO_3^-] are lower than reported values at the same sites, but in the same order of magnitude (Legay et al., 2013; Robson et al., 2007). However, it must be underlined that our values encompass a full snow-free season whereas the previous studies focused on a period from May to July, potentially explaining the lower values obtained here.

Mean annual [NH_4^+] and [NO_3^-] were, in all meadows, significantly lower in soil leachates relative to soil extracts. Leachates N concentrations represented between 4 and 18 % of extract N concentrations, except for the mean [NO_3^-] in the TM meadow that was half as high in the leachates than in the extracts. This highlights the good capacity of soils to retain N in micro-porous sites not easily reached by sub-surface water flows. Mean annual [NH_4^+] in UU soil leachates were significantly higher than in terraced meadows, whereas more nitrate was leached from TM and TU fields compared to the UU meadow.

Mean annual $\Delta^{17}O\text{-}NO_3^-$ was very low (under the analytical error of 0.6 ‰) in both soil extracts and leachates of the terraced meadows, meaning that no $NO_3^-_{atm}$ could be detected on average over the year. Mean $\Delta^{17}O\text{-}NO_3^-$ was significantly higher in the UU meadow, and $NO_3^-_{atm}$ accounted for 4 and 6 % to the nitrate pool in the extracts and leachates, respectively. These values were consistent with measured soils $\Delta^{17}O\text{-}NO_3^-$ (n=2) between 0.5 and 1 ‰ for a mountain site in the south of California (Michalski et al., 2004b) but lower than the mean 3.6 ± 2.4 ‰ (n=4) in soils of a temperate forest of Michigan (Costa et al., 2011).

Note that all reported $\delta^{18}O$ and $\delta^{15}N$ values were corrected for the presence of $NO_3^-_{atm}$ and reflect the isotopic composition of terrestrial nitrate ($NO_3^-_{ter}$). Mean annual $\delta^{18}O\text{-}NO_3^-_{ter}$ were significantly lower in the terraced meadows soil extracts relative to the UU grassland soil extracts, and no significant differences between soil extracts and leachates were measured, exception made of the TM meadow. Mean $\delta^{18}O\text{-}NO_3^-_{ter}$ values of -10 ‰ (in the terraced meadows) are sensibly lower than mostly positive values reported in the literature, as reviewed elsewhere (Rose et al., 2015b). Fang et al. (2012) reported intriguingly low $\delta^{18}O\text{-}NO_3^-$ values around -4 ‰ in

a temperate forest of Japan, still higher than in this study. Similarly, mean δ^{15}N- $NO_3^-{}_{ter}$ ranged from -5.1 ± 6.6 (UU) to -1.3 ± 9.6 ‰ (TU), lower than the -0.1 ± 1.3 ‰ value measured in the organic topsoil of a forested watershed in the Catskill Mountains (Burns and Kendall, 2002). In contrast, Mayer et al. (2001) reported low δ^{15}N-NO_3^- in deciduous forest floors (-10.3 ± 1.7) and coniferous forest floors (-11.3 ± 0.3). Interestingly, these values were in good agreement with the measured mean δ^{15}N-$NO_3^-{}_{ter}$ in leachates in this study, but significantly lower than in the terraced meadows soil extracts.

Table 3-3: Mean annual concentration of NO_3^- and NH_4^+ (µg g^{-1} dw) and concentration-weighted isotopic values of $NO_3^-{}_{ter}$ (‰) in soil extracts and leachates, and associated standard deviation. Bold leachates values indicate significant difference with the corresponding soil extract values. Different letters indicate significant differences across land-use. Note that δ^{15}N and δ^{18}O values are corrected for the atmospheric contribution.

	Terraced Mown		Terraced Unmown		Unterraced Unmown	
	Extracts (n=21)	Leachates (n=21)	Extracts (n=21)	Leachates (n=21)	Extracts (n=18)	Leachates (n=18)
$[NH_4^+]$ (µg N g^{-1} dw)	4.8 ± 3.1	**0.6 ± 1.3** *	13.6 ± 23.2	**0.6 ± 1.4** ^{a}	10.1 ± 10.6	**1.2 ± 1.2** ^{b}
$[NO_3^-]$ (µg N g^{-1} dw)	11.8 ± 11.0 ^{a}	**6.0 ± 12.8** ^{a}	13.3 ± 10.6 ^{a}	**2.4 ± 8.7** ^{ab}	3.3 ± 4.3 ^{b}	**0.5 ± 0.9** ^{b}
Δ^{17}O (‰) f_{atm}	0.3 ± 0.4 ^{a} (0%)	0.5 ± 0.4 ^{a} (0%)	0.5 ± 0.8 ^{a} (0%)	0.7 ± 0.5 ^{a} (3%)	0.9 ± 0.6 ^{b} (4%)	**1.4 ± 1.0** ^{b} (6%)
$\delta^{18}O_{ter}$ (‰)	-10.9 ± 5.1 ^{a}	**-6.7 ± 6.7**	-10.3 ± 6.6 ^{a}	-6.1 ± 6.7	-4.3 ± 6.8 ^{b}	-3.8 ± 7.5
$\delta^{15}N_{ter}$ (‰)	-2.6 ± 6.5	**-8.7 ± 6.0**	-1.3 ± 9.6	**-7.3 ± 7.2**	-5.1 ± 6.6	-6.4 ± 9.7

3.1.3.3 Seasonal trends

Figure 3-4 illustrates the variations of the mean $[NH_4^+]$, $[NO_3^-]$ and NO_3^- isotopic values (Δ^{17}O, δ^{18}O and δ^{15}N) in soil extracts and soil leachates between the early growing season (April-July) and the senescence period (August-October). Such decoupling of periods is common in subalpine studies (Legay et al., 2013; Robson et

al., 2010), as N turnover is expected to be governed by plant uptake in the first period and by microbial uptake in the second (Jaeger et al., 1999). Here, the most remarkable variations concerned [NH_4^+], which significantly decreased in TM soil extracts and leachates and in TU soil extracts after the peak biomass. [NO_3^-] was significantly higher in TU soil extracts in the second part of the year.

$\Delta^{17}O\text{-}NO_3^-$ did not significantly vary between the two periods neither for leachates nor for extracts, whereas $\delta^{18}O\text{-}NO_3^-{}_{ter}$ was significantly lower and higher in soil extracts after the peak biomass in TM and UU meadows, respectively. The most marked isotopic temporal variations occurred for $\delta^{15}N\text{-}NO_3^-{}_{ter}$, which was significantly higher in TM soil extracts and TU soil extracts and leachates in the late part of the growing season.

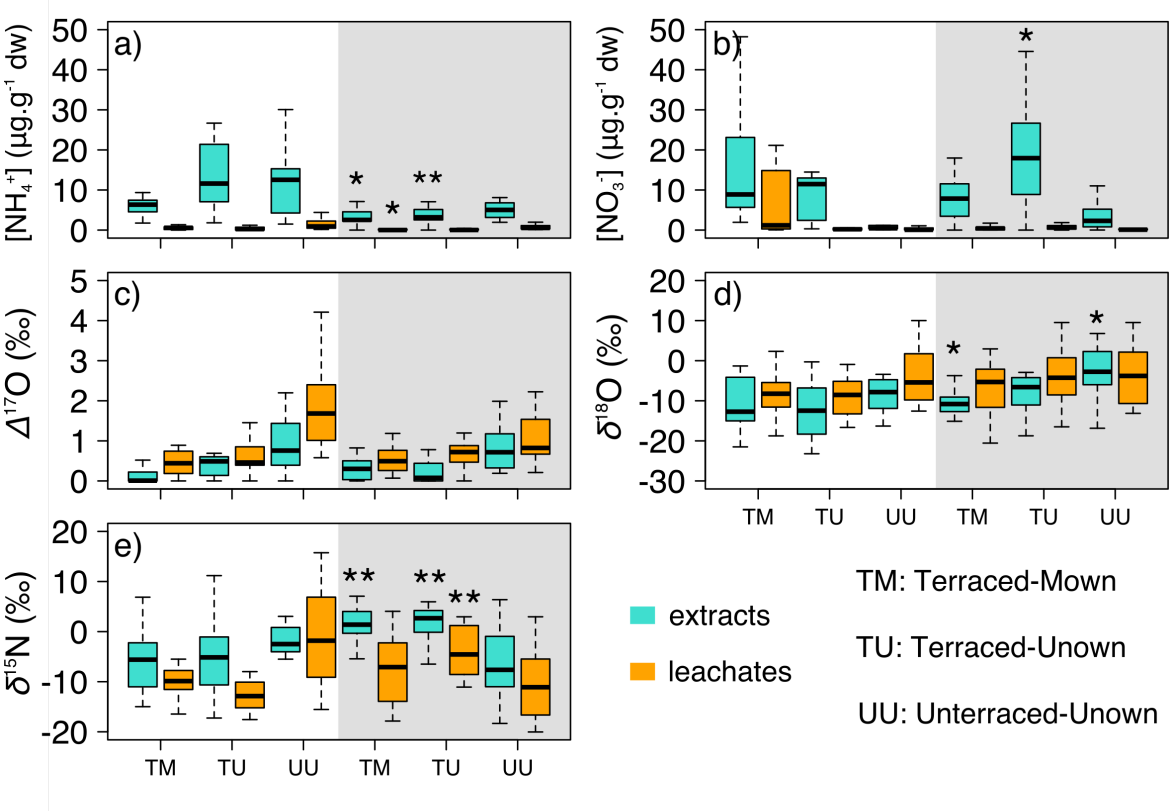

Figure 3-4: Before and after peak biomass values of a) [NH_4^+] (µg g^{-1} dw), b) [NO_3^-] (µg g^{-1} dw), c) $\Delta^{17}O\text{-}NO_3^-$ (‰), d) $\delta^{18}O\text{-}NO_3^-{}_{ter}$ (‰) and e) $\delta^{15}N\text{-}NO_3^-{}_{ter}$ (‰) in soil extracts (blue, n=12) and leachates (orange, n=9). Highlighted in grey is the after peak biomass period. Asterisks indicate that the after peak biomass mean value is significantly different from the before peak biomass value (* for $p<0.05$, ** for $p<0.01$, *** for $p<0.001$). Outliers are not shown. Note that $\delta^{15}N$ and $\delta^{18}O$ values are corrected for the atmospheric contribution (see section 3.1.2.3).

3.1.4 Discussion

3.1.4.1 Low $\Delta^{17}O\text{-}NO_3^-$ in soils

Using the same framework as provided in Costa et al. (2011), we estimated the expected $\Delta^{17}O\text{-}NO_3^-$ if rain was to saturate the pore space in soils, assuming no leaching or nitrification. At the Lautaret pass, the mean soil pore space is 68, 70 and 78 % for TM, TU and UU meadows, respectively (Table 3-1). The average $[NO_3^-]$ in rain over the study period is 5.5-µg mL^{-1} (Table 3-2). Thus, if the pore space was saturated by rain, we would expect an increase of 3.7, 3.9 and 4.3 µg-NO_3^- per cm^{-3} of bulk soil (0.8, 0.9 and 1.0 µg-N cm^{-3}), assuming no soil NO_3^- is displaced by rain. Considering the mean soil extracts NO_3^- concentrations reported in Table 3-3, and the mean soil densities given in Table 3-1, we find an average soil NO_3^- concentration of 8.5, 8.6 and 1.4 µg-N cm^{-3} for TM, TU and UU meadows, respectively. This means that the rain would contribute up to 9, 10 and 71 % of total soil NO_3^- after a rainfall episode, corresponding to $\Delta^{17}O\text{-}NO_3^-$ = 2.2, 2.4 and 17.3 ‰ in TM, TU and UU meadows, respectively. As the aim of this study was not to focus specifically on rain events but rather to capture the background presence of $NO_3^-{}_{atm}$ in soils, it is not surprising that our results are, in average, lower than the calculated values stated above. However, it is interesting to debate the possible sinks for deposited $NO_3^-{}_{atm}$.

Possible sinks of deposited $NO_3^-{}_{atm}$ in soils encompass extensive leaching, fast uptake or immobilization by plants and microorganisms and fast biological recycling of $NO_3^-{}_{atm}$ in soils. Biological recycling will be further expanded on in the section 3.1.4.2, in light of $\delta^{18}O$ and $\delta^{15}N$ data.

The isotopic composition of NO_3^- exported in the streams draining the same watersheds on which soils were sampled here – namely Les Cours and Laurichard, – have been reported elsewhere (Bourgeois et al., *in review*). In the mid montane stream draining the terraced meadows, mean annual $\Delta^{17}O\text{-}NO_3^-$ = 1.0 ± 0.7 ‰ whereas $\Delta^{17}O\text{-}NO_3^-$ = 3.0 ± 1.7 ‰ in the upper montane stream corresponding to UU meadows. Without stream discharge measurements, it is difficult to assess the amount of $NO_3^-{}_{atm}$ that was actually retained in soils. However, higher proportion of

$NO_3^-_{atm}$ (i.e., higher $\Delta^{17}O\text{-}NO_3^-$) in streams compared to soils on an annual basis suggest that direct leaching of deposited $NO_3^-_{atm}$ could be partly responsible for $NO_3^-_{atm}$ removal from the meadows of the Lautaret pass. The magnitude of this removal mechanism is difficult to assess, but the snowmelt period is a good indicator whether $NO_3^-_{atm}$ is efficiently transported to the stream (Campbell et al., 2002, 2007; Kendall et al., 1995; Ohte et al., 2004). In the upper stream, the snowmelt period led to an increase of $\Delta^{17}O\text{-}NO_3^-$, a pattern not observed in the mid montane stream (Bourgeois et al., *in review*). Furthermore, hydrological events such as rainstorms led to an increase of $\Delta^{17}O\text{-}NO_3^-$ in the upper mountain stream (Bourgeois et al., *in review*). This and the significantly higher $\Delta^{17}O\text{-}NO_3^-$ in UU soil leachates relative to soil extracts corroborate leaching as the likely driver of $NO_3^-_{atm}$ flushing from soils of the UU meadow. Yet, it does not explain what becomes of $NO_3^-_{atm}$ in the terraced fields.

Dominance of species with exploitative traits on terraced meadows has been well documented (Quétier et al., 2007), and efficient removal of soil $NO_3^-_{atm}$ by root and leaves uptake is a reasonable hypothesis to explain what becomes of $NO_3^-_{atm}$. Higher f_{atm} in *Dactylis glomerata*, the dominant perennial grass on these terraces, relative to soils has been reported in another study at the Lautaret pass (Bourgeois et al., *in review*). Also, other studies conducted in subalpine grasslands showed an effective scavenging of ^{15}N-enriched NO_3^- by plants in simulated atmospheric deposition experiments, at the expense of the soil reservoirs (Bassin et al., 2015; Boutin, 2015). Given the unvarying $\Delta^{17}O\text{-}NO_3^-$ over time in both soil extracts and leachates (Figure 3-4), it is likely that microbial immobilization also plays a role in $NO_3^-_{atm}$ removal. Indeed, it is widely acknowledged that plant benefit from a decrease in nutrients competition with microbes due to freeze-thaw cycles restricting microbial growth in the first part of the growing season, leading to greater plant N uptake associated with active growth (Freppaz et al., 2007; Legay et al., 2013). By August, most subalpine plants have completed their life cycle (Quétier et al., 2007), leading to enhanced N microbial immobilization in soils (Jaeger et al., 1999), thus driving $NO_3^-_{atm}$ removal in the second part of the snow-free season. Significantly greater microbial biomass in the terraced meadows compared to the UU grassland (Table 3-1) also points at an active role played by microbes in these fields.

Another important characteristic of the UU grassland is the extensive litter cover (Baptist et al., 2013; Gross et al., 2007) that is likely to intercept $NO_3^-_{atm}$ before it reaches the soils. For instance, Michalski et al [2004] reported a $\Delta^{17}O\text{-}NO_3^-$ value of 18.9 ‰ for surface litter in a Californian forest when underlying soils had $\Delta^{17}O\text{-}NO_3^-$ values of 2.5 ‰. To sum up, the combination of soil leaching and litter retention is assumed to drive $NO_3^-_{atm}$ removal in UU grasslands whereas we suggest it is more likely controlled by plant uptake and microbial immobilization in the terraced meadows.

3.1.4.2 Low $\delta^{18}O\text{-}NO_3^-_{ter}$

The low $\delta^{18}O\text{-}NO_3^-_{ter}$ values measured in soils were unexpected. Although the mean annual $\delta^{18}O\text{-}NO_3^-_{ter}$ measured in all fields are comprised in the -15 ‰ to 15 ‰ range expected for microbial nitrification product (Kendall et al., 2007), we measured values as low as -25 ‰, which has very rarely been reported in literature.

It is customary in NO_3^- isotopic studies not to measure directly the isotopic composition of nitrate produced by nitrifiers ($\delta^{18}O\text{-}NO_3^-_{nit}$) but rather to infer it based upon the knowledge of the fractional contributions and isotopic ratios of water (H_2O) and molecular oxygen (O_2) during chemolithoautotrophic nitrification. The oxidation of ammonium to nitrite (NO_2^-) is catalyzed by ammonia monooxygenase and hydroxylamine oxidoreductase, and the oxygen atoms incorporated during this step are derived from O_2 and from H_2O (Andersson and Hooper, 1983; Hollocher et al., 1981). The next oxidation step leading to the formation of nitrate involves another oxygen atom from H_2O (Hollocher, 1984), resulting in a theoretical $\delta^{18}O\text{-}NO_3^-_{nit}$ = 1/3 ($\delta^{18}O\text{-}O_2$) + 2/3 ($\delta^{18}O\text{-}H_2O$). Using this definition, we calculated in a previous study on the same site an expected $\delta^{18}O\text{-}NO_3^-_{nit}$ ranging between -3.3 and 2.3 ‰, using $\delta^{18}O\text{-}O_2$ = 23.5 ‰ and $\delta^{18}O\text{-}H_2O$ = -16.6 ‰ (if water is snow) or -8.2 ‰ (if water is rain) (Bourgeois et al., *in review*). When compared to the infield measured values in this study (Table 3-3), it is clear that this theoretical calculation overestimates microbial nitrate oxygen isotopic composition, which stands in stark contrast with otherwise reported higher field values than theoretically calculated. A number of such studies have been listed in Snider et al. (2010), who also provides a very nice

framework for interpreting higher $\delta^{18}O\text{-}NO_3^-{}_{ter}$ than expected. However, an opposite pattern is observed here (i.e., lower $\delta^{18}O\text{-}NO_3^-{}_{ter}$ values than theoretically calculated and to what was reported in the literature).

The only other study reporting lower $\delta^{18}O\text{-}NO_3^-{}_{ter}$ than expected attributed such pattern to a combination of kinetic isotopic fractionation – during the incorporation of oxygen atoms from water and molecular oxygen process – and equilibrium isotopic fractionation (Figure 3-5) when O-exchange occurs between the intermediary NO_2^- and H_2O (Fang et al., 2012). Using the same two scenarios as presented by the authors – *i.e.*, scenario 1 is "kinetic isotopic fractionation but no O-exchange" and scenario 2 is "complete O-exchange and kinetic isotopic fractionation" –, we calculated a new $\delta^{18}O\text{-}NO_3^-{}_{nit}$. To do so, we assumed kinetic isotopic effects between -37.6 and -17.9 ‰ for the NH_4^+ ➔ NO_2^- step (Casciotti et al., 2010), a kinetic isotopic effect between -18.2 and -12.8‰ for the NO_2^- ➔ NO_3^- step (Buchwald and Casciotti, 2010) and an equilibrium isotopic effect of 14‰ for the O-exchange between NO_2^- and H_2O (Casciotti et al., 2007). Using these reported fractionation factors, we calculated $\delta^{18}O\text{-}NO_3^-{}_{nit}$ from -21.9 to -13.5 ‰ and from -13.0 to -11.5 ‰ for scenarios 1 and 2, respectively, if water is snow. If water is rain, the calculated $\delta^{18}O\text{-}NO_3^-{}_{nit}$ ranges from -16.3 to -7.9 ‰ and from -4.9 to -3.1 ‰ for scenarios 1 and 2, respectively. We reported these values in a dual isotope plot (Figure 3-6) to show that a combination of these two scenarios could very possibly explain the measured low $\delta^{18}O\text{-}NO_3^-{}_{ter}$ in soils at the Lautaret pass. Most of the values fell in line with this predicted $\delta^{18}O\text{-}NO_3^-{}_{ter}$. As the O-exchange rate between NO_2^- and H_2O is pH dependent (Casciotti et al., 2007; Fang et al., 2012; Snider et al., 2010), acidic soils in the UU grasslands certainly favored a greater degree of O-exchange compared to the terraced meadows, where the pH_{H2O} is closer to neutral due to past agricultural practices that mobilized the underlying calcareous substrate (Quétier et al., 2007) (Table 3-1). This would significantly raise the $\delta^{18}O\text{-}NO_3^-{}_{ter}$ in UU grassland compared to the terraced meadows (by overwriting the strong kinetic effects leading to ^{18}O depletion), as observed here (Table 3-3).

We did not measure systematically [NO_2^-] values in soils, however we did measure it in a subset of soil extracts and leachates where no evidence of nitrite accumulation was found (data not shown). Similarly, all stream samples draining the two studied watersheds here had [NO_2^-] = 0, which is another indication that NO_2^- residence time in soils is most likely short, which is quite in contradiction with the scenarios prediction stated above. A more thorough investigation is needed to evaluate whether O-exchange is a determinant step in modifying the oxygen isotopic composition of $NO_3^-{}_{ter}$.

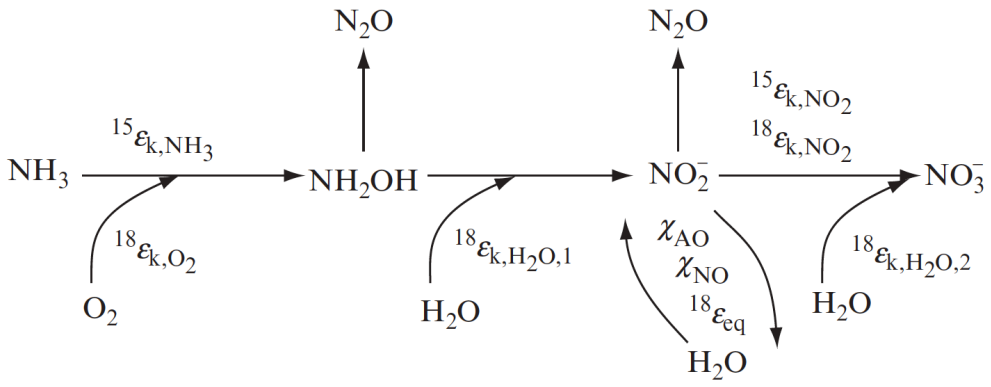

Figure 3-5: Schematic of isotopic fractionation and exchange during nitrification. During ammonia oxidation, N isotopic fractionation occurs at ammonia monooxygenase ($^{15}\varepsilon_{k,NH3}$), and O isotopic fractionation occur during O_2 and H_2O incorporation ($^{18}\varepsilon_{k,O2}$ and $^{18}\varepsilon_{k,H2O,1}$, respectively) and exchange (χ_{AO}, $^{18}\varepsilon_{eq}$). During nitrite oxidation, N and O isotopic fractionation occur at nitrite oxidoreductase ($^{15}\varepsilon_{k,NO2}$ and $^{18}\varepsilon_{k,NO2}$, respectively), and O isotopic fractionation occurs during H_2O incorporation ($^{18}\varepsilon_{k,H2O,2}$) and exchange ($\chi_{NO}$, $^{18}\varepsilon_{eq}$). N and O isotopic fractionation may also occur during N_2O production from NH_2OH and NO_2 by ammonia oxidizers (not shown). After Casciotti et al. (2011).

Anyhow, some δ^{18}O-$NO_3^-{}_{ter}$ fell outside the predictions from scenarios 1 and 2, especially in the UU soil extracts and leachates. Possible explanations are numerous and encompass the possible ^{18}O-enrichment of water by evaporation (Fang et al., 2012), denitrification (Wexler et al., 2014) (which discriminates against heavier isotopes), heterotrophic nitrification (Mayer et al., 2001) or efflux from subalpine roots NO_3^- (Britto and Kronzucker, 2006; Maire et al., 2009; Marty et al., 2009), ^{18}O-enriched by nitrate reductase during the assimilation process (Granger et al., 2004, 2010a). Based on the data presented here, it is difficult to clearly delineate the drivers at play and further investigation would be needed. Quantification of key

microbial gene – relative to the N cycle – abundances and identification of the microbial communities in soils could for example help understand if heterotrophic nitrification or denitrification exerts control on $\delta^{18}O\text{-}NO_3^-{}_{ter}$.

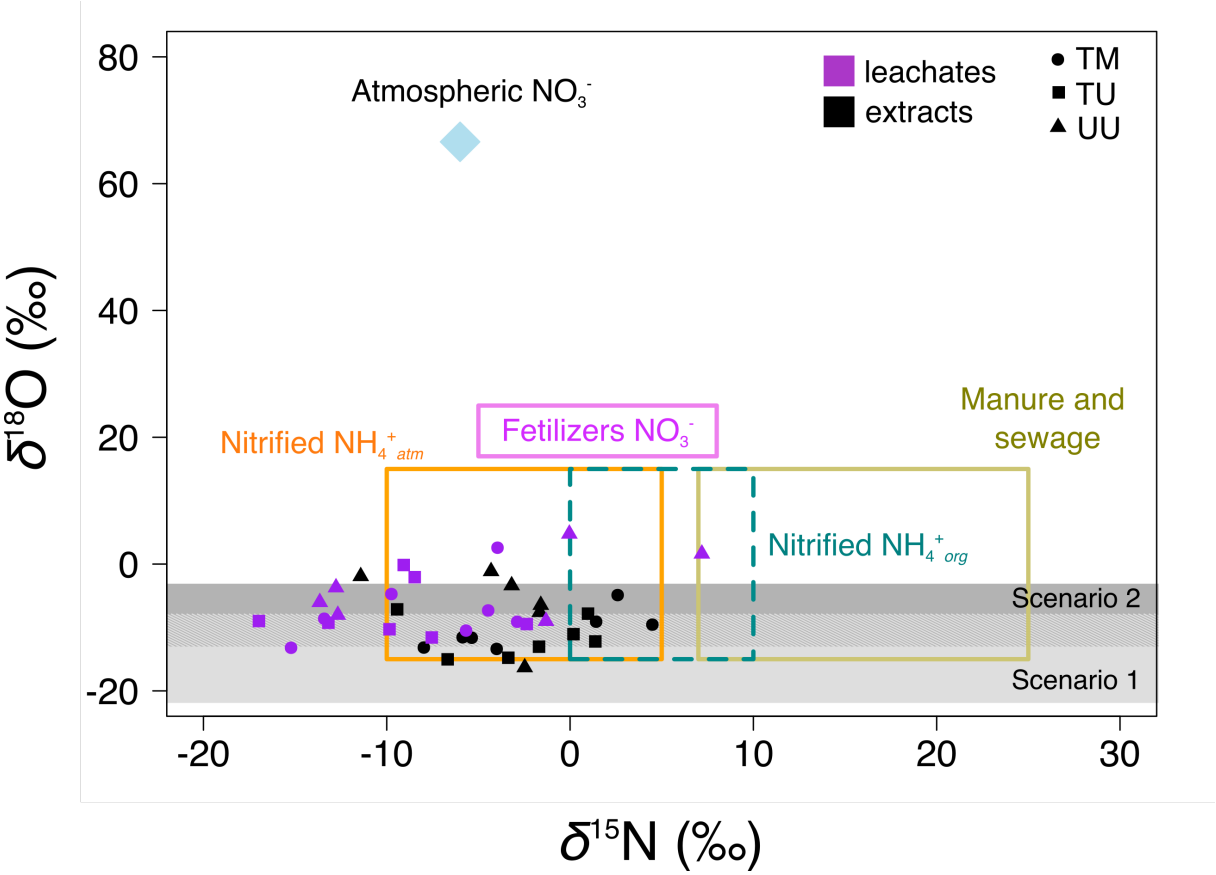

Figure 3-6: Dual isotopes plot ($\delta^{18}O$ *vs* $\delta^{15}N$) illustrating the mixing between distinct sources of $NO_3^-{}_{ter}$ in soil extracts (black) and leachates (purple). All isotopic values were obtained by the $\Delta^{17}O$ transform of NO_3^- collected at all sites (see section 3.1.2.3). The colored boxes represent the reported range for NO_3^- terrestrial sources, featuring atmospheric ammonium ($NH_4^+{}_{atm}$) in orange, mineralized ammonium ($NH_4^+{}_{org}$) in turquoise, manure or sewage derived NH_4^+ in beige and fertilizers NO_3^- in violet. The blue diamond reflects the isotopic composition of $NO_3^-{}_{atm}$ as measured in this study. Point shapes denote management treatments as indicated in legend. The grey boxes indicate the range for expected $\delta^{18}O\text{-}NO_3^-{}_{ter}$ following scenario 1 (kinetic isotopic fractionation but no O-exchange) and scenario 2 (complete O-exchange and kinetic isotopic fractionation). The dashed grey boxes translate the overlapping of predicted ranges.

3.1.4.3 Low $\delta^{15}N\text{-}NO_3^-{}_{ter}$

$\delta^{15}N\text{-}NO_3^-{}_{ter}$ has very largely been used to identify the original N source of NO_3^- before the nitrification process (Kendall et al., 2007). Although some sources have overlapping $\delta^{15}N$ ranges that sometimes complicate the appointment process, when $\delta^{15}N$ is coupled to $\delta^{18}O$ useful insights on sources and processes driving NO_3^-

dynamics in a system can be inferred. Here, the wide range in $\delta^{15}N\text{-}NO_3^-{}_{ter}$ in extracts and leachates suggests that a combination of multiple sources and non-conservative behavior is the main control on $\delta^{15}N$ values of $NO_3^-{}_{ter}$. In this study, the probable sources of $NO_3^-{}_{ter}$ were limited to deposited NH_4^+ ($NH_4^+{}_{atm}$) and soil organic matter (OM) – although manure and cattle waste also represent potential sources – and the primary processes expected to cause variation in $\delta^{15}N$ are mineralization, nitrification and denitrification.

First, the report of the $\delta^{15}N\text{-}NO_3^-{}_{ter}$ values measured in this study in a dual isotope plot (Figure 3-6) points at an origin from $NH_4^+{}_{atm}$, which has also been found to have low $\delta^{15}N$ values (Russell et al., 1998; Xue et al., 2009). It is difficult to ascertain whether $NH_4^+{}_{atm}$ contributes much to total soil NH_4^+, however the release of $NH_4^+{}_{atm}$ at snowmelt and subsequent nitrification was proposed as the reason for the low $\delta^{15}N\text{-}NO_3^-$ in streams at the Lautaret pass in spring (Bourgeois et al., *in review*). This falls in line with the significantly lower $\delta^{15}N\text{-}NO_3^-{}_{ter}$ in the TM and TU soil extracts and leachates in the first part of the growing season compared to later in the year when snowmelt influence is negligible (Figure 3-4). Interestingly, $[NH_4^+]$ was under the detection limit in the quasi totality of stream samples even at snowmelt (data not shown), hinting at a strong retention and utilization of $NH_4^+{}_{atm}$ in soils, also supported by the significantly lower $[NH_4^+]$ in leachates compared to extracts (Table 3-3). However, $NH_4^+{}_{atm}$ is not likely to account for $\delta^{15}N\text{-}NO_3^-{}_{ter}$ as low as -17 ‰.

OM as the main substrate for mineralization and nitrification would lead to higher $\delta^{15}N\text{-}NO_3^-{}_{ter}$ than $NH_4^+{}_{atm}$ as substrate, and cannot account for the low $\delta^{15}N\text{-}NO_3^-{}_{ter}$ in this study. Yet, kinetic isotopic effects favor the incorporation of the light isotope in the microbial product of nitrification (Casciotti et al., 2011). The low $\delta^{15}N\text{-}NO_3^-{}_{ter}$ in this study can only reflect the isotopic segregation during $NO_3^-{}_{ter}$ production process (Mayer et al., 2001; Spoelstra et al., 2007). NH_4^+ availability was shown to drive the magnitude of the kinetic isotopic effect (Mayer et al., 2001), because the isotope effect during nitrification is reduced or not observed if NH_4^+ is limiting to nitrifiers (Mariotti et al., 1981). Here, NH_4^+ pools are of the same order of magnitude as NO_3^- pools in all soil extracts, suggesting that fractionation during nitrification

could possibly occur. Also the concomitant $\delta^{15}N\text{-}NO_3^-{}_{ter}$ increase and $[NH_4^+]$ decrease in soil extracts after peak biomass in the terraced meadows (Figure 3-4) is in line with a dampened kinetic effect due to NH_4^+ limitation. Finally, significantly lower $\delta^{15}N\text{-}NO_3^-{}_{ter}$ in leachates compared to extracts suggest that the newly formed $NO_3^-{}_{nit}$ is ^{15}N-depleted compared to NO_3^- in soils microsites, possibly as a result from kinetic effect during nitrification.

The mineralization process is usually considered as yielding little isotopic fractionation to the produced NH_4^+, however several studies have reported $\delta^{15}N\text{-}NO_3^-{}_{ter}$ approximately lower by 5 ‰ compared to bulk soil $\delta^{15}N$ (Fang et al., 2012; Ostrom et al., 1998; Spoelstra et al., 2007) and could be an additional factor to explain the low $\delta^{15}N\text{-}NO_3^-{}_{ter}$. Here, NMP is significantly higher in the terraced soils (Table 3-1), where $\delta^{15}N\text{-}NO_3^-{}_{ter}$ is the lowest (Table 3-3), suggesting that kinetic isotope effects during mineralization are not the main driver of $\delta^{15}N\text{-}NO_3^-{}_{ter}$ variability in these fields. For the UU grassland with high DON pool and where year-round mineralization rates are low (Table 3-1 and Figure 3-3), it is possible that kinetic fractionation during OM mineralization exert a stronger control on $\delta^{15}N\text{-}NO_3^-{}_{ter}$, also possibly explaining the lack of significant temporal variation observed in this meadow (Figure 3-4).

The dual isotope plot does not reveal any sign of denitrification, *i.e.* no significant correlation between $\delta^{15}N$ and $\delta^{18}O$ of nitrate is evidenced (Figure 3-6). However, it does not mean that denitrification processes did not occur in our soils, because nitrification has been shown to ubiquitously overprint denitrification isotopic effects (Granger and Wankel, 2016). Denitrification can occur in anaerobic microsites of well-drained nitrifying soils (Spoelstra et al., 2007), and discriminates against the heavier isotopes of NO_3^- during the N_2O and N_2 production processes (Mariotti et al., 1981; Andre Mariotti et al., 1982). Therefore, denitrification could be responsible for the higher $\delta^{15}N\text{-}NO_3^-{}_{ter}$ in extracts compared to leachates (Table 3-3) or for the higher values after the peak biomass when warmer temperatures trigger denitrification (Ostrom et al., 1998).

3.1.4.4 Implications for N cycling in mountainous ecosystems

Our findings have several key implications regarding the fate of atmospheric N and the biological processes in subalpine meadows. First, the low f_{atm} in all soils suggest that the studied grasslands have not reached an advanced N saturation stage yet. In UU grassland, the low N cycling rate (Robson et al., 2007) coupled with litter interception and efficient leaching of atmospheric N presumably prevent exogenous N accumulation in soils. In the terraced meadows, the strong seasonal plant-microbe competition for nutrients is assumed to promote a fast uptake of deposited N, in order to meet the biological N demand. This is, per definition, the sign of N limitation as the main limiting factor of net primary production. That O and N isotopes of nitrate are strongly affected by kinetic isotopic effects is also in line with N limited ecosystems. Slow rates of nitrification, and in some case of mineralization, are responsible for such exacerbated isotopic fractionation, and are symptomatic of N limited environments (Burns, 2004). It is likely that the difficult weather conditions still exert a strong control on microbial properties, which were shown to drive N turnover in these N poor soils (Jusselme et al., 2016; Legay et al., 2016).

Second, the decoupling between the oxygen isotopic compositions of nitrate following the land-management regimes is intriguing. Differences in $\delta^{18}O\text{-}NO_3^-{}_{ter}$ can only originate from differences in water composition (unlikely considered the close vicinity of the studied site and a relatively similar snow-covered period) or from isotopic effects during nitrification. These isotopic effects depend on abiotic conditions (pH, temperature) but also on the microbial communities driving the nitrification processes (e.g., bacteria, archeae, anammox microbes, heterotrophic nitrifiers, etc.). Therefore, it would be interesting to couple isotopic considerations with microbial gene abundances and sequencing to better understand the main mechanism of nitrification in natural soils. A very nice example is given in Liu et al. (2017), where the authors evaluated the biotic and abiotic controls of N cycling along an aridity gradient in China.

Third, the considerable variability of $\delta^{15}N\text{-}NO_3^-{}_{ter}$, both spatially and temporally, highlights the complex interaction between biological processes and multiple sources in a life-riche environment such as soils. To further constrain the drivers, there is a

clear need for ancillary data, such as, once again, a thorough study of the microbial communities involved in N cycling (e.g., nitrifiers, denitrifiers, N fixers, etc.).

Finally, it is interesting to note that Burns and Kendall (2002) attributed increasing $\delta^{15}N\text{-}NO_3^-{}_{ter}$ during an incubation experiment to the conservative recycling of N in soils. A ^{15}N-pool dilution study led in Pyreneans subalpine grasslands showed that N was conservatively recycled in the soil-plant continuum (Boutin, 2015). However, low $\delta^{15}N\text{-}NO_3^-{}_{ter}$ in our study rather suggest that $NO_3^-{}_{ter}$ is newly produced in soils, and the causes for such discrepancy (possibly higher leaching rates in the case of the present study) would be worth investigating.

3.2 Complements of information

I started collaborating in 2016 with Catherine Larose, Tim Vogel, and Cécile Thion from the Laboratoire Ampère of Lyon, who have an extensive experience working on environmental microbial genomics. My intent was to further constrain the biological processes (e.g., nitrification, denitrification) that take place in the studied subalpine meadows of the Lautaret pass. By capturing the nature and the diversity of the underlying microbial communities, I hope to clarify their role in controlling N turnover (Legay et al., 2016). Additionally, coupling of isotopic tracers and genomics data has been seldom used in N cycling studies in natural environments. The only other study I could find in literature that combined the two approaches is from Liu et al. (2017). There, the authors show the good match between, on one side, isotopic evidence of NO_3^- sources mixing (and no processing) and low N-related microbial genes abundance in arid areas; and on the other side isotopic imprints of biological processes correlated with higher N-related genes abundance. Another interesting study coupling isotopic and genes abundance, this time focusing on methane, reports evidence of a full methane turnover regulated by microorganisms in a groundwater system of Pennsylvania, US (Vigneron et al., 2017). Therefore, I aim at investigating whether the association of genomic, taxonomic and isotopic data could help further understand the drivers of N cycling in subalpine soils.

In summer 2017 I spent two weeks at the Laboratoire Ampère, where I analyzed the densities of total bacteria, ammonium-oxidizing microbes (bacteria and archaea), nitrate reducers and denitrifiers in a subset of the collected soils presented in the previous section by quantitative PCR (qPCR). I specifically focused on the 16Sb rRNA (bacteria), 16Sa rRNA (archeae), 18S rRNA (fungi), AOB (ammonium-oxidizing bacteria), AOA (ammonium-oxidizing archaea), *narG* and *napA* (nitrate reducers) and *nirK*, *nirS* and *nosZ* (denitrifiers) genes. I also sent DNA extracts to a private American company (Mr DNA, Molecular Research LP, Texas, US), which provided taxonomic analyses on 16S rRNA gene only.

Because of the cost of genomic and taxonomic analyses, only 9 soils samples were analyzed in this first batch, spanning three different management treatments (see section 3.1.2.1) on three different dates (May, July, October) representative of

subalpine ecosystems temporal "hotspots" (*i.e.*, snowmelt, peak biomass, plant senescence). Every sample was pooled from three replicates collected on the meadows.

The results are freshly obtained, and not yet thoroughly dissected. However, we provide here some promising preliminary findings. First, a dendrogram produced by hierarchical clustering of Operational Taxonomic Units (OTU) – *i.e.* groups of non-identified microorganisms showing similar 16S sequences – is given in Figure 3-7. We see that the unterraced grassland (UU in section 3.1) can be clearly distinguished from the terraced meadows (TM and TU in section 3.1) using this taxonomic approach. This is not without echoing the significantly different nitrate isotopic composition in UU soils compared to soils from other management treatments (Table 3-3). Whereas concluding that one is the cause for the other would be a very unscientific shortcut, this nevertheless suggests an interesting possible correlation between isotopic and taxonomic data.

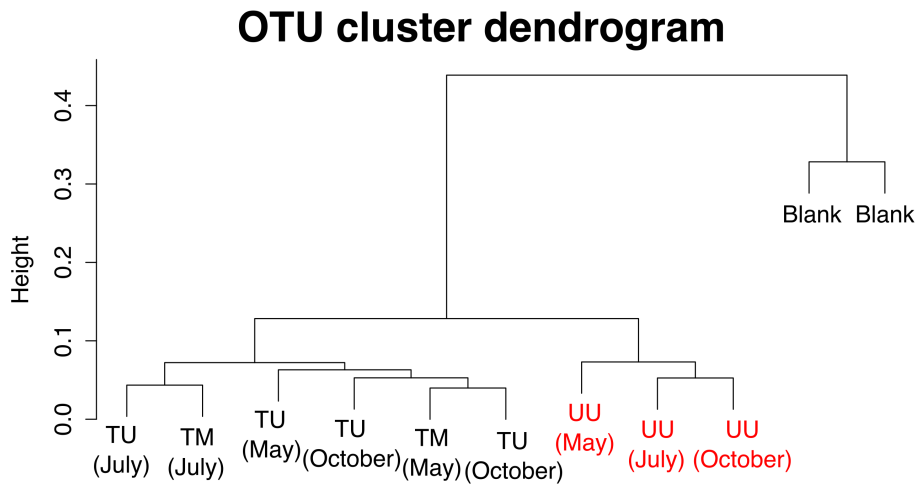

Figure 3-7: Dendrogram of OTU clusters in nine soil samples and two blanks. Samples encompass three different past and current land uses (Unterraced-Unmown (UU), Terraced-Unmown (TU) and Terraced-Mown (TM) and three different dates (May, July and October).

Using an analysis of similarities (ANOSIM) test, it is possible to separate soil samples in two groups that are statistically different (ANOSIM statistic $R = 0.9474$ and $p < 0.01$) with one group constituted of the TM and TU soils and the other

constituted of the UU soils. With an analysis of similarity percentage (SIMPER) test, it is possible to hierarchize the microbial phyla that most explain the statistical difference between the two groups. Five phyla accounting for 71% of the taxonomic difference between soils are given in Table 3-4. A preliminary review of the literature did no provide information on whether species from Verrucomicrobia and Actinobacteria phyla could play a significant role in N cycling, however species from the Chloroflexi, Proteobacteria and Thaumarchaeota phyla are associated with bacterial heterotrophic nitrification, bacterial chemolithoautotrophic nitrification and archaeal ammonia oxidation, respectively. These results point at alternative nitrification pathways from the "classical" autotrophic nitrification, but further tests are required to evaluate how this could relate to isotopic spatial and temporal variations.

Table 3-4: Five phyla explaining 71% of the difference in taxonomy between the terraced meadows (TM and TU) and the unterraced grassland (UU).

Phylum	Difference explained (cumulative %)
Verrucomicrobia	26
Actinobacteria	44
Chloroflexi	55
Proteobacteria	65
Thaumarchaeota	71

It is possible to look even more in details at the taxonomic diversity of microorganisms in soils, by focusing on bacterial classes for instance (Figure 3-8). However, the more details, the more difficulty in interpreting the relationship between isotopic and taxonomic data. Indeed, microorganisms' diversity probing is limited by a number of caveats. First, the choice of primers to perform the gene sequencing will strongly control the access to the taxa diversity in soils, and can potentially bias our understanding of microbial community structure. Second, taxonomy and functionality are not always related because of:

(i) Functional redundancy (*i.e.*, taxa that are phylogenetically very different can have genes coding for the same function). For instance denitrification is

coded by a large number of genes that intervene successively in the denitrification stages, and that are widely (and randomly?) spread among the bacterial phylogeny (Salles et al., 2012).

(ii) Horizontal genes transfer (*i.e.*, an exchange of functional genes between bacterial communities), although this is has been mostly reported for N-fixing genes (Bailly et al., 2007; Bolhuis et al., 2010).

(iii) Significant discrepancy between bacterial genotype and phenotype which sometimes translate the precise control of environmental conditions on a gene expression. It is notably the case for denitrifiers, which allegedly express denitrification only under anaerobic conditions (N playing the role of electron acceptor) because this alternative respiration pathway costs more energy (Ferguson, 1994).

Despite these limitations, there is generally a strong coherence between taxonomy and ecology, and my efforts will be placed on a few relevant taxa regarding N cycling.

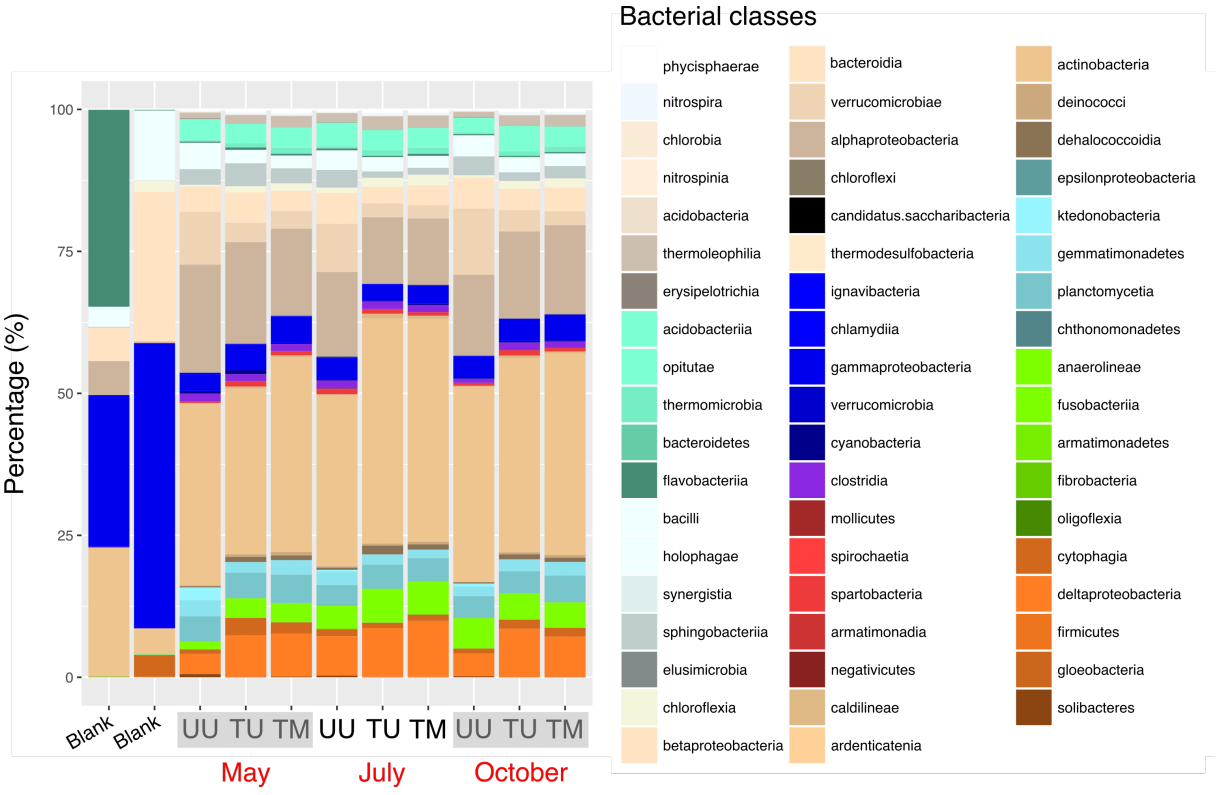

Figure 3-8: Bacterial diversity in nine soil samples spanning three different land past and current use (Unterraced-Unmown (UU), Terraced-Unmown (TU) and Terraced-Mown (TM) and three different dates (May, July and October).

3.3 Synthesis

3.3.1 Summary of the main results

In the first part of this chapter (section 3.1), we specifically focus on quantifying $NO_3^-_{atm}$ proportion in three subalpine meadows. The soils exhibit different $NO_3^-_{atm}$ retention patterns depending on their management. In average over the study period, the terraced meadows (TM and TU) both have undetectable $NO_3^-_{atm}$ in soil extracts and leachates whereas **up to 6 %** of the unterraced grassland (UU) NO_3^- pool has an atmospheric origin. This is likely due to low N cycling rates in the UU grassland favoring a higher transit time of $NO_3^-_{atm}$ in soils without being biologically processed. The overall low amount of $NO_3^-_{atm}$ in the terraced meadows, and no $NO_3^-_{atm}$ exports at the outlet of the watershed during snowmelt together suggest that **$NO_3^-_{atm}$ undergoes a rapid turnover** upon deposition in these fields. In the unterraced grassland, soil and stream data rather suggest that kinetic saturation is the primary driver of $NO_3^-_{atm}$ dynamics in this unamended field.

Low δ^{18}O-$NO_3^-_{ter}$ and δ^{15}N-$NO_3^-_{ter}$ in all soils are intriguing and perplexing. To date, it is difficult to ascertain why this is so, and several hypotheses are provided in sections 3.1.4.2 and 3.1.4.3. Regardless of the reason, it appears that **isotopic fractionations**, due to kinetic or equilibrium effects for instance, could play a major role in controlling the isotopic composition of nitrate in these subalpine soils. A systematic monitoring of nitrate complete isotopic composition (**Δ^{17}O, δ^{18}O and δ^{15}N**) in future environmental studies – and correction for the atmospheric imprint – would help understand whether the low δ^{18}O-$NO_3^-_{ter}$ and δ^{15}N-$NO_3^-_{ter}$ in this study are site-specific or more widely spread than suggested in literature. **This is an important point because most studies – including mine – rely heavily on the assumption that sources mixing rather than processes is the main driver of NO_3^- isotopic composition**. I hope that coupling isotopic with genomic data will alleviate the uncertainties regarding the main processes driving N turnover in subalpine soils and their effect on NO_3^- isotopes.

3.3.2 Results situated in the conceptual framework

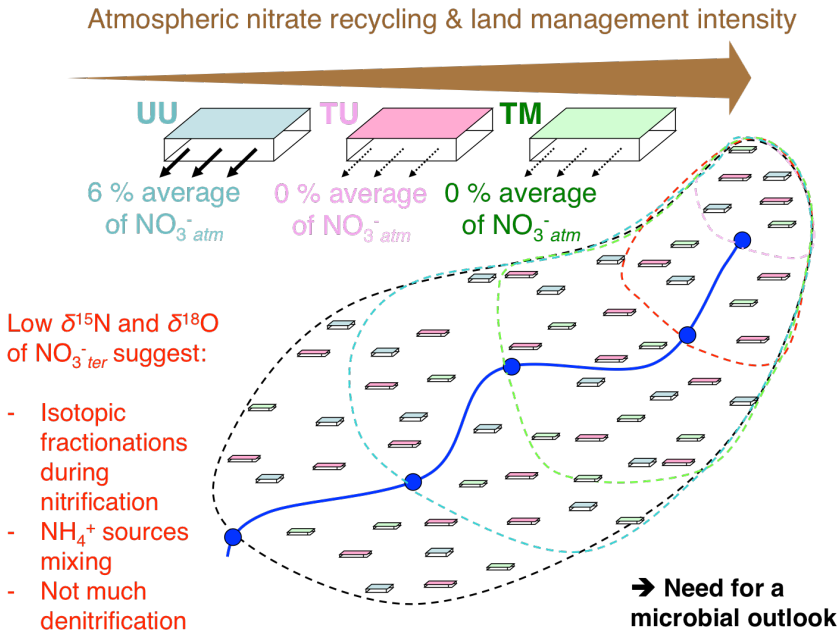

Figure 3-9: Main results from the chapter 3 placed in the study context.

3.3.3 Linkage with the plant compartment

Low fractions of $NO_3^-{}_{atm}$ in soils point at a quick immobilization and uptake by microbes and plants. $NO_3^-{}_{atm}$ contribution to subalpine plants N contents could be particularly important because of the strong competition between plants and microorganisms for resources, tipping in favor of subalpine plants uptake in the early stages of the growing season (Legay et al., 2013). Furthermore, plants have unanimously been recognized as a very sensitive biota to N deposition, especially in nutrient poor environments where the biotic constraint on plant response to N inputs is particularly acute (Bowman et al., 2006; Chapin et al., 1997). An experiment conducted in subalpine meadows in the French Pyrenees showed that plant recovered 43 % and 37 % (19 % and 29 % in soils) of exogenous sprayed N after one and two years following inoculation, respectively (Boutin, 2015). Interestingly, most part of this additional N was found in leaves, hinting at a potential foliar uptake strategy of these subalpine plant species. In the next chapter, we will investigate this

plant compartment at the Lautaret pass and see whether, under natural conditions, plants show higher $NO_3^-{}_{atm}$ contents than in soils.

4 Atmospheric nitrate in plants: seasonal dynamics, uptake pathways and ecological implication

This chapter describes the breakthroughs in our understanding of NO_3^- uptake pathways and strategy used by two dominant subalpine plants at the Lautaret pass. *Dactylis glomerata* and *Festuca paniculata*, collected on the same meadows as presented in Chapter 3, are more specifically the object of the study presented here. The section 4.1 describes the temporal variations of $NO_3^-_{atm}$ proportion in plant organs and how it relates to known nutrients uptake strategies for these species. Based on isotopic considerations, the respective importance of foliar and root uptake is discussed, and the preferred sites for NO_3^- assimilation are dissected. A summary of the scientific conclusions is provided in section 4.2, and the main findings will be put in perspective with the terrestrial N cycle in subalpine meadows.

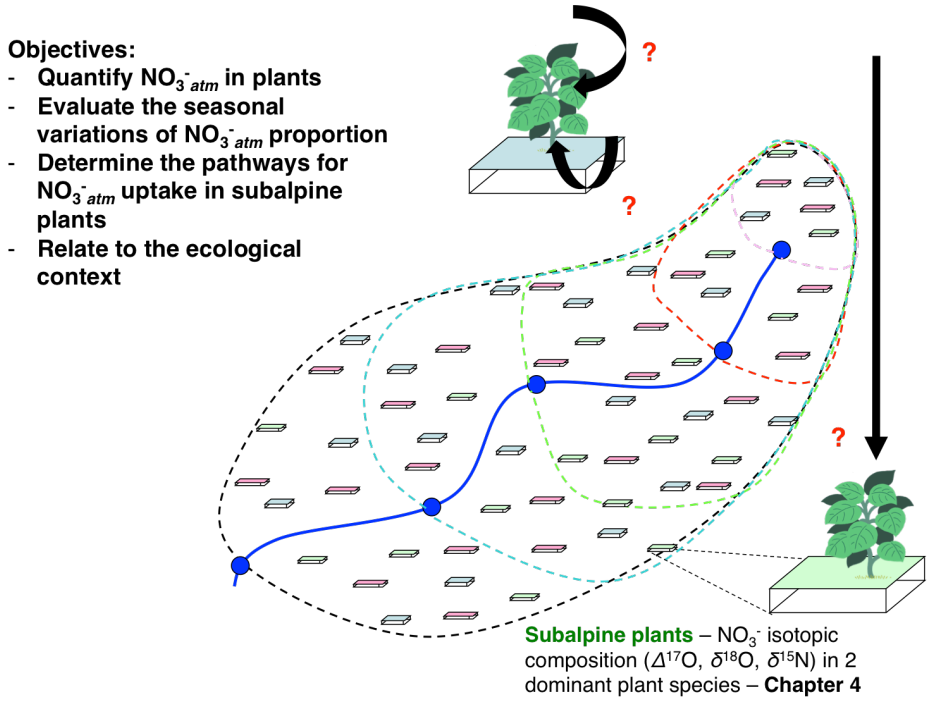

Figure 4-1: Positioning of this chapter in the conceptual framework of this study, and related objectives it will answer to.

4.1 Direct fertilization of subalpine plants by atmospheric nitrate

After:

Bourgeois, I. ; Clément, J.-C. ; Caillon, N. ; Nesti, C. ; Deschamps, N. and Savarino, J. : Direct fertilization of subalpine plants by atmospheric nitrate, in review for the *Proceedings of the National Academy of Sciences*.

Abstract

Despite decades of studies on nitrogen (N) cycling perturbations in ecosystems caused by anthropogenic activities, several caveats remain before we fully understand the fate of increasing atmospherically deposited N. Subalpine meadows are especially relevant in that concern as N is a key-limiting nutrient fostering the dominance of specific subalpine plant communities, with strong impact on essential ecosystems services. Here, we present isotopic evidence ($\Delta^{17}O$, $\delta^{18}O$ and $\delta^{15}N$) of the direct contribution of atmospherically deposited nitrate to subalpine plants nitrate pool (up to 33%). Differences in nitrate isotopic composition between leaves and roots suggest that plants strategies for N uptake reflect on their NO_3^- isotopic composition. We show that direct foliar uptake of atmospheric nitrate (3-16% of plant N demand) is a non-negligible, yet overlooked, pathway for N uptake in grasses under natural conditions, especially when growing on nutrients poor soils. Further, we demonstrate that this multi-isotopic approach has a unique potential to further unravel the global functioning of ecosystems with changing N supplies, and we recommend that more studies use this technique to decouple atmospheric N input pathways into ecosystems.

Significance

Nitrogen (N) is often an essential limiting nutrient for terrestrial plant productivity. However, in excess, it leads to complex ecological consequences on Earth system. Human activities have increased by ten-fold the amount of atmospherically deposited nitrogen over the last century with, as consequence, the alteration of pristine environments. Here, we use natural isotopes of nitrate, one of the preferential N form for plant uptake, to demonstrate that subalpine plants readily

absorb atmospheric nitrogen either after deposition, through the root system, or directly from the air *via* the leaves. These measurements provide the first *in situ* evidence of the direct contribution of atmospheric nitrogen as plants substrate, bypassing soil N cycling, and raise the concern of potentially increased ecological issues under rising anthropogenic nitrogen deposition.

4.1.1 Introduction

Nitrogen (N) atmospheric deposition monitoring has been determinant to assess human global imprint on the environment over the past decades (Fowler et al., 2015; Galloway et al., 2008; Vitousek et al., 1997). Anthropogenic activities (e.g., fossil fuel combustion, agriculture) have led to increased emissions of reactive nitrogen species (Nr = NO_y, NH_x, N_2O), with in turn enhanced inputs of N in a large variety of ecosystems (Galloway et al., 2004). Consequences of such alteration of the N cycle are now well documented, ranging from soil acidification to biodiversity loss, not to mention intensified N leaching, eutrophication and public health issues (Aber et al., 1989; Clark et al., 2013; Galloway et al., 2003; Ward et al., 2005). Mountainous regions are especially vulnerable to this phenomenon because of little acidification buffering capacities in soils and optimized functioning strategies of native plants in response to historical nutrients limitation (Bassin et al., 2013; Boutin et al., 2017; Bowman et al., 2006). For instance, advanced stages of N saturation in elevated sites of the Colorado Front Range, USA have been demonstrated (Baron, 2006; Burns, 2004; Williams and Tonnessen, 2000), and highlight the critical need for further investigation in understanding the fate of deposited N.

Novel isotopic techniques used in recent studies have shed new light on the dramatically high contribution of atmospheric N to remote freshwater bodies (15, Bourgeois et al. *in review*). Yet, N balance in altitude catchments is still poorly understood. Atmospheric N deposition often exceeds streams water losses *via* leaching (Baron and Campbell, 1997; Mast et al., 2014); potential sinks for the missing N may be immobilization by soil microbes, uptake by plants and/or denitrification. Up to date, atmospheric N dynamics in mountainous soil/plant continuum have scarcely been investigated, despite an urgent need for

understanding nutrients partitioning in these ecologically critical ecosystems (Clément et al., 2012; Thébault et al., 2014).

Inorganic N (nitrate and ammonium) is usually considered as more readily absorbed by plants than organic N forms (Haynes and Goh, 1978). Measurements of the triple isotopes ($\Delta^{17}O$, $\delta^{18}O$ and $\delta^{15}N$) composition of nitrate (NO_3^-) provide a unique and powerful tool to identify NO_3^- sources and infer the biological processes governing its dynamics (Kendall et al., 2007). However, this multi-isotopic tracer has, to the best of our knowledge, still never been used to monitor atmospheric nitrate ($NO_3^-_{atm}$) uptake and assimilation by plants in natural condition. The dual isotope technique has been successfully used on mosses to evaluate the sources of NO_3^- contained in their tissues (Liu et al., 2012; Liu et al., 2013b), but interpretation of the $\delta^{18}O$ and $\delta^{15}N$ values of NO_3^- ($\delta^{18}O$-NO_3^- and $\delta^{15}N$-NO_3^- later on) in vascular plants is a much more complicated challenge (Liu et al., 2013a). We suggest that direct measurements of $\Delta^{17}O$-NO_3^- in plants should help to bypass interpretation issues caused by mass-dependent biological fractionation.

To investigate the contribution of $NO_3^-_{atm}$ to the bio-available nutrients pool in subalpine meadows, we measured for the first time the concentration and triple isotopic composition ($\Delta^{17}O$, $\delta^{18}O$ and $\delta^{15}N$) of NO_3^-, along with ammonium (NH_4^+) concentration, in different tissues of two subalpine plants species at the Lautaret pass in the Central French Alps. This site is characterized by a seasonal snow-cover (November to April) and by a short vegetative period (May to September, hereafter referred as annual). The vegetation is dominated by grassland communities whose diversity and functional traits depend on past – terraced *vs*. unterraced – and current – mowing, grazing – land use (Quétier et al., 2007). From May to September 2016, we harvested the roots and the leaves and stems (hereafter referred as leaves) of *Dactylis glomerata* (*D. glomerata*) and *Festuca paniculata* (*F. paniculata*), two dominant perennial tussock grasses featuring exploitative and conservative resource use strategies, respectively (Gross et al., 2007; Quétier et al., 2007). *D. glomerata* was collected on two terraced meadows with different current land-management –

terraced-mown (TM) *vs* terraced-unmown (TU) – while *F. paniculata* was collected on unterraced grassland – unterraced-unmown (UU) – (Figure 4-2).

4.1.2 Methods

4.1.2.1 Site Description

This study focuses on two sub-watersheds (Lautaret and Les Cours), located in the upper Romanche valley, near the Lautaret pass (45°02'N; 6°20'E, 1650-2000 m a.s.l., Figure 4-2). The experimental site is part of the national research infrastructure for the study of continental ecosystems and their biodiversity (AnaEE – France, https://www.anaee-france.fr), and of the Long Term Ecological Research network (LTER, https://lternet.edu). Temperatures in 2016 averaged -3.0°C in January and 13.0°C in August and cumulated annual precipitation was 609 mm. We studied three grasslands featuring three combinations of past (terraced *vs* unterraced) and present (mown *vs* unmown) land uses (Quétier et al., 2007). Two of the grasslands were situated on the terraced slopes of Les Cours watershed. One was mown for hay in August then grazed in autumn (terraced and mown, TM) while the other was not mown but grazed in summer (terraced and unmown, TU). The unterraced grassland has never been mown (unterraced and unmown, UU) and only very lightly grazed during the transhumance of livestock. The management practices in the area have been stable since at least 2003 (Legay et al., 2013) and led to substantial differences in plant communities and soil properties. Briefly, terraced meadows are dominated by species showing exploitative traits such as *D. glomerata* whereas unterraced grasslands are dominated by conservative species like *F. paniculata*. These two species show very different functional traits (Quétier et al., 2007), illustrating different strategies for nutrients uptake and competition with soil microbial biomass (Legay et al., 2013; Robson et al., 2010).

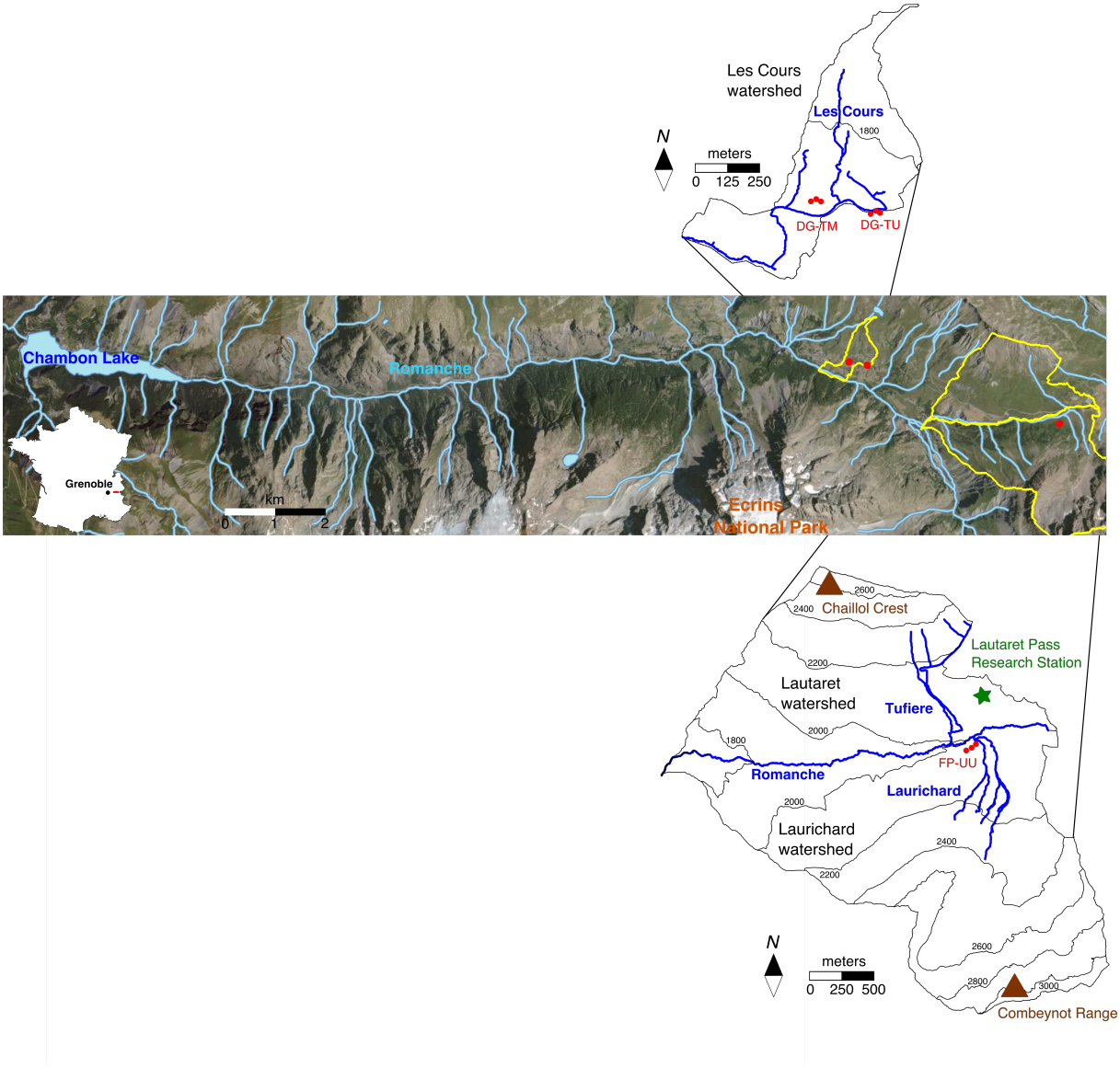

Figure 4-2: Map of the Lautaret pass study area. The central map represents the Romanche Valley in the central French Alps, situated 90 km away from the city of Grenoble (~ 163 000 inhabitants). The boundaries of Lautaret, Laurichard and Les Cours watersheds are delimited in yellow. Streams are shown in blue. The localization of plants and soils sampling in three meadows with different land-management is indicated in red. The meadows are labeled as DG-TM (terraced-mown, *Dactylis glomerata* is dominant), DG-TU (terraced-unmown, *Dactylis glomerata* is dominant) and FP-UU (unterraced-unmown, *Festuca paniculata* is dominant).

4.1.2.2 Samples collect and analysis.

Sampling encompasses three different grasslands as described in the previous section, each of which was divided in three plots, to reach a total number of 9 plant individuals collected per sampling date (3 grasslands * 3 replicates). From May to September 2016, either one *D. glomerata* or *F. paniculata* tussock per

subplot, including several tillers, was harvested based on respective species dominance in the meadow. A soil core of 4.5-cm diameter and 8-cm length was removed from all subplots, in the same place as the biomass harvest. Sampling was performed twice a month until peak biomass (May and June), and on a monthly basis afterward (July, August, September).

Separate wet and dry deposition were collected – every three weeks when possible – using an atmospheric deposition collector (WADOS Kroneis GmbH Austria) from April 2016 to October 2016. Precipitation samples were stored frozen until further analysis. The dry deposition funnel was rinsed with 500-mL of ultrapure water (18.2-MΩ cm^{-1}), and the sample was stored at -20°C.

All plants were thoroughly washed with ultrapure water. Aerial parts (*i.e.*, leaves, shoots and stems) and belowground parts (*i.e.*, roots) were separated, wiped and stored frozen. Samples were later freeze-dried (Heto DryWinner, Allerod, Denmark), grounded to powder (RETSCH Mixer Mill MM400) and homogenized, following a commonly used procedure (Laursen et al., 2013; Mihailova et al., 2014). Dissolved inorganic nitrogen (DIN) was extracted by shaking (300-RPM for 1-h) 1-g and 1.5-g dw of *D. glomerata* and *F. paniculata* powdered tissues, respectively, in 50-mL ultrapure water. Soils were 2-mm sieved to remove rocks and roots, and 10-g dw subsamples of sieved soils were shaken (300-RPM for 1-h) in 50-mL ultrapure water to extract the DIN. After centrifugation (4000-RPM for 10-min), all plants and soils samples were filtered on 0.22-µm quartz filters (QMA Whatman). Precipitation samples were left to melt at ambient temperature prior to being filtered on 0.45-µm quartz filters (QMA Whatman).

All samples were subsequently analyzed for [NH_4^+] and [NO_3^-] using a colorimetric technique (Gallery Plus, Thermo Fisher Scientific, Waltham, Massachusetts, USA) with an analytical error of ± 0.01-mg L^{-1}. All concentrations are given in µg g^{-1} dry tissue weight (dw). Isotopic analyses were conducted on an MAT 253 IRMS using an adapted version of the denitrifier method (Kaiser et al., 2007). The analytical error was ± 0.5, 2.1 and 0.3 ‰ for $\Delta^{17}O$, $\delta^{18}O$ and $\delta^{15}N$ of NO_3^-, respectively.

4.1.2.3 Isotopic end-member mixing model

Oxygen abundances have been successfully used in recent studies to discriminate $NO_3^-_{atm}$ from NO_3^- originating from other sources (Riha et al., 2014; Tsunogai et al., 2016; Wang et al., 2016). Most processes and materials on Earth are subject to isotopic fractionations proportional to the relative difference of isotopes mass (mass-dependent fractionation). Microbial nitrification in soils, for instance, yields NO_3^- of which O isotopes follow the mass-dependent law $\delta^{17}O \approx 0.52*\delta^{18}O$ (Miller, 2002). $NO_3^-_{atm}$ deviates from this mass-dependent law because of its production pathway involving O_3, bearer of a ^{17}O excess between 25 and 35‰ (Vicars and Savarino, 2014). As a result, ^{17}O excess (noted $\Delta^{17}O$, with $\Delta^{17}O = \delta^{17}O - 0.52*\delta^{18}O$) of $NO_3^-_{atm}$ ranges from 20 to 35 ‰ (Savarino et al., 2013), whereas NO_3^- from other sources has $\Delta^{17}O$ of zero (Michalski et al., 2004b). In this study, $\Delta^{17}O$-$NO_3^-_{atm}$ end-member was chosen as the mean concentration-weighted value of $\Delta^{17}O$-NO_3^- in wet and dry deposition collected at the Lautaret pass from May to September 2016 (Table 3-2), with a value of 24.4 ± 2.4 ‰ (-6.0 ± 4.1 and 66.6 ± 5.8 ‰ for $\delta^{15}N$ and $\delta^{18}O$-$NO_3^-_{atm}$, respectively). Respective contribution of atmospheric deposition was thus inferred from the following equation:

$$f_{atm} = \Delta^{17}O\text{-}NO_3^-_{sample} / 24.4 \qquad \text{(Eq. 4.1)}$$

With f_{atm} (= $\%NO_3^-_{atm}$), the mole fraction of the atmospheric contribution and $\Delta^{17}O$-$NO_3^-_{sample}$ the measured value of $\Delta^{17}O$-NO_3^- in a sample.

Mole fractions of NO_3^- (f_{atm} and $f_{ter} = 1 - f_{atm}$) can be used to remove the isotopic influence of $NO_3^-_{atm}$ on $NO_3^-_{sample}$, which allow a better interpretation of biological processes that affect its $\delta^{15}N$ and $\delta^{18}O$ values (Dejwakh et al., 2012; Riha et al., 2014). Dual isotope plots have been intensively used to evaluate sources of N and potential processes (denitrification, assimilation) in the environment (Burns et al., 2009; Durka et al., 1994; Griffiths et al., 2016; Kendall et al., 1995; Liu et al., 2013a). However, because of distinct $\delta^{18}O$-$NO_3^-_{atm}$ values compared to $NO_3^-_{ter}$, even a small f_{atm} can lead to scatter in a dual-isotope plot. Removing the atmospheric $\delta^{15}N$ and $\delta^{18}O$ components from environmental samples lead to an easier assessment of

biological processes, such as assimilation in our case. This isotope correction was applied on our samples using the isotopic mass balances from Riha et al. (2014):

$$\delta^{18}O_{ter} = (\delta^{18}O_{sample} - \delta^{18}O_{atm} * f_{atm})/f_{ter} \quad \text{(Eq. 4.2)}$$

$$\delta^{15}N_{ter} = (\delta^{15}N_{sample} - \delta^{15}N_{atm} * f_{atm})/f_{ter} \quad \text{(Eq. 4.3)}$$

$\delta^{15}N_{atm}$ and $\delta^{18}O_{atm}$ were inferred from NO_3^- in wet and dry deposition, and given in Table 3-2.

4.1.2.4 Plots and statistical analysis

Note that each data point in Figure 4-6 and Figure 4-7 represents the mean value of three plant individuals per sampling date in order to account for spatial variability. All statistical analyses were conducted using R software (v3.2.3). A Mann-Whitney test was applied to determine significant differences of mean concentrations and isotopic values of NO_3^- and NH_4^+ between plants organs and species, on an annual (Figure 4-3) or seasonal (Figure 4-4) basis. Differences and correlations were held significant when the *p* value reached a 0.05 credible interval.

4.1.3 Results

Figure 4-3 shows the mean annual [NH_4^+], [NO_3^-] and NO_3^- isotopic values ($\Delta^{17}O$, $\delta^{18}O$ and $\delta^{15}N$) in *D. glomerata* and *F. paniculata* tissues. Values are also given in Table 4-1. Mean annual plant [NO_3^-] varied between 10.0 ± 5.4 and 38.8 ± 50.8-µg g^{-1} dry weight (dw), and no significant difference was found between plant species or between plants tissues, except for *D. glomerata* in TU fields (Figure 4-3a). Measured [NO_3^-] in plants were consistent with NO_3^- contents in other grasses grown under natural conditions (Gebauer et al., 1988). Mean annual plant [NH_4^+] varied between 1.3 ± 0.8 and 94.0 ± 100.1-µg g^{-1} dw and were very low in all plants leaves. *D. glomerata* roots held significantly higher NH_4^+ amounts compared to adjacent soils (Table 4-2), and compared to *F. paniculata* roots (Figure 4-3b). We found isotopic evidence of unprocessed $NO_3^-{}_{atm}$ in all parts of *D. glomerata* and *F. paniculata* (Figure 4-3c). Mean annual $\Delta^{17}O$-NO_3^- ranged from 1.0 ± 0.7 ‰ in *D. glomerata* roots

to 3.4 ± 3.2 ‰ in *F. paniculata* leaves. Interestingly, mean annual $\Delta^{17}O\text{-}NO_3^-$ was significantly higher in leaves compared to adjacent soils (Table 4-2). Mean annual $\delta^{18}O\text{-}NO_3^-$ and $\delta^{15}N\text{-}NO_3^-$ were significantly higher in all plants compared to soils (Table 4-2). *F. paniculata* exhibited similar mean annual $\delta^{18}O\text{-}NO_3^-$ and $\delta^{15}N\text{-}NO_3^-$ in roots and leaves (Figure 4-3d and e) whereas $\delta^{18}O\text{-}NO_3^-$ and $\delta^{15}N\text{-}NO_3^-$ spanned higher values in *D. glomerata* leaves compared to roots.

Table 4-1: Mean concentration of NO_3^- and NH_4^+ (µg g^{-1} dw) and concentration-weighted isotopic values of NO_3^- (‰) in plants organs and associated standard deviation. UU, TU and TM refer to Unterraced-Unmown, Terraced-Unmown and Terraced-Mown land-uses. Highlighted values exclude one outlier.

Roots	$[NO_3^-]$ (µg g^{-1} dw)	$[NH_4^+]$ (µg g^{-1} dw)	$\Delta^{17}O$ (‰)	$\delta^{18}O$ (‰)	$\delta^{15}N$ (‰)
F. paniculata (UU meadows)	14.4 ± 18.3	2.1 ± 2.9	1.9 ± 0.6	23.6 ± 5.4	15.9 ± 6.7
D. glomerata (TU meadows)	10.0 ± 5.4	94.0 ± 100.1	1.2 ± 1.2	4.9 ± 5.6	-2.4 ± 5.5
D. glomerata (TM meadows)	29.4 ± 52.8	43.6 ± 27.1	1.0 ± 0.7	3.8 ± 3.1	4.4 ± 8.4
Leaves	$[NO_3^-]$ (µg g^{-1} dw)	$[NH_4^+]$ (µg g^{-1} dw)	$\Delta^{17}O$ (‰)	$\delta^{18}O$ (‰)	$\delta^{15}N$ (‰)
F. paniculata (UU meadows)	19.2 ± 12.9	1.3 ± 0.8	3.4 ± 3.2	25.6 ± 6.6	14.8 ± 14.8
D. glomerata (TU meadows)	38.8 ± 50.8	2.0 ± 1.4	2.7 ± 1.7	13.6 ± 16.2	4.4 ± 11.8
D. glomerata (TM meadows)	36.5 ± 23.7	3.6 ± 2.5	2.5 ± 2.0	18.2 ± 6.2	16.8 ± 7.7

Table 4-2: Mean annual concentration of NO_3^- and NH_4^+ (µg g^{-1} dw) and concentration-weighted isotopic values of NO_3^- (‰) in soils extracts and leachates, and associated standard deviation. UU, TU and TM refer to Unterraced-Unmown, Terraced-Unmown and Terraced-Mown land-uses.

Soils extracts	$[NO_3^-]$ (µg g^{-1} dw)	$[NH_4^+]$ (µg g^{-1} dw)	$\Delta^{17}O$ (‰)	$\delta^{18}O$ (‰)	$\delta^{15}N$ (‰)
UU meadows (n=18)	14.6 ± 19.0	13.0 ± 13.7	0.9 ± 0.6	-4.3 ± 6.8	-5.1 ± 6.6
TU meadows (n=21)	58.9 ± 46.9	17.5 ± 29.9	0.5 ± 0.8	-10.3 ± 6.6	-1.3 ± 9.6
TM meadows (n=21)	52.3 ± 48.7	6.2 ± 4.0	0.3 ± 0.4	-10.9 ± 5.1	-2.6 ± 6.5

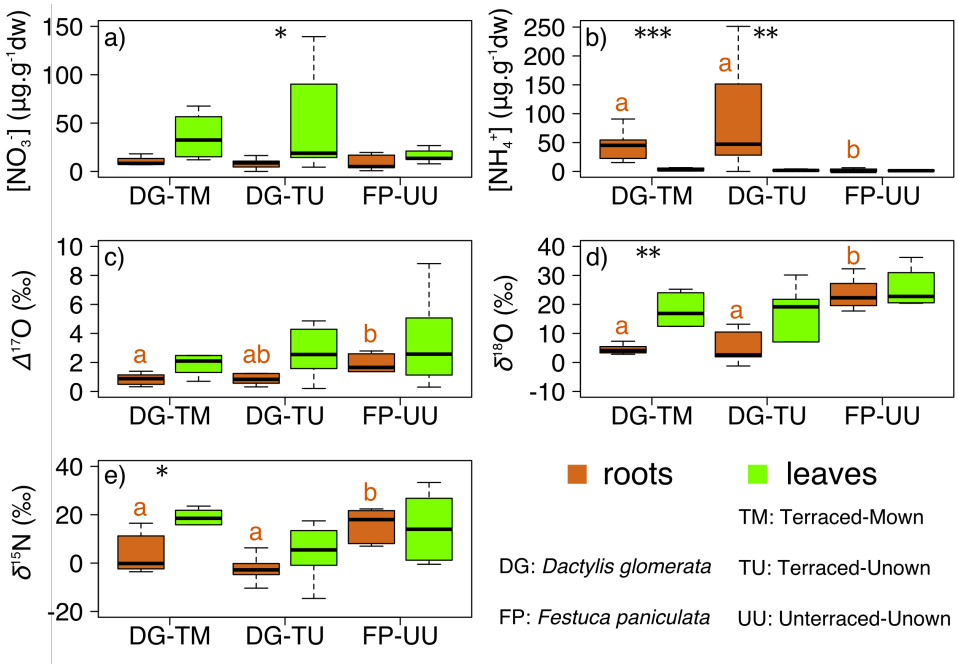

Figure 4-3: Mean annual a) $[NO_3^-]$ (µg g^{-1} dw) and b) $[NH_4^+]$ (µg g^{-1} dw) along with c) $\Delta^{17}O$ (‰), d) $\delta^{18}O$ (‰) and e) $\delta^{15}N$ (‰) of NO_3^- in *Dactylis glomerata* and *Festuca paniculata* leaves (n= 55 and 33 for concentration and isotopic data, respectively) and roots (n= 56 and 47 for concentration and isotopic data, respectively), sampled between May and September 2016. Box plots show median, 25th and 75th percentiles. Different letters indicate significant differences between plant species. Asterisks indicate significant differences between plant organs for a given species (* for p<0.05, ** for p<0.01, *** for p<0.001).

Figure 4-4 presents the variations of $[NH_4^+]$, $[NO_3^-]$ and NO_3^- isotopic values ($\Delta^{17}O$ and $\delta^{15}N$) in pooled plants before and after the peak biomass early July ($\delta^{18}O$ is given in Figure 4-5). Mean $[NO_3^-]$ in leaves was significantly higher after peak biomass in all plants compared to prior peak biomass (Figure 4-4a), whereas mean

$[NH_4^+]$ did not significantly vary accordingly (Figure 4-4b). Interestingly, the after peak biomass period was also characterized by significantly higher mean $\Delta^{17}O\text{-}NO_3^-$ in leaves and significantly lower mean $\delta^{15}N\text{-}NO_3^-$ in roots, compared the earlier period (Figure 4-4c and d).

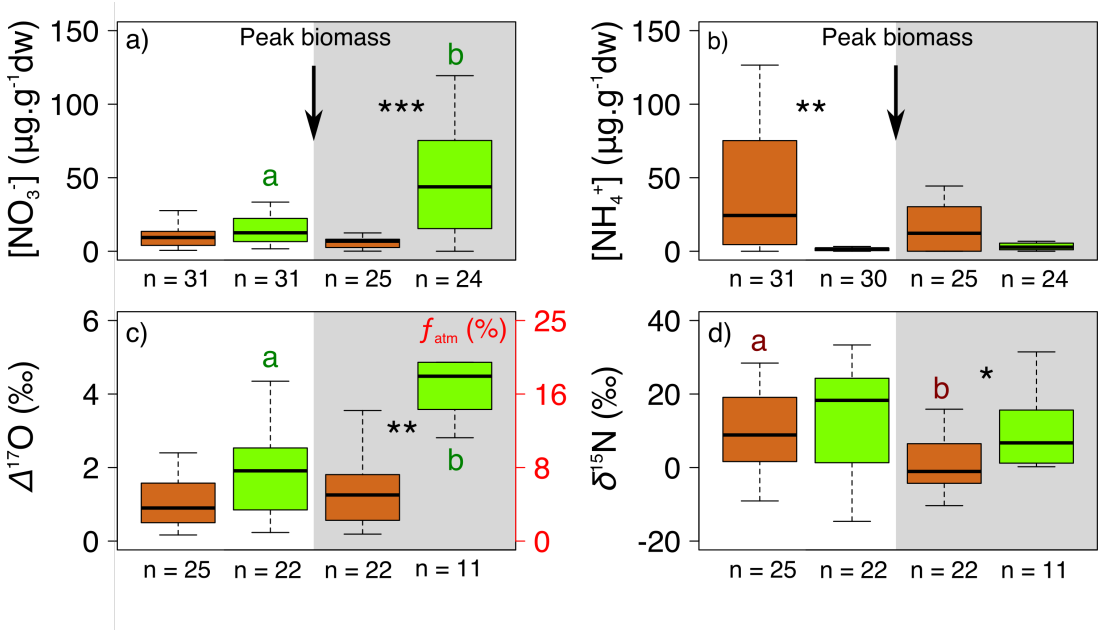

Figure 4-4: Before and after peak biomass values of a) $[NO_3^-]$ (µg g^{-1} dry tissue), b) $[NH_4^+]$ (µg g^{-1} dry tissue), c) $\Delta^{17}O\text{-}NO_3^-$ (‰) and corresponding f_{atm} (%, the proportion of $NO_3^-{}_{atm}$) and d) $\delta^{15}N\text{-}NO_3^-$ (‰) in pooled plant leaves (green) and roots (brown). The black arrow delineates the peak biomass (beginning of July). Highlighted in grey is the after peak biomass period. Different letters indicate significant differences between the two periods. Asterisks indicate significant differences between plant organs for a given period (* for $p<0.05$, ** for $p<0.01$, *** for $p<0.001$).

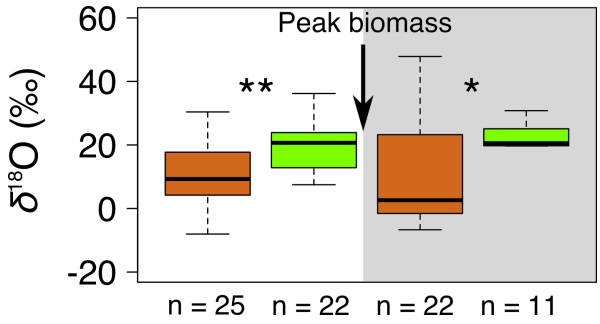

Figure 4-5: Before and after peak biomass values of $\delta^{18}O\text{-}NO_3^-$ (‰) in pooled plant leaves (green) and roots (brown). The black arrow delineates the peak biomass (beginning of July). Highlighted in grey is the after peak biomass period. Different letters indicate significant differences between the two periods. Asterisks indicate significant differences between plant organs for a given period (* for p<0.05, ** for p<0.01, *** for p<0.001).

4.1.4 Discussion

4.1.4.1 Isotopic framework

Atmospheric NO_3^- ($NO_3^-_{atm}$) is characterized by high $\Delta^{17}O$ values gained during its production process and ranging from 20 to 35 ‰ (Savarino et al., 2013), whereas terrestrial NO_3^- ($NO_3^-_{ter}$) exhibits $\Delta^{17}O$ values of 0 ‰ (Michalski et al., 2004b), enabling the quantification of $NO_3^-_{atm}$ contribution using a simple two end-member mixing model (see section 4.1.2). Not only does this multi-isotopic tracer of NO_3^- reveal unequivocal direct $NO_3^-_{atm}$ inputs in environmental matrices, it also provides a more robust assessment of biological induced fractionation of NO_3^- isotopes compared to the traditional dual isotopes technique (*i.e.*, $\delta^{18}O$ and $\delta^{15}N$) (Fang et al., 2015). In other words, positive values of $\Delta^{17}O\text{-}NO_3^-$ in a plant sample reflect the uptake of unprocessed $NO_3^-_{atm}$ in the tissues.

4.1.4.2 $NO_3^-_{atm}$ uptake

Photoautotrophic plants are not able to produce autonomously the nitrogen they need for biomass growth and therefore depend on external N availability to meet their needs. NO_3^- uptake is regulated by a large number of environmental and physiological parameters (Liu et al., 2014), with soils regarded as the almost exclusive pool of available N for vascular plants (Haynes and Goh, 1978). Here, *D. glomerata* and *F. paniculata* both showed unequivocal year-round presence of NO_3^-

$_{atm}$ in roots and leaves, which contributed punctually up to 33% ($\Delta^{17}O$ = 8.1 ‰) of total NO_3^- pool (Figure 4-3c). This result highlights that, in natural conditions, atmospheric nitrate serves as substrate for vascular plants uptake, and this before being recycled in soils. Increasing $NO_3^-{}_{atm}$ proportion in leaves after peak biomass may illustrate a shift of plants strategy from roots uptake in spring after snowmelt to foliar uptake in summer, when competition by microbial immobilization is stronger (Legay et al., 2013; Robson et al., 2010), and foliar exchange surface with the atmosphere is maximum. A recent study in French Pyrenees subalpine meadows highlighted the strong foliar uptake capacity of *Poaceae* (*i.e.*, *F. paniculata* and *D. glomerata* family) in an experiment where $\delta^{15}N$-labeled NO_3^- and NH_4^+ were sprayed at different concentrations on natural grasslands (Boutin, 2015). To assess the plausibility of such foliar uptake under natural conditions, we evaluated the possible pathways of $NO_3^-{}_{atm}$ entry in plants organs based on isotopic considerations (Liu et al., 2014).

One possible scenario for $NO_3^-{}_{atm}$ uptake is the foliar absorption of gaseous species (NO_2, HNO_3) and/or the incorporation of NO_3^- dissolved in precipitation when water forms a film layer on plant tissues (Vallano and Sparks, 2007). These compounds enter plant leaves either via the stomata or through the cuticles, depending on the chemical and physical characteristics of the pollutants and the plant species (Sparks, 2009; Vallano and Sparks, 2007). HNO_3, NO_3^- and hypothetically NO_2 (Savarino et al., 2008), will lead to a similarly $\Delta^{17}O$ enriched $NO_3^-{}_{atm}$ when assimilated in leaves. However, our results cannot discriminate one pathway against the other.

Another possible scenario is the translocation of deposited $NO_3^-{}_{atm}$ in soils to aboveground biomass (Boutin, 2015). Roots-to-shoot transport of NO_3^- *via* the xylem is well-documented for herbaceous species, with NO_3^- being either stored in petioles or reduced in mesophyll cells (Hachiya and Sakakibara, 2016). On the way up, NO_3^- could also be partly reduced in roots or stored in the vacuole. In this study, year-round positive $\Delta^{17}O$-NO_3^- values in *D. glomerata* and *F. paniculata* roots indicated that at least part of $NO_3^-{}_{atm}$ in plants was acquired *via* roots uptake from the soil N pool, then partly stored in roots and transported to above-ground plant tissues. However, the increasing $\Delta^{17}O$-NO_3^- in leaves, compared to roots or soils, after peak

biomass could only be explained by foliar uptake. Indeed, an enrichment of leaves $NO_3^-{}_{atm}$ (increasing $\Delta^{17}O\text{-}NO_3^-$) should have reflected the respective $NO_3^-{}_{atm}$ enrichment of its reservoir (increasing $\Delta^{17}O\text{-}NO_3^-$), as biological and transport processes do not affect $\Delta^{17}O$ signal (Michalski et al., 2004b). Here, neither soils (Table 4-2) nor roots (Figure 4-4c) – which would be the reservoirs of leaves $NO_3^-{}_{atm}$ in this scenario – showed similar increase in exogenous NO_3^-. Figure 4-6a shows a significant positive correlation between organs differences in $[NO_3^-]$ and $\Delta^{17}O\text{-}NO_3^-$, further supporting the assumption of an increased contribution of foliar uptake to plants NO_3^- content. 3-16 % of leaves NO_3^- was $NO_3^-{}_{atm}$ from foliar uptake (calculated from the 0.8 and 3.8 ‰ range of the positive $\Delta^{17}O\text{-}NO_3^-$ difference between leaves and roots), in perfect agreement with a modeled estimate of 3-16 % of plant N demand sustained by direct foliar incorporation (Holland et al., 2005).

These findings shed new light on the direct contribution of atmospheric nitrogen to plants-available N reservoir. Indeed, we can hypothesize that along with $NO_3^-{}_{atm}$, atmospheric NH_4^+ ($NH_4^+{}_{atm}$) might be also quantitatively absorbed by plants to fuel plants metabolism, a mechanism which has been evidenced in *Poaceae* species (Boutin, 2015; Hanstein et al., 1999). However, the quantification of such input based on isotopic consideration ($\delta^{15}N\text{-}NH_4^+$) would be complicated due to overlapping effects of sources mixing and processes induced fractionation (Kolb and Evans, 2002; Sparks, 2009; Vallano and Sparks, 2007). If plants N comes from direct uptake of atmospheric N species, it means that the buffering effect of soil – where microbial N immobilization, N leaching, denitrification and volatilization in part dampen N accumulation in ecosystems – is bypassed, highlighting the urgent need to further constrain this process (Sparks, 2009).

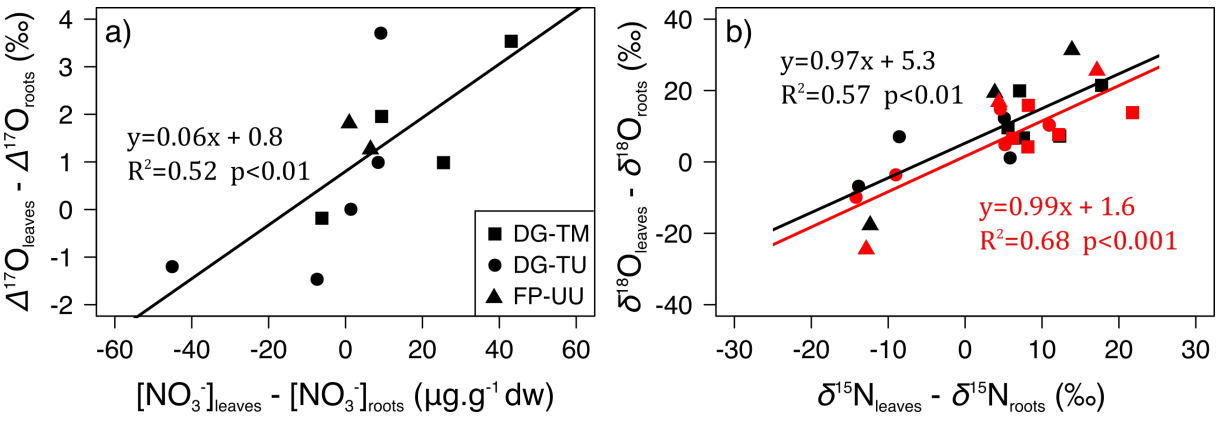

Figure 4-6: Difference between leaves and roots values of a) $\Delta^{17}O$ (‰) *vs* $[NO_3^-]$ (µg g^{-1} dw) and b) $\delta^{18}O$ (‰) *vs* $\delta^{15}N$ (‰). In panel b) are shown corrected for $NO_3^-_{atm}$ contribution data (in red) and uncorrected data (in black). See section 4.1.2.3 for information on the correction.

4.1.4.3 Isotopic evidence of NO_3^- assimilation in roots and leaves

Uptake and subsequent transport of NO_3^- in plants is commonly regarded as yielding little, if none, isotopic fractionation due to the lack of bond breakage in the process (Mariotti et al., 1982). In contrast, the co-variation of O and N isotopic fractionation can be a good indicator of biological processes such as denitrification (Fang et al., 2015; Wexler et al., 2014), but also assimilation (Granger et al., 2004, 2010b). In plants, variations of $\delta^{18}O$-NO_3^- and $\delta^{15}N$-NO_3^- are thus mainly influenced by NO_3^- reduction (NR) into NH_4^+ in the protein-making process (Tcherkez and Farquhar, 2006). Laboratory and hydroponic experiments on NR induced isotopic fractionations showed that the $\delta^{18}O$ and $\delta^{15}N$ values of residual NO_3^- covariate accordingly, along a 1:1 slope (Estrada et al., 2017; Karsh et al., 2012). These findings were supported by the only in field analysis of NR fractionation effect in natural plants, where a slope of 1.27 was found between $\delta^{18}O$-NO_3^- and $\delta^{15}N$-NO_3^- in tree roots (Liu et al., 2013a). To investigate in which organ NR takes place, we plotted in Figure 4-7a the $\delta^{18}O$ and $\delta^{15}N$ values of NO_3^- in roots and leaves. However, uptake of $NO_3^-_{atm}$ was likely to shift up the correlation slope due to its high $\delta^{18}O$ values (66.6 ± 5.8 ‰ in this study, see Table 3-2). Correction for the isotopic influence of $NO_3^-_{atm}$ enables a better assessment of biological processes such as assimilation (Dejwakh et al., 2012; Riha et al., 2014), and was used here to remove the atmospheric component caused by foliar uptake on $\delta^{18}O$ and $\delta^{15}N$ values of NO_3^- (see section 4.1.2.3). We found similar significant correlation slopes for both tissues (0.76 and 0.71 in roots and leaves, respectively), somewhat lower than the expected

1:1 line. Weaker denitrification slopes in natural conditions (0.4 - 0.7) when compared to laboratory experiments (1.0) have been reported elsewhere (Wexler et al., 2014), and were in part attributed to the recharge of new $NO_3^-{}_{ter}$ (with low $\delta^{18}O$ and $\delta^{15}N$) in a given system (Granger and Wankel, 2016). Here, uptake of $NO_3^-{}_{ter}$ by roots and subsequent translocation to the leaves represent a reasonable hypothesis to explain the observed pattern. In Figure 4-7b, the significant positive correlation observed between $\Delta^{17}O\text{-}NO_3^-$ and $\delta^{18}O\text{-}NO_3^-$ in roots, with a slope of 0.08, also pointed at NR-driven $\delta^{18}O$ enrichment of $NO_3^-{}_{ter}$. Also, the strong deviation of $\delta^{18}O\text{-}NO_3^-$ in all plant leaves from the mixing line between $NO_3^-{}_{atm}$ and $NO_3^-{}_{ter}$ compared to roots suggested that additional NR occurred in aboveground organs after transport from roots (Figure 4-7b). To explore this hypothesis, we reported in Figure 4-6b the corrected $\delta^{18}O_{leaves\text{-}roots}$ and $\delta^{15}N_{leaves\text{-}roots}$ ($\delta_{leaves\text{-}roots} = \delta_{leaves} - \delta_{roots}$) values in all plants. We found a significant correlation between $\delta^{18}O_{leaves\text{-}roots}$ and $\delta^{15}N_{leaves\text{-}roots}$ with a slope of 0.99, unambiguously evidencing that an additional NR step occurred in leaves after NO_3^- partial assimilation in roots and transport to leaves.

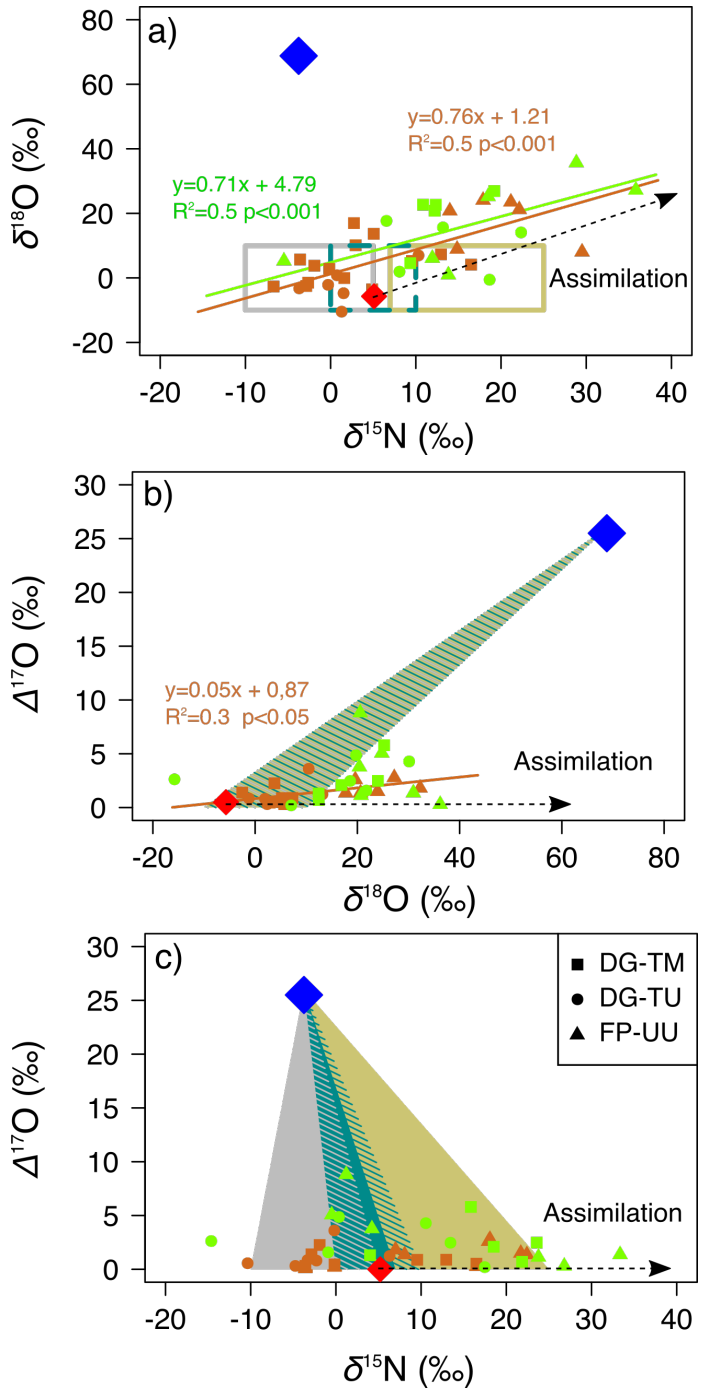

Figure 4-7: Roots (brown) and leaves (green) NO_3^- isotopic values featuring a) $\delta^{18}O$ (‰) *vs* $\delta^{15}N$ (‰), b) $\Delta^{17}O$ (‰) *vs* $\delta^{18}O$ (‰) and c) $\Delta^{17}O$ (‰) *vs* $\delta^{15}N$ (‰). The boxes in the first panel (a) delineate the isotopic range of potential terrestrial NO_3^- sources, featuring atmospheric ammonium ($NH_4^+{}_{atm}$) in grey, mineralized organic matter ($NH_4^+{}_{org}$) in turquoise and manure NH_4^+ in beige. The colored full triangles in the second and third panels indicate the mixing area between the atmospheric end-member (blue diamond) and the above-mentioned terrestrial NO_3^- poles. The blue diamond corresponds to the mean isotopic values of $NO_3^-{}_{atm}$ given in Table 3-2. The red diamond corresponds to the expected mean isotopic values of $NO_3^-{}_{ter}$ at the Lautaret pass (Bourgeois et al., *in review*). In all panels, the arrows indicate the expected variation of residual soil NO_3^- isotopic values following assimilation.

4.1.4.4 Different plant strategies for NO_3^- uptake

Further isotopic considerations highlighted different N uptake strategies by *D. glomerata* and *F. paniculata*. We reported in Figure 4-7c the $\Delta^{17}O\text{-}NO_3^-$ and $\delta^{15}N\text{-}NO_3^-$ measured in roots and leaves. Dual isotope plots have been extensively used to evaluate the sources of N used during nitrification (Kendall et al., 2007), and to provide insights on biological processes, as shown in the previous section. Surprisingly, $\delta^{15}N\text{-}NO_3^-$ in *D. glomerata* roots was generally lower than the estimated $NO_3^-{}_{ter}$ isotopic values at this site ($\delta^{18}O$ = -5.7 ‰ and $\delta^{15}N$ = 5.1 ‰ (Bourgeois et al., *in review*)). Lower values of $\delta^{15}N\text{-}NO_3^-$ in *D. glomerata* roots indicated that absorbed NO_3^- could derive from $NH_4^+{}_{atm}$ nitrification rather than from nitrification of NH_4^+ mineralized from organic N ($NH_4^+{}_{org}$), which is in line with the demonstrated nitrification of $NH_4^+{}_{atm}$ at this site (Bourgeois et al., *in review*). Another explanation holds in the initial production of $\delta^{15}N$-depleted NO_3^- in subalpine soils where N cycling is slow (Robson et al., 2007), hypothesis also brought forward in another study to explain ^{15}N-depleted NO_3^- in tree roots compared to soils (Liu et al., 2013a). Occasionally high *D. glomerata* roots $\delta^{15}N\text{-}NO_3^-$ values in TM meadows are likely related to manure derived NO_3^- inputs on this fertilized meadow (see section 4.1.2.1). In contrast, we measured ^{15}N-enriched NO_3^- in *F. paniculata* roots compared to $NO_3^-{}_{ter}$, which could have resulted from several distinct or concomitant sources and processes. Possible explanations encompass:

(i) The contribution of manure derived NO_3^- as suggested by isotopic sources partitioning (Figure 4-7a), but this remains improbable considering the rare and scattered occurrence of grazing in unterraced grasslands (see section 4.1.2.1).

(ii) Nitrate reduction in the roots that would lead to isotopic enrichment of residual root-NO_3^-, as highlighted in the previous section. Yet, *F. paniculata* exhibits conservative functional traits (Quétier et al., 2007) that are unlikely to account for the year-round high $\delta^{18}O$ and $\delta^{15}N$ enrichment observed in roots (Figure 4-3d and e).

(iii) The well-documented association of *F. paniculata* with mycorrhizal fungi (Binet et al., 2013; Mouhamadou et al., 2011), which impact on N and O isotopes of NO_3^- has never been investigated. However, in a recent review on

the isotopic imprint of plants-fungi association, mycorrhizal plants were ^{15}N-depleted compared to their fungal symbionts (Hobbie and Hogberg, 2012), hinting at opposite isotopic effects to what was found here.

(iv) The relative abundance of previous year stored NO_3^-, ^{15}N-enriched by NR (Baptist et al., 2013). This last hypothesis is supported by the low N turnover measured for subalpine *Poaceae* species (Boutin, 2015) and by year-round elevated δ^{15}N and δ^{18}O (Figure 4-3d and e).

In any case, the isotopic values of NO_3^- found in *D. glomerata* and *F. paniculata* organs are consistent with their nutrients uptake strategies. Significantly higher [NH_4^+] and lower δ^{15}N-NO_3^- in *D. glomerata* roots (Figure 4-3b and d). reflected its exploitative strategy, characterized by fast uptake (*i.e.*, low δ^{15}N-NO_3^- due to frequent turn-over with new $NO_3^-{}_{ter}$) and intensive assimilation rates (*i.e.*, production of NH_4^+). For *F. paniculata*, which is more conservative, data show a significantly higher proportion of $NO_3^-{}_{atm}$ in roots (Figure 4-3c), mirroring the slower N cycling rates in adjacent UU soils which has been well documented (Robson et al., 2007). For this subalpine plant species growing on nutrients poor soils, uptake of $NO_3^-{}_{atm}$ appears to be a non-negligible alternative source of nutrients, hypothesis also supported by higher spanning Δ^{17}O-NO_3^- in its leaves compared to *D. glomerata* (Figure 4-3c).

Using a multi-isotopic tracer of NO_3^-, we managed to evidence, for the first time in natural conditions, the direct contribution of $NO_3^-{}_{atm}$ to subalpine grasses N pools, and to unravel organ respective role in the fate of absorbed NO_3^-. We showed that foliar uptake accounted for up to 16 % of plant N, and we provided an in field evaluation of assimilation isotopic fractionation effect on residual soil NO_3^-. These results also enabled a refined understanding of the different strategies for N uptake adopted by *D. glomerata* and *F. paniculata*. It is necessary, in the close future, to generalize this isotopic approach over a larger span of species and ecosystems and evaluate whether our findings are globally unifying features. This would improve current process models which either do not consider foliar uptake of reactive N separate from total N deposition, or make this separation without firm experimental

evidence (Sparks, 2009). A systematic isotopic quantification of species foliar N uptake is the key to better constrain model estimates of N deposition alteration of ecosystem functioning, and more particularly when coupled to other drivers of change. For instance, global temperature increase is projected to drive a strong N/P decoupling in alpine soils above treeline, which could possibly be further exacerbated by plants foliar uptake, a variable not taken into account in the study (Mayor et al., 2017).

4.2 Synthesis

4.2.1 Summary of the main results

In the first part of this chapter (section 4.1), we specifically focus on quantifying $NO_3^-{}_{atm}$ proportion in two dominant plant species harvested at the Lautaret pass. The plants exhibit different $NO_3^-{}_{atm}$ contents depending on the period of the year, but on average over the study period **a minimum of 4 %** of NO_3^- in subalpine plants derives directly from atmospheric deposition. Interestingly, $\Delta^{17}O$-NO_3^- in leaves is generally higher than in roots, reflecting a **significant uptake of $NO_3^-{}_{atm}$ through the leaves** of these subalpine species. This direct uptake of $NO_3^-{}_{atm}$ is quantified as accounting for 3 to 16 % of plants NO_3^- content, and could explain the exacerbated sensitivity of this biota to atmospheric N deposition.

Co-variations of $\delta^{18}O$-$NO_3^-{}_{ter}$ and $\delta^{15}N$-$NO_3^-{}_{ter}$ in all plants provide very interesting results. Distributed along a 1:1 line, they clearly point at **assimilation taking place in both roots and leaves**. Differences between plant organs also suggest that NO_3^- entering in roots is partly reduced there, transported to leaves and further reduced before entering the glutamine synthetase and glutamate synthase systems. These findings highlight once again the convenient association of the three isotopic markers of NO_3^- (**$\Delta^{17}O$, $\delta^{18}O$ and $\delta^{15}N$**) in environmental studies. Even more, they point at a raw, unexploited potential of this multi-isotopic tracer to be used in new fields, such as biological physiology, ecology and microbiology.

4.2.2 Results situated in the conceptual framework

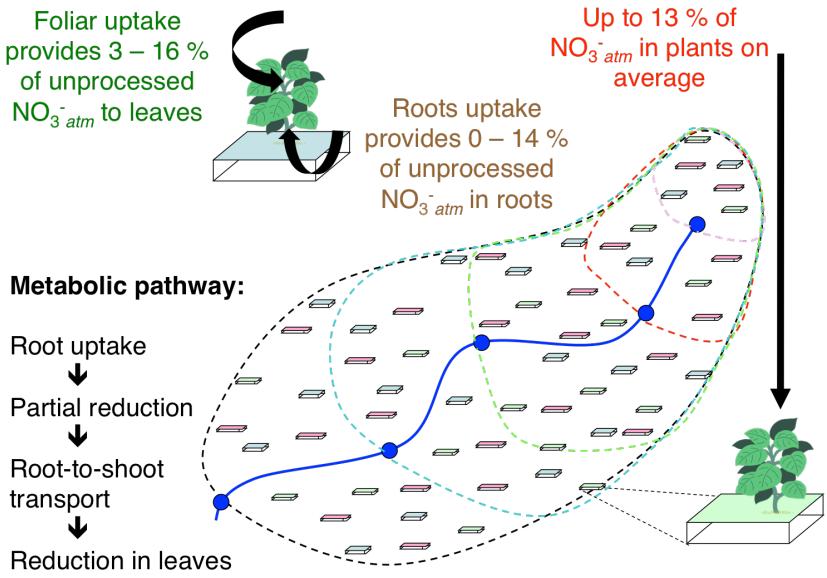

Figure 4-8: Main results from the chapter 4 put back in the context of the study.

5 General conclusion and perspectives

5.1 Conclusion

N deposition is of global concern on Earth because it brings an imbalance to biogeochemical cycles and leads to a large number of ecological issues that are now well documented. High altitude ecosystems are particularly sensitive to additional inputs of N due to harsh bioclimatic conditions rendering these systems oligotrophic. However, the drivers and processes that promote these ecological changes are still to be fully comprehended. Here, the goal was to grasp **what becomes of atmospheric N in subalpine ecosystems upon deposition**. I was also animated by the will to push the limits of NO_3^- triple isotopes application in biogeochemical studies. Thanks to different funding sources, acknowledged throughout this Ph.D. manuscript, I was able to deploy atmospheric monitoring instruments at the Lautaret pass and to perform two full years of field and laboratory work. Based on thus obtained data, I aimed at improving our understanding of the drivers and processes controlling $NO_3^-{}_{atm}$ dynamics in subalpine ecosystems.

The main results obtained in this doctoral work are summarized here. First, I was able to **characterize the isotopic composition of $NO_3^-{}_{atm}$** in the different forms of atmospheric N deposition collected onsite. On annual average, $\Delta^{17}O\text{-}NO_3^-$ ≈ 25 and 29 ‰ in total deposition (wet & dry) and in snow, respectively. This is an important value to measure, as it is a necessary input in the mixing model that enables $NO_3^-{}_{atm}$ quantification. I have thus been able to choose the more adapted atmospheric end-member value following the studied compartment (*i.e.*, rivers, soils or plants).

Two years of monitoring $NO_3^-{}_{atm}$ exports in streams unequivocally confirmed that **snowmelt is responsible for seasonal variations in subalpine streams $NO_3^-{}_{atm}$ proportion**. The magnitude of the control exerted by snowmelt likely depends on a range of topographic and geomorphic variables that are specific to each watershed.

Our findings also lifted the incertitude surrounding the real proportion of $NO_3^-_{atm}$ in streams draining seasonally snow-covered catchments. Previous studies relying only on dual isotope quantification of $NO_3^-_{atm}$ reported a much lower contribution of atmospheric deposition to streams NO_3^- contents (Burns and Kendall, 2002; Campbell et al., 2002; Kendall et al., 1995; Ohte et al., 2004). Here, the use of the $\Delta^{17}O$-NO_3^- tracer shows that $NO_3^-_{atm}$ constitute *ca* 20% of total NO_3^- exports at the outlet of the Romanche Valley. **It is difficult to speculate on the origin of the ionic pulse** usually monitored at snowmelt in alpine/subalpine streams as such ionic pulse was not clearly recorded over the past two years. This could be due to the sampling temporal resolution (weekly basis), but even during the intensive field campaign in April 2016 no such pulse was recorded. Interestingly, this manuscript results showed that all streams, urban or subalpine, had a **year-round quantifiable proportion of $NO_3^-_{atm}$**. This suggests that atmospheric N inputs exceed the capacity of water reservoirs to process this additional source of N, and is a primary indicator of **ubiquitous eutrophication risks**. Additionally, I showed that the main source of NO_3^- in streams is the nitrification of ammonium. The way $NO_3^-_{ter}$ isotopic composition points at a **potentially high contribution of atmospheric ammonium** to this process is very intriguing and would definitively need further investigation.

Monitoring the fate of $NO_3^-_{atm}$ in subalpine soils yielded results difficult to fully comprehend in light of the few parameters that were simultaneously measured. At this point, it is difficult to provide firm conclusions on the main biological processes that drive $NO_3^-_{atm}$ dynamics in soils. Soils are very complex environmental matrixes where N turnover is affected by a large number of sources, abiotic and biotic processes and environmental parameters. However, **the fate of $NO_3^-_{atm}$ in subalpine soils seems to depend on:**

i) **The land management treatment** (past or current) that controls N cycling rates through abiotic (pH) or biotic (microbial immobilization, plant uptake) constraints.

ii) ii) **The topographic and geomorphic characteristics** of the watershed, which promote or impede runoff and leaching.

iii) iii) **The interception** by dead (litter) or living plants prior to reaching the soil compartment.

A combination of **low rate nitrification** (yielding isotopic fractionation), **occasional denitrification** outbursts and **mixing of NH_4^+ sources** (atmospheric deposition and mineralization) are advanced to explain $NO_3^-{}_{ter}$ isotopic composition. These results will be put in perspective with **genomic and taxonomic data** with the objective to further constrain the biological processes driving the N cycle in subalpine soils.

Monitoring the fate of $NO_3^-{}_{atm}$ in plants was doubtless the most demanding challenge of this doctoral work, first because of the novelty of this approach and second because there was a large unknown regarding the feasibility of such isotopic analyses on plant-extracted NO_3^- (*i.e.*, sufficient amount of NO_3^- in plants relative to the minimum quantity necessary for isotopic measurements). With the help of two students, I had to **adapt existing protocols to the analytical chain constraints** (see Appendix A – Methods). However, these efforts were rewarded by findings that provided precise insights on why are **subalpine plants sensitive to atmospheric N deposition.** Results showed that the **entry pathways of $NO_3^-{}_{atm}$ in plants are twofold**: i) root uptake (0-14%) and ii) foliar uptake, accounting up to 16% of leaves NO_3^- contents. This is the first **evidence of infield foliar uptake**, and it points at the need for more investigation on the spread of this process across ecosystems. $NO_3^-{}_{ter}$ isotopic composition in plants also highlights the **two-step process of NO_3^- assimilation** by subalpine grasses, first in the roots than in the leaves.

Writing these final words, I feel that the originality of this work mainly holds in its multidisciplinary approach. I combined tools from multiple fields of research (e.g., atmospheric chemistry, hydrology, ecology, biology, microbiology) to capture a snapshot of $NO_3^-{}_{atm}$ dynamics in a subalpine watershed, tools that are responsible for the novel results presented here. A particular stress should be put upon the utilization of $\Delta^{17}O$, initially a pure atmospheric chemistry tool, but with so much potential when applied to other scientific fields. Because this project had the ambitious objective to

understand how atmospheric nitrate fares in all compartments of a subalpine watershed, and because three years of PhD is too short a time to do so, I believe that a lot of work is still needed to unravel all the mysteries surrounding the fate of atmospheric nitrate in altitude catchments and in the environment more generally. However, I have hope that this work can serve as a milestone towards achieving this objective.

5.2 Perspectives

Owing to the deployment of atmospheric deposition collectors (rain, aerosols), to intensive field and laboratory work and to a novel isotopic approach, I believe this work cleared the ground for more in depth study of $NO_3^-{}_{atm}$ fate in the environment, and more generally of the N cycle in the environment. Rather than to saturate the literature with studies focusing on NO_3^- dual isotopes ($\delta^{15}N$ and $\delta^{18}O$), it now appears primordial to me that scientists systematically analyze $\Delta^{17}O$-NO_3^-. This would help remove the large uncertainty that tarnish the interpretation of dual isotope plots. Only then we will start gaining useful insights on the sources and processes involved in N turnover in a given system under natural conditions. In the meantime, several axes that could help further constrain our understanding of the N cycle are provided hereafter.

5.2.1 On the local scale

As stated above, there a lot of work yet to be done to fully understand the fate of atmospheric N is subalpine ecosystems. However, this thesis will serve to lay the foundation of a more ambitious project aiming at – if funded – totally constraining the N budget at a small watershed (*ca* 0.5-km^2) scale. It will associate microbiologists, ecologists, hydrologists, biogeochemists and atmospheric chemists in an attempt to fully capture the ins and outs of nitrogen at the subalpine stage. I actively collaborated to the setting up of this project, and here were my recommendations:

A better understanding of soil processes is first required. Further work on the association of genomic, taxonomic and isotopic data will help to do so. Additionally, contingent measurements of NO_3^- isotopes ($\Delta^{17}O$, $\delta^{15}N$ and $\delta^{18}O$), but also $\delta^{15}N$-

NH_4^+ and $\delta^{15}N$ of bulk soil are necessary to discriminate isotopic fractionation during nitrification or mineralization processes and sources mixing (Mayer et al., 2001; Spoelstra et al., 2007). A year-round survey of soil-water isotopic composition (δ^2H and $\delta^{18}O$) in parallel to NO_3^- isotopic composition seems also inevitable to understand nitrification pathways (Casciotti et al., 2011; Snider et al., 2010).

In order to constrain the full nitrogen budget, entering and outgoing nitrogen fluxes need to be quantified. This starts by a systematic monitoring of subalpine streams discharge. Tufiere (S-upper montane) stream has recently been equipped with an automatic water-level gauge, a first step towards this objective. The annual total deposition flux also need to be quantified. This was one of my Ph.D. objectives that I couldn't achieve, mostly because of the inadequacy of the sampling collectors with the harsh climatic conditions in winter on site, which prevented me from gathering a full and continuous year of atmospheric deposition data. Finally, measurements of NO, NO_2, N_2O (and N2) and NH_3 from the soils are necessary to evaluate the gaseous losses from the soils and the snow.

The next step is to implement all these data in a simple box model and see if the observed patterns in N fluxes can be reproduced. The ultimate goal would be to input observation and isotopic data into a more complex model, such as ParFlow-CLM (*i.e.*, a coupled hydrologic and land model) in order to be able to predict N partitioning in terrestrial and aquatic compartments globally. This model seems the most suitable in that account because of its historical importance in setting climate science and policy (e.g., only model to consider N in CO_2 and climate change simulations in the IPCC report from 2013 (Stocker, 2014)).This would definitely help to anticipate the ecological and climatic consequences of a forecasted to increase atmospheric N deposition (Fowler et al., 2015; Galloway et al., 2004). The necessity for N isotopic benchmarks in global change models has been underlined recently (Houlton et al., 2015), and in line with this recommendation, a recent review paper has set a nice base to foster the interlocking of $\delta^{15}N$ measurements and ecosystem modeling (Denk et al., 2017).

A bit aside from the work I have doing over the past three years, but interesting nonetheless is the identification of the sources of $NO_3^-{}_{atm}$ that deposits at the Lautaret pass. By running back trajectories of air masses, it is possible to get a sense of atmospheric species spatial origin. Furthermore, variations of $NO_3^-{}_{atm}$ isotopic composition have been widely used to infer the emitting sources and subsequent oxidation pathways prior to deposition (see section 1.1.4).

5.2.2 On the global scale

Throughout this manuscript, I have advocated for a more systematic utilization of NO_3^- triple isotopes ($\Delta^{17}O$, $\delta^{18}O$, $\delta^{15}N$) in ecosystem studies. Here I reiterate by summarizing the two main issues that I feel are inherent to the NO_3^- dual isotope ($\delta^{18}O$, $\delta^{15}N$) approach. First, sources partitioning can be biased: when comparing results obtained from the two approaches (triple isotopes and dual isotopes), all studies in the literature provided evidence of misevaluation of the atmospheric source, and therefore of other sources as well (Michalski et al., 2004; Riha et al., 2014; Rose et al., 2015, this study). This stems from the high variability of terrestrial $\delta^{18}O\text{-}NO_3^-$ due to i) possible enrichment from the atmospheric source, ii) possible enrichment due to biological processes (denitrification, assimilation) and iii) high dependency on the nitrification pathway and rate. Second, biological processes assessment can be hindered, for the reasons listed above. Isotope plots combining $\Delta^{17}O\text{-}NO_3^-$ *vs* $\delta^{18}O\text{-}NO_3^-$, $\Delta^{17}O\text{-}NO_3^-$ *vs* $\delta^{15}N\text{-}NO_3^-$ and $\delta^{18}O\text{-}NO_3^-{}_{ter}$ *vs* $\delta^{15}N\text{-}NO_3^-{}_{ter}$ provide more robust evaluation of NO_3^- dynamics in a system (this study, Tsunogai et al., 2016). Therefore, there is a need for more studies to establish to what extent we could have missed key information on N cycle in the environment.

Investigation of foliar uptake magnitude worldwide, and especially in forests appears as a priority (Sparks, 2009). Forested ecosystems are widely recognized as very sensitive to N deposition (Aber et al., 1989; Costa et al., 2011; Durka et al., 1994; Lequy, 2012; McLauchlan et al., 2007; Templer et al., 2012; Vitousek et al., 1997), and evidence of vegetation foliar uptake goes back as far as 1971 (Hill, 1971). However, to date the assessment of foliar uptake mostly relied on the evaluation of bulk plant $\delta^{15}N$ (Vallano, 2009; Vallano and Sparks, 2007), a tenuous task

considering the difficulty to precisely measure the isotopic fractionation effect associated with foliar uptake. The use of $\Delta^{17}O\text{-}NO_3^-$, not affected by mass-dependent fractionation, can be a very good alternative to estimate the amount of incorporated oxidized N species, although it would not account for NH_3 / NH_4^+ foliar uptake. This approach has a unique potential to increase our understanding of canopies role in biogeochemical cycles, and has already been successfully used to evidence biological nitrification and atmospheric N processing in forests of the United Kingdom (Guerrieri et al., 2015).

Recent studies show a shift towards an increasing proportion of reduced N species (NH_3 / NH_4^+), but also of organic N species, in total N deposition (Li et al., 2016; Sun et al., 2016). This is line with my findings hinting at a possibly high contribution of atmospheric NH_4^+ at the Lautaret pass, especially at snowmelt. NO_3^- isotopic composition monitoring should provide information on the relative increase of these N forms addition to the environment. However, more work is needed to characterize the variability in reduced and organic nitrogen $\delta^{15}N$ values in order to grasp the magnitude of this speciation shift in atmospheric N deposition, but also to better understand emitting sources (Felix et al., 2017; Lin et al., 2016). NH_3 emissions are subject to little or none regulations worldwide, and sources are highly variable in space and time, making it arduous to provide precise emissions inventories (Paulot et al., 2014). Undoubtedly, N deposition issues will yet continue to occupy scientists for a number of years.

Bibliography

Aber, J.D., Nadelhoffer, K.J., Steudler, P., Melillo, J.M., 1989. Nitrogen Saturation in Northern Forest Ecosystems. BioScience 39, 378–386. https://doi.org/10.2307/1311067

Alexander, B., Hastings, M.G., Allman, D.J., Dachs, J., Thornton, J.A., Kunasek, S.A., 2009. Quantifying atmospheric nitrate formation pathways based on a global model of the oxygen isotopic composition (Δ 17 O) of atmospheric nitrate. Atmospheric Chem. Phys. 9, 5043–5056.

Andersson, K.K., Hooper, A.B., 1983. O2 and H2O are each the source of one O in NO−2 produced from NH3 by Nitrosomonas: 15N-NMR evidence. FEBS Lett. 164, 236–240. https://doi.org/10.1016/0014-5793(83)80292-0

Bai, Y., Wu, J., Clark, C.M., Naeem, S., Pan, Q., Huang, J., Zhang, L., Han, X., 2010. Tradeoffs and thresholds in the effects of nitrogen addition on biodiversity and ecosystem functioning: evidence from inner Mongolia Grasslands. Glob. Change Biol. 16, 358–372. https://doi.org/10.1111/j.1365-2486.2009.01950.x

Bailly, X., Olivieri, I., Brunel, B., Cleyet-Marel, J.C., Béna, G., 2007. Horizontal gene transfer and homologous recombination drive the evolution of the nitrogen-fixing symbionts of Medicago species. J. Bacteriol. 189, 5223–5236. https://doi.org/10.1128/JB.00105-07

Balestrini, R., Arese, C., Freppaz, M., Buffagni, A., 2013. Catchment features controlling nitrogen dynamics in running waters above the tree line (central Italian Alps). Hydrol. Earth Syst. Sci. 17, 989–1001. https://doi.org/10.5194/hess-17-989-2013

Bao, H., Cao, X., Hayles, J.A., 2016. Triple Oxygen Isotopes: Fundamental Relationships and Applications. Annu. Rev. Earth Planet. Sci. 44, 463–492. https://doi.org/10.1146/annurev-earth-060115-012340

Baptist, F., 2007. Impact de la durée d'enneigement sur les cycles biogéochimiques dans les écosystèmes alpins. Université Joseph-Fourier-Grenoble I.

Baptist, F., Secher-Fromell, H., Viard-Cretat, F., Aranjuelo, I., Clement, J.-C., Creme, A., Desclos, M., Laine, P., Nogues, S., Lavorel, S., 2013. Carbohydrate and nitrogen

stores in *Festuca paniculata* under mowing explain dominance in subalpine grasslands: Carbohydrate and N storage in *F. paniculata* under mowing. Plant Biol. 15, 395–404. https://doi.org/10.1111/j.1438-8677.2012.00652.x

Barkan, E., Luz, B., 2005. High precision measurements of 17O/16O and 18O/16O ratios in H2O. Rapid Commun. Mass Spectrom. 19, 3737–3742. https://doi.org/10.1002/rcm.2250

Barnes, R.T., Raymond, P.A., 2010. Land-use controls on sources and processing of nitrate in small watersheds: insights from dual isotopic analysis. Ecol. Appl. 20, 1961–1978. https://doi.org/10.1890/08-1328.1

Barnes, R.T., Williams, M.W., Parman, J.N., Hill, K., Caine, N., 2014. Thawing glacial and permafrost features contribute to nitrogen export from Green Lakes Valley, Colorado Front Range, USA. Biogeochemistry 117, 413–430. https://doi.org/10.1007/s10533-013-9886-5

Baron, J.S., 2006. Hindcasting nitrogen deposition to determine an ecological critical load. Ecol. Appl. 16, 433–439.

Baron, J.S., Campbell, D.H., 1997. Nitrogen fluxes in a high elevation Colorado Rocky Mountain basin. Hydrol. Process. 11, 783–799.

Baron, J.S., Driscoll, C.T., Stoddard, J.L., Richer, E.E., 2011. Empirical Critical Loads of Atmospheric Nitrogen Deposition for Nutrient Enrichment and Acidification of Sensitive US Lakes. BioScience 61, 602–613. https://doi.org/10.1525/bio.2011.61.8.6

Baron, J.S., Nydick, K.R., Rueth, H.M., Lafrançois, B.M., Wolfe, A.P., 2005. High Elevation Ecosystem Responses to Atmospheric Deposition of Nitrogen in the Colorado Rocky Mountains, USA, in: Huber, U.M., Bugmann, H.K.M., Reasoner, M.A. (Eds.), Global Change and Mountain Regions. Springer Netherlands, Dordrecht, pp. 429–436.

Baron, J.S., Rueth, H.M., Wolfe, A.M., Nydick, K.R., Allstott, E.J., Minear, J.T., Moraska, B., 2000. Ecosystem Responses to Nitrogen Deposition in the Colorado Front Range. Ecosystems 3, 352–368. https://doi.org/10.1007/s100210000032

Bassin, S., Käch, D., Valsangiacomo, A., Mayer, J., Oberholzer, H.-R., Volk, M., Fuhrer, J., 2015. Elevated ozone and nitrogen deposition affect nitrogen pools of subalpine grassland. Environ. Pollut. 201, 67–74. https://doi.org/10.1016/j.envpol.2015.02.038

Bassin, S., Volk, M., Fuhrer, J., 2013. Species Composition of Subalpine Grassland is Sensitive to Nitrogen Deposition, but Not to Ozone, After Seven Years of Treatment. Ecosystems 16, 1105–1117. https://doi.org/10.1007/s10021-013-9670-3

Beirle, S., Boersma, K.F., Platt, U., Lawrence, M.G., Wagner, T., 2011. Megacity Emissions and Lifetimes of Nitrogen Oxides Probed from Space. Science 333, 1737–1739. https://doi.org/10.1126/science.1207824

Bettez, N.D., Groffman, P.M., 2013. Nitrogen Deposition in and near an Urban Ecosystem. Environ. Sci. Technol. 47, 6047–6051. https://doi.org/10.1021/es400664b

Beyn, F., Matthias, V., Dähnke, K., 2014. Changes in atmospheric nitrate deposition in Germany – An isotopic perspective. Environ. Pollut. 194, 1–10. https://doi.org/10.1016/j.envpol.2014.06.043

Bilbrough, C.J., Welker, J.M., Bowman, W.D., 2000. Early Spring Nitrogen Uptake by Snow-Covered Plants: A Comparison of Arctic and Alpine Plant Function under the Snowpack. Arct. Antarct. Alp. Res. 32, 404. https://doi.org/10.2307/1552389

Binet, M.N., Sage, L., Malan, C., Clément, J.C., Redecker, D., Wipf, D., Geremia, R.A., Lavorel, S., Mouhamadou, B., 2013. Effects of mowing on fungal endophytes and arbuscular mycorrhizal fungi in subalpine grasslands. Fungal Ecol. 6, 248–255. https://doi.org/10.1016/j.funeco.2013.04.001

Bobbink, R., Hettelingh, J.-P., Review and revision of empirical critical loads and dose-response relationships, 2011. Review and revision of empirical critical loads and dose-response relationships: proceedings of an expert workshop, Noordwijkerhout, 23-25 June 2010. RIVM, Bilthoven.

Bodin, X., 2007. Geodynamique du pergélisol alpin : fonctionnement, distribution et évolution récente. L'exemple du massif du Combeynot (Hautes Alpes). Université Paris-Diderot - Paris VII.

Bodin, X., Thibert, E., Fabre, D., Ribolini, A., Schoeneich, P., Francou, B., Reynaud, L., Fort, M., 2009. Two decades of responses (1986–2006) to climate by the Laurichard rock glacier, French Alps. Permafr. Periglac. Process. 20, 331–344. https://doi.org/10.1002/ppp.665

Böhlke, J.K., Mroczkowski, S.J., Coplen, T.B., 2003. Oxygen isotopes in nitrate: new reference materials for 18O:17O:16O measurements and observations on nitrate-

water equilibration. Rapid Commun. Mass Spectrom. 17, 1835–1846. https://doi.org/10.1002/rcm.1123

Bolhuis, H., Severin, I., Confurius-Guns, V., Wollenzien, U.I.A., Stal, L.J., 2010. Horizontal transfer of the nitrogen fixation gene cluster in the cyanobacterium Microcoleus chthonoplastes. ISME J. 4, 121–130. https://doi.org/10.1038/ismej.2009.99

Bourgeois, I., Clement, J.-C., Caillon, N., Nesti, C., Deschamps, N., Savarino, J., n.d. Direct fertilization of subalpine plants by atmospheric nitrate. Proc. Natl. Acad. Sci. submitted.

Bourgeois, I., Savarino, J., Caillon, N., Angot, H., Barbero, A., Delbart, F., Voisin, D., Clement, J.-C., n.d. Tracing the fate of atmospheric nitrate in a subalpine watershed using Δ17O. Environ. Sci. Technol. in review.

Bourgeois, I., Savarino, J., Némery, J., Caillon, N., Albertin, S., Delbart, F., Voisin, D., Clément, J.-C., n.d. Atmospheric nitrate exports along a montane to urban gradient. Sci. Total Environ. submitted.

Boutin, M., 2015. Impacts des dépôts atmosphériques azotés sur la biodiversité et le fonctionnement des pelouses subalpines pyrénéennes. Université de Toulouse, Université Toulouse III-Paul Sabatier.

Boutin, M., Corcket, E., Alard, D., Villar, L., Jiménez, J.-J., Blaix, C., Lemaire, C., Corriol, G., Lamaze, T., Pornon, A., 2017. Nitrogen deposition and climate change have increased vascular plant species richness and altered the composition of grazed subalpine grasslands. J. Ecol. https://doi.org/10.1111/1365-2745.12743

Boutin, M., Lamaze, T., Couvidat, F., Pornon, A., 2015. Subalpine Pyrenees received higher nitrogen deposition than predicted by EMEP and CHIMERE chemistry-transport models. Sci. Rep. 5. https://doi.org/10.1038/srep12942

Bowman, W.D., Gartner, J.R., Holland, K., Wiedermann, M., 2006. Nitrogen Critical Loads For Alpine Vegetation And Terrestrial Ecosystem Response: Are We There Yet? Ecol. Appl. 16, 1183–1193. https://doi.org/10.1890/1051-0761(2006)016[1183:NCLFAV]2.0.CO;2

Briand, C., 2014. Approche multi-traceurs pour la détermination de l'origine des nitrates dans les eaux souterraines: exemple d'une source karstique dans les Landes. Université Pierre et Marie Curie-Paris VI.

Britto, D.T., Kronzucker, H.J., 2013. Ecological significance and complexity of N-source preference in plants. Ann. Bot. 112, 957–963. https://doi.org/10.1093/aob/mct157

Britto, D.T., Kronzucker, H.J., 2006. Futile cycling at the plasma membrane: a hallmark of low-affinity nutrient transport. Trends Plant Sci. 11, 529–534. https://doi.org/10.1016/j.tplants.2006.09.011

Brookes, P.C., Landman, A., Pruden, G., Jenkinson, D.S., 1985. Chloroform fumigation and the release of soil nitrogen: A rapid direct extraction method to measure microbial biomass nitrogen in soil. Soil Biol. Biochem. 17, 837–842. https://doi.org/10.1016/0038-0717(85)90144-0

Brooks, P.D., Campbell, D.H., Tonnessen, K.A., Heuer, K., 1999. Natural variability in N export from headwater catchments: snow cover controls on ecosystem N retention. Hydrol. Process. 13, 2191–2201.

Brooks, P.D., Grogan, P., Templer, P.H., Groffman, P., Öquist, M.G., Schimel, J., 2011. Carbon and Nitrogen Cycling in Snow-Covered Environments. Geogr. Compass 5, 682–699. https://doi.org/10.1111/j.1749-8198.2011.00420.x

Brooks, P.D., Williams, M.W., 1999. Snowpack controls on nitrogen cycling and export in seasonally snow-covered catchments. Hydrol. Process. 13, 2177–2190.

Buchwald, C., Casciotti, K.L., 2010. Oxygen isotopic fractionation and exchange during bacterial nitrite oxidation. Limnol. Oceanogr. 55, 1064–1074. https://doi.org/10.4319/lo.2010.55.3.1064

Burns, D.A., 2004. The effects of atmospheric nitrogen deposition in the Rocky Mountains of Colorado and southern Wyoming, USA—a critical review. Environ. Pollut. 127, 257–269. https://doi.org/10.1016/S0269-7491(03)00264-1

Burns, D.A., 2003. Atmospheric nitrogen deposition in the Rocky Mountains of Colorado and southern Wyoming—a review and new analysis of past study results. Atmos. Environ. 37, 921–932. https://doi.org/10.1016/S1352-2310(02)00993-7

Burns, D.A., Boyer, E.W., Elliott, E.M., Kendall, C., 2009. Sources and Transformations of Nitrate from Streams Draining Varying Land Uses: Evidence from Dual Isotope Analysis. J. Environ. Qual. 38, 1149. https://doi.org/10.2134/jeq2008.0371

Burns, D.A., Kendall, C., 2002. Analysis of δ15N and δ18O to differentiate NO3–

sources in runoff at two watersheds in the Catskill Mountains of New York. Water Resour. Res. 38, 9–1. https://doi.org/10.1029/2001WR000292

Campbell, D.H., Clow, D.W., Ingersoll, G.P., Mast, M.A., Spahr, N.E., Turk, J.T., 1995. Nitrogen deposition and release in alpine watersheds, Loch Vale, Colorado, USA. IAHS Publ.-Ser. Proc. Rep.-Intern Assoc Hydrol. Sci. 228, 243–254.

Campbell, D.H., Kendall, C., Chang, C.C.Y., Silva, S.R., Tonnessen, K.A., 2002. Pathways for nitrate release from an alpine watershed: Determination using δ^{15}N and δ^{18}O: ALPINE WATERSHED NITRATE δ^{15}N AND δ^{18}O. Water Resour. Res. 38, 10-1-10–9. https://doi.org/10.1029/2001WR000294

Campbell, J.L., Mitchell, M.J., Mayer, B., Groffman, P.M., Christenson, L.M., 2007. Mobility of Nitrogen-15-Labeled Nitrate and Sulfur-34-Labeled Sulfate during Snowmelt. Soil Sci. Soc. Am. J. 71, 1934. https://doi.org/10.2136/sssaj2006.0283

Casciotti, K.L., Böhlke, J.K., McIlvin, M.R., Mroczkowski, S.J., Hannon, J.E., 2007. Oxygen Isotopes in Nitrite: Analysis, Calibration, and Equilibration. Anal. Chem. 79, 2427–2436. https://doi.org/10.1021/ac061598h

Casciotti, K.L., Buchwald, C., Santoro, A.E., Frame, C., 2011. Assessment of Nitrogen and Oxygen Isotopic Fractionation During Nitrification and Its Expression in the Marine Environment. Methods Enzymol. 486, 253.

Casciotti, K.L., McIlvin, M., Buchwald, C., 2010. Oxygen isotopic exchange and fractionation during bacterial ammonia oxidation. Limnol. Oceanogr. 55, 753–762.

Casciotti, K.L., Sigman, D.M., Hastings, M.G., Böhlke, J.K., Hilkert, A., 2002. Measurement of the Oxygen Isotopic Composition of Nitrate in Seawater and Freshwater Using the Denitrifier Method. Anal. Chem. 74, 4905–4912. https://doi.org/10.1021/ac020113w

Chapin, F.S., Walker, B.H., Hobbs, R.J., Hooper, D.U., Lawton, J.H., Sala, O.E., Tilman, D., 1997. Biotic control over the functioning of ecosystems. Science 277, 500–504.

Charrois, L., 2017. Assimilation de réflectances satellitaires du domaine visible et proche infrarouge dans un modèle détaillé de manteau neigeux. Université Grenoble Alpes.

Clark, C.M., Bell, M.D., Boyd, J.W., Compton, J.E., Davidson, E.A., Davis, C., Fenn, M.E., Geiser, L., Jones, L., Blett, T.F., 2017. Nitrogen-induced terrestrial

eutrophication: cascading effects and impacts on ecosystem services. Ecosphere 8, e01877. https://doi.org/10.1002/ecs2.1877

Clark, C.M., Morefield, P.E., Gilliam, F.S., Pardo, L.H., 2013. Estimated losses of plant biodiversity in the United States from historical N deposition (1985–2010). Ecology 94, 1441–1448. https://doi.org/10.1890/12-2016.1

Clément, J.-C., Aquilina, L., Bour, O., Plaine, K., Burt, T.P., Pinay, G., 2003a. Hydrological flowpaths and nitrate removal rates within a riparian floodplain along a fourth-order stream in Brittany (France). Hydrol. Process. 17, 1177–1195. https://doi.org/10.1002/hyp.1192

Clément, J.-C., Holmes, R.M., Peterson, B.J., Pinay, G., 2003b. Isotopic investigation of denitrification in a riparian ecosystem in western France. J. Appl. Ecol. 40, 1035–1048. https://doi.org/10.1111/j.1365-2664.2003.00854.x

Clément, J.-C., Pinay, G., Marmonier, P., 2002. Seasonal Dynamics of Denitrification Along Topohydrosequences in Three Different Riparian Wetlands. J. Environ. Qual. 31, 1025–1037. https://doi.org/10.2134/jeq2002.1025

Clément, J.C., Robson, T.M., Guillemin, R., Saccone, P., Lochet, J., Aubert, S., Lavorel, S., 2012. The effects of snow-N deposition and snowmelt dynamics on soil-N cycling in marginal terraced grasslands in the French Alps. Biogeochemistry 108, 297–315. https://doi.org/10.1007/s10533-011-9601-3

Clow, D.W., Sueker, J.K., 2000. Relations between basin characteristics and stream water chemistry in alpine/subalpine basins in Rocky Mountain National Park, Colorado. Water Resour. Res. 36, 49–61. https://doi.org/10.1029/1999WR900294

Coplen, T.B., 2011. Guidelines and recommended terms for expression of stable-isotope-ratio and gas-ratio measurement results. Rapid Commun. Mass Spectrom. 25, 2538–2560. https://doi.org/10.1002/rcm.5129

Costa, A.W., Michalski, G., Schauer, A.J., Alexander, B., Steig, E.J., Shepson, P.B., 2011. Analysis of atmospheric inputs of nitrate to a temperate forest ecosystem from Δ^{17} O isotope ratio measurements: ATMOSPHERIC NITRATE INPUTS TO A FOREST. Geophys. Res. Lett. 38, n/a-n/a. https://doi.org/10.1029/2011GL047539

Cowie, R.M., Knowles, J.F., Dailey, K.R., Williams, M.W., Mills, T.J., Molotch, N.P., 2017. Sources of streamflow along a headwater catchment elevational gradient. J. Hydrol. 549, 163–178. https://doi.org/10.1016/j.jhydrol.2017.03.044

Crutzen, P.J., 1970. The influence of nitrogen oxides on the atmospheric ozone content. Q. J. R. Meteorol. Soc. 96, 320–325. https://doi.org/10.1002/qj.49709640815

Darrouzet-Nardi, A., Erbland, J., Bowman, W.D., Savarino, J., Williams, M.W., 2012. Landscape-level nitrogen import and export in an ecosystem with complex terrain, Colorado Front Range. Biogeochemistry 109, 271–285. https://doi.org/10.1007/s10533-011-9625-8

De Vries, F., Van Groenigen, J.W., Hoffland, E., Bloem, J., 2011. Nitrogen losses from two grassland soils with different fungal biomass. Soil Biol. Biochem. - SOIL BIOL BIOCHEM 43, 997–1005. https://doi.org/10.1016/j.soilbio.2011.01.016

Decina, S.M., Templer, P.H., Hutyra, L.R., Gately, C.K., Rao, P., 2017. Variability, drivers, and effects of atmospheric nitrogen inputs across an urban area: Emerging patterns among human activities, the atmosphere, and soils. Sci. Total Environ. 609, 1524–1534. https://doi.org/10.1016/j.scitotenv.2017.07.166

Dejwakh, N.R., Meixner, T., Michalski, G., McIntosh, J., 2012. Using ^{17} O to Investigate Nitrate Sources and Sinks in a Semi-Arid Groundwater System. Environ. Sci. Technol. 46, 745–751. https://doi.org/10.1021/es203450z

Denk, T.R.A., Mohn, J., Decock, C., Lewicka-Szczebak, D., Harris, E., Butterbach-Bahl, K., Kiese, R., Wolf, B., 2017. The nitrogen cycle: A review of isotope effects and isotope modeling approaches. Soil Biol. Biochem. 105, 121–137. https://doi.org/10.1016/j.soilbio.2016.11.015

Devito, K.J., Fitzgerald, D., Hill, A.R., Aravena, R., 2000. Nitrate dynamics in relation to lithology and hydrologic flow path in a river riparian zone. J. Environ. Qual. 29, 1075–1084.

Dietzel, M., Leis, A., Abdalla, R., Savarino, J., Morin, S., Böttcher, M.E., Köhler, S., 2014. ¹⁷O excess traces atmospheric nitrate in paleo-groundwater of the Saharan desert. Biogeosciences 11, 3149–3161. https://doi.org/10.5194/bg-11-3149-2014

Dodds, W.K., Bouska, W.W., Eitzmann, J.L., Pilger, T.J., Pitts, K.L., Riley, A.J., Schloesser, J.T., Thornbrugh, D.J., 2009. Eutrophication of U.S. Freshwaters: Analysis of Potential Economic Damages. Environ. Sci. Technol. 43, 12–19. https://doi.org/10.1021/es801217q

Durka, W., Schulze, E.-D., Gebauer, G., Voerkeliust, S., 1994. Effects of forest

decline on uptake and leaching of deposited nitrate determined from 15N and 18O measurements. Nature 372, 765–767. https://doi.org/10.1038/372765a0

Dutordoir, S., 2014. Bilan des flux de métaux, carbone organique et nutriments contenus dans une rivière alpine: part des rejets urbains de l'agglomération de Grenoble et apports amont (Isère et Drac). Université Grenoble Alpes.

Elliott, E.M., Kendall, C., Boyer, E.W., Burns, D.A., Lear, G.G., Golden, H.E., Harlin, K., Bytnerowicz, A., Butler, T.J., Glatz, R., 2009. Dual nitrate isotopes in dry deposition: Utility for partitioning NO_x source contributions to landscape nitrogen deposition. J. Geophys. Res. 114. https://doi.org/10.1029/2008JG000889

Elliott, E.M., Kendall, C., Wankel, S.D., Burns, D.A., Boyer, E.W., Harlin, K., Bain, D.J., Butler, T.J., 2007. Nitrogen Isotopes as Indicators of NO_x Source Contributions to Atmospheric Nitrate Deposition Across the Midwestern and Northeastern United States. Environ. Sci. Technol. 41, 7661–7667. https://doi.org/10.1021/es070898t

Elser, J.J., Andersen, T., Baron, J.S., Bergström, A.-K., Jansson, M., Kyle, M., Nydick, K.R., Steger, L., Hessen, D.O., 2009. Shifts in lake N:P stoichiometry and nutrient limitation driven by atmospheric nitrogen deposition. Science 326, 835–837. https://doi.org/10.1126/science.1176199

Emmerton, K.S., Callaghan, T.V., Jones, H.E., Leake, J.R., Michelsen, A., Read, D.J., 2001. Assimilation and Isotopic Fractionation of Nitrogen by Mycorrhizal and Nonmycorrhizal Subarctic Plants. New Phytol. 151, 513–524. https://doi.org/10.2307/1353802

Epstein, E., Bloom, A., 2016. Mineral Nutrition of Plants Principles and Perspectives, 2nd Edition. John Wiley & Sons.

Erbland, J., 2011. Contraintes isotopiques sur l'interprétation de l'enregistrement en nitrate dans la carotte de glace de Vostok. Université de Grenoble.

Estrada, N.L., Böhlke, J.K., Sturchio, N.C., Gu, B., Harvey, G., Burkey, K.O., Grantz, D.A., McGrath, M.T., Anderson, T.A., Rao, B., Sevanthi, R., Hatzinger, P.B., Jackson, W.A., 2017. Stable isotopic composition of perchlorate and nitrate accumulated in plants: Hydroponic experiments and field data. Sci. Total Environ. 595, 556–566. https://doi.org/10.1016/j.scitotenv.2017.03.223

Fang, Y., Koba, K., Makabe, A., Takahashi, C., Zhu, W., Hayashi, T., Hokari, A.A.,

Urakawa, R., Bai, E., Houlton, B.Z., Xi, D., Zhang, S., Matsushita, K., Tu, Y., Liu, D., Zhu, F., Wang, Z., Zhou, G., Chen, D., Makita, T., Toda, H., Liu, X., Chen, Q., Zhang, D., Li, Y., Yoh, M., 2015. Microbial denitrification dominates nitrate losses from forest ecosystems. Proc. Natl. Acad. Sci. 112, 1470–1474. https://doi.org/10.1073/pnas.1416776112

Fang, Y., Koba, K., Makabe, A., Zhu, F., Fan, S., Liu, X., Yoh, M., 2012. Low δ ^{18} O Values of Nitrate Produced from Nitrification in Temperate Forest Soils. Environ. Sci. Technol. 46, 8723–8730. https://doi.org/10.1021/es300510r

Fang, Y., Yoh, M., Koba, K., Zhu, W., Takebayashi, Y., Xiao, Y., Lei, C., Mo, J., Zhang, W., Lu, X., 2011. Nitrogen deposition and forest nitrogen cycling along an urban-rural transect in southern China: FOREST N CYCLING IN SOUTHERN CHINA. Glob. Change Biol. 17, 872–885. https://doi.org/10.1111/j.1365-2486.2010.02283.x

Faure, G., 1998. Principles and applications of geochemistry : a comprehensive textbook for geology students. Prentice Hall.

Felix, J.D., Elliott, E.M., Gay, D.A., 2017. Spatial and temporal patterns of nitrogen isotopic composition of ammonia at U.S. ammonia monitoring network sites. Atmos. Environ. 150, 434–442. https://doi.org/10.1016/j.atmosenv.2016.11.039

Ferguson, S.J., 1994. Denitrification and its control. Antonie Van Leeuwenhoek 66, 89–110.

Fewtrell, L., 2004. Drinking-Water Nitrate, Methemoglobinemia, and Global Burden of Disease: A Discussion. Environ. Health Perspect. 112, 1371–1374. https://doi.org/10.1289/ehp.7216

Fowler, D., Coyle, M., Skiba, U., Sutton, M.A., Cape, J.N., Reis, S., Sheppard, L.J., Jenkins, A., Grizzetti, B., Galloway, J.N., Vitousek, P., Leach, A., Bouwman, A.F., Butterbach-Bahl, K., Dentener, F., Stevenson, D., Amann, M., Voss, M., 2013. The global nitrogen cycle in the twenty-first century. Philos. Trans. R. Soc. B Biol. Sci. 368, 20130164–20130164. https://doi.org/10.1098/rstb.2013.0164

Fowler, D., Steadman, C.E., Stevenson, D., Coyle, M., Rees, R.M., Skiba, U.M., Sutton, M.A., Cape, J.N., Dore, A.J., Vieno, M., Simpson, D., Zaehle, S., Stocker, B.D., Rinaldi, M., Facchini, M.C., Flechard, C.R., Nemitz, E., Twigg, M., Erisman, J.W., Butterbach-Bahl, K., Galloway, J.N., 2015. Effects of global change during the

21st century onthe nitrogen cycle. Atmospheric Chem. Phys. 15, 13849–13893. https://doi.org/10.5194/acp-15-13849-2015

Freppaz, M., Williams, B.L., Edwards, A.C., Scalenghe, R., Zanini, E., 2007. Simulating soil freeze/thaw cycles typical of winter alpine conditions: Implications for N and P availability. Appl. Soil Ecol. 35, 247–255. https://doi.org/10.1016/j.apsoil.2006.03.012

Freyer, H.D., 1991. Seasonal variation of 15N/14N ratios in atmospheric nitrate species. Tellus B 43, 30–44. https://doi.org/10.1034/j.1600-0889.1991.00003.x

Galloway, J.N., Aber, J.D., Erisman, J.W., Seitzinger, S.P., Howarth, R.W., Cowling, E.B., Cosby, B.J., 2003. The Nitrogen Cascade. BioScience 53, 341. https://doi.org/10.1641/0006-3568(2003)053[0341:TNC]2.0.CO;2

Galloway, J.N., Dentener, F.J., Capone, D.G., Boyer, E.W., Howarth, R.W., Seitzinger, S.P., Asner, G.P., Cleveland, C.C., Green, P.A., Holland, E.A., Karl, D.M., Michaels, A.F., Porter, J.H., Townsend, A.R., V�osmarty, C.J., 2004. Nitrogen Cycles: Past, Present, and Future. Biogeochemistry 70, 153–226. https://doi.org/10.1007/s10533-004-0370-0

Galloway, J.N., Townsend, A.R., Erisman, J.W., Bekunda, M., Cai, Z., Freney, J.R., Martinelli, L.A., Seitzinger, S.P., Sutton, M.A., 2008. Transformation of the nitrogen cycle: recent trends, questions, and potential solutions. Science 320, 889–892.

Gao, Y.Q., Marcus, R.A., 2001. Strange and Unconventional Isotope Effects in Ozone Formation. Science 293, 259–263. https://doi.org/10.1126/science.1058528

Gavazov, K., Ingrisch, J., Hasibeder, R., Mills, R.T.E., Buttler, A., Gleixner, G., Pumpanen, J., Bahn, M., 2017. Winter ecology of a subalpine grassland: Effects of snow removal on soil respiration, microbial structure and function. Sci. Total Environ. 590–591, 316–324. https://doi.org/10.1016/j.scitotenv.2017.03.010

Gebauer, G., Rehder, H., Wollenweber, B., 1988. Nitrate, nitrate reduction and organic nitrogen in plants from different ecological and taxonomic groups of Central Europe. Oecologia 75, 371–385.

Gill, R.A., 2014. The influence of 3-years of warming and N-deposition on ecosystem dynamics is small compared to past land use in subalpine meadows. Plant Soil 374, 197–210. https://doi.org/10.1007/s11104-013-1868-9

Girel, J., Quétier, F., Bignon, A., Aubert, S., 2010. Histoire de l'agriculture en Oisans

(Haute Romanche et pays faranchin, Villar d'Arène , Hautes-Alpes).
Granger, J., Sigman, D.M., 2009. Removal of nitrite with sulfamic acid for nitrate N and O isotope analysis with the denitrifier method. Rapid Commun. Mass Spectrom. 23, 3753–3762. https://doi.org/10.1002/rcm.4307
Granger, J., Sigman, D.M., Lehmann, M.F., Tortell, P.D., 2008. Nitrogen and oxygen isotope fractionation during dissimilatory nitrate reduction by denitrifying bacteria. Limnol. Oceanogr. 53, 2533.
Granger, J., Sigman, D.M., Needoba, J.A., Harrison, P.J., 2004. Coupled nitrogen and oxygen isotope fractionation of nitrate during assimilation by cultures of marine phytoplankton. Limnol. Oceanogr. 49, 1763–1773.
Granger, J., Sigman, D.M., Rohde, M.M., Maldonado, M.T., Tortell, P.D., 2010a. N and O isotope effects during nitrate assimilation by unicellular prokaryotic and eukaryotic plankton cultures. Geochim. Cosmochim. Acta 74, 1030–1040. https://doi.org/10.1016/j.gca.2009.10.044
Granger, J., Sigman, D.M., Rohde, M.M., Maldonado, M.T., Tortell, P.D., 2010b. N and O isotope effects during nitrate assimilation by unicellular prokaryotic and eukaryotic plankton cultures. Geochim. Cosmochim. Acta 74, 1030–1040. https://doi.org/10.1016/j.gca.2009.10.044
Granger, J., Wankel, S.D., 2016. Isotopic overprinting of nitrification on denitrification as a ubiquitous and unifying feature of environmental nitrogen cycling. Proc. Natl. Acad. Sci. 113, E6391–E6400. https://doi.org/10.1073/pnas.1601383113
Grassein, F., 2009. Mécanismes de variation des traits fonctionnels dans les prairies des Alpes. Université Joseph-Fourier-Grenoble I.
Griffiths, N.A., Jackson, C.R., McDonnell, J.J., Klaus, J., Du, E., Bitew, M.M., 2016. Dual nitrate isotopes clarify the role of biological processing and hydrologic flow paths on nitrogen cycling in subtropical low-gradient watersheds: N CYCLING IN LOW-RELIEF WATERSHEDS. J. Geophys. Res. Biogeosciences 121, 422–437. https://doi.org/10.1002/2015JG003189
Groffman, P.M., Law, N.L., Belt, K.T., Band, L.E., Fisher, G.T., 2004. Nitrogen Fluxes and Retention in Urban Watershed Ecosystems. Ecosystems 7. https://doi.org/10.1007/s10021-003-0039-x
Gross, N., Suding, K.N., Lavorel, S., 2007. Leaf dry matter content and lateral spread

predict response to land use change for six subalpine grassland species. J. Veg. Sci. 18, 289–300.

Guerrieri, R., Vanguelova, E.I., Michalski, G., Heaton, T.H.E., Mencuccini, M., 2015. Isotopic evidence for the occurrence of biological nitrification and nitrogen deposition processing in forest canopies. Glob. Change Biol. 21, 4613–4626. https://doi.org/10.1111/gcb.13018

Guha, T., Lin, C.T., Bhattacharya, S.K., Mahajan, A.S., Ou-Yang, C.-F., Lan, Y.-P., Hsu, S.C., Liang, M.-C., 2017. Isotopic ratios of nitrate in aerosol samples from Mt. Lulin, a high-altitude station in Central Taiwan. Atmos. Environ. 154, 53–69. https://doi.org/10.1016/j.atmosenv.2017.01.036

Hachiya, T., Sakakibara, H., 2016. Interactions between nitrate and ammonium in their uptake, allocation, assimilation, and signaling in plants. J. Exp. Bot. erw449. https://doi.org/10.1093/jxb/erw449

Hall Jr, R.O., Baker, M.A., Arp, C.D., Koch, B.J., 2009. Hydrologic control of nitrogenremoval, storage and export in a mountain stream. Limnol. Oceanogr. 54, 2128.

Hall, S.J., Maurer, G., Hoch, S.W., Taylor, R., Bowling, D.R., 2014. Impacts of anthropogenic emissions and cold air pools on urban to montane gradients of snowpack ion concentrations in the Wasatch Mountains, Utah. Atmos. Environ. 98, 231–241. https://doi.org/10.1016/j.atmosenv.2014.08.076

Hall, S.J., Weintraub, S.R., Eiriksson, D., Brooks, P.D., Baker, M.A., Bowen, G.J., Bowling, D.R., 2016. Stream Nitrogen Inputs Reflect Groundwater Across a Snowmelt-Dominated Montane to Urban Watershed. Environ. Sci. Technol. 50, 1137–1146. https://doi.org/10.1021/acs.est.5b04805

Hanstein, S., Mattsson, M., Jaeger, H.-J., Schjoerring, J.K., 1999. Uptake and utilization of atmospheric ammonia in three native Poaceae species: leaf conductances, composition of apoplastic solution and interactions with root nitrogen supply. New Phytol. 141, 71–83.

Hastings, M.G., 2004. Seasonal variations in N and O isotopes of nitrate in snow at Summit, Greenland: Implications for the study of nitrate in snow and ice cores. J. Geophys. Res. 109. https://doi.org/10.1029/2004JD004991

Hastings, M.G., Jarvis, J.C., Steig, E.J., 2009. Anthropogenic Impacts on Nitrogen

Isotopes of Ice-Core Nitrate. Science 324, 1288–1288. https://doi.org/10.1126/science.1170510

Hathorn, B.C., Marcus, R.A., 2000. An intramolecular theory of the mass-independent isotope effect for ozone. II. Numerical implementation at low pressures using a loose transition state. J. Chem. Phys. 113, 9497–9509. https://doi.org/10.1063/1.1321045

Hayes, J.M., 2004. An introduction to isotopic calculations. Woods Hole Oceanogr. Inst. Woods Hole MA 2543.

Haynes, R.J., Goh, K.M., 1978. Ammonium and Nitrate Nutrition of Plants. Biol. Rev. 53, 465–510. https://doi.org/10.1111/j.1469-185X.1978.tb00862.x

Hertel, O., Skjøth, C.A., Reis, S., Bleeker, A., Harrison, R.M., Cape, J.N., Fowler, D., Skiba, U., Simpson, D., Jickells, T., Kulmala, M., Gyldenkærne, S., Sørensen, L.L., Erisman, J.W., Sutton, M.A., 2012. Governing processes for reactive nitrogen compounds in the European atmosphere. Biogeosciences 9, 4921–4954. https://doi.org/10.5194/bg-9-4921-2012

Hill, A.C., 1971. Vegetation: A Sink for Atmospheric Pollutants. J. Air Pollut. Control Assoc. 21, 341–346. https://doi.org/10.1080/00022470.1971.10469535

Hiltbrunner, E., Schwikowski, M., Körner, C., 2005. Inorganic nitrogen storage in alpine snow pack in the Central Alps (Switzerland). Atmos. Environ. 39, 2249–2259. https://doi.org/10.1016/j.atmosenv.2004.12.037

Hipkin, C.R., Simpson, D.J., Wainwright, S.J., Salem, M.A., 2004. Nitrification by plants that also fix nitrogen. Nature 430, 98–101. https://doi.org/10.1038/nature02635

Hobbie, E.A., Hogberg, P., 2012. Nitrogen isotopes link mycorrhizal fungi and plants to nitrogen dynamics. New Phytol. 196, 367–382. https://doi.org/10.1111/j.1469-8137.2012.04300.x

Hobbs, W.O., Lafrancois, B.M., Stottlemyer, R., Toczydlowski, D., Engstrom, D.R., Edlund, M.B., Almendinger, J.E., Strock, K.E., VanderMeulen, D., Elias, J.E., Saros, J.E., 2016. Nitrogen deposition to lakes in national parks of the western Great Lakes region: Isotopic signatures, watershed retention, and algal shifts: NITROGEN DEPOSITION TO NORTHERN LAKES. Glob. Biogeochem. Cycles 30, 514–533. https://doi.org/10.1002/2015GB005228

Holland, E., Guenther, B., Lee-Taylor, M., Bertman, S., Carroll, M., Shepson, P.,

Sparks, J., 2005. U.S. nitrogen science plan focuses collaborative efforts. Eos 86, 253–260.

Hollocher, T.C., 1984. Source of the oxygen atoms of nitrate in the oxidation of nitrite by Nitrobacter agilis and evidence against a P-O-N anhydride mechanism in oxidative phosphorylation. Arch. Biochem. Biophys. 233, 721–727.

Hollocher, T.C., Tate, M.E., Nicholas, D.J., 1981. Oxidation of ammonia by Nitrosomonas europaea. Definite 18O-tracer evidence that hydroxylamine formation involves a monooxygenase. J. Biol. Chem. 256, 10834–10836.

Holtgrieve, G.W., Schindler, D.E., Hobbs, W.O., Leavitt, P.R., Ward, E.J., Bunting, L., Chen, G., Finney, B.P., Gregory-Eaves, I., Holmgren, S., Lisac, M.J., Lisi, P.J., Nydick, K., Rogers, L.A., Saros, J.E., Selbie, D.T., Shapley, M.D., Walsh, P.B., Wolfe, A.P., 2011. A Coherent Signature of Anthropogenic Nitrogen Deposition to Remote Watersheds of the Northern Hemisphere. Science 334, 1545–1548. https://doi.org/10.1126/science.1212267

Hood, E., Scott, D., 2008. Riverine organic matter and nutrients in southeast Alaska affected by glacial coverage. Nat. Geosci. 1, 583–587. https://doi.org/10.1038/ngeo280

Houlton, B.Z., Marklein, A.R., Bai, E., 2015. Representation of nitrogen in climate change forecasts. Nat. Clim. Change 5, 398–401. https://doi.org/10.1038/nclimate2538

Hundey, E.J., Russell, S.D., Longstaffe, F.J., Moser, K.A., 2016. Agriculture causes nitrate fertilization of remote alpine lakes. Nat. Commun. 7, 10571. https://doi.org/10.1038/ncomms10571

Ishino, S., Hattori, S., Savarino, J., Jourdain, B., Preunkert, S., Legrand, M., Caillon, N., Albane, B., Kuribayashi, K., Yoshida, N., 2017. Seasonal variations of triple oxygen isotopic compositions of atmospheric sulfate, nitrate, and ozone at Dumont d'Urville, coastal Antarctica. Atmospheric Chem. Phys. 17, 3713–3727. https://doi.org/10.5194/acp-17-3713-2017

Jaeger, C.H., Monson, R.K., Fisk, M.C., Schmidt, S.K., 1999. Seasonal partitioning of nitrogen by plants and soil microorganisms in an alpine ecosystem. Ecology 80, 1883–1891.

Jaffrezo, J.-L., Aymoz, G., Cozic, J., 2005. Size distribution of EC and OC in the

aerosol of Alpine valleys during summer and winter. Atmospheric Chem. Phys. 5, 2915–2925. https://doi.org/10.5194/acp-5-2915-2005

Janssen, C., Marcus, R.A., 2001. Does Symmetry Drive Isotopic Anomalies in Ozone Isotopomer Formation? Science 294, 951–951. https://doi.org/10.1126/science.294.5544.951a

Jin, Z., Qin, X., Chen, L., Jin, M., Li, F., 2015. Using dual isotopes to evaluate sources and transformations of nitrate in the West Lake watershed, eastern China. J. Contam. Hydrol. 177–178, 64–75. https://doi.org/10.1016/j.jconhyd.2015.02.008

Jusselme, M.-D., Saccone, P., Zinger, L., Faure, M., Le Roux, X., Guillaumaud, N., Bernard, L., Clement, J.-C., Poly, F., 2016. Variations in snow depth modify N-related soil microbial abundances and functioning during winter in subalpine grassland. Soil Biol. Biochem. 92, 27–37. https://doi.org/10.1016/j.soilbio.2015.09.013

Kaiser, J., 2011. Technical note: Consistent calculation of aquatic gross production from oxygen triple isotope measurements. Biogeosciences 8, 1793–1811. https://doi.org/10.5194/bg-8-1793-2011

Kaiser, J., Hastings, M.G., Houlton, B.Z., Röckmann, T., Sigman, D.M., 2007. Triple Oxygen Isotope Analysis of Nitrate Using the Denitrifier Method and Thermal Decomposition of N_2O. Anal. Chem. 79, 599–607. https://doi.org/10.1021/ac061022s

Karsh, K.L., Granger, J., Kritee, K., Sigman, D.M., 2012. Eukaryotic Assimilatory Nitrate Reductase Fractionates N and O Isotopes with a Ratio near Unity. Environ. Sci. Technol. 46, 5727–5735. https://doi.org/10.1021/es204593q

Karsh, K.L., Trull, T.W., Sigman, D.M., Thompson, P.A., Granger, J., 2014. The contributions of nitrate uptake and efflux to isotope fractionation during algal nitrate assimilation. Geochim. Cosmochim. Acta 132, 391–412. https://doi.org/10.1016/j.gca.2013.09.030

Kaye, J.P., Hart, S.C., 1997. Competition for nitrogen between plants and soil microorganisms. Trends Ecol. Evol. 12, 139–143. https://doi.org/10.1016/S0169-5347(97)01001-X

Kean, A.J., Harley, R.A., Littlejohn, D., Kendall, G.R., 2000. On-Road Measurement of Ammonia and Other Motor Vehicle Exhaust Emissions. Environ. Sci. Technol. 34, 3535–3539. https://doi.org/10.1021/es991451q

Kendall, C., Campbell, D.H., Burns, D.A., Shanley, J.B., Silva, S.R., Chang, C.C., 1995. Tracing sources of nitrate in snowmelt runoff using the oxygen and nitrogen isotopic compositions of nitrate. IAHS Publ.-Ser. Proc. Rep.-Intern Assoc Hydrol. Sci. 228, 339–348.

Kendall, C., Elliott, E.M., Wankel, S.D., 2007. Tracing anthropogenic inputs of nitrogen to ecosystems. Stable Isot. Ecol. Environ. Sci. 2, 375–449.

Kirchner, M., Fegg, W., Römmelt, H., Leuchner, M., Ries, L., Zimmermann, R., Michalke, B., Wallasch, M., Maguhn, J., Faus-Kessler, T., Jakobi, G., 2014. Nitrogen deposition along differently exposed slopes in the Bavarian Alps. Sci. Total Environ. 470–471, 895–906. https://doi.org/10.1016/j.scitotenv.2013.10.036

Kolb, K.J., Evans, R.D., 2002. Implications of leaf nitrogen recycling on the nitrogen isotope composition of deciduous plant tissues. New Phytol. 156, 57–64.

Körner, C., 2004. Mountain biodiversity, its causes and function. Ambio Spec No 13, 11–17.

Körner, C., 2003. Alpine Plant Life. Springer Berlin Heidelberg, Berlin, Heidelberg. https://doi.org/10.1007/978-3-642-18970-8

Laursen, K.H., Mihailova, A., Kelly, S.D., Epov, V.N., Bérail, S., Schjoerring, J.K., Donard, O.F.X., Larsen, E.H., Pedentchouk, N., Marca-Bell, A.D., Halekoh, U., Olesen, J.E., Husted, S., 2013. Is it really organic? – Multi-isotopic analysis as a tool to discriminate between organic and conventional plants. Food Chem. 141, 2812–2820. https://doi.org/10.1016/j.foodchem.2013.05.068

Lavorel, S., Grigulis, K., Lamarque, P., Colace, M.-P., Garden, D., Girel, J., Pellet, G., Douzet, R., 2011. Using plant functional traits to understand the landscape distribution of multiple ecosystem services: Plant functional traits and provision of multiple ecosystem services. J. Ecol. 99, 135–147. https://doi.org/10.1111/j.1365-2745.2010.01753.x

Lefebvre, S., Clément, J.-C., Pinay, G., Thenail, C., Durand, P., Marmonier, P., 2007. 15n-Nitrate Signature in Low-Order Streams: Effects of Land Cover and Agricultural Practices. Ecol. Appl. 17, 2333–2346. https://doi.org/10.1890/06-1496.1

Legay, N., 2013. Une approche fonctionnelle des relations plantes-microorganismes dans le cadre du cycle de l'azote. Cas des prairies de montagnes. Grenoble.

Legay, N., Grassein, F., Robson, T.M., Personeni, E., Bataillé, M.-P., Lavorel, S.,

Clément, J.-C., 2013. Comparison of inorganic nitrogen uptake dynamics following snowmelt and at peak biomass in subalpine grasslands. Biogeosciences 10, 7631–7645. https://doi.org/10.5194/bg-10-7631-2013

Legay, N., Lavorel, S., Baxendale, C., Krainer, U., Bahn, M., Binet, M.-N., Cantarel, A.A.M., Colace, M.-P., Foulquier, A., Kastl, E.-M., Grigulis, K., Mouhamadou, B., Poly, F., Pommier, T., Schloter, M., Clément, J.-C., Bardgett, R.D., 2016. Influence of plant traits, soil microbial properties, and abiotic parameters on nitrogen turnover of grassland ecosystems. Ecosphere 7, e01448. https://doi.org/10.1002/ecs2.1448

Leighton, P., 1961. Photochemistry of Air Pollution. Elsevier.

Lepori, F., Barbieri, A., Ormerod, S.J., 2003. Causes of episodic acidification in Alpine streams. Freshw. Biol. 48, 175–189.

Lequy, E., 2012. Dépôts atmosphériques particulaires sur les écosystèmes forestiers de la moitié nord de la France: influence sur les cycles biogéochimiques. Université de Lorraine.

Li, Y., Schichtel, B.A., Walker, J.T., Schwede, D.B., Chen, X., Lehmann, C.M.B., Puchalski, M.A., Gay, D.A., Collett, J.L., 2016. Increasing importance of deposition of reduced nitrogen in the United States. Proc. Natl. Acad. Sci. 113, 5874–5879. https://doi.org/10.1073/pnas.1525736113

Lin, C.T., Jickells, T.D., Baker, A.R., Marca, A., Johnson, M.T., 2016. Aerosol isotopic ammonium signatures over the remote Atlantic Ocean. Atmos. Environ. 133, 165–169. https://doi.org/10.1016/j.atmosenv.2016.03.020

Lipson, D.A., Schadt, C.W., Schmidt, S.K., 2002. Changes in Soil Microbial Community Structure and Function in an Alpine Dry Meadow Following Spring Snow Melt. Microb. Ecol. 43, 307–314. https://doi.org/10.1007/s00248-001-1057-x

Liu, D., Zhu, W., Wang, X., Pan, Y., Wang, C., Xi, D., Bai, E., Wang, Y., Han, X., Fang, Y., 2017. Abiotic versus biotic controls on soil nitrogen cycling in drylands along a 3200 km transect. Biogeosciences 14, 989–1001. https://doi.org/10.5194/bg-14-989-2017

Liu, F., Williams, M.W., Caine, N., 2004. Source waters and flow paths in an alpine catchment, Colorado Front Range, United States: SOURCE WATERS AND FLOW PATHS IN ALPINE CATCHMENTS. Water Resour. Res. 40. https://doi.org/10.1029/2004WR003076

Liu, T., Wang, F., Michalski, G., Xia, X., Liu, S., 2013. Using ^{15} N, ^{17} O, and ^{18} O To Determine Nitrate Sources in the Yellow River, China. Environ. Sci. Technol. 47, 13412–13421. https://doi.org/10.1021/es403357m

Liu, X.-Y., Koba, K., Makabe, A., Liu, C.-Q., 2014. Nitrate dynamics in natural plants: insights based on the concentration and natural isotope abundances of tissue nitrate. Front. Plant Sci. 5. https://doi.org/10.3389/fpls.2014.00355

Liu, X.-Y., Koba, K., Takebayashi, Y., Liu, C.-Q., Fang, Y.-T., Yoh, M., 2013a. Dual N and O isotopes of nitrate in natural plants: first insights into individual variability and organ-specific patterns. Biogeochemistry 114, 399–411. https://doi.org/10.1007/s10533-012-9721-4

Liu, X.-Y., Koba, K., Takebayashi, Y., Liu, C.-Q., Fang, Y.-T., Yoh, M., 2012. Preliminary insights into δ15N and δ18O of nitrate in natural mosses: A new application of the denitrifier method. Environ. Pollut. 162, 48–55. https://doi.org/10.1016/j.envpol.2011.09.029

Liu, X.-Y., Koba, K., Yoh, M., Liu, C.-Q., 2013b. Nitrogen and oxygen isotope effects of tissue nitrate associated with nitrate acquisition and utilisation in the moss Hypnum plumaeforme. Funct. Plant Biol. 39, 598. https://doi.org/10.1071/FP12014

Louiseize, N.L., Lafrenière, M.J., Hastings, M.G., 2014. Stable isotopic evidence of enhanced export of microbially derived $${\text{NO}}_{3}^{ - }$$ NO 3 - following active layer slope disturbance in the Canadian High Arctic. Biogeochemistry 121, 565–580. https://doi.org/10.1007/s10533-014-0023-x

Lovett, G.M., Goodale, C.L., 2011. A New Conceptual Model of Nitrogen Saturation Based on Experimental Nitrogen Addition to an Oak Forest. Ecosystems 14, 615–631. https://doi.org/10.1007/s10021-011-9432-z

Maire, V., Gross, N., da Silveira Pontes, L., Picon-Cochard, C., Soussana, J.-F., 2009. Trade-off between root nitrogen acquisition and shoot nitrogen utilization across 13 co-occurring pasture grass species. Funct. Ecol. 23, 668–679. https://doi.org/10.1111/j.1365-2435.2009.01557.x

Mano, V., 2008. Processus fondamentaux conditionnant les apports de sediments fins dans les retenues-Optimisation des methodes de mesure et modelisation statistique. Université Joseph-Fourier-Grenoble I.

Mano, V., Nemery, J., Belleudy, P., Poirel, A., 2009. Assessment of suspended

sediment transport in four alpine watersheds (France): influence of the climatic regime. Hydrol. Process. 23, 777–792. https://doi.org/10.1002/hyp.7178

Mara, P., Mihalopoulos, N., Gogou, A., Daehnke, K., Schlarbaum, T., Emeis, K.-C., Krom, M., 2009. Isotopic composition of nitrate in wet and dry atmospheric deposition on Crete in the eastern Mediterranean Sea: ISOTOPIC COMPOSITION OF NITRATE IN DEPOSITION. Glob. Biogeochem. Cycles 23, n/a-n/a. https://doi.org/10.1029/2008GB003395

Mariotti, A., 1984. Natural 15N abundance measurements and atmospheric nitrogen standard calibration. Nature 311, 251–252. https://doi.org/10.1038/311251a0

Mariotti, A., Germon, J.C., Hubert, P., Kaiser, P., Letolle, R., Tardieux, A., Tardieux, P., 1981. Experimental determination of nitrogen kinetic isotope fractionation: some principles; illustration for the denitrification and nitrification processes. Plant Soil 62, 413–430.

Mariotti, A., Leclerc, A., Germon, J.C., 1982. Nitrogen isotope fractionation associated with the NO2-→ N2O step of denitrification in soils. Can. J. Soil Sci. 62, 227–241.

Mariotti, A., Mariotti, F., Champigny, M.-L., Amarger, N., Moyse, A., 1982. Nitrogen isotope fractionation associated with nitrate reductase activity and uptake of NO3- by Pearl Millet. Plant Physiol. 69, 880–884.

Marty, C., Pornon, A., Lamaze, T., 2009. High NH4+ efflux from roots of the common alpine grass, Festuca nigrescens, at field-relevant concentrations restricts net uptake. Environ. Exp. Bot. 67, 84–86. https://doi.org/10.1016/j.envexpbot.2009.03.020

Mast, M.A., Clow, D.W., Baron, J.S., Wetherbee, G.A., 2014. Links between N Deposition and Nitrate Export from a High-Elevation Watershed in the Colorado Front Range. Environ. Sci. Technol. 48, 14258–14265. https://doi.org/10.1021/es502461k

Matson, P., Lohse, K.A., Hall, S.J., 2002. The Globalization of Nitrogen Deposition: Consequences for Terrestrial Ecosystems. AMBIO J. Hum. Environ. 31, 113. https://doi.org/10.1639/0044-7447(2002)031[0113:TGONDC]2.0.CO;2

Mayer, B., Bollwerk, S.M., Mansfeldt, T., Hütter, B., Veizer, J., 2001. The oxygen isotope composition of nitrate generated by nitrification in acid forest floors. Geochim. Cosmochim. Acta 65, 2743–2756. https://doi.org/10.1016/S0016-7037(01)00612-3

Mayer, B., Boyer, E.W., Goodale, C., Jaworski, N.A., Van Breemen, N., Howarth, R.W., Seitzinger, S., Billen, G., Lajtha, K., Nadelhoffer, K., others, 2002. Sources of nitrate in rivers draining sixteen watersheds in the northeastern US: Isotopic constraints. Biogeochemistry 57, 171–197.

Mayor, J.R., Sanders, N.J., Classen, A.T., Bardgett, R.D., Clément, J.-C., Fajardo, A., Lavorel, S., Sundqvist, M.K., Bahn, M., Chisholm, C., Cieraad, E., Gedalof, Z., Grigulis, K., Kudo, G., Oberski, D.L., Wardle, D.A., 2017. Elevation alters ecosystem properties across temperate treelines globally. Nature 542, 91–95. https://doi.org/10.1038/nature21027

McDonnell, T.C., Belyazid, S., Sullivan, T.J., Sverdrup, H., Bowman, W.D., Porter, E.M., 2014. Modeled subalpine plant community response to climate change and atmospheric nitrogen deposition in Rocky Mountain National Park, USA. Environ. Pollut. 187, 55–64. https://doi.org/10.1016/j.envpol.2013.12.021

McGovern, S.T., Evans, C.D., Dennis, P., Walmsley, C.A., Turner, A., McDonald, M.A., 2014. Increased inorganic nitrogen leaching from a mountain grassland ecosystem following grazing removal: a hangover of past intensive land-use? Biogeochemistry 119, 125–138. https://doi.org/10.1007/s10533-014-9952-7

McLauchlan, K.K., Craine, J.M., Oswald, W.W., Leavitt, P.R., Likens, G.E., 2007. Changes in nitrogen cycling during the past century in a northern hardwood forest. Proc. Natl. Acad. Sci. 104, 7466–7470. https://doi.org/10.1073/pnas.0701779104

Mensinga, T.T., Speijers, G.J., Meulenbelt, J., 2003. Health implications of exposure to environmental nitrogenous compounds. Toxicol. Rev. 22, 41–51.

Michalski, G., Böhlke, J.K., Thiemens, M., 2004a. Long term atmospheric deposition as the source of nitrate and other salts in the Atacama Desert, Chile: New evidence from mass-independent oxygen isotopic compositions. Geochim. Cosmochim. Acta 68, 4023–4038. https://doi.org/10.1016/j.gca.2004.04.009

Michalski, G., Kolanowski, M., Riha, K.M., 2015. Oxygen and nitrogen isotopic composition of nitrate in commercial fertilizers, nitric acid, and reagent salts. Isotopes Environ. Health Stud. 51, 382–391. https://doi.org/10.1080/10256016.2015.1054821

Michalski, G., Meixner, T., Fenn, M., Hernandez, L., Sirulnik, A., Allen, E., Thiemens, M., 2004b. Tracing Atmospheric Nitrate Deposition in a Complex Semiarid Ecosystem Using Δ17O. Environ. Sci. Technol. 38, 2175–2181.

https://doi.org/10.1021/es034980+

Michalski, G., Savarino, J., Böhlke, J.K., Thiemens, M., 2002. Determination of the Total Oxygen Isotopic Composition of Nitrate and the Calibration of a Δ17O Nitrate Reference Material. Anal. Chem. 74, 4989–4993. https://doi.org/10.1021/ac0256282

Michener, R.H., Lajtha, K. (Eds.), 2007. Stable isotopes in ecology and environmental science, 2nd ed. ed, Ecological methods and concepts series. Blackwell Pub, Malden, MA.

Mihailova, A., Pedentchouk, N., Kelly, S.D., 2014. Stable isotope analysis of plant-derived nitrate – Novel method for discrimination between organically and conventionally grown vegetables. Food Chem. 154, 238–245. https://doi.org/10.1016/j.foodchem.2014.01.020

Miller, A.E., Schimel, J.P., Sickman, J.O., Meixner, T., Doyle, A.P., Melack, J.M., 2007. Mineralization responses at near-zero temperatures in three alpine soils. Biogeochemistry 84, 233–245. https://doi.org/10.1007/s10533-007-9112-4

Miller, A.J., Cramer, M.D., 2005. Root Nitrogen Acquisition and Assimilation. Plant Soil 274, 1–36. https://doi.org/10.1007/s11104-004-0965-1

Miller, M.F., 2002. Isotopic fractionation and the quantification of 17 O anomalies in the oxygen three-isotope system: an appraisal and geochemical significance. Geochim. Cosmochim. Acta 66, 1881–1889.

Mladenov, N., Williams, M.W., Schmidt, S.K., Cawley, K., 2012. Atmospheric deposition as a source of carbon and nutrients to an alpine catchment of the Colorado Rocky Mountains. Biogeosciences 9, 3337–3355. https://doi.org/10.5194/bg-9-3337-2012

Morin, S., 2008. Analyse de la composition isotopique de l'ion nitrate dans la basse atmosphère polaire et marine. Université Paris-Est.

Morin, S., Sander, R., Savarino, J., 2011. Simulation of the diurnal variations of the oxygen isotope anomaly (Δ¹⁷O) of reactive atmospheric species. Atmospheric Chem. Phys. 11, 3653–3671. https://doi.org/10.5194/acp-11-3653-2011

Morin, S., Savarino, J., Bekki, S., Gong, S., Bottenheim, J.W., 2007. Signature of Arctic surface ozone depletion events in the isotope anomaly (Δ17O) of atmospheric nitrate. Atmos Chem Phys 7, 1451–1469. https://doi.org/10.5194/acp-7-1451-2007

Morin, S., Savarino, J., Frey, M.M., Domine, F., Jacobi, H.-W., Kaleschke, L., Martins, J.M.F., 2009. Comprehensive isotopic composition of atmospheric nitrate in the Atlantic Ocean boundary layer from 65°S to 79°N. J. Geophys. Res. 114. https://doi.org/10.1029/2008JD010696

Morin, S., Savarino, J., Frey, M.M., Yan, N., Bekki, S., Bottenheim, J.W., Martins, J.M.F., 2008. Tracing the Origin and Fate of NOx in the Arctic Atmosphere Using Stable Isotopes in Nitrate. Science 322, 730–732. https://doi.org/10.1126/science.1161910

Mouhamadou, B., Molitor, C., Baptist, F., Sage, L., Clément, J.-C., Lavorel, S., Monier, A., Geremia, R.A., 2011. Differences in fungal communities associated to Festuca paniculata roots in subalpine grasslands. Fungal Divers. 47, 55–63. https://doi.org/10.1007/s13225-011-0091-3

Nanus, L., McMurray, J.A., Clow, D.W., Saros, J.E., Blett, T., Gurdak, J.J., 2017. Spatial variation of atmospheric nitrogen deposition and critical loads for aquatic ecosystems in the Greater Yellowstone Area. Environ. Pollut. 223, 644–656. https://doi.org/10.1016/j.envpol.2017.01.077

Nanus, L., Williams, M.W., Campbell, D.H., Elliott, E.M., Kendall, C., 2008. Evaluating Regional Patterns in Nitrate Sources to Watersheds in National Parks of the Rocky Mountains using Nitrate Isotopes. Environ. Sci. Technol. 42, 6487–6493. https://doi.org/10.1021/es800739e

Nemergut, D.R., Townsend, A.R., Sattin, S.R., Freeman, K.R., Fierer, N., Neff, J.C., Bowman, W.D., Schadt, C.W., Weintraub, M.N., Schmidt, S.K., 2008. The effects of chronic nitrogen fertilization on alpine tundra soil microbial communities: implications for carbon and nitrogen cycling. Environ. Microbiol. 10, 3093–3105. https://doi.org/10.1111/j.1462-2920.2008.01735.x

Némery, J., Mano, V., Coynel, A., Etcheber, H., Moatar, F., Meybeck, M., Belleudy, P., Poirel, A., 2013. Carbon and suspended sediment transport in an impounded alpine river (Isère, France). Hydrol. Process. 27, n/a–n/a. https://doi.org/10.1002/hyp.9387

Nesti, C., 2016. Study of the isotopic composition of nitrate in alpine plants at the Col du Lautaret (Hautes-Alpes) and evaluation of atmospheric contribution in its balance. (Masters thesis). University of Florence.

Ohte, N., NAGATA, T., TAYASU, I., KOHZU, A., YOSHIMIZU, C., 2008. Nitrogen and oxygen isotope measurements of nitrate to survey the sources and transformation of nitrogen loads in rivers.

Ohte, N., Sebestyen, S.D., Shanley, J.B., Doctor, D.H., Kendall, C., Wankel, S.D., Boyer, E.W., 2004. Tracing sources of nitrate in snowmelt runoff using a high-resolution isotopic technique: TRACING SOURCES OF NITRATE IN SNOWMELT RUNOFF. Geophys. Res. Lett. 31, n/a-n/a. https://doi.org/10.1029/2004GL020908

Ostrom, N.E., Knoke, K.E., Hedin, L.O., Robertson, G.P., Smucker, A.J.M., 1998. Temporal trends in nitrogen isotope values of nitrate leaching from an agricultural soil. Chem. Geol. 146, 219–227. https://doi.org/10.1016/S0009-2541(98)00012-6

Ozenda, P., 1985. La végétation de la chaîne alpine: dans l'espace montagnard européen. Masson.

Paulot, F., Jacob, D.J., Pinder, R.W., Bash, J.O., Travis, K., Henze, D.K., 2014. Ammonia emissions in the United States, European Union, and China derived by high-resolution inversion of ammonium wet deposition data: Interpretation with a new agricultural emissions inventory (MASAGE_NH3). J. Geophys. Res. Atmospheres 119, 4343–4364. https://doi.org/10.1002/2013JD021130

Pellerin, B.A., Saraceno, J.F., Shanley, J.B., Sebestyen, S.D., Aiken, G.R., Wollheim, W.M., Bergamaschi, B.A., 2012. Taking the pulse of snowmelt: in situ sensors reveal seasonal, event and diurnal patterns of nitrate and dissolved organic matter variability in an upland forest stream. Biogeochemistry 108, 183–198. https://doi.org/10.1007/s10533-011-9589-8

Phoenix, G.K., Booth, R.E., Leake, J.R., Read, D.J., Grime, J.P., Lee, J.A., 2003. Effects of enhanced nitrogen deposition and phosphorus limitation on nitrogen budgets of semi-natural grasslands. Glob. Change Biol. 9, 1309–1321. https://doi.org/10.1046/j.1365-2486.2003.00660.x

Phoenix, G.K., Hicks, W.K., Cinderby, S., Kuylenstierna, J.C.I., Stock, W.D., Dentener, F.J., Giller, K.E., Austin, A.T., Lefroy, R.D.B., Gimeno, B.S., Ashmore, M.R., Ineson, P., 2006. Atmospheric nitrogen deposition in world biodiversity hotspots: the need for a greater global perspective in assessing N deposition impacts. Glob. Change Biol. 12, 470–476. https://doi.org/10.1111/j.1365-2486.2006.01104.x

Powlson, D.S., Addiscott, T.M., Benjamin, N., Cassman, K.G., de Kok, T.M., van Grinsven, H., L'hirondel, J.-L., Avery, A.A., van Kessel, C., 2008. When Does Nitrate Become a Risk for Humans? J. Environ. Qual. 37, 291. https://doi.org/10.2134/jeq2007.0177

Preunkert, S., 2003. A seasonally resolved alpine ice core record of nitrate: Comparison with anthropogenic inventories and estimation of preindustrial emissions of NO in Europe. J. Geophys. Res. 108. https://doi.org/10.1029/2003JD003475

Quétier, F., 2006. Vulnérabilité des écosystèmes semi-naturels européens aux changements d'utilisation des terres : application aux prairies subalpines de Villar d'Arène, France. Montpellier, ENSA.

Quétier, F., Thébault, A., Lavorel, S., 2007. PLANT TRAITS IN A STATE AND TRANSITION FRAMEWORK AS MARKERS OF ECOSYSTEM RESPONSE TO LAND-USE CHANGE. Ecol. Monogr. 77, 33–52. https://doi.org/10.1890/06-0054

Rao, P., Hutyra, L.R., Raciti, S.M., Templer, P.H., 2014. Atmospheric nitrogen inputs and losses along an urbanization gradient from Boston to Harvard Forest, MA. Biogeochemistry 121, 229–245. https://doi.org/10.1007/s10533-013-9861-1

Ravazzani, G., Curti, D., Gattinoni, P., Della Valentina, S., Fiorucci, A., Rosso, R., 2016. Assessing Groundwater Contribution to Streamflow of a Large Alpine River with Heat Tracer Methods and Hydrological Modelling. River Res. Appl. 32, 871–884. https://doi.org/10.1002/rra.2921

Riha, K.M., 2014. The use of stable isotopes to constrain the nitrogen cycle. Purdue University.

Riha, K.M., Michalski, G., Gallo, E.L., Lohse, K.A., Brooks, P.D., Meixner, T., 2014. High Atmospheric Nitrate Inputs and Nitrogen Turnover in Semi-arid Urban Catchments. Ecosystems 17, 1309–1325. https://doi.org/10.1007/s10021-014-9797-x

Robson, T., Lavorel, S., Clement, J., Roux, X., 2007. Neglect of mowing and manuring leads to slower nitrogen cycling in subalpine grasslands. Soil Biol. Biochem. 39, 930–941. https://doi.org/10.1016/j.soilbio.2006.11.004

Robson, T.M., Baptist, F., ClÃ©ment, J.-C., Lavorel, S., 2010. Land use in subalpine grasslands affects nitrogen cycling via changes in plant community and soil microbial uptake dynamics: Land-use gradients affect N cycle via plants and microbes. J. Ecol. 98, 62–73. https://doi.org/10.1111/j.1365-2745.2009.01609.x

Rogora, M., Mosello, R., Arisci, S., Brizzio, M.C., Barbieri, A., Balestrini, R., Waldner, P., Schmitt, M., Stähli, M., Thimonier, A., Kalina, M., Puxbaum, H., Nickus, U., Ulrich, E., Probst, A., 2006. An Overview of Atmospheric Deposition Chemistry over the Alps: Present Status and Long-term Trends. Hydrobiologia 562, 17–40. https://doi.org/10.1007/s10750-005-1803-z

Rose, L.A., Elliott, E.M., Adams, M.B., 2015a. Triple Nitrate Isotopes Indicate Differing Nitrate Source Contributions to Streams Across a Nitrogen Saturation Gradient. Ecosystems 18, 1209–1223. https://doi.org/10.1007/s10021-015-9891-8

Rose, L.A., Sebestyen, S.D., Elliott, E.M., Koba, K., 2015b. Drivers of atmospheric nitrate processing and export in forested catchments. Water Resour. Res. 51, 1333–1352. https://doi.org/10.1002/2014WR015716

Russell, K.M., Galloway, J.N., Macko, S.A., Moody, J.L., Scudlark, J.R., 1998. Sources of nitrogen in wet deposition to the Chesapeake Bay region. Atmos. Environ. 32, 2453–2465. https://doi.org/10.1016/S1352-2310(98)00044-2

Sabo, R.D., Nelson, D.M., Eshleman, K.N., 2016. Episodic, seasonal, and annual export of atmospheric and microbial nitrate from a temperate forest: MICROBIAL AND ATMOSPHERIC NITRATE EXPORT. Geophys. Res. Lett. 43, 683–691. https://doi.org/10.1002/2015GL066758

Saccon, P., Leis, A., Marca, A., Kaiser, J., Campisi, L., Böttcher, M.E., Savarino, J., Escher, P., Eisenhauer, A., Erbland, J., 2013. Determination of Nitrate Pollution Sources in the Marano Lagoon (Italy) by using a Combined Approach of Hydrochemical and Isotopic Techniques. Procedia Earth Planet. Sci., Proceedings of the Fourteenth International Symposium on Water-Rock Interaction, WRI 14 7, 758–761. https://doi.org/10.1016/j.proeps.2013.03.019

Saccone, P., Morin, S., Baptist, F., Bonneville, J.-M., Colace, M.-P., Domine, F., Faure, M., Geremia, R., Lochet, J., Poly, F., Lavorel, S., Clément, J.-C., 2013. The effects of snowpack properties and plant strategies on litter decomposition during winter in subalpine meadows. Plant Soil 363, 215–229. https://doi.org/10.1007/s11104-012-1307-3

Sala, O.E., Chapin III, F.S., Armesto, J.J., Berlow, E., Bloomfield, J., Huenneke, L., Jackson, R., Kinzig, A., Leemans, R., Lodge, D., Mooney, H.A., Oesterheld, M., Poff, N., Sykes, M.R., Walker, B., Walker, M., Wall, D., 2000. Biodiversity: global

biodiversity scenarios for the year 2100. Science 287, 1770–1774.

Salles, J.F., Le Roux, X., Poly, F., 2012. Relating Phylogenetic and Functional Diversity among Denitrifiers and Quantifying their Capacity to Predict Community Functioning. Front. Microbiol. 3. https://doi.org/10.3389/fmicb.2012.00209

Saros, J.E., Rose, K.C., Clow, D.W., Stephens, V.C., Nurse, A.B., Arnett, H.A., Stone, J.R., Williamson, C.E., Wolfe, A.P., 2010. Melting Alpine Glaciers Enrich High-Elevation Lakes with Reactive Nitrogen. Environ. Sci. Technol. 44, 4891–4896. https://doi.org/10.1021/es100147j

Savarino, J., Bhattacharya, S.K., Morin, S., Baroni, M., Doussin, J.-F., 2008. The NO+O3 reaction: A triple oxygen isotope perspective on the reaction dynamics and atmospheric implications for the transfer of the ozone isotope anomaly. J. Chem. Phys. 128, 194303. https://doi.org/10.1063/1.2917581

Savarino, J., Kaiser, J., Morin, S., Sigman, D.M., Thiemens, M.H., 2007. Nitrogen and oxygen isotopic constraints on the origin of atmospheric nitrate in coastal Antarctica. Atmospheric Chem. Phys. 7, 1925–1945. https://doi.org/10.5194/acp-7-1925-2007

Savarino, J., Morin, S., Erbland, J., Grannec, F., Patey, M.D., Vicars, W., Alexander, B., Achterberg, E.P., 2013. Isotopic composition of atmospheric nitrate in a tropical marine boundary layer. Proc. Natl. Acad. Sci. 110, 17668–17673. https://doi.org/10.1073/pnas.1216639110

Schmidt, S.K., Lipson, D.A., 2004. Microbial growth under the snow: implications for nutrient and allelochemical availability in temperate soils. Plant Soil 259, 1–7.

Sebestyen, S.D., Shanley, J.B., Boyer, E.W., Kendall, C., Doctor, D.H., 2014. Coupled hydrological and biogeochemical processes controlling variability of nitrogen species in streamflow during autumn in an upland forest: STREAM N DYNAMICS DURING AUTUMN. Water Resour. Res. 50, 1569–1591. https://doi.org/10.1002/2013WR013670

Sebilo, M., Billen, G., Grably, M., Mariotti, A., 2003. Isotopic composition of nitrate-nitrogen as a marker of riparian and benthic denitrification at the scale of the whole Seine River system. Biogeochemistry 63, 35–51. https://doi.org/10.1023/A:1023362923881

Sebilo, M., Billen, G., Mayer, B., Billiou, D., Grably, M., Garnier, J., Mariotti, A., 2006.

Assessing Nitrification and Denitrification in the Seine River and Estuary Using Chemical and Isotopic Techniques. Ecosystems 9, 564–577. https://doi.org/10.1007/s10021-006-0151-9

Semaoune, P., Sebilo, M., Templier, J., Derenne, S., 2012. Is there any isotopic fractionation of nitrate associated with diffusion and advection? Environ. Chem. 9, 158–162. https://doi.org/10.1071/EN11143

Sigman, D.M., Casciotti, K.L., Andreani, M., Barford, C., Galanter, M., Böhlke, J.K., 2001. A Bacterial Method for the Nitrogen Isotopic Analysis of Nitrate in Seawater and Freshwater. Anal. Chem. 73, 4145–4153. https://doi.org/10.1021/ac010088e

Silva, S.R., Kendall, C., Wilkison, D.H., Ziegler, A.C., Chang, C.C.Y., Avanzino, R.J., 2000. A new method for collection of nitrate from fresh water and the analysis of nitrogen and oxygen isotope ratios. J. Hydrol. 228, 22–36. https://doi.org/10.1016/S0022-1694(99)00205-X

Slemmons, K.E.H., Saros, J.E., Simon, K., 2013. The influence of glacial meltwater on alpine aquatic ecosystems: a review. Environ. Sci. Process. Impacts 15, 1794. https://doi.org/10.1039/c3em00243h

Snider, D.M., Spoelstra, J., Schiff, S.L., Venkiteswaran, J.J., 2010. Stable Oxygen Isotope Ratios of Nitrate Produced from Nitrification: 18O-Labeled Water Incubations of Agricultural and Temperate Forest Soils. Environ. Sci. Technol. 44, 5358–5364. https://doi.org/10.1021/es1002567

Sorensen, P.O., Templer, P.H., Christenson, L., Duran, J., Fahey, T., Fisk, M.C., Groffman, P.M., Morse, J.L., Finzi, A.C., 2016. Reduced snow cover alters root-microbe interactions and decreases nitrification rates in a northern hardwood forest. Ecology 97, 3359–3368. https://doi.org/10.1002/ecy.1599

Spalding, R.F., Exner, M.E., 1993. Occurrence of Nitrate in Groundwater—A Review. J. Environ. Qual. 22, 392–402. https://doi.org/10.2134/jeq1993.00472425002200030002x

Sparks, J.P., 2009. Ecological ramifications of the direct foliar uptake of nitrogen. Oecologia 159, 1–13. https://doi.org/10.1007/s00442-008-1188-6

Spaulding, S.A., Otu, M.K., Wolfe, A.P., Baron, J.S., 2015. Paleolimnological Records of Nitrogen Deposition in Shallow, High-Elevation Lakes of Grand Teton National Park, Wyoming, U.S.A. Arct. Antarct. Alp. Res. 47, 703–717.

https://doi.org/10.1657/AAAR0015-008

Spoelstra, J., Schiff, S.L., Hazlett, P.W., Jeffries, D.S., Semkin, R.G., 2007. The isotopic composition of nitrate produced from nitrification in a hardwood forest floor. Geochim. Cosmochim. Acta 71, 3757–3771. https://doi.org/10.1016/j.gca.2007.05.021

Stevens, C.J., 2004. Impact of Nitrogen Deposition on the Species Richness of Grasslands. Science 303, 1876–1879. https://doi.org/10.1126/science.1094678

Stocker, T. (Ed.), 2014. Climate change 2013: the physical science basis: Working Group I contribution to the Fifth assessment report of the Intergovernmental Panel on Climate Change. Cambridge University Press, New York.

Stoewer, M.M., Knöller, K., Stumpp, C., 2015. Tracing freshwater nitrate sources in pre-alpine groundwater catchments using environmental tracers. J. Hydrol. 524, 753–767. https://doi.org/10.1016/j.jhydrol.2015.03.022

Sun, J., Fu, J.S., Huang, K., 2016. Organic nitrates and other oxidized nitrogen compounds contribute significantly to the total nitrogen depositions in the United States. Proc. Natl. Acad. Sci. 113, E4433–E4434. https://doi.org/10.1073/pnas.1608717113

Sutton, M.A. (Ed.), 2011. The European nitrogen assessment: sources, effects, and policy perspectives. Cambridge University Press, Cambridge, UK ; New York.

Swart, P.K., Evans, S., Capo, T., Altabet, M.A., 2014. The fractionation of nitrogen and oxygen isotopes in macroalgae during the assimilation of nitrate. Biogeosciences 11, 6147–6157. https://doi.org/10.5194/bg-11-6147-2014

Tcherkez, G., Farquhar, G.D., 2006. *Viewpoint*: Isotopic fractionation by plant nitrate reductase, twenty years later. Funct. Plant Biol. 33, 531. https://doi.org/10.1071/FP05284

Templer, P.H., Pinder, R.W., Goodale, C.L., 2012. Effects of nitrogen deposition on greenhouse-gas fluxes for forests and grasslands of North America. Front. Ecol. Environ. 10, 547–553. https://doi.org/10.1890/120055

Templer, P.H., Weathers, K.C., 2011. Use of mixed ion exchange resin and the denitrifier method to determine isotopic values of nitrate in atmospheric deposition and canopy throughfall. Atmos. Environ. 45, 2017–2020. https://doi.org/10.1016/j.atmosenv.2011.01.035

Templer, P.H., Weathers, K.C., Lindsey, A., Lenoir, K., Scott, L., 2015. Atmospheric inputs and nitrogen saturation status in and adjacent to Class I wilderness areas of the northeastern US. Oecologia 177, 5–15. https://doi.org/10.1007/s00442-014-3121-5

Thamdrup, B., Dalsgaard, T., 2002. Production of N(2) through anaerobic ammonium oxidation coupled to nitrate reduction in marine sediments. Appl. Environ. Microbiol. 68, 1312–1318.

Thébault, A., Clément, J.-C., Ibanez, S., Roy, J., Geremia, R.A., Pérez, C.A., Buttler, A., Estienne, Y., Lavorel, S., 2014. Nitrogen limitation and microbial diversity at the treeline. Oikos 123, 729–740. https://doi.org/10.1111/j.1600-0706.2013.00860.x

Thiemens, M.H., 2006. History and applications of mass-independent isotope effects. Annu Rev Earth Planet Sci 34, 217–262.

Thiemens, M.H., Heidenreich, J.E., 1983. The mass-independent fractionation of oxygen: a novel isotope effect and its possible cosmochemical implications. Science 219, 1073–1075. https://doi.org/10.1126/science.219.4588.1073

Townsend, A.R., Howarth, R.W., Bazzaz, F.A., Booth, M.S., Cleveland, C.C., Collinge, S.K., Dobson, A.P., Epstein, P.R., Holland, E.A., Keeney, D.R., others, 2003. Human health effects of a changing global nitrogen cycle. Front. Ecol. Environ. 1, 240–246.

Treibergs, L.A., Granger, J., 2017. Enzyme level N and O isotope effects of assimilatory and dissimilatory nitrate reduction: Enzyme level N and O isotope effects. Limnol. Oceanogr. 62, 272–288. https://doi.org/10.1002/lno.10393

Trimmer, M., Nicholls, J.C., 2009. Production of nitrogen gas via anammox and denitrification in intact sediment cores along a continental shelf to slope transect in the North Atlantic. Limnol. Oceanogr. 54, 577–589. https://doi.org/10.4319/lo.2009.54.2.0577

Tsunogai, U., Daita, S., Komatsu, D.D., Nakagawa, F., Tanaka, A., 2011. Quantifying nitrate dynamics in an oligotrophic lake using Δ¹⁷O. Biogeosciences 8, 687–702. https://doi.org/10.5194/bg-8-687-2011

Tsunogai, U., Komatsu, D.D., Ohyama, T., Suzuki, A., Nakagawa, F., Noguchi, I., Takagi, K., Nomura, M., Fukuzawa, K., Shibata, H., 2014. Quantifying the effects of clear-cutting and strip-cutting on nitrate dynamics in a forested watershed using triple

oxygen isotopes as tracers. Biogeosciences 11, 5411–5424. https://doi.org/10.5194/bg-11-5411-2014

Tsunogai, U., Miyauchi, T., Ohyama, T., Komatsu, D.D., Nakagawa, F., Obata, Y., Sato, K., Ohizumi, T., 2016. Accurate and precise quantification of atmospheric nitrate in streams draining land of various uses by using triple oxygen isotopes as tracers. Biogeosciences 13, 3441–3459. https://doi.org/10.5194/bg-13-3441-2016

Vallano, D., 2009. Foliar Uptake Of Atmospheric Reactive Nitrogen Pollution.

Vallano, D.M., Sparks, J.P., 2007. Foliar δ 15 N values as indicators of foliar uptake of atmospheric nitrogen pollution. Terr. Ecol. 1, 93–109.

Van Grinsven, H.J., Ward, M.H., Benjamin, N., De Kok, T.M., 2006. Does the evidence about health risks associated with nitrate ingestion warrant an increase of the nitrate standard for drinking water? Environ. Health 5, 26.

Vankoughnett, M.R., Henry, H.A.L., 2013. Combined Effects of Soil Freezing and N Addition on Losses and Interception of N Over Winter and Summer. Ecosystems 16, 694–703. https://doi.org/10.1007/s10021-013-9642-7

Viard-Crétat, F., Baptist, F., Secher-Fromell, H., Gallet, C., 2012. The allelopathic effects of Festuca paniculata depend on competition in subalpine grasslands. Plant Ecol. 213, 1963–1973. https://doi.org/10.1007/s11258-012-0143-0

Vicars, W.C., Savarino, J., 2014. Quantitative constraints on the 17O-excess (Δ17O) signature of surface ozone: Ambient measurements from 50°N to 50°S using the nitrite-coated filter technique. Geochim. Cosmochim. Acta 135, 270–287. https://doi.org/10.1016/j.gca.2014.03.023

Vigneron, A., Bishop, A., Alsop, E.B., Hull, K., Rhodes, I., Hendricks, R., Head, I.M., Tsesmetzis, N., 2017. Microbial and Isotopic Evidence for Methane Cycling in Hydrocarbon-Containing Groundwater from the Pennsylvania Region. Front. Microbiol. 8. https://doi.org/10.3389/fmicb.2017.00593

Vitousek, P.M., Aber, J.D., Howarth, R.W., Likens, G.E., Matson, P.A., Schindler, D.W., Schlesinger, W.H., Tilman, D.G., 1997. HUMAN ALTERATION OF THE GLOBAL NITROGEN CYCLE: SOURCES AND CONSEQUENCES. Ecol. Appl. 7, 737–750. https://doi.org/10.1890/1051-0761(1997)007[0737:HAOTGN]2.0.CO;2

Vitousek, P.M., Howarth, R.W., 1991. Nitrogen limitation on land and in the sea: How can it occur? Biogeochemistry 13, 87–115. https://doi.org/10.1007/BF00002772

Wang, F., Ge, W., Luo, H., Seo, J.-H., Michalski, G., 2016. Oxygen-17 anomaly in soil nitrate: A new precipitation proxy for desert landscapes. Earth Planet. Sci. Lett. 438, 103–111. https://doi.org/10.1016/j.epsl.2016.01.002

Wankel, S.D., Kendall, C., Francis, C.A., Paytan, A., 2006. Nitrogen sources and cycling in the San Francisco Bay Estuary: A nitrate dual isotopic composition approach. Limnol. Oceanogr. 51, 1654–1664.

Ward, M.H., deKok, T.M., Levallois, P., Brender, J., Gulis, G., Nolan, B.T., VanDerslice, J., 2005. Workgroup Report: Drinking-Water Nitrate and Health—Recent Findings and Research Needs. Environ. Health Perspect. 113, 1607–1614. https://doi.org/10.1289/ehp.8043

Waring, S.A., Bremner, J.M., 1964. Ammonium Production in Soil under Waterlogged Conditions as an Index of Nitrogen Availability. Nature 201, 951–952. https://doi.org/10.1038/201951a0

Wasiuta, V., Lafrenière, M.J., Norman, A.-L., 2015a. Atmospheric deposition of sulfur and inorganic nitrogen in the Southern Canadian Rocky Mountains from seasonal snowpacks and bulk summer precipitation. J. Hydrol. 523, 563–573. https://doi.org/10.1016/j.jhydrol.2015.01.073

Wasiuta, V., Lafrenière, M.J., Norman, A.-L., Hastings, M.G., 2015b. Summer deposition of sulfate and reactive nitrogen to two alpine valleys in the Canadian Rocky Mountains. Atmos. Environ. 101, 270–285. https://doi.org/10.1016/j.atmosenv.2014.10.041

Weijs, S.V., Mutzner, R., Parlange, M.B., 2013. Could electrical conductivity replace water level in rating curves for alpine streams?: ELECTRICAL CONDUCTIVITY STREAMFLOW RATING CURVES. Water Resour. Res. 49, 343–351. https://doi.org/10.1029/2012WR012181

Wexler, S.K., Goodale, C.L., McGuire, K.J., Bailey, S.W., Groffman, P.M., 2014. Isotopic signals of summer denitrification in a northern hardwood forested catchment. Proc. Natl. Acad. Sci. 111, 16413–16418. https://doi.org/10.1073/pnas.1404321111

Williams, J.J., Nurse, A., Saros, J.E., Riedel, J., Beutel, M., 2016. Effects of glaciers on nutrient concentrations and phytoplankton in lakes within the Northern Cascades Mountains (USA). Biogeochemistry 131, 373–385. https://doi.org/10.1007/s10533-016-0264-y

Williams, M.W., Brooks, P.D., Mosier, A., Tonnessen, K.A., 1996. Mineral nitrogen transformations in and under seasonal snow in a high-elevation catchment in the Rocky Mountains, United States. Water Resour. Res. 32, 3161–3171. https://doi.org/10.1029/96WR02240

Williams, M.W., Knauf, M., Cory, R., Caine, N., Liu, F., 2007. Nitrate content and potential microbial signature of rock glacier outflow, Colorado Front Range. Earth Surf. Process. Landf. 32, 1032–1047. https://doi.org/10.1002/esp.1455

Williams, M.W., Melack, J.M., 1991. Solute chemistry of snowmelt and runoff in an Alpine Basin, Sierra Nevada. Water Resour. Res. 27, 1575–1588. https://doi.org/10.1029/90WR02774

Williams, M.W., Seibold, C., Chowanski, K., 2009. Storage and release of solutes from a subalpine seasonal snowpack: soil and stream water response, Niwot Ridge, Colorado. Biogeochemistry 95, 77–94. https://doi.org/10.1007/s10533-009-9288-x

Williams, M.W., Tonnessen, K.A., 2000. Critical loads for inorganic nitrogen deposition in the Colorado Front Range, USA. Ecol. Appl. 10, 1648–1665.

Winter, T.C., 2007. The Role of Ground Water in Generating Streamflow in Headwater Areas and in Maintaining Base Flow1. JAWRA J. Am. Water Resour. Assoc. 43, 15–25. https://doi.org/10.1111/j.1752-1688.2007.00003.x

Wolfe, A.P., Van Gorp, A.C., Baron, J.S., 2003. Recent ecological and biogeochemical changes in alpine lakes of Rocky Mountain National Park (Colorado, USA): a response to anthropogenic nitrogen deposition. Geobiology 1, 153–168.

Wood, E.D., Armstrong, F.A.J., Richards, F.A., 1967. Determination of nitrate in sea water by cadmium-copper reduction to nitrite. J. Mar. Biol. Assoc. U. K. 47, 23. https://doi.org/10.1017/S002531540003352X

Xue, D., Botte, J., De Baets, B., Accoe, F., Nestler, A., Taylor, P., Van Cleemput, O., Berglund, M., Boeckx, P., 2009. Present limitations and future prospects of stable isotope methods for nitrate source identification in surface- and groundwater. Water Res. 43, 1159–1170. https://doi.org/10.1016/j.watres.2008.12.048

Yang, Y.-Y., Toor, G.S., 2016. δ^{15} N and δ^{18} O Reveal the Sources of Nitrate-Nitrogen in Urban Residential Stormwater Runoff. Environ. Sci. Technol. https://doi.org/10.1021/acs.est.5b05353

Ye, C., Gao, H., Zhang, N., Zhou, X., 2016. Photolysis of Nitric Acid and Nitrate on

Natural and Artificial Surfaces. Environ. Sci. Technol. 50, 3530–3536. https://doi.org/10.1021/acs.est.5b05032

Young, E.D., Galy, A., Nagahara, H., 2002. Kinetic and equilibrium mass-dependent isotope fractionation laws in nature and their geochemical and cosmochemical significance. Geochim. Cosmochim. Acta 66, 1095–1104.

Young, G.L., 2002. NOx formation in rotary kilns producing cement clinker applicable NOx control techniques and cost effectiveness of these control techniques, in: IEEE-IAS/PCS 2002 Cement Industry Technical Conference. Conference Record (Cat. No.02CH37282). Presented at the IEEE-IAS/PCS 2002 Cement Industry Technical Conference. Conference Record (Cat. No.02CH37282), pp. 239–254. https://doi.org/10.1109/.2002.1006510

Zong, N., Shi, P., Song, M., Zhang, X., Jiang, J., Chai, X., 2016. Nitrogen Critical Loads for an Alpine Meadow Ecosystem on the Tibetan Plateau. Environ. Manage. 57, 531–542. https://doi.org/10.1007/s00267-015-0626-6

List of Tables

List of Figures

Appendix A – Methods

The following section presents simplified versions of field and laboratory techniques that were deployed during this Ph.D., and most are routinely used at IGE and LECA. Unless specified otherwise, all the work presented hereafter has been part of the routine sampling and analysis protocol I performed over the pas three years. This could not have been achieved without the precious help of students and colleagues, who were always willing to lend a hand when needed. Here, the aim is to give an overview of the main techniques that have been used, and more extensive documentation on the procedures can be found in published papers or theses, of which references will be distilled throughout the text. Ultrapure water designates MilliQ water (18.2-MΩ cm^{-1} at 25°C).

Field work

Atmospheric nitrate sampling

Aerosols collect

I installed at the Lautaret pass a homemade apparatus (similar to a DIGITEL DA77), equipped with a DIGITEL $PM_{2.5}$ cutting head (Figure A-0-1a). Similar equipment has been routinely used in Antarctica with the same purpose (*i.e.*, to collect NO_3^- in aerosols) (Ishino et al., 2017). This equipment served all year 2015, and was later (in 2016) replaced by an automatic SDEC CAV-A aerosols collector with a PM_{10} cutting head, which proved to be highly inadequate to on-site winter conditions (Figure A-0-1b). The SDEC collector is operated through a LCD that doesn't support below freezing temperature. Therefore, a specific housing – not provided by the manufacturer - is needed to operate this instrument in mountainous regions. Another alternative is to keep the instrument in a warmed shelter with only the collecting head exiting outside.

Sampling was done on a weekly basis. Filters for the aerosols collect were always prepared at IGE using QMA Whatman quartz filters burnt at 800°C for 1-h to lower the blank signal (Jaffrezo et al., 2005). Airflow was set at 30-m^3 h^{-1}. A 1-min

blank was performed every month. A simplified version of the procedure, adapted to the automatic collect in 2016, is provided hereafter:

- When arriving on site, stop the collector and note the date, time, and value of the volumetric counter.
- Remove the filter holder, wrap in clean aluminum foil, and bring back to laboratory.
- Remove the filter from the filter holder with clean pliers under a hood; fold it in two (so that the collecting surface is protected) and wrap it in aluminum foil.
- Put the aluminum containing the filter in a clean zip lock bag.
- Store at -20°C.
- Clean the pliers and the filter holder; leave them to dry under the hood.
- Take a clean filter holder; insert a new filter; wrap in clean aluminum foil.
- Insert in the collector; launch it and note the date, time, and value on the volumetric counter.

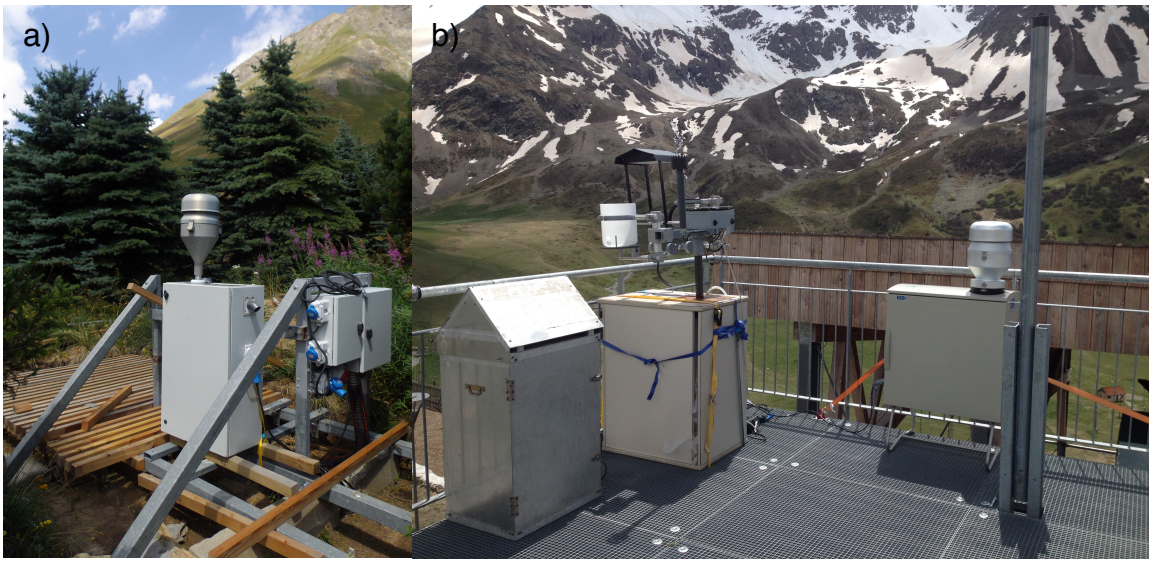

Figure A-0-1: The atmospheric collectors at the Lautaret pass, with a) the homemade aerosols collector on the experimental platform and b) from left to right: a bulk aerosols collector, a deposition (wet and dry) collector and an automatic aerosols collector on the roof of the Galerie de l'Alpe.

Deposition (wet and dry) collect

We also added a wet & dry deposition collector (WADOS Kroneis GmbH Austria) in 2016 to capture precipitation and dry particles / gases (Beyn et al., 2014; Mara et al., 2009). Monitoring of dry deposition has been a challenge for the scientific

community, and the method employed here cannot account quantitatively for the dry deposition flux. The collector is constituted of two funnels, dedicated to the collect of dry deposition and wet deposition separately. A moving lid is operated by a heated rain gauge, and depending on the precipitation status (*i.e.*, rain or not), it alternatively covers the wet or the dry funnel. Under snow conditions, the heated rain gauge melts snowflakes and thus triggers the opening of the wet funnel. The wet funnel is connected to a collecting bucket inside a fridge at 4 °C to prevent any further biological or chemical transformation (Figure A-0-2). Sampling was done every three weeks or so. A simplified version of the procedure is provided hereafter:`

- When arriving on site, note the date and time and retrieve the two collecting buckets.
- In the laboratory, pour the wet deposition sample in a weighted clean Nalgene bottle; weight the sample.
- Rinse the dry deposition bucket with 1-L ultrapure water; pour into a clean Nalgene bottle. Store the samples at -20°C.
- Clean both buckets three times with ultrapure water; leave them to dry upside down.
- When dry, put the buckets back in place. Write down the date and time.

Figure A-0-2: The WADOS collector being installed on the roof of the Galerie de l'Alpe. The wet deposition funnel is connected to a fridge where rain (or snow) samples are conserved (left panel).

The dry deposition funnel is just a bucket (right panel). The rain gauge was still under plastic when the picture was taken.

Snow collect

I performed snow pits on a monthly basis throughout winter 2015, and collected bulk snow throughout winter 2016 (Figure A-0-3), in agreement with the procedure used in Antarctica by IGE (Erbland, 2011). As most of the bulk snow samples have not been analyzed to date, I will only provide a simplified version of the snow pits sampling procedure hereafter:

- Before the first snow pit, spot a flat area with consistent snowpack that is not on a ridge (to avoid blowing snow bias) and neither in an accumulation zone.
- Delineate the sampling zone with visible landmarks to avoid skiers and hikers trespassing.
- Dig a pit until soil is reached; make a hole large enough so that a person can fit in easily.
- Clean the vertical profile; measure the snowpack height.
- Collect snow in Whirl-Pack® bags with a clean shovel every 2-5 cm depending on the snowpack.
- Label every samples and store in a cold box.
- When done, refill the hole and mark the location.
- Store samples at -20°C.

Figure A-0-3: Snow pit digging in winter 2015 (left panel) and surface snow sampling in winter 2016 with the help of Albane Barbero (right panel). © S. Hattori and F. Delbart.

Terrestrial nitrate sampling

Stream samples collect

I sampled (hand grab) six streams and one artificial lake spanning an altitude gradient from Grenoble to the Lautaret pass on a weekly basis in 2015 and 2016. In April 2016, I also performed an intensive stream sampling campaign (Figure A-0-4). For three weeks, I collected samples in Tufiere, Les Cours and Romanche streams every three hours using automatic water samplers (Teledyne ISCO® 3700). A simplified version of the manual procedure, which was adapted to the automatic sampling period, is provided hereafter:

- In laboratory, prepare and clean Nalgene bottles by rinsing them three times with ultrapure water.
- Go to the first stream; rinse the bottle and cap three more times with stream water.
- Fill the bottle; note the date and time.
- Proceed to the next stream and start over.
- Don't forget to label the bottles.
- Store all samples at -20°C.

Figure A-0-4: Manual sampling (left panel) and automatic sampling (right panel) of the Romanche stream.

Soil and plant samples collect

Starting at snowmelt 2016, I collected the soils of three meadows with different management treatments on a monthly basis at the Lautaret pass (Figure A-0-5). The

land uses of the meadows encompass a management gradient, featuring a) Terraced-Mown, b) Terraced-Unmown and c) Unterraced-Unmown treatments

I used a soil coring system (Eijkelkamp Inc., Netherlands) to extract soil without too much disturbing its physical and chemical properties and the microbial communities within (Legay et al., 2013; Robson et al., 2010). At the beginning of the experiment, each meadow was divided in three parts separated by *ca* 100m from one another, to account (a minimum) for spatial variability. The three parts were visibly marked.

On the same dates of soil sampling, entire grass (*i.e.*, roots + aerial parts) specimens were collected in close vicinity to the soils sampling location. Plants species were chosen based on their abundance on the three meadows elected for this experimentation. On the terraced meadows, it was *Dactylis glomerata* that was harvested, and *Festuca paniculata* for the abandoned grassland (Figure A-0-6). A simplified version of the manual procedure is provided hereafter:

- The day before sampling, prepare and clean the soil corer and the metallic cores; gather cool boxes, ice packs, plastic bags and a shovel.
- On sampling day, go to the first meadow; proceed to the first landmark.
- Collect two soil cores (8-cm high and 4.5-cm diameter); leave about 10-cm between the two soil coring locations.
- Wrap the cores, label them and store in a cold box.
- Spot a grass of interest (*Dactylis glomerata* or *Festuca paniculata* depending on the meadow); dig around the grass to a depth of *ca* 50-cm.
- Carefully remove the grass from the soil with its roots; put it in a plastic bag.
- Store the plant in a cold box after it is labeled.
- Proceed to the next landmark (or meadow) and start over.
- Store all samples at -20°C.

Figure A-0-5: The three sampled meadows with a) Terraced-Mown, b) Terraced-Unmown and c) Unterraced-Unmown treatments (left panel). Hélène Angot helping with the soil corer in front of the Laurichard glacier (right panel).

Figure A-0-6: *Festuca paniculata* tussock (left panel) and *Dactylis glomerata* inflorescence (right panel).

Samples treatment

Aerosols filters

The CERMO lab at IGE first collected punches on all filters for major ions, elementary and organic carbon and tracer compounds (e.g., levoglucosan). I dissolved what remained of the filters in ultrapure to extract nitrate, as follows:

- In laboratory, rinse four centrifugal ultrafiltration units (Milipore Centricon plus-70, 100 000 Daltons) with ultrapure water.
- Fill the units with 40-mL ultrapure water.
- Centrifuge for 2-min at 4500-RPM.
- Remove the water and clean again the units three times with ultrapure water.
- Carefully place one filter per unit with clean pliers; fill with 40-mL ultrapure water.
- Shake manually for 30-sec.
- Centrifuge for 20-min at 4500 -PM.
- Retrieve the extracts in clean 50-mL Corning tubes; throw the filters.
- Start over.

After being extracted, all extracts were straight away concentrated on resin (see nitrate concentration). Blanks were regularly performed.

Liquid samples (stream, snow, wet and dry deposition)

All samples were left to unfreeze at room temperature the day prior to treatment. All samples were filtered using 0.45-µm Whatman GD/X syringe filters linked to a peristaltic pump, as follows:

- Prepare and clean Nalgene bottles by washing them three times with ultrapure water.
- Rinse the peristaltic pump tubes with ultrapure water.
- Connect all incoming tubes to samples (12 at a time).
- Rinse all tubes again with samples for 2-min.

- Connect the filters to the outgoing tubes.
- Place each filter in a clean funnel on top of a clean Nalgene bottle.
- Filter until all samples have been flown to the Nalgene bottles.
- Collect an aliquot for major ions analyses in a clean 50-mL Corning tube.
- Start over

After being extracted, all extracts were straight away concentrated on resin (see nitrate concentration). Blanks were regularly performed.

Soil samples

Soil samples were left to unfreeze at room temperature prior to any treatment. The two soil cores collected per sampling location (section A.1.2.2) underwent a different fate in laboratory. The first soil core was used for nitrate, ammonium and total dissolved nitrogen (TDN) extraction, along with other parameters measurements. The second soil core was dedicated to leaching simulation experiments, to extract labile ions from soils macro sites.

Extraction and other parameters

Sieve (5.6 mm) and homogenize soil cores; remove apparent rocks, roots and insects.

Extraction

- Weight 10-g of fresh soil in a clean extraction vial; note the exact weight.
- Add 50-mL ultrapure water; shake mechanically at 300-RPM for 1-h.
- Centrifuge at 4000-RPM for 10-min.
- Recover the supernatant and filter using 0.22-µm Whatman GD/X syringe filters linked to a peristaltic pump as described above.
- Collect an aliquot for nitrate, ammonium and TDN analyses in a clean 50-mL Corning tube.
- Start over.

After being extracted, all extracts were straight away concentrated on resin (see nitrate concentration). Blanks were regularly performed.

Net Mineralization Potential (NMP)

- Weight 10-g of fresh soil in a clean extraction vial; note the exact weight.
- Fill the vial with ultrapure water and weight again to infer the added water volume.
- Place at 40°C for seven days.
- Add 50-mL ultrapure water and proceed to extraction as described above.
- Centrifuge at 4000-RPM for 10-min.
- Recover the supernatant and filter using 0.22-µm Whatman GD/X syringe filters linked to a peristaltic pump as described above.
- Start over.

Note that these samples are analyzed for ammonium concentration only.

Microbial biomass

- Weight 10-g of fresh soil in a clean weighted open glass vial; note the exact weight.
- Prepare clean chloroform under the hood.
- Add wet paper at the bottom of a 20-L desiccator placed under the hood.
- Place the samples in the desiccator; pour 75-mL of chloroform in a glass vial with pumice; place it in the desiccator.
- Make sure that all samples are sufficiently wet (*i.e.*, at least half field capacity); otherwise spray ultrapure water on them.
- Close the desiccator; evacuate the air to create gauge-controlled vacuum and cover with a black plastic bag for five days.
- When done, open the desiccator under the hood and remove the chloroform.
- Purge the air several times.
- Remove the samples.
- Proceed to extraction as describes above.
- Start over.

Note that these samples are analyzed for TDN concentration only.

Soil humidity and organic matter content

- Weight 5-g of fresh soil in a clean weighted Pyrex cup; note the exact weight.
- Bake the samples at 70°C for seven days.
- Weight again the samples; note the exact weight.
- Bake the same samples at 550°C for 5-h.
- Weight again the samples; note the exact weight.

Leaching experiment

In order to do this experiment, soil cores need to be intact:

- Wrap all soil cores in clean aluminum foil; leave the top of the core uncovered; weight all soil cores.
- With a clean sharp tool, pierce holes in the aluminum at the bottom of the soil cores; don not pierce the soil cores.
- Place each soil core in a clean funnel on top of a measuring cylinder.
- Prepare around 100-mL ultrapure water in another measuring cylinder; note the volume.
- Spray homogeneously the water on a soil core; avoid lateral flow paths.
- Once the water starts to leach, continue to spray until a volume of *ca* 40-mL is collected in the measuring cylinder; note the collected and sprayed volumes.
- Weight the water saturated soil core.
- Proceed to the next sample.
- Bake all soil cores at 70°C for seven days then weight the soil cores.
- Centrifuge and filter all leachates using the protocol described above; collect an aliquot for nitrate, ammonium and TDN analyses.
- Start over.

After being extracted, all extracts were straight away concentrated on resin (see nitrate concentration). Blanks were regularly performed.

Plant samples

All plant samples were left to unfreeze at room temperature before further treatment. I choose to adapt the nitrate extraction protocol from Laursen et al. (2013) to perform the plants nitrate extraction in this study. The original protocol uses a 30-min heated water (90°C) extraction method, but there was no adapted machine to do so at LECA, especially considering the large number of samples I had. Therefore, I checked whether extractions using water at room temperature (mild water) would yield the same recovery efficiencies as the original protocol. I also compared the effect of an increase of extraction time and if the sample is extracted three times successively (*i.e.*, three consecutive extractions on the same plant sample). I performed these tests on *Dactylis glomerata* and *Festuca paniculata* samples collected during previous field campaigns. Overall, the 30-min heated water extraction (original protocol), the 1-h mild water extraction and the three successive 30-min extractions yielded the same nitrate concentrations. The 30-min mild water extraction produced lower nitrate concentrations (Figure A-0-7). The fact that the 3 successive extractions led to the same nitrate concentrations as other methods also suggests that nitrate recovery is total. The protocol ultimately used is provided hereafter:

- Rinse all plants thoroughly with ultrapure water; make sure to remove of trace of soil and dirt.
- Separate aboveground organs (leaves hereafter) from underground organs (roots hereafter).
- Dry all samples with clean laboratory paper.
- Weight about 50-g (for *Dactylis glomerata*) and 70-g (for *Festuca paniculata*) of plant organs and put them in a clean zip lock bag.
- Store at -20°C.
- Freeze-dry all samples (Heto DryWinner, Allerod, Denmark) for 48 hours.
- Grind all samples (RETSCH Mixer Mill MM400) for 45 sec at 30-Hz.
- Extract 1.5-g (for *Dactylis glomerata*) and 1-g (for *Festuca paniculata*) of ground powder with 50-mL ultrapure water for 1 h at 300 RPM.
- Centrifuge at 4000-RPM for 10-min.

- Recover the supernatant and filter using 0.22-µm Whatman GD/X syringe filters linked to a peristaltic pump as described above.
- Collect an aliquot for nitrate and ammonium in a clean 50-mL Corning tube.
- Start over.

After being extracted, all extracts were straight away concentrated on resin (see nitrate concentration) so that all samples had the same matrix (*i.e.*, NaCl). Blanks were regularly performed. Note that Liu et al. (2012) did not recommend freeze-drying after comparing plants nitrate extraction methods. However, to be consistent with the already analyzed plant samples using the freeze-drying method, I continued with this protocol.

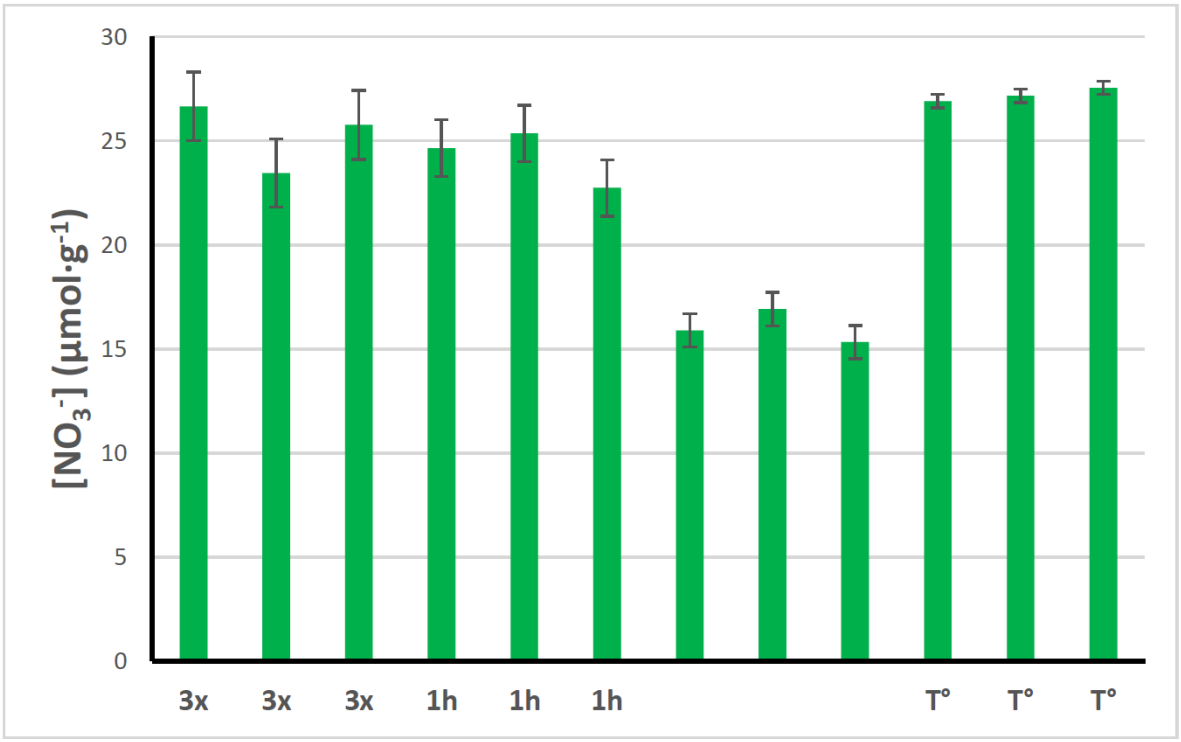

Figure A-0-7: Example of a method comparison test for nitrate extraction from plants tissues. Here the samples are *Dactylis glomerata* leaves. "3x" refers to the three successive extractions method, "1h" refers to the 1 h mild water extraction method, unlabeled bars are for the 30 min mild water extraction method and "T°" designates the 30 min heated water extraction method. Error bars indicate the standard deviation of three replicates for each test. After Nesti (2016).

Concentration on anionic resin

The analytical chain prior to the isotopic analyses requires that all samples have a minimum of 100-nmol of nitrate in a maximum of 10-mL sample volume. Nitrate concentrations in environmental matrixes are often lower than this requirement. Therefore, a necessary step of nitrate concentration on an anionic resin (AG 1-X8 resin, Cl^--form, Bio-Rad) was performed on all samples prior to isotopic analyses. The trapping of nitrate in resins have been widely used in both field and laboratory experiments (Boutin, 2015; Silva et al., 2000; Templer and Weathers, 2011), and is routinely used at IGE to concentrate nitrate from Antarctic snow and ice (Figure A-0-8). Its recovery efficiency is over 98.5%, a level at which potential isotopic fractionation effects are estimated as negligible (Erbland, 2011).

After samples nitrate concentrations were determined, I calculated the required volume of sample needed to trap *ca* 300-nmol of nitrate on the resin. The protocol used is provided hereafter:

- Prepare a 50:50 (in volume) resin solution by adding 1-M NaCl solution to a new solid resin.
- Shake the solution for 30-sec; wait until the resin deposits.
- Remove the supernatant; add the same volume of a 1-M NaCl solution.
- Do this steps three times.
- Pour 0.6-mL of mixed resin bed in a clean funnel; wait until the liquid has flown through.
- Rinse the funnel and the sample connecting tube with 20-mL of 1-M NaCl solution; wait until all liquid has flown through the resin.
- Rinse the funnel and the sample connecting tube with 20-mL of ultrapure water; wait until all liquid has flown through the resin.
- Pour the sample into the funnel; wait until all liquid has flown through the resin.
- Retrieve the funnel and place it over a clean 15-mL Corning tube.
- Elute the sample with 5-mL of a 1-M NaCl solution; wait until all liquid has flown through the resin.

- Elute again the sample with another 5-mL of a 1-M NaCl solution; wait until all liquid has flown through the resin.
- Store concentrated samples at -20°C until isotopic analysis.
- Start over.

Note that if not too dirty, a resin bed can be reused, after thorough cleaning, for another extraction. Blanks were performed regularly. I also regularly checked that the concentration process was going smoothly by i) collecting about 10-mL of liquid flowing through the resin towards the end of the concentration process and ii) eluting the resin with additional 10-mL NaCl after the first elution. Over 95 % of these tests showed nitrate concentrations lower than samples concentrations by two orders of magnitude. During my Ph.D., I automated this concentration step by using Gilson 215 and 402 automats, and this automated method is now routinely used at IGE.

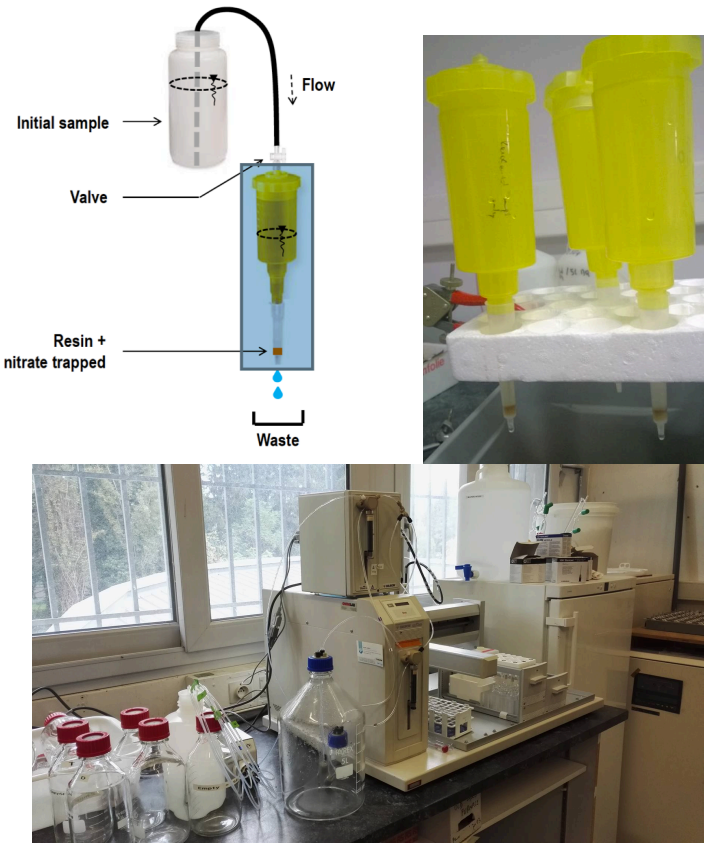

Figure A-0-8: A graphical representation of the nitrate concentration on resin process (top left panel, after Erbland (2011)) and what it looks like in real (top right panel). The bottom panel illustrates the automated version of the concentration step on Gilson 215 and 402 automats.

Analytical procedures

Concentrations

Major ions

Nitrate and nitrite concentrations were first analyzed on a Continuous Flow Analysis spectrophotometer (SEAL Analyzer QuAAtro) based on cadmium-reduction of NO_3^- to nitrite (Wood et al., 1967) in 2015. In 2016, the LECA bought a new, more complex spectrophotometer (Gallery Plus, Thermo Fisher Scientific, Waltham, Massachusetts, USA), which enabled ammonium, sulfate, calcium and chloride concentration monitoring in addition to nitrate and nitrite concentrations (see Table 1-1). Considering that these analytical techniques are widely used and thoroughly described on the manufacturers' websites, the protocols will not be thoroughly described here. Analytical routine includes analytical calibration, regular blanks and data control.

Due to excessive analytical costs, nitrite was not analyzed in all samples. However, I did analyze nitrite concentration in a sub-set of all matrix samples, chosen to span the entire study period. All samples thus analyzed had either undetectable nitrite concentrations or concentrations two orders of magnitude under nitrate levels. Therefore, all subsequent isotopic results were considered as unbiased estimations of nitrate isotopic composition. Note that addition of sulfamic acid to samples has been shown to remove nitrite and to be compatible with the denitrifier method (Granger and Sigman, 2009).

Total Dissolved Nitrogen (TDN)

TDN represents the total amount of dissolved nitrogen (organic and inorganic) in a sample, and can be determined by oxidizing all dissolved N forms to nitrate as follows:

- Prepare an oxidative solution by mixing 26-g $K_2S_2O_8$, 15.6-g H_3BO_3 and 50-mL 3.75N NaOH with ultrapure water in a 500-mL vial.
- Mix 5-mL of sample with 1-mL of oxidative solution in glass tubes.

- Prepare 5 control tubes with 5-mL of urea solution of known concentration and 1-mL of oxidative solution.
- Prepare 3 blank tubes with 5-mL ultrapure water and 1-mL of oxidative solution.
- Put the samples in the autoclave for 1-h at 121°C.
- Analyze nitrate concentration in all samples.

TDN analyses were performed only on soil extracts.

Isotopes

The dentirifier method that enables nitrate isotopic composition determination was first used to measure nitrate isotopes in freshwater and marine environments (Casciotti et al., 2002; Sigman et al., 2001). It was later improved by Kaiser et al. (2007) to allow for $\Delta^{17}O$, $\delta^{18}O$ and $\delta^{15}N$ simultaneous measurements of nitrate. Here we use an adapted version of this protocol, extensively described elsewhere (Morin, 2008; Morin et al., 2009). Here, I will provide a quick outlook of this method, routinely used at IGE.

Preparation of the samples

The denitrifier method relies on the incomplete reduction of nitrate during the denitrification process by *Pseudomonas aureofaciens* leading to the production of N_2O while conserving at least one N and one O atom from the initial nitrate.

Briefly, *Pseudomonas aureofaciens* is grown in 250-mL batches of nutrients-rich broth during 5 days at 30°C. After control of the good “health” of the bacteria by monitoring nitrite level in the medium, bacteria are harvested and concentrated 5–8-fold in 20-mL glass vials (2-mL per vial) and closed with septa. The vials were then purged with a helium (He) flux for at least 3 hours. This step enables the removal of residual N_2O and ensures anaerobic conditions necessary to trigger bacterial denitrification. Automated injection of samples, standards and matrix (1-M NaCl) maintains identical processing conditions for all vials (e.g., total volume, matrix, etc.). The complete reduction of nitrate to N_2O requires a few hours; therefore, all samples and standards are left to incubate overnight. The next day, bacteria are killed by

adding 0.5-mL of 1M NaOH solution to the vials. A summary of these steps is presented in Figure A-0-9.

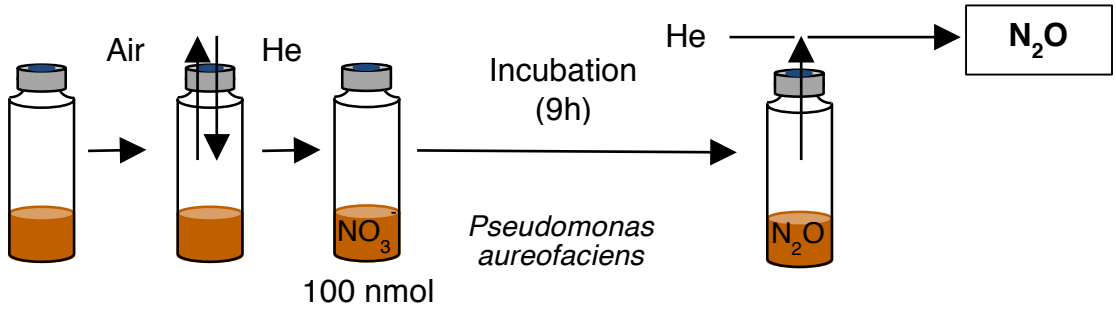

Figure A-0-9: A schematic representation of the successive steps before samples are ready for isotopic analysis. From left to right are represented the flushing step, the sample injection, the overnight incubation (NO_3^- ➔ N_2O) and the flushing of the gas to the mass spectrometer. © A. Barbero.

Mass spectrometer analysis

When all samples have been incubated, they are placed on the rack of an automated injector. The sample (now gaseous) is flushed with He for 10 min and sent through consecutive traps aiming at removing H_2O, CO_2 and volatil organic compounds (VOCs). N_2O is then trapped at liquid N temperature. At this stage, only N_2O should remains in the line. N_2O is then decomposed into N_2 and O_2 in a gold trap at 880 °C, which are seperated on a chromatographic column (10 m Agilent J&W CP-Molsieve 5Å GC Column CP7535I5). N2 and O2 can thus be sequentially analyzed on Thermo Finnigan MAT 253 using the *peak jump* function of the mass spectrometer. A summary of these steps is presented in Figure A-0-10.

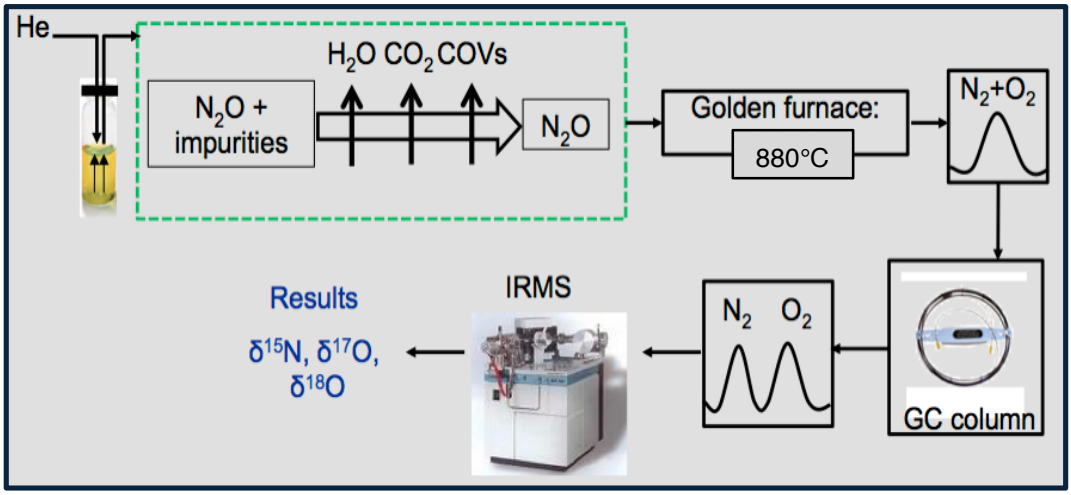

Figure A-0-10: The consecutive steps of N2O journey in the sampling line connected to the mass spectrometer. After Erbland (2011).

Data correction

All samples isotopic values were corrected for any isotopic effect possibly occurring during the procedure by processing simultaneously international reference materials (International Atomic Energy Agency USGS 32, USGS 34 and USGS 35 (Böhlke et al., 2003; Michalski et al., 2002; Morin, 2008)) through the same analytical batch. The isotopic standards were prepared in the same background matrix. An algorithm was used to calibrate the results to account for blank effects and isotopic exchange that could occur during the denitrification process. Standard deviation of the residuals from the linear regression between the measured reference standards (n=20) and their expected values served as indicator of the accuracy of the method.

Appendix B – Summary of activities

This section aims to present succinctly the academic and scientific activities I have pursued during the three years of my doctoral work.

Conferences

Bourgeois, I.; Savarino, J.; Clement, J.-C.: Response of a subalpine watershed to atmospheric NO_3^- deposition using $\Delta^{17}O$. Oral communication.
Goldschmidt Conference 2017, Paris, France.

Bourgeois, I.; Savarino, J.; Clement, J.-C.: Export of atmospheric nitrate in streams along an elevation gradient in the French Alps. Oral communication.
8th International Symposium on Isotopomers 2016, Nantes, France.

Bourgeois, I.; Savarino, J.; Clement, J.-C.: Response of subalpine vegetation to N deposition and land-use changes from a new isotopic perspective. Oral communication.
Joint European Stable Isotopes User group Meeting 2016, Ghent, Belgium.

Bourgeois, I.; Savarino, J.; Clement, J.-C.: MIF from an ecological point of view: insights on the synergy between nitrogen deposition and past land-use in mountainous basins. Oral communication.
Goldschmidt Conference 2016, Yokohama, Japan.

Bourgeois, I. ; Savarino, J. ; Clement, J.-C. : Characterisation of atmospheric nitrate dynamics in a subalpine watershed using $\Delta^{17}O$ and $\delta^{15}N$. Poster.
American Geosciences Union Fall Meeting 2015, San Francisco, USA.

Bourgeois, I.; Savarino, J.; Clement, J.-C.; Barbero, A.: DEPONIT: Dépôts des nitrates atmosphériques sur les prairies subalpines du Lautaret. Poster.
Colloque biennal des Zones-Ateliers 2015, Paris, France.

Bourgeois, I.; Savarino, J.; Clement, J.-C.: Ins and outs of atmospheric nitrate in the French Alps: a triple oxygen isotopes method implementation. Oral communication.
Goldschmidt Conference 2015, Prague, Czech Republic.

Training and collaborations

Laboratoire Ampère, Ecole Centrale de Lyon, France (July 2017): training on DNA extraction and qPCR technique.

ILTER Nitrogen Initiative Training Course, Hokkaido University, Sapporo, Japan (June 2016): summer school on N biogeochemical cycle.

INSTAAR & Niwot Ridge LTER visit, University of Colorado, Boulder, USA (December 2015): training on deposition (wet and dry) monitoring techniques in mountains.

Teaching and supervision

Environmental Chemistry, undergraduate level, tutorial and practical courses, *72h*
Ecology, undergraduate level, tutorial and practical courses, *38h*
Vegetal Biology, undergraduate level, practical courses, *21h*

Main supervisor to:
Sarah Albertin: “Exports of nitrate in subalpine streams”. *Undergraduate Student* (2 months).
Cristiano Nesti: “Study of nitrate isotopic composition in subalpine plants at the Lautaret pass, French Alps”. *Master’s Student* (6 months).
Nicolas Deschamps: “Characterization of atmospheric nitrate inputs to a subalpine meadow”. *Master’s Student* (4 months).

Co-supervisor to
Mathilde Weick: “Characterization of organic nitrogen and its evolution in the snowpack of the Lautaret pass”. *Master’s Student* (4 months).
Julien Alex: “Origin of atmospheric nitrogen deposition at the Lautaret pass”. *Master’s Student* (4 months).

Outreach

Tribulations Savantes

Small experiments related to Earth and the Universe sciences, set up by Ph.D. students, and presented to high school pupils.

Les lundi de la Galerie

Open conferences held at the Lautaret pass on atmospheric pollution related issues in mountainous areas.

Field missions

Stromboli island: two weeks field campaign for the FOFAMIFS project in May 2017.

Ny-Ålesund: two weeks field campaign for the ARCSNOW project in September 2016.

Résumé

L'accroissement des dépôts de nitrate atmosphérique ($NO_3^-{}_{atm}$) sur les bassins versants d'altitude, limités en ressources, entraîne des changements nets de disponibilité d'azote. Ces apports modifient la diversité biologique (végétation, microorganismes), les processus des sols liés à l'azote et conduisent à l'eutrophisation des cours d'eau. A terme, l'impact sur les populations humaines se traduira par la perte d'importants services fournis par ces écosystèmes (alimentation en eau, qualité du fourrage, contrôle de l'érosion, biodiversité). Si les effets des dépôts de $NO_3^-{}_{atm}$ sur les bassins versants pauvres en azote sont maintenant bien documentés, il n'en reste pas moins à comprendre les processus régissant la rétention de $NO_3^-{}_{atm}$ dans les écosystèmes de montagne. Pour ce faire, la variabilité spatio-temporelle de la répartition du $NO_3^-{}_{atm}$ dans tous les compartiments subalpins est ici étudiée en utilisant un traceur multi-isotopique (^{17}O, ^{18}O, ^{15}N) du NO_3^-. L'importante proportion de $NO_3^-{}_{atm}$ dans les cours d'eau de montagne, tout au long de l'année et plus particulièrement à la fonte des neiges, laisse à penser que les bassins versants sont cinétiquement saturés en azote. La composition isotopique du NO_3^- dans les eaux de surface illustre la transformation rapide de l'ammonium de la neige et confirme que la fonte des neiges est une période cruciale du cycle de l'azote dans les montagnes enneigées. La proportion de $NO_3^-{}_{atm}$ dans les sols varie, quant à elle, en fonction du type d'occupation des sols et des propriétés biotiques et abiotiques afférentes. Le suivi de la végétation a montré une forte teneur en $NO_3^-{}_{atm}$ dans les tissus, par assimilation racinaire et foliaire. Ces avancées scientifiques permettront, à terme, de mieux comprendre comment les dépôts de $NO_3^-{}_{atm}$ affectent l'environnement.

Mots-clés : Nitrate, dépôts atmosphériques, isotopes, subalpin, prairies